MEASUREMENTS OF THE POLARIZATION OF STARLIGHT

by

NEIL M. PRATT

A Thesis presented for the Degree of

Doctor of Philosophy

of the University of Edinburgh

Royal Observatory,

Edinburgh.

SEPTEMBER, 1968.

ABSTRACT.

A computer catalogue of photoelectric measurements of the polarization of starlight is being compiled, together with other relevant data about the measured stars. There is a deficiency of measurements of the fainter stars due to the large amounts of telescope time required. A new photographic method, potentially very rapid with the advent of automatic measuring engines, is described. This method, using a polaroid filter, allows also the simultaneous measurement of brightness differences between successive star images at different orientations of the analyser not due to polarization effects, and hence the polarization can be isolated. Overlapping of star images limits the use of the method, with the Edinburgh Schmidt telescope, to areas of sky with < 6000 stars per square degree, or V = 16 on average at the galactic equator.

527 stars in h and chi Persei to V = 13 have been measured. Using the Stokes parameters, comparison with published photoelectric measures for 54 stars gives an r.m.s. deviation of $\pm$ 0m.029 per star, and the photoelectric and photographic means agree to within 0m.003 and 1 degree. Proper motions from the literature and original photographic UBV photometry of the 527 stars has allowed the separation of the measured stars into groups within the local and Perseus spiral arms. From the mean polarization parameters for these groups of stars, it is concluded that the observed polarization towards h and chi Persei is largely produced within the local arm; that the orientation of the presumed magnetic field in the Perseus arm is different to that in the local arm; and that there is a possibility of local magnetic fields associated with the star clusters themselves.

CONTENTS.

(continued)

CONTENTS (cont.).

To my wife

Margaret

INTRODUCTION.

It is twenty-one years since the discovery of the interstellar polarization of starlight. The original discovery was made accidentally during a search for a stellar effect predicted by Chandrasekhar (1946). In the atmospheres of early-type stars, energy transport is by electron scattering and so polarization should occur at the limb of such a star, and be observable during the eclipse of that star in a suitable binary system. Observation showed that the polarization of the binary remained constant, within the errors, and that nearby comparison stars were also polarized. Further measures indicated that the polarization was independent of spectral type and that heavily polarized stars were also heavily obscured, although the converse was not always true. It was therefore concluded that the polarization was interstellar in origin.

This discovery implied that the dust grains of the interstellar medium are asymmetrical and at least partially aligned. The alignment mechanism is believed to be a galactic magnetic field. Such a magnetic field was first inferred in the theory of cosmic rays by Alfven and Fermi, and has also been inferred by radio astronomers to explain galactic radio phenomena.

The optical and radio observations do not delineate the magnetic field itself, but only describe its effect on the interstellar grains and charged particles, principally electrons, respectively. Whether the magnetic field lines run along the spiral arms of the galaxy, as suggested by Chandrasekhar and Fermi (1953), or are wound round the arms in tight helices, as

favoured by Behr (1959), Hoyle and Ireland (1961), Ireland (1961), is still under discussion. Little is known about local deviations in the general magnetic field, for example, in the neighbourhood of recently formed star associations and clusters, or near stars with circumstellar dust clouds.

Within twelve years of the original discovery, the general pattern of the optical polarization vectors had been determined over the whole sky. The amount of polarization is rarely larger than five percent and usually much less. The first attempts to measure optical polarization were made photographically, but these were indeterminate. Photoelectric methods proved successful and measurement of the polarization of starlight has been one of the principal spurs for improving photoelectric techniques. Accuracies of $\pm$ 0m.0005 (this convention will be used to denote 'magnitude' throughout this thesis) and better are now attained, but for the brighter stars only.

Behr (1956) was the first to achieve a mean error of $\pm$ 0m.0005 for stars with $V < 8.75$, with a 13-inch astrograph using a differential method, but the error rose to $\pm$ 0m.002 for $V = 10$. Few stars fainter than $V = 12$ have been investigated. In a study of some star clusters with two 21-inch reflectors, Serkowski (1965a) reported mean errors of $< \pm$ 0m.005 for $V < 9.5$, rising to $\pm$ 0m.015 for $V = 12$. The faintest objects so far investigated for polarization are quasi-stellar radio sources. For 3C446, with $B \sim 16$, Kinman, Lamla and Wirtanen (1966) using the Lick 120-inch reflector found $p = 0m.227$ and 0m.189 on two different nights, with r.m.s. deviations of $\pm$ 0m.034 and $\pm$ 0m.022 respectively. More recently, Visvanathan (1968), using the Mt Wilson 100-inch, has attained mean errors of $\pm$ 0m.004 for 3C273 at $V = 12.8$, but for PHL1377,

V = 16.5, they rise to ± 0m.030.

Photoelectric measures of polarization require large amounts of telescope time – Hall (1958) required about 12 minutes per star and Hiltner (1951) rather longer. To observe fainter stars with a particular telescope, either the observing time must be increased or the accuracy reduced. The investigation of faint stars can be made economic by the use of a photographic method. Considerably less telescope time is required as large numbers of stars are recorded simultaneously and, further, errors are nearly constant until the plate limit is approached. Comparing photographic with photoelectric measures of the same star, Serkowski (1960) attained r.m.s. deviations of ± 0m.020 for photographic measures of stars with m(pg) < 10.

There are two main types of analyser for the measurement of polarization: 1) birefringent crystals, which split the incident light into two beams polarized perpendicularly to each other; 2) polaroid sheet, which transmits only light whose electric vector is vibrating in the preferred direction of transmission of the polaroid. Both have been used in photoelectric polarimeters, with the analyser rotated either continuously or in discrete steps. Absolute photographic measures of polarization have been made with birefringent crystals only – preferably pairs of calcite plates with their principal planes perpendicular (e.g. Serkowski, 1960). At least two images are recorded for each star at a fixed separation; care is required in regions where the star density is high. Photographic measures of polarization using polareid sheet had yielded relative measures only (Tripp, 1956). The principal difficulty is to make the several exposures at different position

angles exactly equal – differences between images due to changes in observing conditions mask the small differences due to polarization.

This thesis describes a new photographic method which is being developed at Edinburgh using a specially designed polaroid filter. This filter allows the simultaneous measurement of the differences between images due to changes in observing conditions, thus enabling the polarization effects to be isolated. The filter is used in the Edinburgh 40/60/150 cm. Schmidt telescope; the fine optical properties of this type of system reduce overlapping in regions of high star density.

Since three exposures are required on each polarization plate, the magnitude limit of the polarization plates is approximately one magnitude brighter than the normal plate limit, B~17 in the present case. The limitation on the method is the star density in the region studied; if the density is too high, an unfavourable proportion of the stars are visibly overlapped.

The accuracy so far attained is ± 0m.029, which is comparable with the errors achieved with the largest reflectors observing quasars of about 16th magnitude photoelectrically. The measurement photographically of large numbers of faint stars and a knowledge of the intrinsic accuracy of the method allow significant mean polarizations to be derived, if the spatial distribution of the stars can be derived from other astronomical observations.

The region of the double cluster, h and chi Persei, was chosen to test the method as it contains a large concentration of photoelectric measures of polarization. The new method will be described and magnitudes and polarization

parameters presented for 527 stars brighter than V = 13 in a one degree diameter field containing h and chi Persei. The 16 polarization plates used required two hours of telescope time: a similar set to B = 17 requires about ten hours of telescope time, several thousand stars being recorded in a typical field. For stars of that magnitude, the largest telescopes using photoelectric polarimeters can only observe 3 or 4 stars in ten hours, and then only with an accuracy similar to that of the new photographic method. To complete the polarization program, approximately 50,000 individual measures were required, a task much facilitated by the use of a semi-automatic digital iris photometer. The program required about 200 hours of measurement, and the reductions were carried out by digital computer.

To separate out the spatial star groups, proper motions were available from the literature and photographic UBV photometry of the stars measured for polarization has been carried out.

Another photographic method for the measurement of the polarization of starlight is being developed by Treanor (1968). This ingenious method gives an immediate indication of stars having moderate, or larger, polarization and of the position angle of the polarization.

Before describing the new Edinburgh photographic polarization method, the polarizations derived, the UBV photometry and the mean polarizations derived for the groups of stars along the line of sight to h and chi Persei, the photoelectric observations of the polarization of starlight will be described.

CHAPTER 1.

PHOTOELECTRIC MEASUREMENTS OF THE POLARIZATION OF STARLIGHT.

The interstellar polarization of starlight is produced by asymmetrical dust grains partially aligned by a presumed galactic magnetic field. The work of Neckel (1966) and Fitzgerald (1967) has shown the dust grains to lie in dust clouds 3 to 40 parsecs across, aggregated in larger complexes, concentrated to the galactic plane and lying in the spiral arms. The areas between the clouds and between the spiral arms have a very tenuous component only.

Suppose the light emitted by a distant star is unpolarized. On traversing a dust cloud in the line of sight, the starlight becomes partially polarized. Should other clouds be encountered by the starlight, further polarization will be produced but, since it is improbable that the dust grains in successive clouds are aligned in exactly the same direction, although not impossible, the starlight will become, to some extent, 'depolarized'. The observed interstellar polarization of a distant star is therefore, in general, the result of a series of complex interactions between the starlight and successive clouds of interstellar dust grains.

The determination of the orientation of the dust grains in each dust cloud, from which the configuration of the galactic magnetic field might be deduced, therefore requires knowledge of the positions and dimensions of the dust clouds and observations of stars within and beyond each individual cloud.

Measurements of nearby stars, the light from which has traversed relatively few dust clouds, will give the most effective information on the problems under consideration. For these stars, distances and obscurations must be known from other astronomical observations.

To facilitate such a study, a catalogue of photoelectric observations of the polarization of starlight is being compiled using the facilities of the Elliott 4130 digital computer of the Royal Observatory, Edinburgh. In addition to the data on a star's designation, position and polarization parameters, additional information contained in the catalogues on spectral types, UBV photometry, distance etc. is included, when available, in a standard format 'block' on magnetic tape for each observation of each star. At present, the stars are ordered in equatorial coordinates for the epoch 1900, with different observations of the same star in successive blocks, but it is intended to order the stars in new galactic coordinates, which are more suited to the investigation envisaged. The format of the catalogue is such that new observations can be incorporated in the catalogue by means of a standard Algol program. At present the following catalogues are included in the photoelectric polarization catalogue (PPC):

1) Hiltner (1951) 186 stars,
2) Hiltner (1954) 61 stars,
3) Hiltner (1956) 1259 stars,
4) Smith (1956) 223 stars,
5) Hall (1958) 1455 stars,
6) Behr (1959) 547 stars.

Only those stars in Hiltner (1951) and Hiltner (1954) which are not contained in Hiltner (1956) have been included. From the comprehensive Hall (1958) catalogue, the stars measured by Hall himself have been extracted. There is a total of 3731 observations of 3090 individual stars.

Spectral types are stored as coded six-digit numbers, e.g. the code 115300 refers to a B1.5III star, 200503 to a A0V star with peculiarities, etc. For stars with spectral types, the PPC includes absolute magnitudes and intrinsic colours derived by Fitzgerald (1967) from the Blanco-Fitzgerald catalogue of photoelectric UBV photometry for 17,000 stars, and for stars with UBV colours, new distances have been computed. The position of and position angle of the polarization for each star have been derived in new galactic coordinates.

To deal with the polarization vectors statistically, it is more convenient to use resolved components of the vectors, the Stokes parameters, Q and U, as shown in Fig. 1. If p and θ_o are the amount of polarization and its position angle in some coordinate system, then the corresponding Stokes parameters are $Q = p \cos 2\theta_o$ and $U = p \sin 2\theta_o$. For the star X in Fig. 1, with Stokes parameters Q_X and U_X, the amount of polarization, $p = (Q_X^2 + U_X^2)^{1/2}$, is the distance from the origin, O, and the position angle, $\theta_c = [\arctan(U_X/Q_X)]/2$, is half the angle subtended at the origin, measured anticlockwise from the positive Q-axis.

Of the 3090 individual stars in the PPC, 2497 stars have been measured once only, the remaining 593 stars appear in two or more source catalogues. Comparison of the polarization parameters of the same star in different source

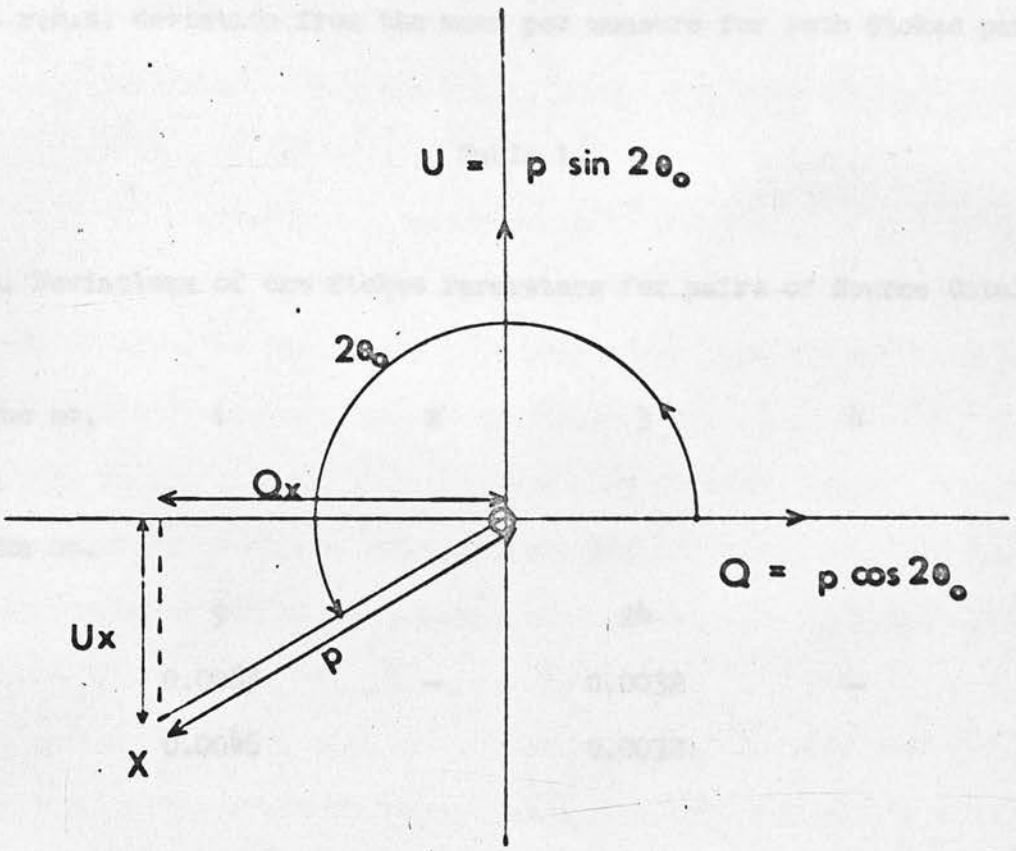

Figure 1. The Stokes parameters, Q and U.
p is the amount of polarization and θ_o the position angle.

catalogues gives an indication of the errors in the measurements. In Table 1 are given, for each pair of source catalogues, the number of stars in common and the r.m.s. deviation from the mean per measure for both Stokes parameters.

Table 1.

R.m.s. Deviations of the Stokes Parameters for pairs of Source Catalogues.

Catalogue no. and Catalogue no.	1	2	3	4	5
	9		24		
4	0.0065	–	0.0032	–	–
	0.0046		0.0032		
	77	10	350	79	
5	0.0046	0.0026	0.0048	0.0049	–
	0.0036	0.0039	0.0044	0.0050	
	9	2	15	1	114
6	0.0022	0.0017	0.0033	0.0095	0.0022
	0.0016	0.0020	0.0021	0.0069	0.0024

For catalogue pairs with more than ten stars in common, the r.m.s. deviation in p ranges from ± 0m.003 for Hall (1958) and Behr (1959) to ± 0m.007 for Smith (1956) and Hall (1958). The error in θ depends on the value for p: for Smith (1956) and Hall (1958), if p = 0m.100 then the r.m.s. deviation in θ is $\pm 4^{\circ}$ and if p = 0m.020, it is $\pm 19^{\circ}$; for Hall (1958) and Behr (1959), the corresponding values are $\pm 2^{\circ}$ and $\pm 9^{\circ}$.

Most of the stars in the PPC have V magnitudes, except for 111 variable stars with no given magnitude and some magnitudes from the BD or HD catalogues. The numbers of stars in half magnitude intervals are shown in Fig. 2. There is a steep drop in the numbers at V = 10 and only 39 stars fainter than V = 11. Over the whole sky there are approximately 900,000 stars brighter than V = 11. The distribution of the stars measured photographically in h and chi Persei in the present investigation is also shown in Fig. 2.

The numbers of stars with amounts of polarization in 0m.005 intervals are shown in Fig. 3. There are 12 stars with p > 0m.150, 220 with p > 0m.100 and 1080, or 29 percent, with p < 0m.010. Except for Behr's catalogue, luminous stars at great distances were selected for measurement.

The numbers of stars in 5° intervals of position angle, in galactic coordinates, are shown in Fig.4. There are 401 stars with polarization so small that no position angle could be measured. The tendency for the polarization vectors to be aligned parallel to the galactic plane is evident, and the distribution is closely symmetrical about the galactic plane.

In order to give an overall impression of the observed polarization vectors on the sky, the celestial sphere in galactic coordinates has been

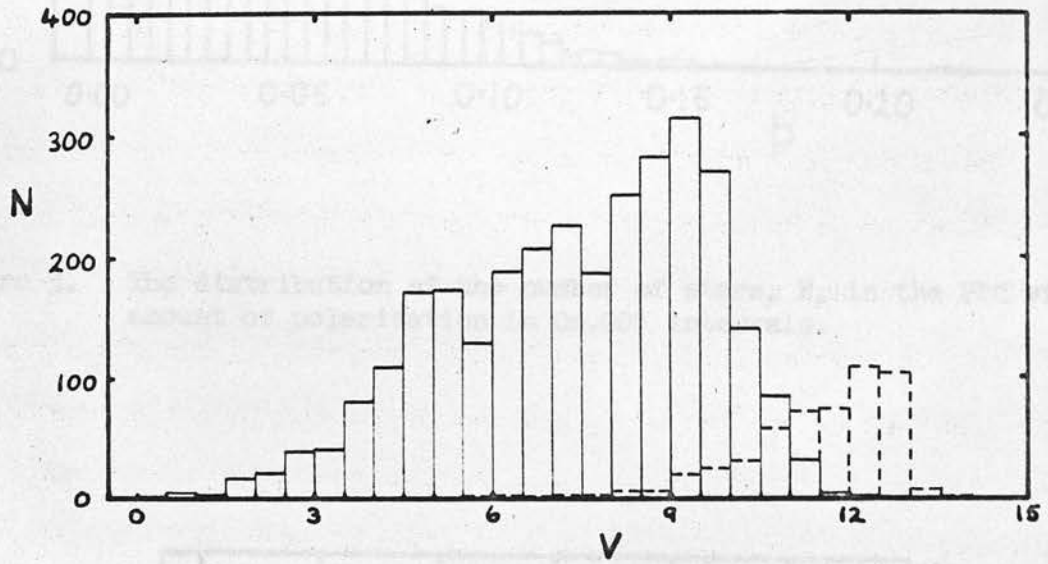

Figure 2. The distribution of the number of stars, N, in the PPC with V magnitudes, in half magnitude intervals.
The magnitude distribution of the stars measured photographically in this thesis is shown by the dashed histogram.

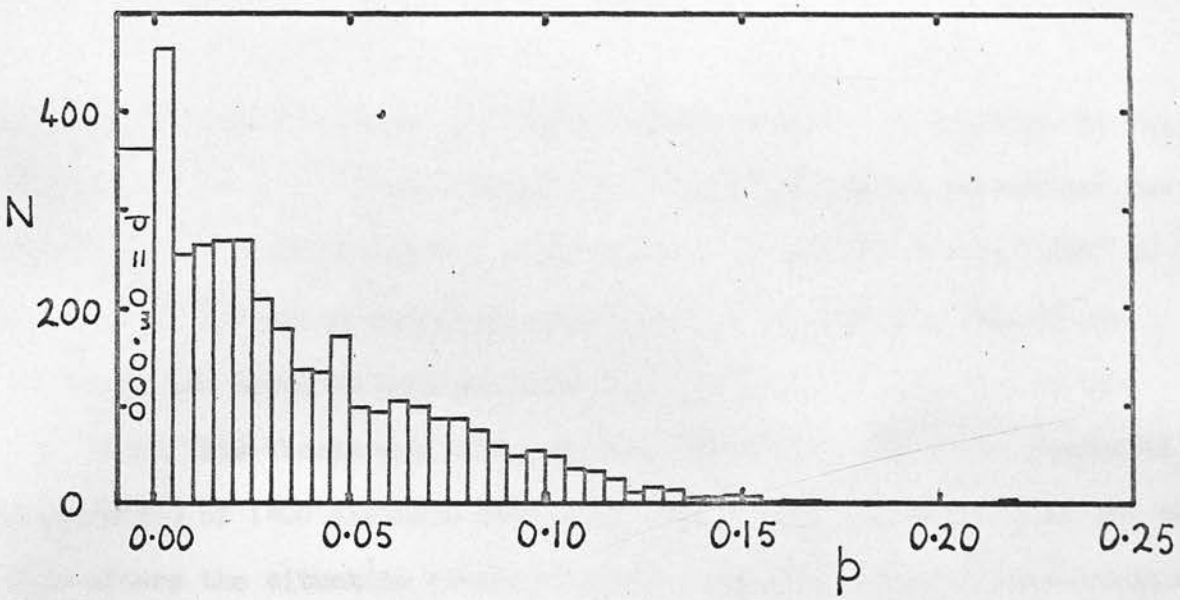

Figure 3. The distribution of the number of stars, N, in the PPC with amount of polarization in 0m.005 intervals.

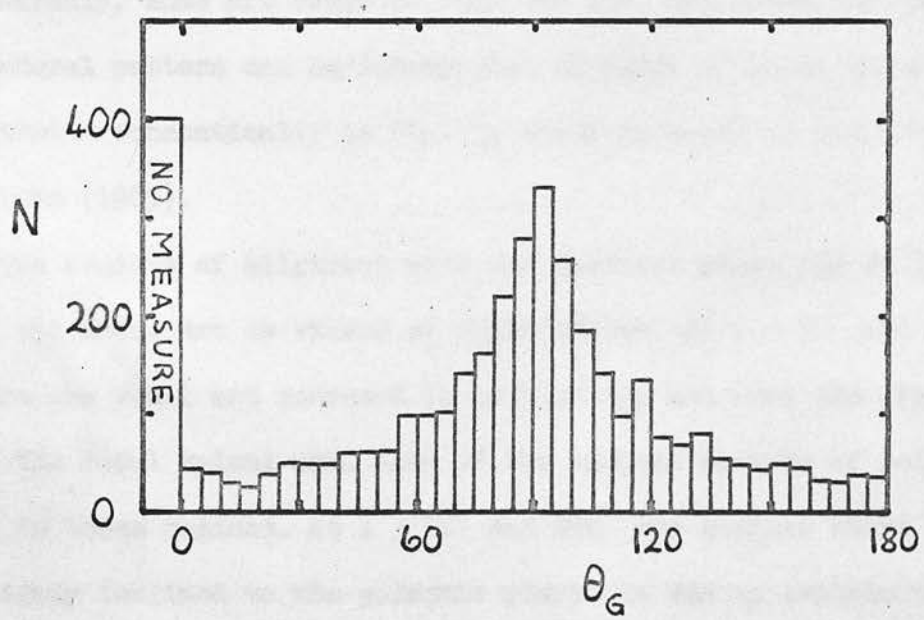

Figure 4. The distribution of the number of stars, N, with position angle, θ_G, in 5° intervals. The position angle is in new galactic coordinates.

divided into 410 areas. The number of stars in each area is given in Fig. 5. The concentration of observed stars to the galactic plane is evident, as is the scarcity of observations in the galactic longitude interval 240° to 350° – the part of the sky observed from the southern hemisphere. 82, or one fifth, of the areas contain no stars and a further 68 only one or two.

While this thesis was being written, Mathewson (1968) has announced the measurement of 1400 southern hemisphere stars, most of them within 500 parsecs. This alters the situation described above, and, combining his new measures with northern hemisphere measures, Mathewson has obtained strong evidence that the helical configuration of the galactic magnetic field is correct.

Using the Stokes parameters, the mean polarization vectors have been derived for all the stars in each of the 410 areas with stars present, and these are shown in Fig. 6. The weights of the individual vectors vary considerably, some are based on only one star and others on approximately 100. The general pattern can be interpreted in terms of local galactic structure, illustrated schematically in Fig. 7, which is based on the diagrams given by Sharpless (1965).

The regions of alignment with the galactic plane lie at $l = 140^\circ$ and 320°, where the local arm is viewed at right angles. At $l = 60^\circ$ and 220°, the mean vectors are small and confused in orientation and here the line of sight lies along the local spiral arm. Some of the largest amounts of polarization are found in these regions. At $l = 10^\circ$ and 260° are regions where the mean vectors are highly inclined to the galactic plane. It was to explain this remarkable appearance that the helical model of the galactic magnetic field was

1 8 0	1 7 0	1 6 0	1 5 0	1 4 0	1 3 0	1 2 0	1 1 0	1 0 0	9 0	8 0	7 0	6 0	5 0	4 0	3 0	2 0	1 0	0	L(2) B(2)
10																		×	90/ 80
×			12			×			12			×			15			×	80/ 60
×			20			×			16			×			24			×	60/ 40
×		9	×		6	×		6	×		5	×		7	×		11	×	40/ 20
×	5	8	3	3	1	1	2	5	6	6	7	16	10	3	3	7	3	3×	20/ 10
×	1	1	1	5	2	2	2	17	9	3	6	6	8	2	3	0	1	7×	10/ 6
×	8	5	5	10	6	4	14	20	9	14	22	10	9	3	0	0	6	3×	6/ 3
×	11	8	2	24	40	53	21	18	7	21	102	12	4	5	1	4	33	1×	3/ 1
×	11	6	1	5	30	39	21	9	1	14	34	9	6	2	0	3	27	16×	1/ 0
×	9	3	1	6	20	27	28	40	8	10	10	8	6	3	2	6	41	32×	0/ -1
×	11	8	4	3	76	41	27	65	14	10	9	7	5	2	3	8	49	38×	-1/ -3
×	3	4	7	8	97	22	17	13	8	9	9	4	5	0	3	6	13	3×	-3/ -6
×	5	1	4	17	13	11	9	6	4	9	5	2	1	7	0	3	7	3×	-6/-10
×	8	15	9	10	12	18	9	12	13	3	6	3	4	2	7	4	9	0×	-10/-20
×		31	×		17	×		14	×		15	×		2	×		1	×	-20/-40
×			10			×			15			×			4			×	-40/-60
×			1			×			1			×			0			×	-60/-80
1																		×	-80/-90

Figure 5. The number of stars in each of the 410 areas of sky. The galactic longitude boundaries of some of the areas are indicated by ×.

L(2)	360	350	340	330	320	310	300	290	280	270	260	250	240	230	220	210	200	190	180
B(2)																			
90/ 80	×																		10
80/ 60	×			8			×			10			×			15			×
60/ 40	×			8			×			10			×			20			×
40/ 20	×		18	×		1	×		0	×		3	×		9	×		12	×
20/ 10		11	0	0	0	0	0	0	0	0	0	1	1	1	1	6	1	4	5	3×
10/ 6		1	1	0	0	0	0	0	0	0	0	0	0	1	1	1	2	0	2	2×
6/ 3		3	3	0	0	1	1	0	0	0	1	1	0	2	2	3	3	6	18×
3/ 1		6	7	2	0	3	18	3	2	0	1	0	4	3	4	3	9	4	10×
1/ 0		3	1	0	1	3	3	7	17	0	4	0	2	2	1	6	7	7	13×
0/ -1		8	0	1	4	1	9	2	7	4	0	0	3	2	4	7	11	6	4×
-1/ -3		10	0	6	3	0	5	4	1	9	0	3	3	4	14	6	26	13	12×
-3/ -6		4	0	0	0	1	0	0	0	2	1	0	10	4	4	5	4	4	13×
-6/-10		1	0	0	0	0	0	0	0	0	0	0	3	4	7	8	3	5	6×
-10/-20		0	0	0	0	0	0	0	0	0	0	0	0	3	5	11	57	14	6×
-20/-40	×		0	×		0	×		0	×		0	×		11	×		36	×
-40/-60	×			0			×			0			×			2			×
-60/-80	×			0			×			0			×			1			×
-80/-90	×																		1

Figure 5 (cont.).

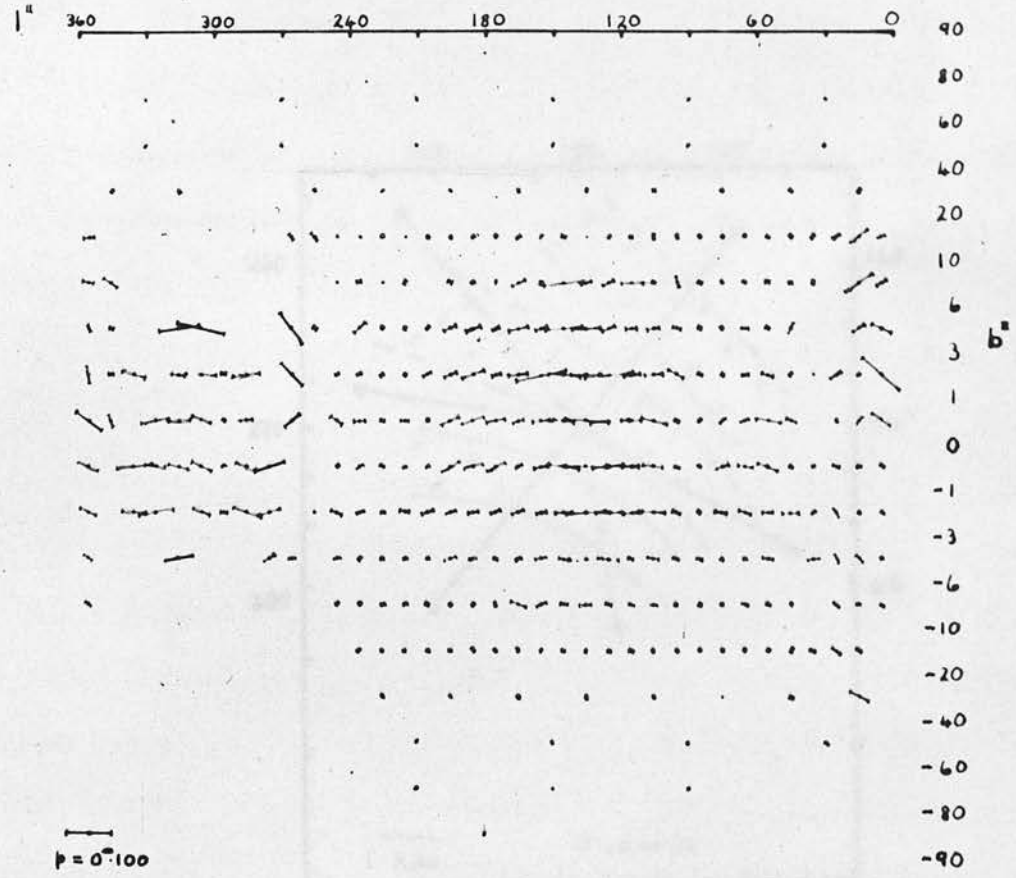

Figure 6. The mean polarization vectors in the 410 areas of sky.

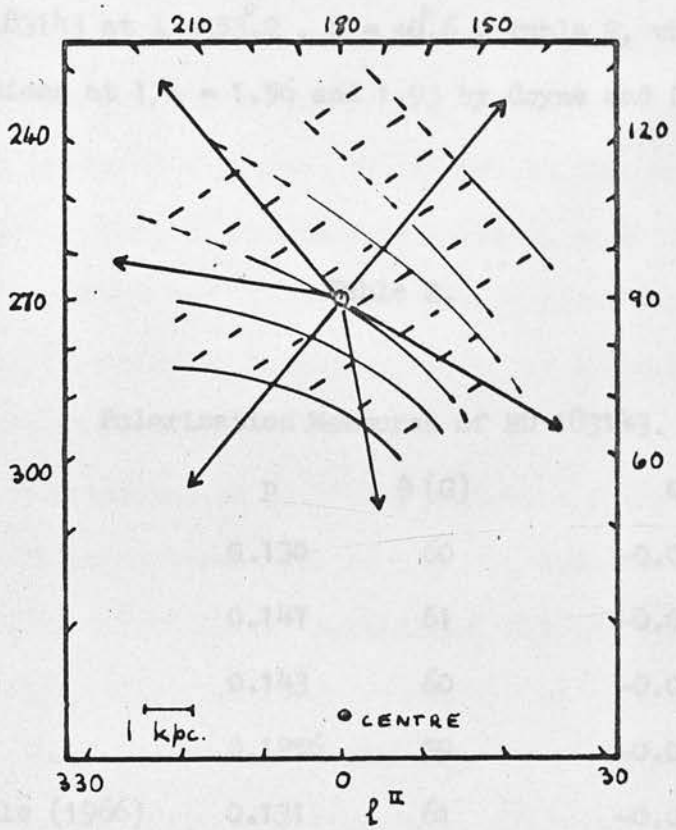

Figure 7. Schematic galactic structure near the sun. The estimated positions of the spiral arms are shown shaded.

introduced. These are just the regions where there were few observations until the work of Mathewson (1968).

There is one star in the PPC which has been measured by all four observers, HD 183143 at $l = 53^{\circ}.2$, $b = +0^{\circ}.6$, Table 2, where the mean values of the observations at $1/\lambda = 1.56$ and 1.93 by Coyne and Gehrels (1966) have been added.

Table 2.

Polarization Measures of HD 183143.

Source	p	θ (G)	Q	U
Hiltner (1956)	0.130	60	−0.0650	0.1126
Smith (1956)	0.147	61	−0.0779	0.1247
Hall (1958)	0.143	60	−0.0715	0.1239
Behr (1959)	0.1256	59	−0.0589	0.1109
Coyne and Gehrels (1966)	0.131	61	−0.0694	0.1111

Comparing half the differences in the Stokes parameters between pairs of catalogues with the r.m.s. deviations given in Table 1, it is found, e.g. for Hall (1958) and Behr (1959), the actual half difference, 0m.0065, is 3 times the r.m.s. deviation. The observations are all approximately in the V waveband. This situation, where the differences between measures of one star by different observers differ by several times the quoted errors, is quite common in interstellar polarization measurements.

The cause is as yet unknown but it may be one of several possibilities, or a combination of some of these. Stars are known with intrinsic variable polarization (Serkowski, 1966), and with circumstellar dust clouds (Reddish, 1967), which may be subjected to magnetic disturbances on the star. Events, such as nova explosions, may cause the configuration of the magnetic field to change. As dust grains of different sizes realign themselves to the new field at different rates, a continuously changing mean alignment of the dust grains will arise. There may be larger scale magnetic field changes at present unknown. Instrumental polarization in the observing system may also contribute to the differences.

Many more observations of all these phenomena are required.

The PPC contains distances for 1833 stars. Some of these, from Behr's catalogue, are from trigonometric parallaxes, but the majority are derived from UBV photometry, colour excesses and estimates of absolute magnitudes. Uncertainties in these distances of the order of a factor of two may occur.

For five galactic longitude ranges with the greatest concentrations of stars, the polarization parameters for all stars with distance estimates have been plotted in the following manner. Let X, Y and Z be distance galactic coordinates in parsecs, with X towards the galactic centre, Y towards $l = 90^{\circ}$, $b = 0^{\circ}$ and Z towards $b = +90^{\circ}$. The distance, D, to the star projected onto the galactic plane, $D = (X^2 + Y^2)^{1/2}$, and Z are used as coordinates for the position of each star and the polarization vector is drawn at 90° to the actual line of sight. As one passes from right to left in the diagrams which follow, the polarization vectors of more and more distant stars are seen.

The galactic longitude intervals illustrated in Fig. 8 are:

8a) $358.0 < l < 5.0$, 49 stars towards the galactic centre,

8b) $76.0 < l < 78.0$, 48 stars towards Cygnus,

8c) $102.0 < l < 105.0$, 45 stars towards Cepheus and Lacerta,

8d) $134.0 < l < 135.0$, 55 stars towards Cassiopeia and Perseus,

8e) $204.0 < l < 210.0$, 46 stars towards Monoceros and Orion.

The observed polarizations are discussed with reference to Fig. 7. In Fig. 8a, the polarization vectors are inclined to the galactic plane and the polarization is stronger above the plane. Stars at the outer edge of the inner arm, at 800 parsecs, are nearly as polarized as those beyond 2 kiloparsecs. In Fig. 8b, the line of sight is along the local arm and the vectors are confused. In Fig. 8c, the outer, Perseus, arm is viewed, apparently through a 'window' in the local arm, where the amount of polarization is small. In Fig. 8d, the local arm is viewed at right angles and the Perseus arm is at its nearest. However, the polarization observed within 1 kiloparsec, i.e. within the local arm, is as large as that observed for stars in the Perseus arm. Hall (1958) in his Fig. 5 had indicated a similar result, suggesting that the polarization observed in this direction is produced within the local arm. Further information on this result will be derived from the observations in this thesis. In Fig. 8e, the line of sight is again along the local arm and the vectors are confused.

Many more polarization observations of stars at known distances are required to complete similar diagrams for all galactic longitudes.

Since 1959 telescopes have been designed and built solely for

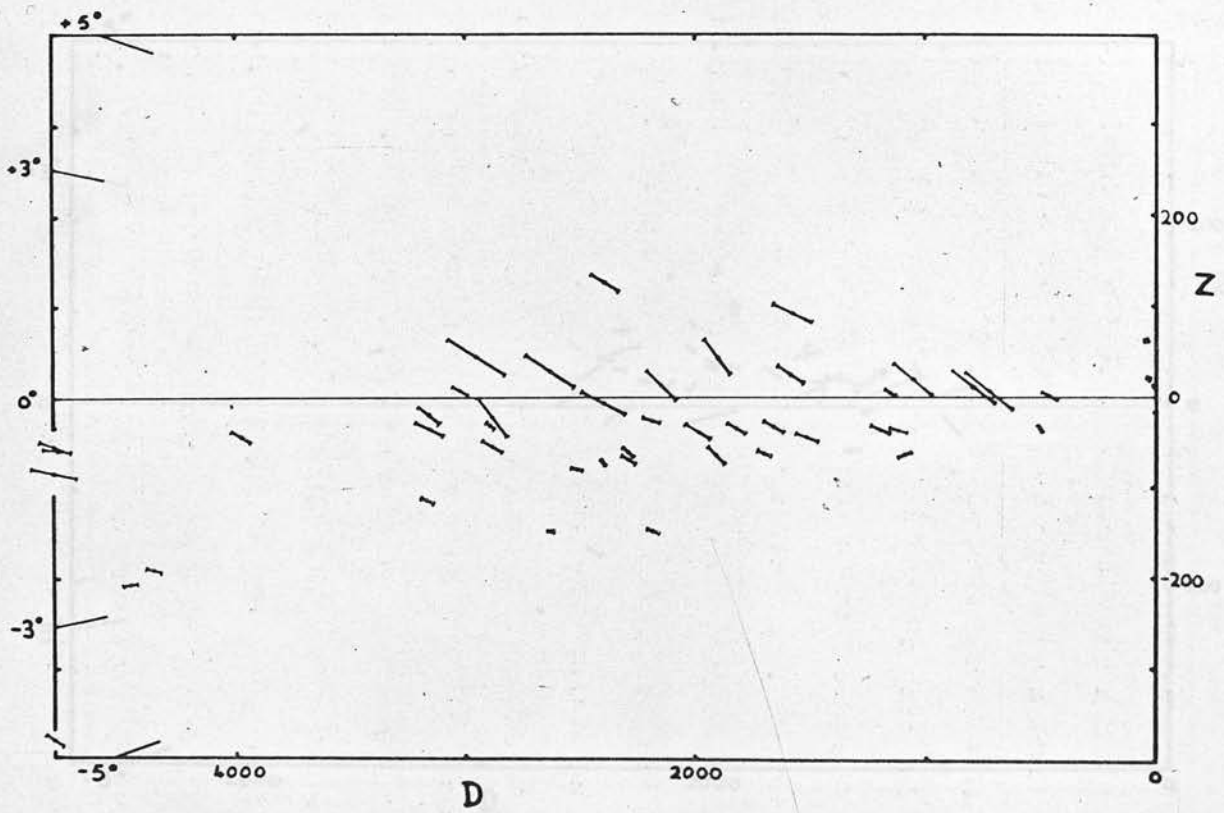

Figure 8a. Stars in $358.0 < l < 5.0$. See text for explanation.

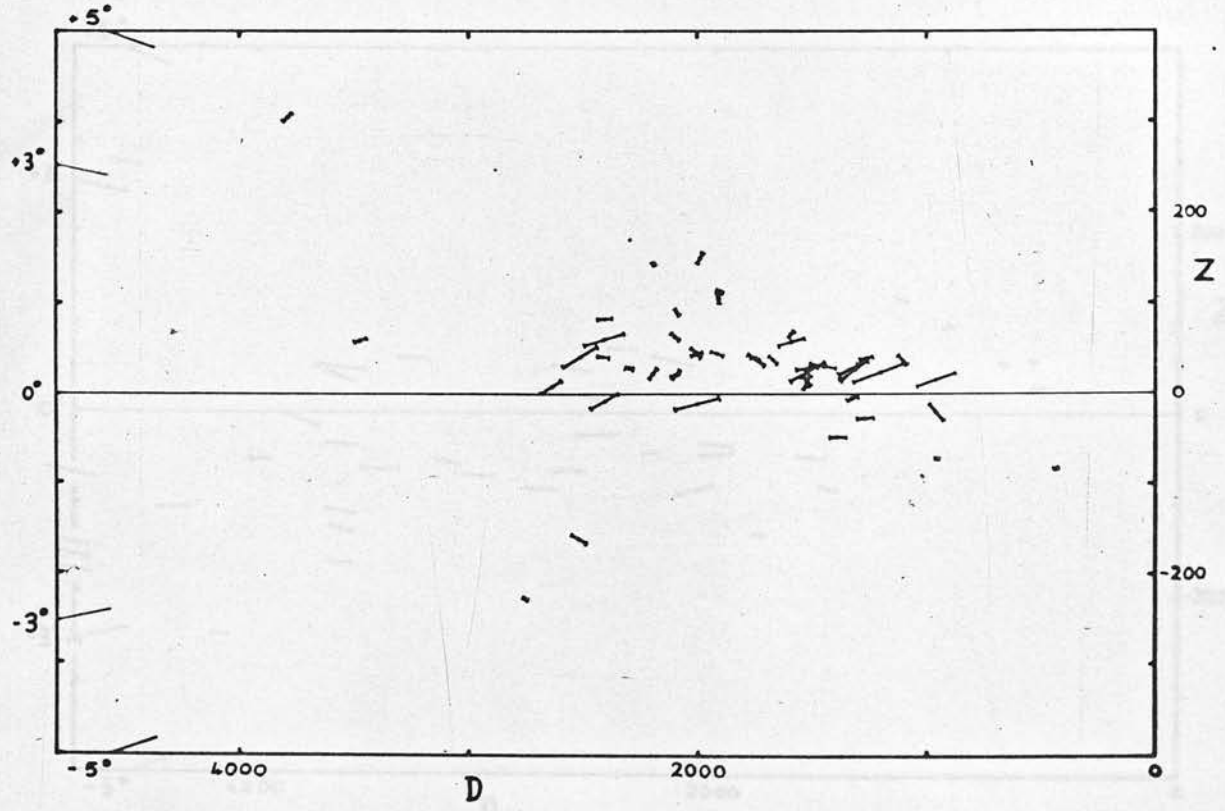

Figure 8b. Stars in $76.0 < l < 78.0$. See text for explanation.

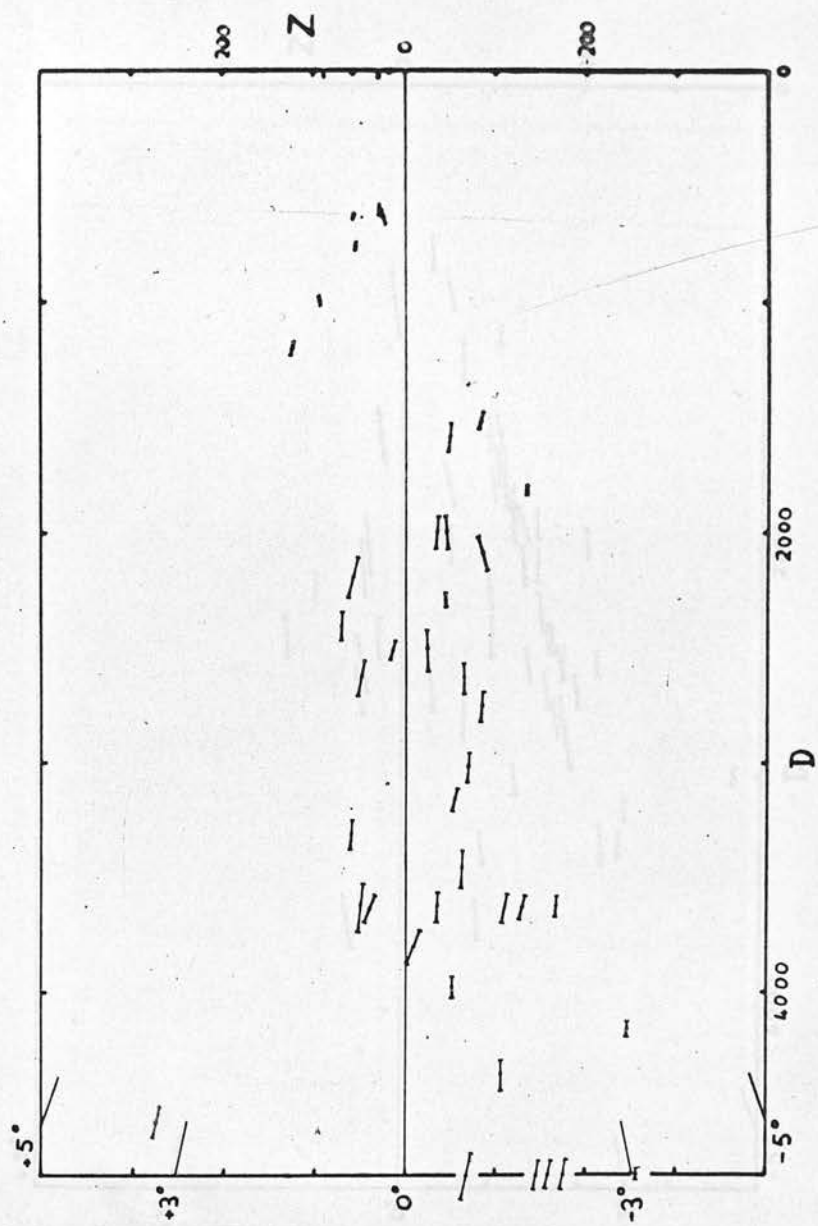

Figure 8c. Stars in $102.0 < l < 105.0$. See text for explanation.

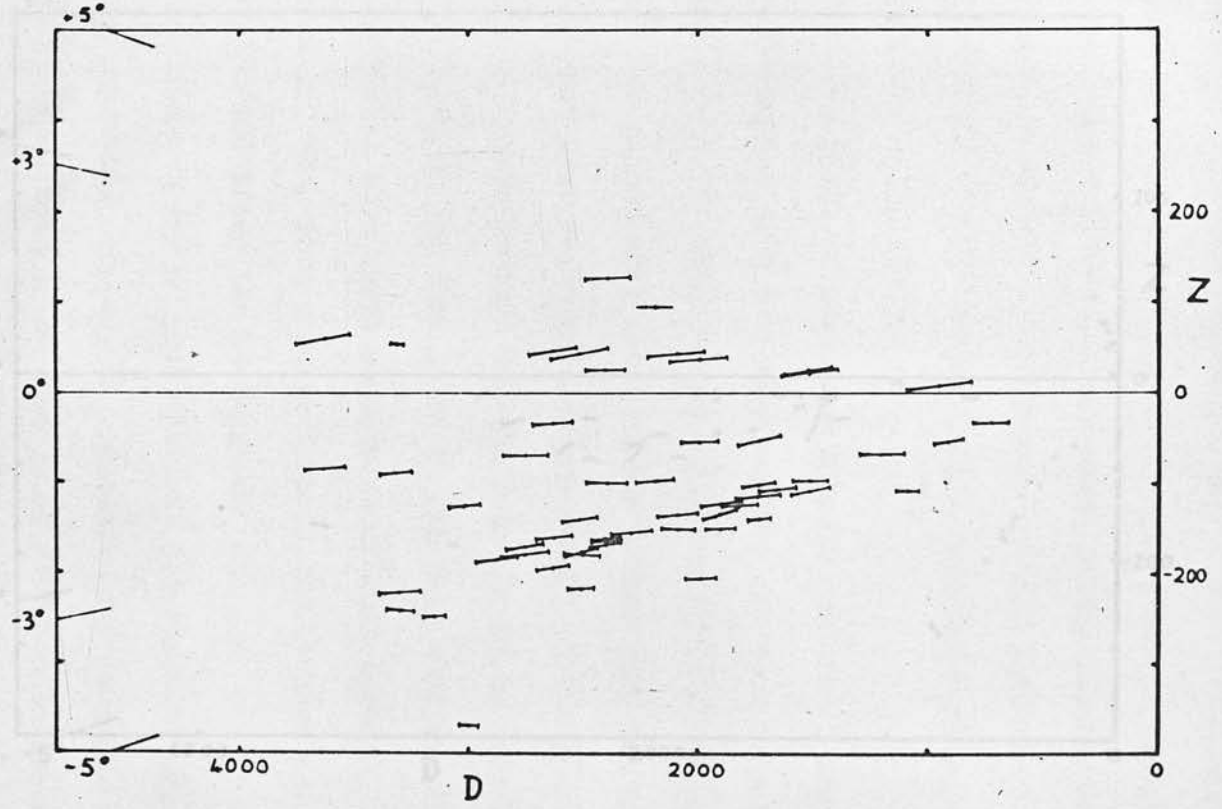

Figure 8d. Stars in 134.0 < l < 135.0. See text for explanation.

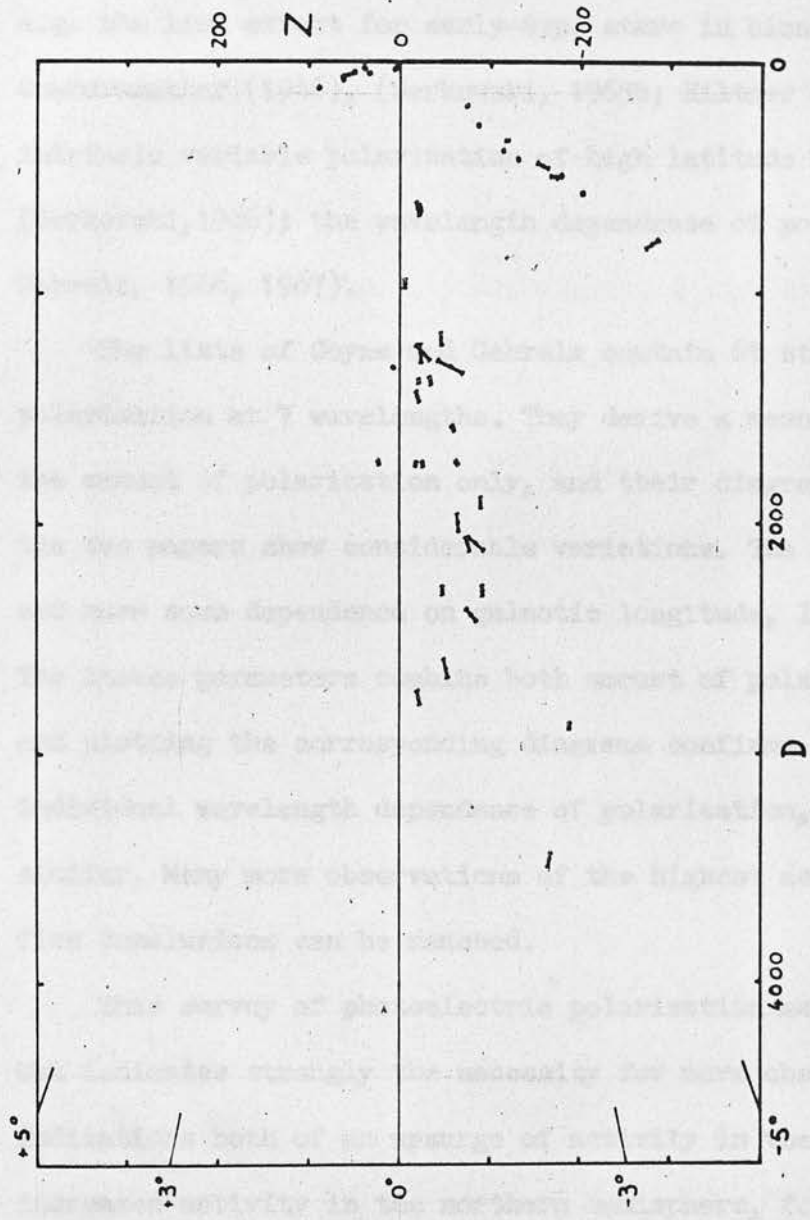

Figure 8e. Stars in $204.0 < l < 210.0$. See text for explanation.

measuring polarization. Most recent photoelectric studies of high accuracy have been concerned with particular characteristics of bright stars, e.g. the limb effect for early-type stars in binary systems, as predicted by Chandrasekhar (1946), (Serkowski, 1965b; Hiltner and Mook, 1966); the intrinsic variable polarization of high latitude Mira-type variables (Serkowski, 1966); the wavelength dependence of polarization (Coyne and Gehrels, 1966, 1967).

The lists of Coyne and Gehrels contain 61 stars with non-variable polarization at 7 wavelengths. They derive a mean wavelength dependence for the amount of polarization only, and their diagrams for individual stars in the two papers show considerable variations. The position angles also vary and have some dependence on galactic longitude, Ireland and others (1966). The Stokes parameters combine both amount of polarization and position angle and plotting the corresponding diagrams confirms that each star has an individual wavelength dependence of polarization, although some stars are similar. Many more observations of the highest accuracy are required before firm conclusions can be reached.

This survey of photoelectric polarization measurements has been brief, but indicates strongly the necessity for more observations. There are indications both of an upsurge of activity in the southern hemisphere and of increased activity in the northern hemisphere, for in both 'rotatable' polarization telescopes are available, Hiltner and Schild (1965) and Mathewson (1968). But these observations, for economic reasons, will be largely confined to the brighter stars. A method for systematically surveying

the fainter stars to the faintest possible magnitude limits is required.

This thesis describes a photographic method for use in fast Schmidt telescopes. Several thousand stars to B$\sim$ 17 in a 1 or 2 degree diameter field can be observed in about 10 hours of telescope time. A similar program carried out with a photoelectric polarimeter on a large reflector would require some thousands of hours of telescope time, to the same accuracy for the same number of stars. The present method, therefore, allows investigations which are quite impracticable by any other method at present available.

CHAPTER 2.

THE NEW PHOTOGRAPHIC METHOD.

The polaroid filter is shown in Fig.9a. The dashed lines indicate the direction of preferred transmission of the polaroid. The three outer segments (one indicated by dotted lines) have this direction radial.

The filter is held in the plateholder of the Edinburgh 40/60/150 cm. Schmidt telescope 11 mm. above the centre of the plate in a mounting which can be rotated into three locations separated by 120°. The three positions of the filter are shown in Figs. 9a, 9b and 9c. An exposure is taken at each position of the filter and the three images of each star are separated by small displacements of the telescope in right ascension between exposures.

For the outer segments, the effect of the rotations is to replace each segment with another similar one: the three images for each star then differ only because of variations in exposure time, seeing and transparency conditions, guiding etc. – the resolved component of any intrinsic polarization of the starlight is constant. In the central region, the successive images of the program stars differ also in having the direction of preferred transmission of the polaroid set at three different position angles – any intrinsic polarization of the starlight is resolved into the corresponding components. The differences between the images of the stars in the areas of sky exposed through the outer segments give the corrections to be applied to the measures of the program stars to compensate for variations in

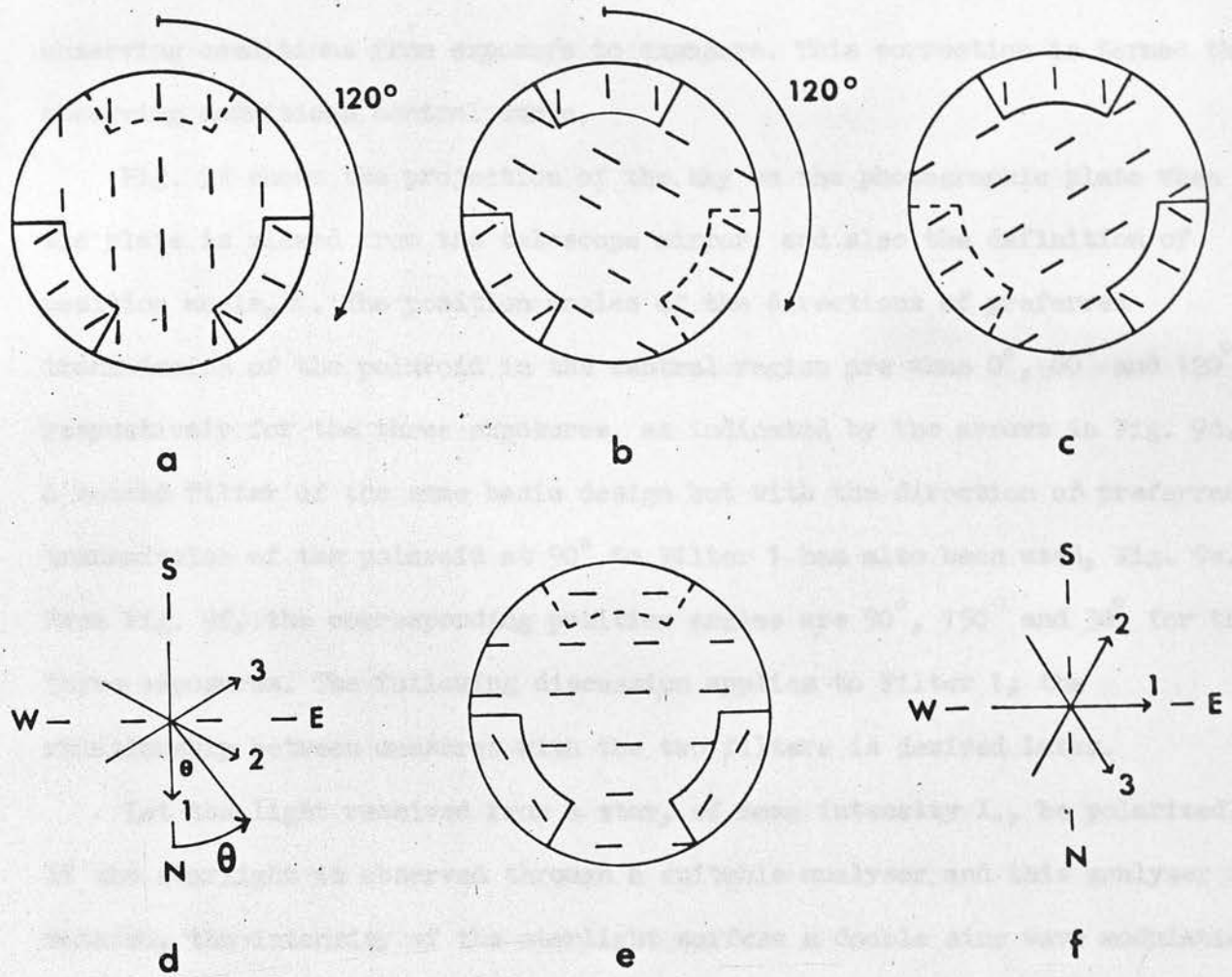

Figure 9. The design and use of the filter.
The direction of preferred transmission of the polaroid shown by dashed lines: a) b) and c) are the three positions of Filter 1, separated by 120°, at which exposures are made; d) shows the projection of the sky on the plate as seen from the telescope mirror, the definition of position angle, θ, and the position angles of the three exposures; e) is the design of Filter 2 and f) gives the corresponding position angles.

observing conditions from exposure to exposure. This correction is termed the observing conditions control curve.

Fig. 9d shows the projection of the sky on the photographic plate when the plate is viewed from the telescope mirror, and also the definition of position angle, θ. The position angles of the directions of preferred transmission of the polaroid in the central region are thus 0°, 60° and 120° respectively for the three exposures, as indicated by the arrows in Fig. 9d. A second filter of the same basic design but with the direction of preferred transmission of the polaroid at 90° to Filter 1 has also been used, Fig. 9e. From Fig. 9f, the corresponding position angles are 90°, 150° and 30° for the three exposures. The following discussion applies to Filter 1; the relationship between measures with the two filters is derived later.

Let the light received from a star, of mean intensity I_o, be polarized. If the starlight is observed through a suitable analyser and this analyser is rotated, the intensity of the starlight suffers a double sine wave modulation.

Let the maximum and minimum intensities be I_X and I_N respectively, and let the position angle of maximum intensity, in the range $0^\circ < \theta < 180^\circ$, be θ_o.

Then

$$I_o = (I_X + I_N)/2. \qquad (1)$$

The degree of polarization, P, is defined by

$$P = (I_X - I_N)/(I_X + I_N). \qquad (2)$$

The intensity when the analyser is at position angle θ, I_θ, is given by

$$I_\theta = I_o + \left[(I_X - I_N) \cos 2(\theta - \theta_o)\right]/2.$$

Dividing both sides by I_o, and using equations (1) and (2),

$$I_\theta / I_o = 1 + P \cos 2(\theta - \theta_o). \qquad (3)$$

The difference in magnitude, m, between two intensities I_1 and I_2 is defined by

$$m = -2.5 \log_{10} (I_1/I_2). \qquad (4)$$

The amount of polarization of starlight in magnitudes, p, is defined by

$$p = -2.5 \log_{10} (I_N/I_X). \qquad (5)$$

From equation (3),

$I_\theta = I_X$ when $\theta = \theta_o$, so $I_X/I_o = 1 + P$

and $I_\theta = I_N$ when $\theta = \theta_o \pm 90^\circ$, so $I_N/I_o = 1 - P$.

Hence, from equation (5),

$$p = +2.5 \log (1 + P)/(1 - P). \qquad (6)$$

Magnitude differences, δm_1, δm_2 and δm_3, corresponding to intensities I_1, I_2 and I_3 at position angles 0°, 60° and 120° respectively, from the magnitude corresponding to I_o, (see also below) are given by

$$-\delta m_1 = 2.5 \log (I_1/I_o) = 2.5 \log [1 + P \cos 2(0^\circ - \theta_o)], \qquad (7)$$

etc., from equations (4) and (3).

Rearranging these equations,

$$\cos 2\theta_o = (10^{-\delta m_1/2.5} - 1)/P, \qquad (8)$$

$$\left.\begin{aligned} &\cos 2(60^\circ - \theta_o) = (10^{-\delta m_2/2.5} - 1)/P, \\ \text{and} \quad &\cos 2(120^\circ - \theta_o) = (10^{-\delta m_3/2.5} - 1)/P. \end{aligned}\right\} \qquad (9)$$

Expanding the left hand sides of the equations (9), inserting numerical values and subtracting,

$$\sqrt{3} \sin 2\theta_o = (10^{-\delta m_2/2.5} - 10^{-\delta m_3/2.5})/P. \qquad (10)$$

Since $\cos^2 \times + \sin^2 \times = 1$, from equations (8) and (10),

$$P = [(10^{-\delta m_1/2.5} - 1)^2 + (10^{-\delta m_2/2.5} - 10^{-\delta m_3/2.5})^2/3]^{1/2}. \quad (11)$$

Also from equations (8) and (11),

$$\sin 2\theta_o/\cos 2\theta = \tan 2\theta_o$$
$$= (10^{-\delta m_2/2.5} - 10^{-\delta m_3/2.5})/[\sqrt{3}(10^{-\delta m_1/2.5} - 1)] \quad (12)$$

The amount of polarization, p, is obtained from equations (11) and (6) and the position angle of the polarization, θ_o, from equation (12).

The relationship between filters is now derived. For the magnitude differences δm_4, δm_5 and δm_6, corresponding to intensities I_4, I_5 and I_6 at position angles 90°, 150° and 30°, obtained with Filter 2, there is a set of equations analogous to the equations (7) for Filter 1. Expanding the right hand side of the first of these equations and inserting numerical values,

$$-\delta m_4 = 2.5 \log [1 - P \cos 2\theta_o]$$
$$= 2.5 \log [2 - (1 + P \cos 2\theta_o)]$$
$$= 2.5 \log [2 - 10^{-\delta m_1/2.5}],$$

from equation (7).

Hence inverting,

$$-\delta m_1 = 2.5 \log [2 - 10^{-\delta m_4/2.5}] \quad (13)$$

and similarly for δm_2 and δm_5, and for δm_3 and δm_6.

Observations using Filter 2, transformed by such equations, can be directly combined with observations using Filter 1.

The magnitude differences, δm_i, used above are relative to a magnitude, m_o, corresponding to the mean intensity, I_o. Let the magnitudes of the three images of a star (corrected by the Observing Conditions Control Curve) be m_i,

m_2 and m_3. The mean magnitude is $\bar{m} = \sum_{i=1}^{3} m_i/3$. The measured magnitude differences are of the form $dm_i = m_i - \bar{m}$. Then $\sum_{i=1}^{3} dm_i = 0$. Since the magnitude scale is logarithmic, $\bar{m} \neq m_o$ unless $p = 0$.

From equations (7) above,

$$-\sum_{i=1}^{3} \delta m_i = 2.5 \log\left\{1 - P^2 [3 - P \cos 2\theta_o (1 - 4 \sin^2 2\theta_o)]/4\right\} \quad (14)$$

$$= 3C, \text{ say, where } C = \bar{m} - m_o.$$

Thus $-\delta m_i = -dm_i + C$, $i = 1,2,3$. The correction term, C, is shown in Fig. 10.

The following method has been used to estimate C from the measured magnitude differences. From equations (7),

$$\sum_{i=1}^{3} |\delta m_i| \simeq 2.5 \log [1 + PZ],$$

where $Z = |\cos 2\theta_o| + |-\frac{1}{2}\cos 2\theta_o + \frac{\sqrt{3}}{2} \sin 2\theta_o| + |-\frac{1}{2}\cos 2\theta_o - \frac{\sqrt{3}}{2} \sin 2\theta_o|$ neglecting P^2 and higher terms. This expression has maximum values at $\theta_o = 0^\circ + n \times 30^\circ$, $n = 0$ to 5 when $\sum_{i=1}^{3} |\delta m_i| = p$, and minimum values at $\theta_o = 15^\circ + n \times 30^\circ$, $n = 0$ to 5 when

$$\sum_{i=1}^{3} |\delta m_i| = p\,[\log (1 + 1.732\, P/\log (1 + 2P)]$$

and so, for $p = 0.10$, $\sum_{i=1}^{3} |\delta m_i| = 0.87\ p$. Thus $\sum_{i=1}^{3} |dm_i| \leq p$, to within 13 percent. Equation (6) can be written in the approximate form $p = 2.5 \times \log e \times 2P = P/0.4605$, from which P is determined to within 1 percent. C, in equation (14), is nearly independent of θ_o. If θ_o is set equal to 0°, equation (14) becomes $3C = 2.5 \log [1 - P^2(3 - P)/4]$ to within 5 percent. The total error in this estimate of C is 13 percent. When $p = 0.130$, $C = 0.001$, so that the error introduced by the approximations is negligible.

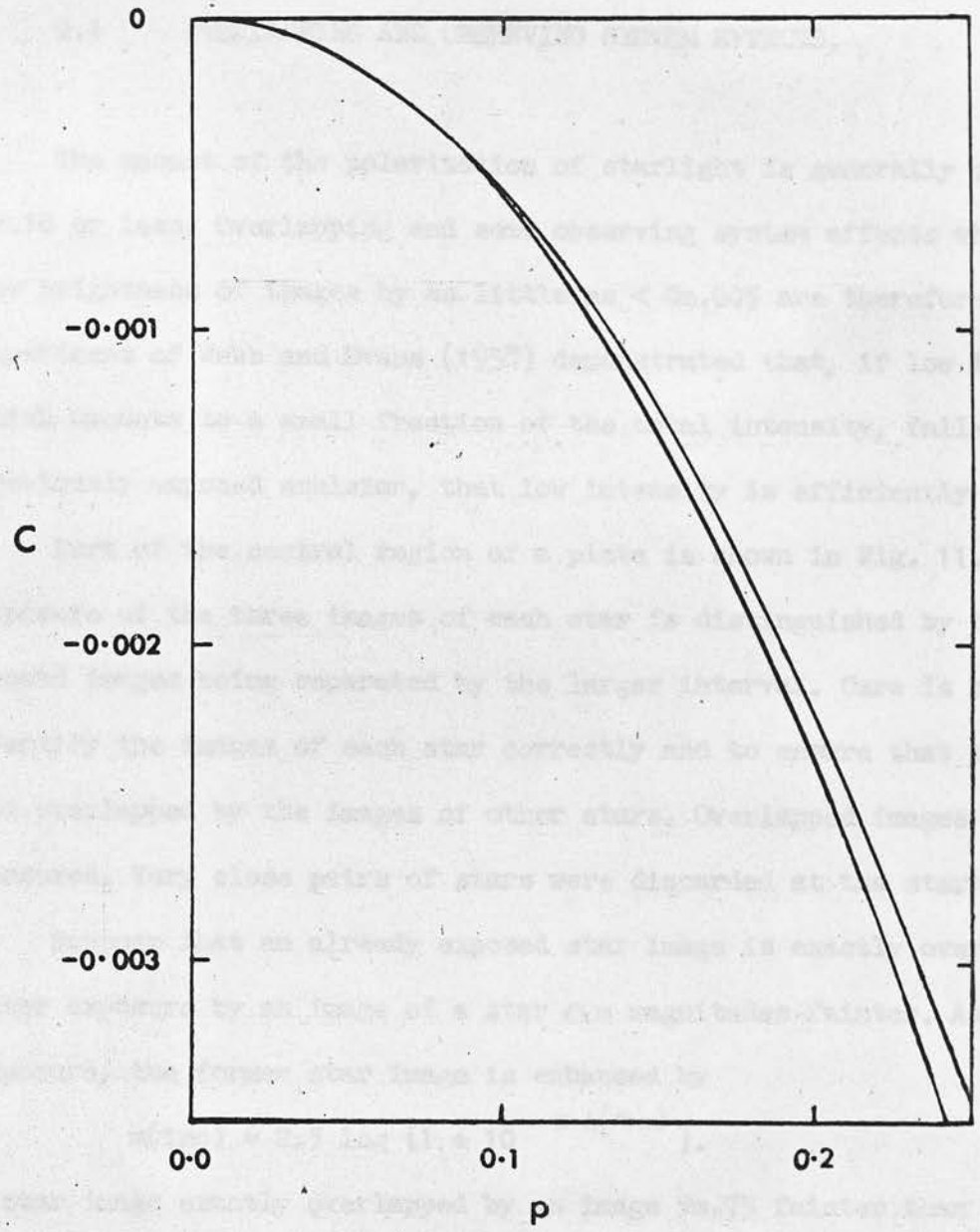

Figure 10. The correction term, C, against amount of polarization, p, from equation (14).

The extreme values are shown, maximum when $\theta_o = 0°$, 60° and 120° and minimum when $\theta_o = 30°$, 90° and 150°.

2.1 OVERLAPPING AND OBSERVING SYSTEM EFFECTS.

The amount of the polarization of starlight is generally of the order of 0m.10 or less. Overlapping and some observing system effects which can alter the brightness of images by as little as < 0m.005 are therefore important. The experiment of Webb and Evans (1938) demonstrated that, if low intensity light, which amounts to a small fraction of the total intensity, falls on an area of previously exposed emulsion, that low intensity is efficiently recorded.

Part of the central region of a plate is shown in Fig. 11. The order of exposure of the three images of each star is distinguished by the first and second images being separated by the larger interval. Care is required to identify the images of each star correctly and to ensure that these images are not overlapped by the images of other stars. Overlapped images were not measured. Very close pairs of stars were discarded at the start of the program.

Suppose that an already exposed star image is exactly overlapped in a later exposure by an image of a star Δm magnitudes fainter. As it is a post-exposure, the former star image is enhanced by

$$m(\text{inc}) = 2.5 \log [1 + 10^{-0.4(\Delta m)}]. \qquad (15)$$

A star image exactly overlapped by an image 5m.75 fainter than itself is enhanced by 0m.005. This is the maximum effect – the enhancement will be reduced in non-exact overlaps.

Care was taken during measurement to avoid bright overlaps, but the identification of all the images of faint stars is extremely difficult, especially in crowded regions. It follows from the Webb and Evans experiment

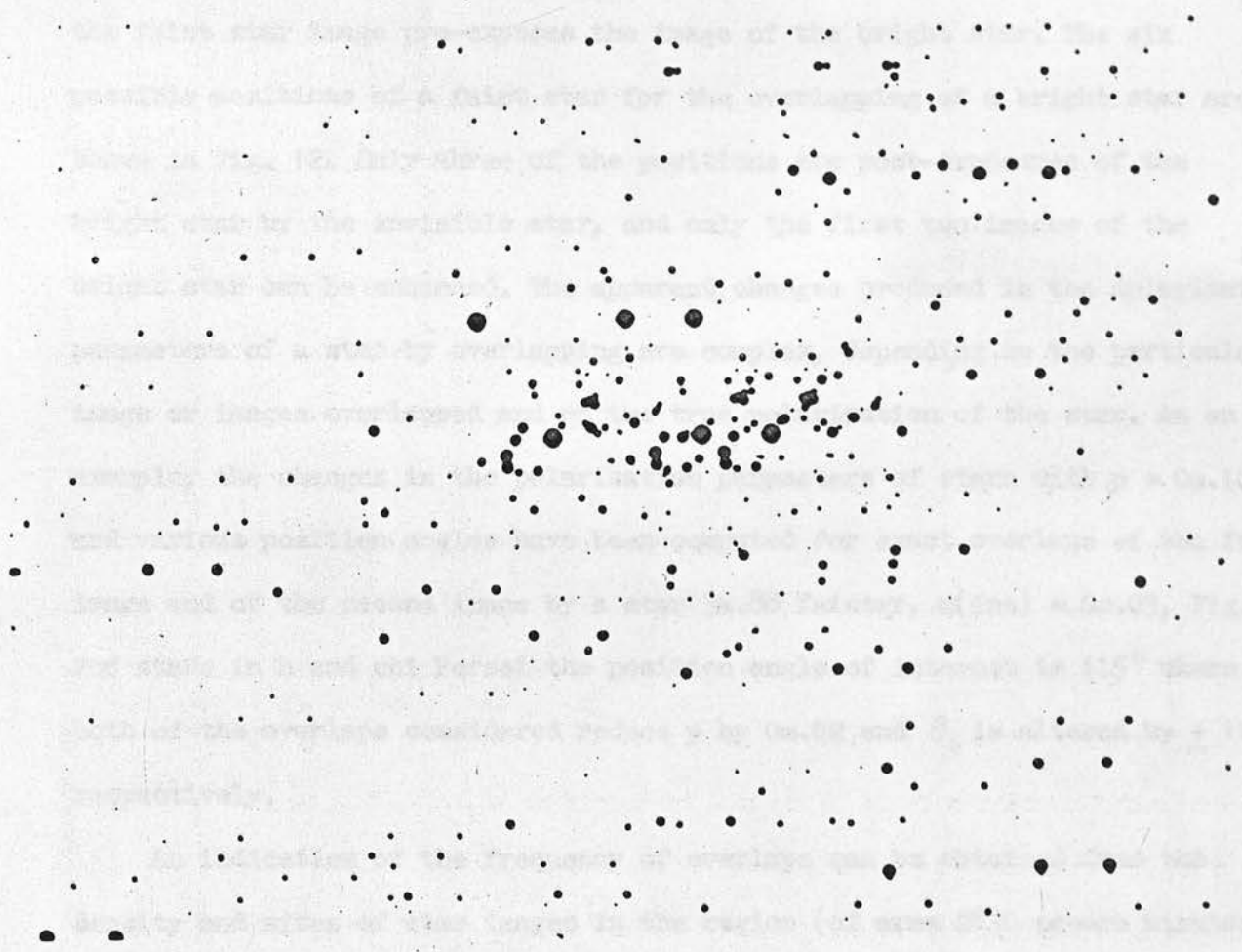

Figure 11. Part of the central region of a polarization plate, showing the three images for each star and overlapping.

that overlapping by stars fainter than the plate limit can only be ignored if the faint star image pre-exposes the image of the bright star. The six possible positions of a faint star for the overlapping of a bright star are shown in Fig. 12. Only three of the positions are post-exposures of the bright star by the invisible star, and only the first two images of the bright star can be enhanced. The apparent changes produced in the polarization parameters of a star by overlapping are complex, depending on the particular image or images overlapped and on the true polarization of the star. As an example, the changes in the polarization parameters of stars with p = 0m.10 and various position angles have been computed for exact overlaps of the first image and of the second image by a star 3m.88 fainter, m(inc) = 0m.03, Fig. 13. For stars in h and chi Persei the position angle of interest is 115° where both of the overlaps considered reduce p by 0m.02 and θ_0 is altered by $\pm$ 11° respectively.

An indication of the frequency of overlaps can be obtained from the density and sizes of star images in the region (of area 2830 square minutes of arc) containing the program stars. Not all stars brighter than V = 13 have been measured – accurate magnitudes for the stars were not available when the program stars were selected. It is unlikely that any stars brighter than V = 12 were omitted, apart from 42 stars which were members of close pairs. Together with the 308 stars measured, there are 350 stars brighter than V = 12 in the region. The numbers of stars to magnitude limits brighter than this, derived from the measured stars, are given in column 2 of Table 3. Allen (1963, p.234) lists the numbers of stars to various V magnitude limits. The

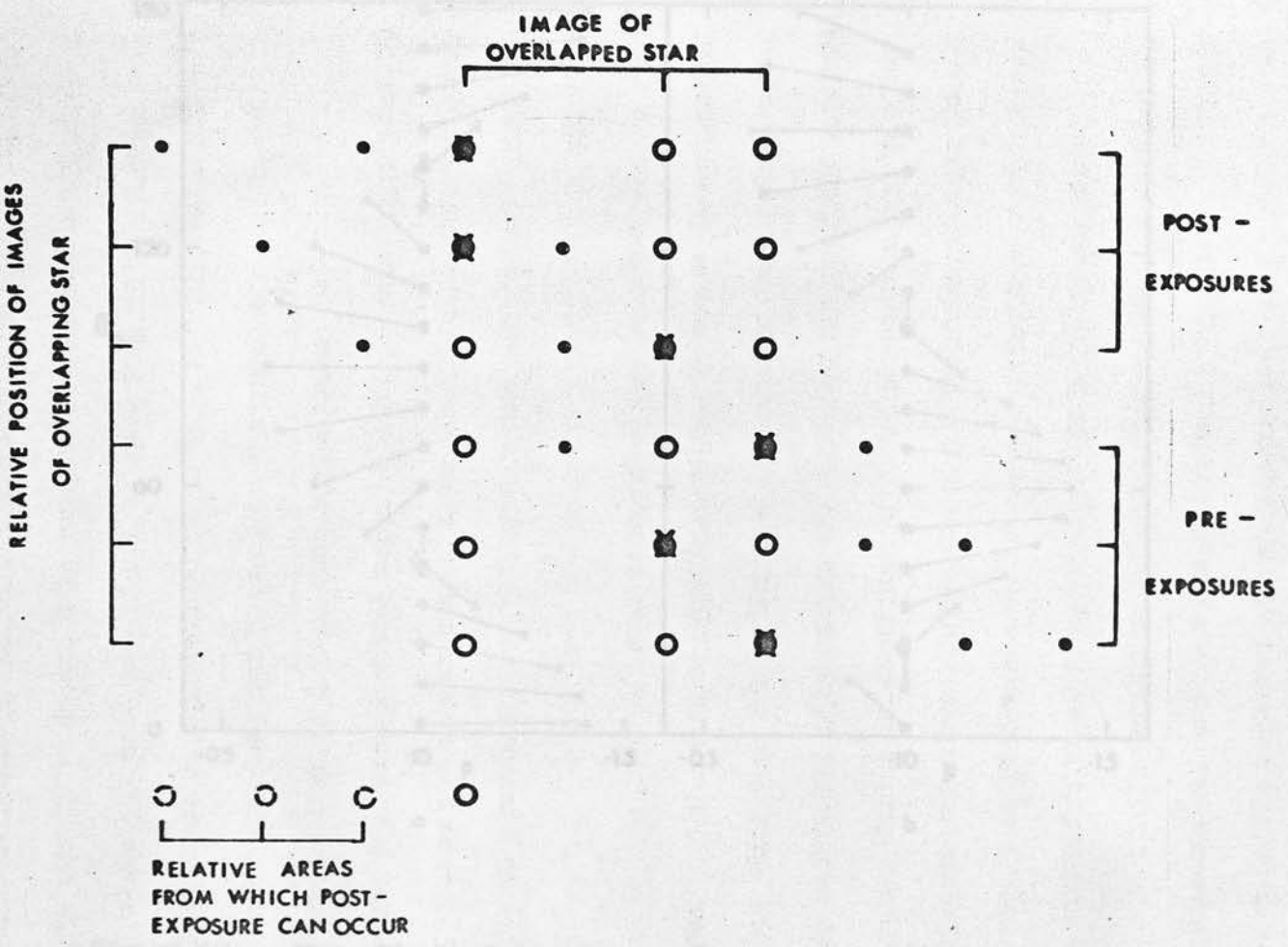

Figure 12. Relative areas of sky from which overlaps, X, can occur.

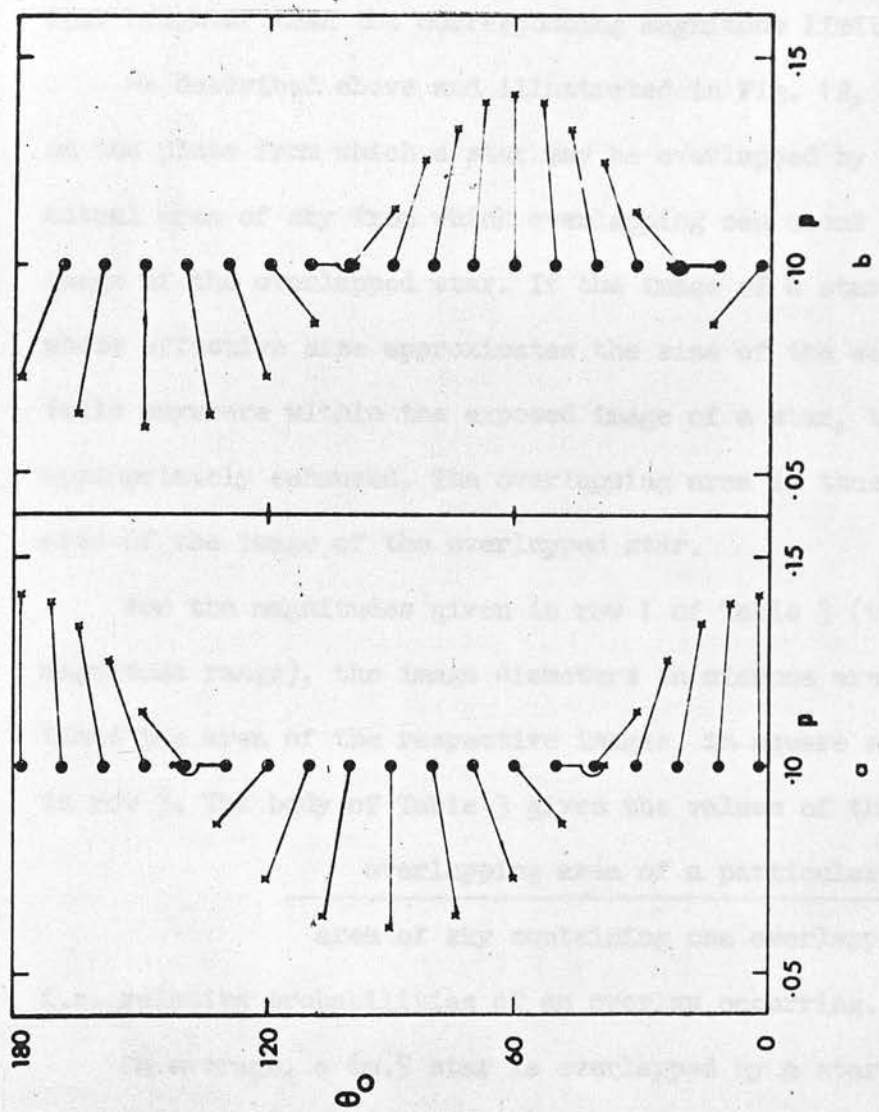

Figure 13. The effect of overlapping by a star 3m.88 fainter on stars with p = 0m.10 and various position angles.
(a) first image overlapped;
(b) 2 nd image overlapped.

ratios of these numbers for the appropriate magnitudes were used to extrapolate the numbers of stars at fainter magnitudes. The extrapolation beyond V = 18 is a continuation of the apparent trend. Column 3 gives the average area of sky, in square minutes of arc, in the region containing one star brighter than the corresponding magnitude limit.

As described above and illustrated in Fig. 12, there are three positions on the plate from which a star may be overlapped by a post-exposure. The actual area of sky from which overlapping can occur depends on the size of the image of the overlapped star. If the image of a star below the plate limit, whose effective size approximates the size of the seeing disc – 20 microns, falls anywhere within the exposed image of a star, the latter image will be appropriately enhanced. The overlapping area is thus closely three times the area of the image of the overlapped star.

For the magnitudes given in row 1 of Table 3 (which covers the entire magnitude range), the image diameters in microns are given in row 2, and three times the area of the respective images, in square minutes of arc, is given in row 3. The body of Table 3 gives the values of the ratio

$$\frac{\text{overlapping area of a particular star}}{\text{area of sky containing one overlapping star}},$$

i.e. relative probabilities of an overlap occurring.

On average, a 6m.5 star is overlapped by a star of ~16m.5, while only one in five 13m.5 stars is overlapped by a 19m star. If the stars in the area brighter than 13m were uniformly distributed, the number of overlaps by stars brighter than 13m is given by

Table 3.

Relative Overlapping Probabilities.

Magnitude of Star			6.5	7.5	8.5	9.5	10.5	11.5	12.5	13.5
Diameter (microns)			130	110	90	71	52	35	27	21
3×Area (sq.min.arc)			0.16	0.14	0.097	0.060	0.032	0.015	0.0087	0.0053
Mag. Limit	No. of Stars	Area of One								
7	4	700	.0002	.0002	.0001	.0001	–	–	–	–
8	8	350	.0005	.0004	.0003	.0002	.0001	–	–	–
9	22	130	.0012	.0011	.0007	.0005	.0002	.0001	.0001	–
10	80	35	.0046	.0040	.0028	.0017	.0009	.0004	.0002	.0002
11	180	16	.010	.0088	.0061	.0038	.0020	.0009	.0005	.0003
12	350	8.1	.020	.017	.012	.0074	.0040	.0019	.0011	.0007
13	870	3.3	.048	.042	.029	.018	.0097	.0045	.0026	.0016
14	2150	1.3	.12	.11	.073	.045	.024	.011	.0066	.0040
15	5200	.54	.30	.26	.18	.11	.059	.028	.016	.0098
16	12000	.24	.67	.58	.40	.25	.13	.062	.036	.022
17	26000	.11	1.45	1.3	.88	.55	.29	.14	.079	.048
18	54000	.052	3.1	2.7	1.9	1.2	.62	.29	.17	.10
19	107000	.026	6.2	5.4	3.7	2.3	1.2	.58	.33	.20
20	200000	.014	11	10	6.9	4.3	2.3	1.1	.62	.38

$\sum_{m=6.5}^{13.5}$ (no. of stars brighter than m)×(relative probability of overlap at m = 13),

i.e. the number of bright star overlaps which should have been avoided during measurement is ~8. However, the majority of stars lie in the cluster regions where the star density is about 10 times greater and so, for these regions, all the relative probabilities must also be increased tenfold. Also, the distribution of stars is not uniform but shows a tendency to form clumps, which will also increase the number of overlaps. The number of expected overlaps by the stars visible on the plates is therefore about 80.

During the measurement of a plate, on average 83 percent of the 527 stars were fully measured, leaving 17 percent, or about 90 stars, which were either overlapped or had an image spoilt by the rare occurrence of some emulsion defect.

Overlapping by stars fainter than the plate limit cannot be detected visually. An estimate of the seriousness of the effect can be made using the data of Table 3. For the stars in the dense cluster regions, where the probabilities are ten times those shown, all stars are overlapped by invisible stars of the magnitudes tabulated in Table 4. The corresponding magnitude differences, Δ m, and magnitude enhancements, m(inc), derived from equation (15) in this section are also given.

The effect is significant for almost all stars and is larger for the fainter stars.

Table 4.

Effect of Faint Overlaps.

Mag. of overlapped star	6.5	7.5	8.5	9.5	10.5	11.5	12.5	13.5
Mag. of overlapping star	13.8	14.0	14.2	15.0	15.5	16.5	17.2	18.0
Mag. difference (Δm)	7.3	6.5	5.7	5.5	5.0	5.0	4.7	4.5
m(inc.)	0.001	0.003	0.005	0.007	0.011	0.011	0.014	0.017

Because the separations of the images on the various plates were not exactly equal, the overlaps are not the same from plate to plate. Each polarization measure must therefore be treated individually.

The observing system used can also introduce enhancements of images by the post-exposure of intensities below the plate limit. The photographic plate causes halation rings. The classical Schmidt system introduces diffraction patterns from the plateholder and its supports and also produces 'ghosts'. When they appear in normal direct photometry, the star image is overexposed and is ignored. Similar effects in the present case of successively exposed separated images cannot be ignored even for faint stars if the spurious light post-exposes an existing image. However, there is no visible indication of their occurrence.

Another effect not often encountered is caused by the design of the filter. Usually there are no discontinuities in a filter except at the edge of

the field. The present filter has additional discontinuities at the boundaries of the observing conditions control regions. As the filter is 11 mm. above the plate and the f-ratio of the telescope is 3.75, a 'shadow' of any discontinuity in the filter nearly 3 mm. in diameter is cast on the plate. The position of this shadow can be measured and is usually apparent from deformation of the images within it.

Overlapping is now considered for the method of Treanor (1968). If the radius of the 'ring' image is a, then the area from which overlapping can occur is a circle of radius approximately 2a, and all overlapping can be considered as post-exposure as there are many cycles in each exposure. If the image of the star has radius a/f, then overlapping can occur from an area $4f^2$ times the area of the star image. The radius of the ring image is approximately 200 microns and the star images vary in radius from 10 to 100 microns approximately, i.e. f varies from 20 to 2. The area for overlapping therefore varies from 1600 to 16 times the area of the star image. In the present method, overlapping can occur from an area 3 times the area of the star image i.e. 1/5 to 1/500 the overlapping probability in Treanor's method.

2.2 THE 1.5 R.M.S. DEVIATION CYCLE.

The preceding discussion suggests that star measures with large deviations from the general trend are to be expected. Inspection of the measures in the observing conditions control (OCC) regions confirmed this. To

illustrate the presence of these interlopers, after the polarization measures corrected by the OCC curves had been stored in the computer, the numbers of deviations from the straight means of these measures for each star were counted in various magnitude intervals, as shown in Fig. 14, where ln N is plotted against (deviation)^2. The majority of measures form a Gaussian distribution with an r.m.s. deviation of $\pm$ 0m.041, but there is a considerable 'tail', amounting to nearly 5 percent of the total number.

As the complete reduction was to be performed by computer, some numerical method of finding and discarding these erroneous measures had to be devised. The following method was used.

Suppose that N(1) sets of magnitude differences are available for a particular mean – N(1) stars in a OCC region or N(1) plates for a polarization reduction – and these are dm_{j1}, dm_{j2} and dm_{j3} for the j^{th} set. The first approximation to the mean is given by

$$DM_i(1) = \sum_{j=1}^{N(1)} dm_{ji}/N(1), \quad i = 1, 2, 3.$$

The r.m.s. deviation of the j^{th} set from the first mean is

$$R_j(1) = \left[\sum_{i=1}^{3} (dm_{ji} - DM_i)^2/3 \right]^{1/2}$$

and the first mean r.m.s. deviation of the set is

$$R(1) = \left\{ \sum_{j=1}^{N(1)} \left[\sum_{i=1}^{3} (dm_{ji} - DM_i)^2/3 \right]/N(1) \right\}^{1/2}.$$

Any set with $R_j(1) > 1.5 \times R(1)$ is discarded and a new mean, $DM_i(2)$, is calculated for the N(2) sets remaining which leads to new r.m.s. deviations $R_j(2)$ and R(2). Once again those sets, if any, with $R_j(2) > 1.5 \times R(2)$ are discarded, all the N(1) stars being tested in every cycle. This cycle is discontinued in the k^{th} cycle when

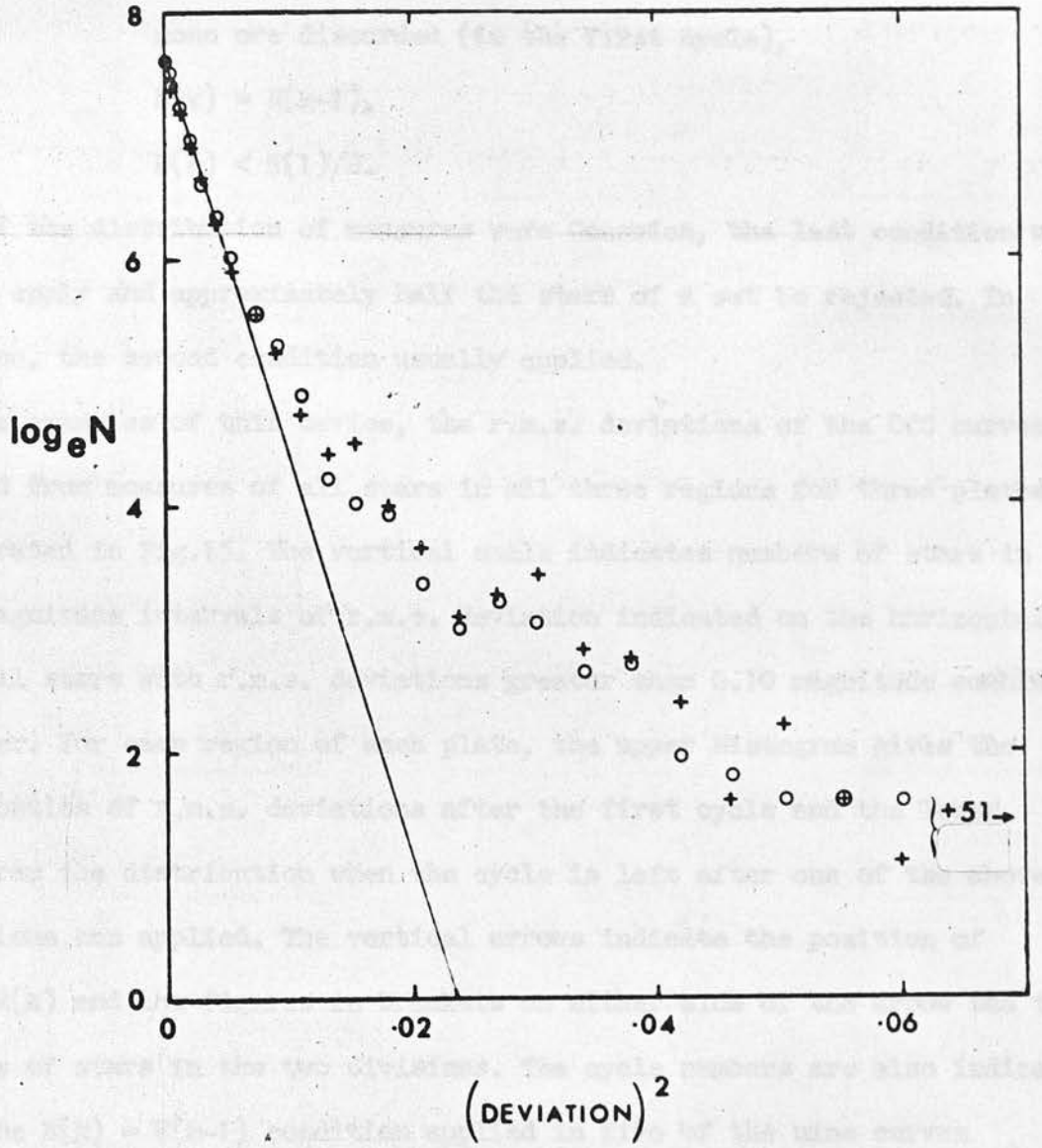

Figure 14. The number, N, of deviations from the mean polarization magnitude differences per star against (deviation)^2.
+ positive deviations, 0 negative deviations.
The straight line is a Gaussian distribution. Of the 21,000 deviations, approximately 1,000 lie to the right of this line.

either none are discarded (in the first cycle),

or $N(k) = N(k-1)$,

or $N(k) < N(1)/2$.

If the distribution of measures were Gaussian, the last condition would always apply and approximately half the stars of a set be rejected. In practice, the second condition usually applied.

As examples of this device, the r.m.s. deviations of the OCC curves derived from measures of all stars in all three regions for three plates are illustrated in Fig.15. The vertical scale indicates numbers of stars in the 0.01 magnitude intervals of r.m.s. deviation indicated on the horizontal scale, with all stars with r.m.s. deviations greater than 0.10 magnitude combined together. For each region of each plate, the upper histogram gives the distribution of r.m.s. deviations after the first cycle and the lower histogram the distribution when the cycle is left after one of the above conditions has applied. The vertical arrows indicate the position of $1.5 \times R(k)$ and the figures in brackets on either side of the arrow the total numbers of stars in the two divisions. The cycle numbers are also indicated.

The $N(k) = N(k-1)$ condition applied in five of the nine curves illustrated. In all the OCC curves derived, no star once rejected by the cycle was reinstated.

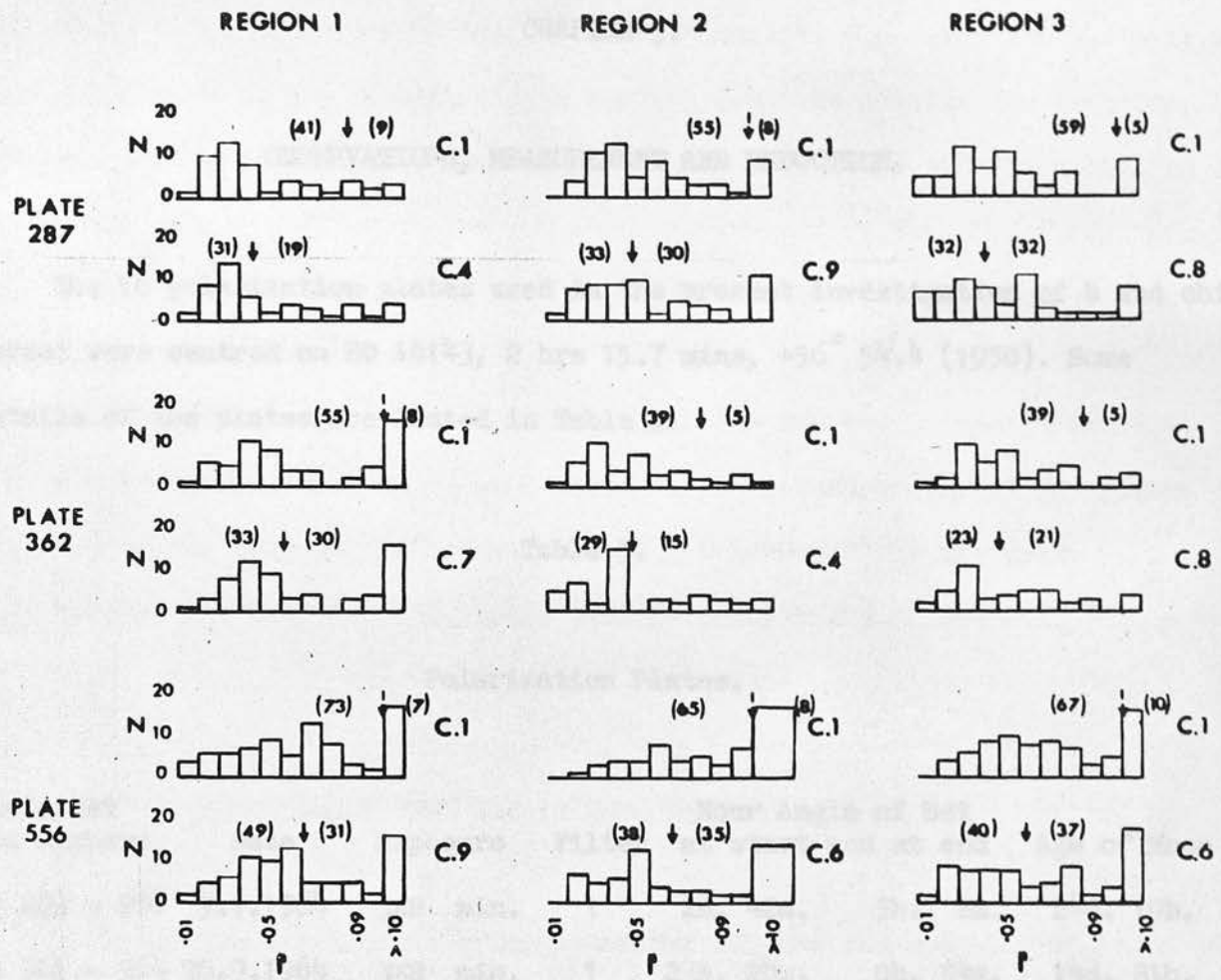

Figure 15. Effect of the 1.5 r.m.s. deviation cycle on the OCC measures of 3 plates.

CHAPTER 3.

OBSERVATIONS, MEASUREMENT AND REDUCTION.

The 16 polarization plates used in the present investigation of h and chi Persei were centred on HD 14143, 2 hrs 15.7 mins, +56° 54'.4 (1950). Some details of the plates are listed in Table 5.

Table 5.

Polarization Plates.

Plate Set and numbers	Date	Exposure	Filter	Hour Angle of Set at start	at end	Age of Moon
1) 283 – 288	9.1.1964	3x2 min.	1	2h. 42m.	5h. 2m.	24d. 19h.
2) 361 – 364	20.9.1964	3x2 min.	1	23h. 28m.	0h. 54m.	14d. 21h.
3) 555 – 560	28.2.1966	3x3.5 min.	2	5h. 18m.	7h. 48m.	8d. 11h.

The plates were all Ilford R40 panchromatic fine grain emulsion. The polaroid filters were butyrate laminations and each was cut from a single piece of polaroid, Filter 1 being of type HN38 and Filter 2 HN22. The three plate sets are of differing quality depending on the hour angle at which they were obtained: set 2 is of high quality, being obtained very near the meridian; set 3 is of poor quality and set 1 intermediate. The telescope

mirror was aluminized in 1963 August and 1965 August. The first two plate sets were obtained with the same aluminium coating when the coating was five and thirteen months old respectively, and the third set with a different coating six months old.

Details of the position of the Moon will be given in the discussion of the OCC curves in Chapter 4.

The UBV plates were also centred on HD 14143 and are listed in Table 6.

All the plates were taken on Eastman Kodak emulsions. Except for plate 622 at 3 hours, they were all taken within 1.5 hours of the meridian.

The results from the UBV plates will be described in Chapter 6.

3.1 MEASUREMENT WITH THE IRIS PHOTOMETER.

A semi-automatic digital iris photometer (Seddon and Jones, 1966) was used for the measurement of all the plates. The polarization program required 200 hours of measurement.

The paper tape output from the iris photometer for one measure consists of the X and Y coordinates and the iris reading, in EDSAC code. One coordinate unit corresponds to 127 microns on the plate (7.40 microns corresponding to 1 arc second). The diameters of the star images range from 140 to 15 microns. In crowded regions on a direct plate a star image cannot be specified uniquely by the coordinate system available. On polarization plates, the situation is still more confused as each star has three images, see

Table 6.

UBV Plates.

Colour	Date	Plate No.	Emulsion	Filter	Exposure
V	23.10.1966	628	IIaD	Ilford 804 + 111	2 min.
V	"	629	"	"	"
V	"	632	"	"	"
V	"	635	"	"	"
V	"	638	"	"	"
B	22.10.1966	622	IIaO	Schott GG13	2 min.
B	23.10.1966	630	"	"	"
B	"	633	"	"	"
B	"	636	"	"	"
B	25.10.1966	639	"	"	"
U	23.10.1966	631	IIaO	Schott UG2	15 min.
U	"	637	"	"	"
U	25.10.1966	640	"	"	"
U	"	641	"	"	"
U	"	642	"	"	7 min.

Fig. 11. The stars were therefore measured in strict numerical order.

Also, due to overlapping of one or other of the images of a star, not all stars could be measured fully. The measurement of a star always commenced with a measure of the background fog level (BFL) near the first image and was terminated by inserting a row of blank tape with a manual switch. The total number of photometer measures for any star depended on the overlapping, if any, of its images as follows:

(1) first image overlapped – one measure – BFL (blank);

(2) second or third images (or both) overlapped – two measures – BFL plus the first image (blank);

(3) no overlapping – four measures – BFL plus the three images in order (blank).

Two additional rows of blank tape were inserted after every fifth star for checking purposes. Magnitude calibration was obtained from measures of the first image only.

The average time needed to measure each plate was about twelve hours, four to six measuring runs per plate being required. Each run commenced with the measurement of the photoelectric standard stars for magnitude calibration (Chapter 5). The OCC region stars were measured first, followed by the program stars. Measurement time was distributed thus:

program stars	53 percent,
observing conditions control stars	24 percent,
photometric standard stars	23 percent.

The UBV plates were measured in the same format.

The 527 program stars are identified in the UBV and polarization catalogues and Charts 1 to 9 at the end of this thesis.

The measurement of the polarization plates with the iris photometer was carried out in three sessions – in 1965 November (plate set 2), 1966 March – April (set 1) and 1966 July – August (set 3). The first session commissioned the instrument following the transistorisation of the amplifier units (Seddon and Jones,1966). The iris and coordinate counting unit ran continuously day and night (as did an air conditioning system to maintain a constant temperature in the measuring room) and was not altered from the initial settings for each plate, except, for example, when the photometer light source had to be replaced.

To check for drift, the iris readings of four stars covering the whole range of brightness, together with the iris reading for an identifiable area of background fog, were recorded at intervals during each measuring run. The readings showed that drift was less than one iris unit (corresponding to 0m.01) over intervals of several days, allowing the complete measurement of one plate.

The calibration measures for each plate were therefore averaged for as many measuring runs as possible. Ten plates required only one calibration curve each, the others two or more. Plate 361 required six measuring runs with no measurable drift during them. For the mean calibration curve required for this plate, the r.m.s. deviation per measure in iris units for each standard star measured is plotted against iris reading in Fig. 16a. The crosses indicate the mean r.m.s. deviation per measure in five magnitude intervals:

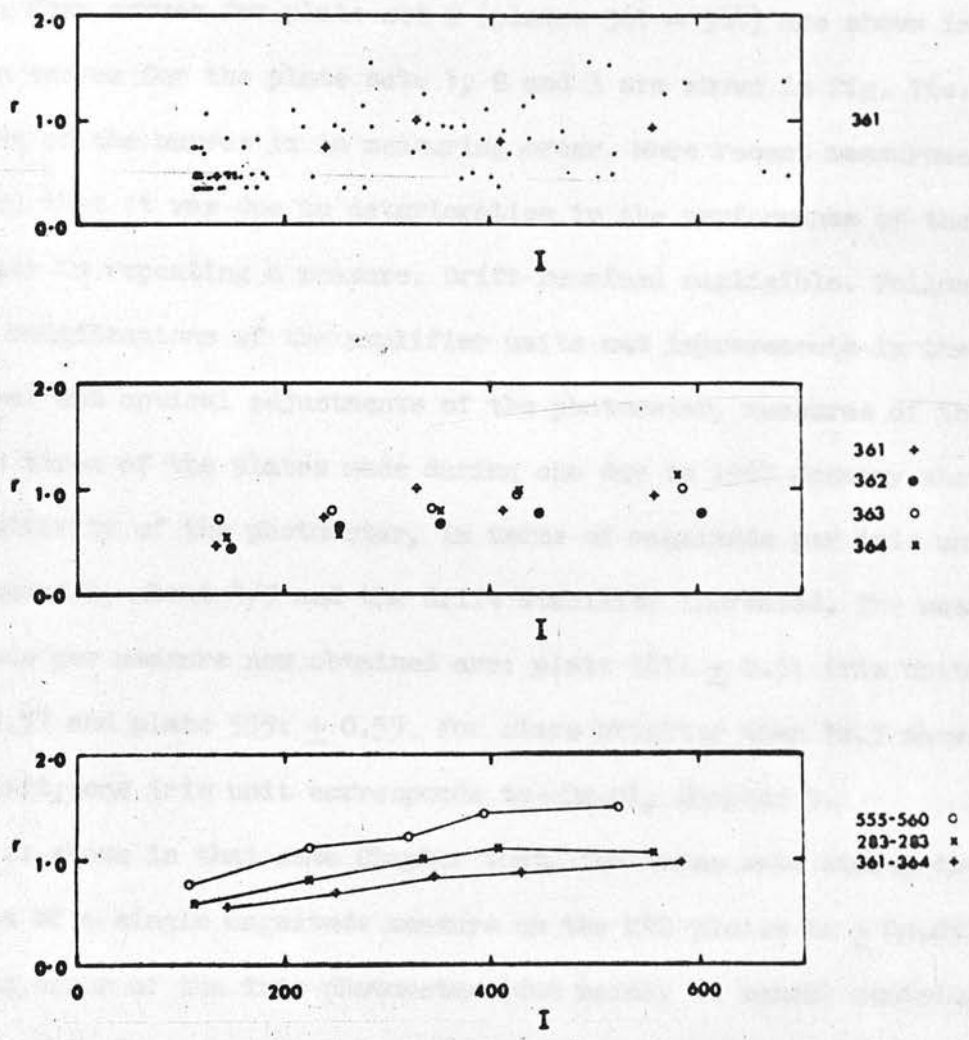

Figure 16. The r.m.s. deviation per measure, r, against iris reading, I, for plates and plate sets.

fainter than V = 12, 12 to 10.5, 10.5 to 9.5, 9.5 to 8.5 and brighter than V = 8.5. Mean curves for plate set 2 (plates 361 – 364) are shown in Fig. 16b. The mean curves for the plate sets 1, 2 and 3 are shown in Fig. 16c. The worsening of the curves is in measuring order. More recent measurements have confirmed that it was due to deterioration in the performance of the iris photometer in repeating a measure. Drift remained negligible. Following further modifications of the amplifier units and improvements in the mechanical and optical adjustments of the photometer, measures of the standard stars on three of the plates made during one day in 1967 January show that the sensitivity of the photometer, in terms of magnitude per iris unit, has been reduced by about 4/5 and the drift stability increased. The mean r.m.s. deviations per measure now obtained are: plate 361: $\pm$ 0.51 iris units; plate 283: $\pm$ 0.57 and plate 555: $\pm$ 0.55. For stars brighter than 1m.5 above the plate limit, one iris unit corresponds to~0m.01, Chapter 5.

It is shown in that same Chapter that, for these same stars, the r.m.s. deviation of a single magnitude measure on the R40 plates is $\pm$ 0m.050. The measuring error of the iris photometer (due mainly to manual centring of the image) is therefore very small compared with the intrinsic errors of the photographic photometry.

3.2 COMPUTER REDUCTION PROGRAMS.

The reduction of the iris photometer measures of the polarization plates

was carried out on an Elliott 803 digital computer. As access to the computer was limited, a series of programs was written, each program performing some aspect of the reduction and providing data for succeeding programs. Some programming redundancy followed from this approach, but with little inconvenience as a subroutine structure was used. The programs were written in Autocode, leaving only 4934 locations in the store available for use. For storing and sorting large amounts of data, two magnetic film handlers were used.

In the following, the overall organisation of the data-handling will be described. Details of the numerical analysis are given elsewhere.

(1) Photometric calibration.

The iris photometer measures of the photometric standards are input for as many measuring runs as required, a code conversion from EDSAC code to Elliott 803 code is carried out and the output tape tabulates the mean iris reading, the r.m.s. deviation per measure and the photoelectric magnitudes available for each star. These results have already been discussed above; the calibration curves themselves are discussed in Chapter 5. Some statistics of the background fog levels are also derived, see below.

(2) Observing Conditions Control Curves.

The photometer measures of the three sets of stars in the OCC regions for each plate are input, the code conversion is carried out and magnitudes and magnitude differences for each star are derived from the calibration. These are averaged using the 1.5 r.m.s. deviation cycle to give the OCC curves, Chapter 4.

(3) Magnitude conversion.

The photometer measures of the program stars for each plate are input, the code conversion is carried out, magnitudes and magnitude differences are derived from the calibration, and the appropriate OCC correction is applied. For each of the 527 stars, the output tape contains the following: star serial number, a code number giving the number of photometer measures and specifying which measures follow, x- and y-coordinates, difference of the background fog level near the star from the mean fog level of the standards, magnitude and three magnitude differences. Some statistics of the background fog levels are also derived, see below.

(4) Magnitude combination.

It is now necessary to collect together the measures for each star. Each magnetic film handler has 4096 blocks, each containing 64 locations. As each film 'read' or 'write' operation automatically causes the film to move to the next block, it is convenient to write onto one handler and read from the other alternately, although one film could contain the 68,000 numbers involved.

There are up to eight numbers for each star per plate, depending on the code number. The block number is used for the serial number of the star and so each block can contain all the measures for one star from eight plates. All the measures from the first 8 plates are read into, in the present case, blocks 1 to 527 and the measures from the second 8 plates into blocks 528 to 1054. A final sort routine brings together on one film all the measures for each star in successive blocks. This technique can be extended to any number of stars on any number of plates, up to the capacity of three film handlers.

The program can also: convert measures with Filter 2 to the Filter 1 system using equations (13) during the reading-in of the plate measures; print the contents of any film block; print the measures of any star; and substitute corrected values for any measure of any star (the tape readers occasionally misread original data).

(5) Polarization reduction.

The measures for each star are read from the film handler in turn. The program calculates for that star:

(1) mean coordinates;

(2) mean background fog level and its r.m.s. deviation, see below;

(3) mean magnitude and its r.m.s. deviation per measure, Chapter 5;

(4) the mean magnitude differences using a 1.5 r.m.s. deviation cycle, the polarization parameters p and θ_o using the equations of Chapter 2, and the Stokes parameters, Chapter 5.

In addition, the numbers of measures available etc. are recorded, see the Catalogue at the end of this thesis. Two examples of the full output from this program are given in Fig. 27, Chapter 5.

The reduction of the UBV measures was carried out on the Elliott 4130 computer of the Royal Observatory, Edinburgh. Algol programs analagous to programs (1), (3) and (4) above were written, incorporating some improvements, and producing, for each star, a block on magnetic tape containing all the measures of that star. Additional programs averaged the measures, applied colour equations and derived the final magnitudes, colours and errors, Chapter 6.

3.3 BACKGROUND FOG LEVELS.

The background fog level (BFL) was measured near (usually about 150 microns east of) the first image of every star measured. The measures for the program stars and for the photometric standards from the polarization plates will be discussed here; the measures in the OCC regions are summarised in Chapter 4.

During measurement it was observed that, near any star, a range of BFL existed, extending over most of the total range observed. Some of the BFL distributions are shown in Fig. 17a – some are symmetric and some quite skew. The distribution, however, is closely Gaussian – the apparent skewness is due to the large sample width and non-integral values of the mean. Some Gaussian distributions with similar characteristics are shown in Fig. 17b.

The BFL data for each plate set are given in Table 7; all measures are in iris units.

The difference between the mean BFL of the program stars and that of the standard stars is small except for plate set 3, where it is almost one digit. This plate set was taken far from the meridian and relatively more standard stars are in crowded regions where scattered light increases the BFL.

The r.m.s. deviations per measure from the two sets of stars are nearly equal. Part of the scatter is due to errors in the iris reading itself. These can be obtained from the r.m.s. deviations of Fig. 16c at the faint star end. The final row of Table 7 gives the r.m.s. deviation per measure of BFL for each of the plate sets. Since the exposures were so short, the BFL density

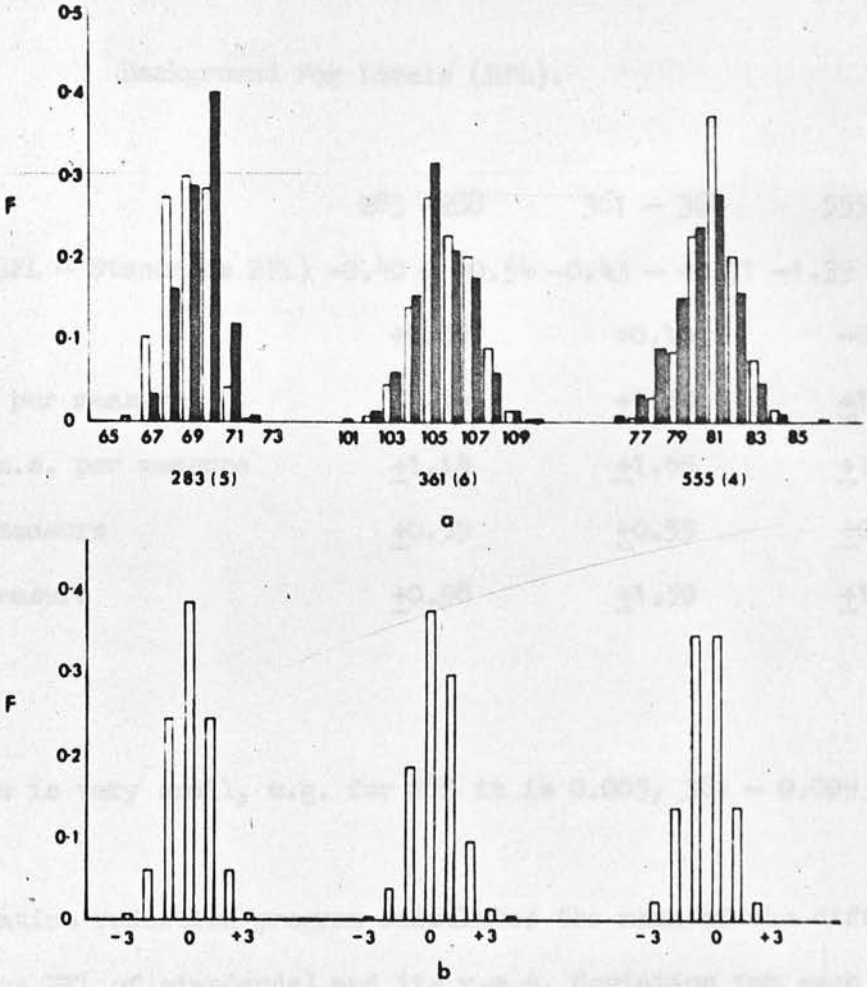

Figure 17. Distributions of the fraction, F, of the total numbers of background fog level readings against iris reading.
(a) measures from the standard stars, open columns, and from the program stars, filled columns.
(b) Gaussian distributions with large sample widths and non-integral values of the mean.

Table 7.

Background Fog Levels (BFL).

Plate Set	283 –288	361 – 364	555 – 560
Range of (Prog. BFL – Standards BFL)	–0.40 – +0.54	–0.43 – +0.71	–1.39 – +0.08
Mean Difference	+0.08	+0.10	–0.93
Standards r.m.s. per measure	±1.14	±1.54	±1.50
Program Stars r.m.s. per measure	±1.14	±1.65	±1.52
Iris r.m.s. per measure	±0.59	±0.55	±0.78
BFL r.m.s. per measure	±0.98	±1.50	±1.29

of all the plates is very small, e.g. for 283 it is 0.003, 361 – 0.009 and 560 – 0.018.

The polarization reduction program calculates the mean of the differences (BFL of star minus BFL of standards) and its r.m.s. deviation for each star. Mean values for some magnitude ranges are:

	Mean BFL	r.m.s. deviation of mean BFL per measure	mean r.m.s. deviation
69 stars brighter than m(E) = 10	–0.44	±0.48	±1.47,
307 stars brighter than m(E) = 12	–0.33	±0.48	±1.47,
220 stars fainter than m(E) = 12	+0.13	±0.42	±1.30.

The negative values of the mean BFL for the brighter stars indicate a tendency to measure the BFL of a bright star further away from the first image than usual, where the fog level is not so affected by scattered light.

CHAPTER 4.

OBSERVING CONDITIONS CONTROL CURVES.

To begin this Chapter, the various means and r.m.s. deviations derived for the observing conditions control (OCC) curves will be defined.

Suppose that, in OCC region r, r = 1,2,3, of a particular plate, N(r) stars have been selected by the 1.5 r.m.s. deviation cycle described in Chapter 3. A star n_r of this set has magnitude differences dm_{in_r}, i = 1,2,3 being the image number.

The OCC curve of the region r is

$$O_{ir} = \sum_{n_r=1}^{N(r)} dm_{in_r}/N(r)$$

and the mean OCC curve for the plate is

$$MO_i = \sum_{r=1}^{3} \left[\sum_{n_r=1}^{N(r)} dm_{in_r}/N(r) \right]/3, \quad i = 1,2,3.$$

The r.m.s. deviation of a star, n_r, from the O_r is

$$\left[\sum_{i=1}^{3} (dm_{in_r} - O_{ir})^2/3 \right]^{1/2},$$

the r.m.s. deviation per star of one O_r is

$$\left\{ \sum_{n_r=1}^{N(r)} \left[\sum_{i=1}^{3} (dm_{in_r} - O_{ir})^2/3 \right]/N(r) \right\}^{1/2},$$

and the r.m.s. deviation per star of the MO is

$$\left(\sum_{r=1}^{3} \left\{ \sum_{n_r=1}^{N(r)} \left[\sum_{i=1}^{3} (dm_{in_r} - O_{ir})^2/3 \right]/N(r) \right\}/3 \right)^{1/2}.$$

Before discussing the OCC curves of the polarization plates themselves, results from two multiple image plates will be described.

4.1 MULTIPLE IMAGE OCC CURVES.

In 1964 February, two plates were obtained, both on Ilford R40 emulsion, with 20 exposures of 90 sec. duration on each, the images being separated by small displacements of the telescope between exposures. Plate 309 was taken with polaroid Filter 1, but the filter was not rotated. Plate 315 had no filter, and was obtained on a night of poor seeing. The region observed was that of the cluster Praesepe, M44, 7 hours 37.5 mins., $+19^{\circ}\ 52'$ (1950), which was conveniently placed for observation at the time. Photometric calibration was obtained from standard stars observed by Johnson (1952).

On both plates, the images of 40 stars were measured with the iris photometer. The MO(40) – i.e. the mean OCC curve for all 40 stars – of both plates are shown in Fig. 18. Vertical lines indicate the r.m.s. deviations of each mean point – the mean r.m.s. deviation of a mean point is $\pm$ 0m.007 for plate 309 and $\pm$ 0m.012 for plate 315. In general, the image size decreases with time, indicating an improvement in seeing conditions near the dome as the exposures proceeded. The physical diameter decreases by about 5 percent and 8 percent for the two plates respectively.

There is no correlation between the r.m.s. deviation of one mean point and the magnitude difference between it and its predecessor.

The r.m.s deviations per measure for the individual stars are plotted against magnitude for both plates in Fig. 19. There is an apparent magnitude effect – the brightest and faintest stars having larger errors. In an attempt to correct this effect, the 40 stars were placed in magnitude order and

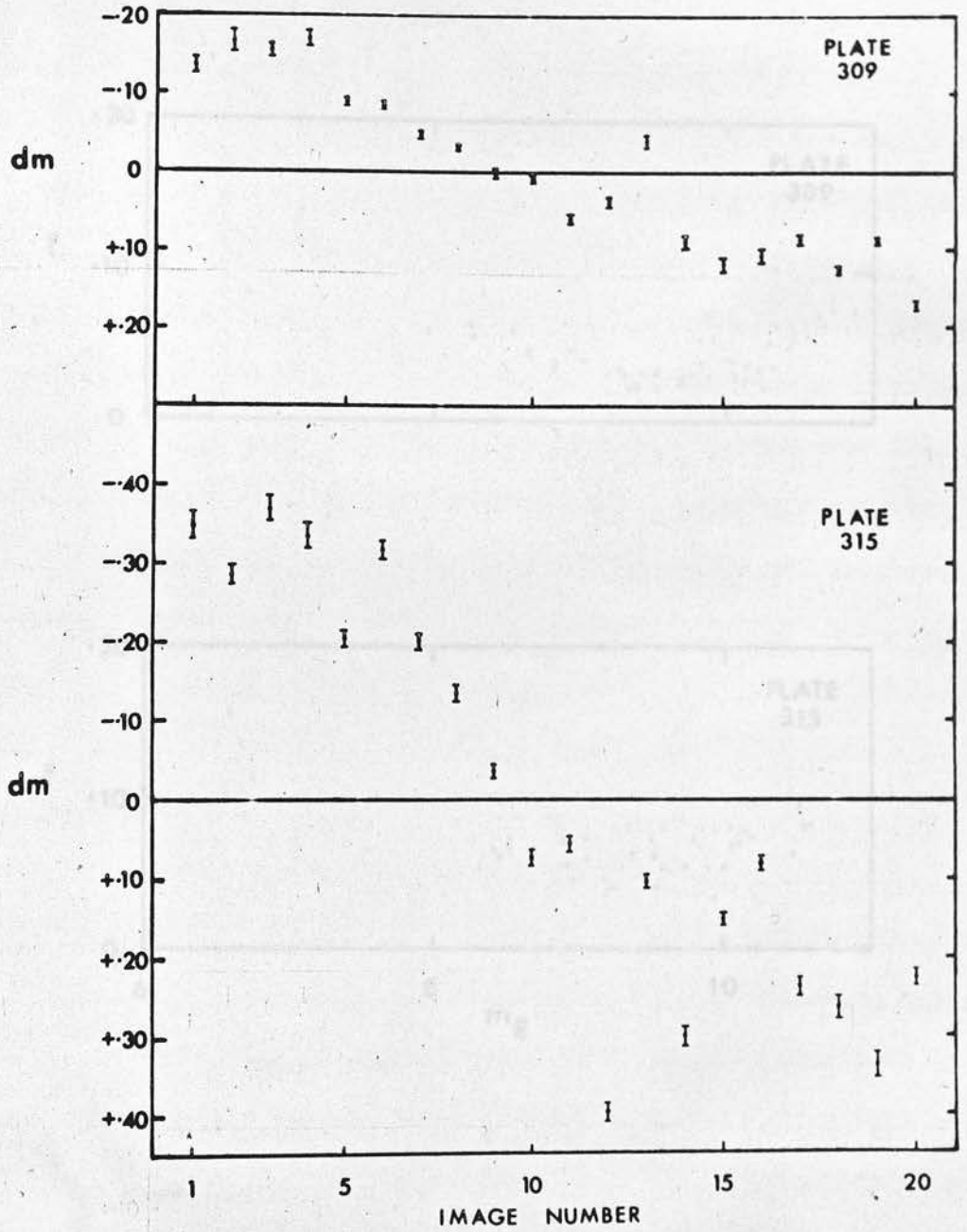

Figure 18. MO(40) curves for two multiple image plates.

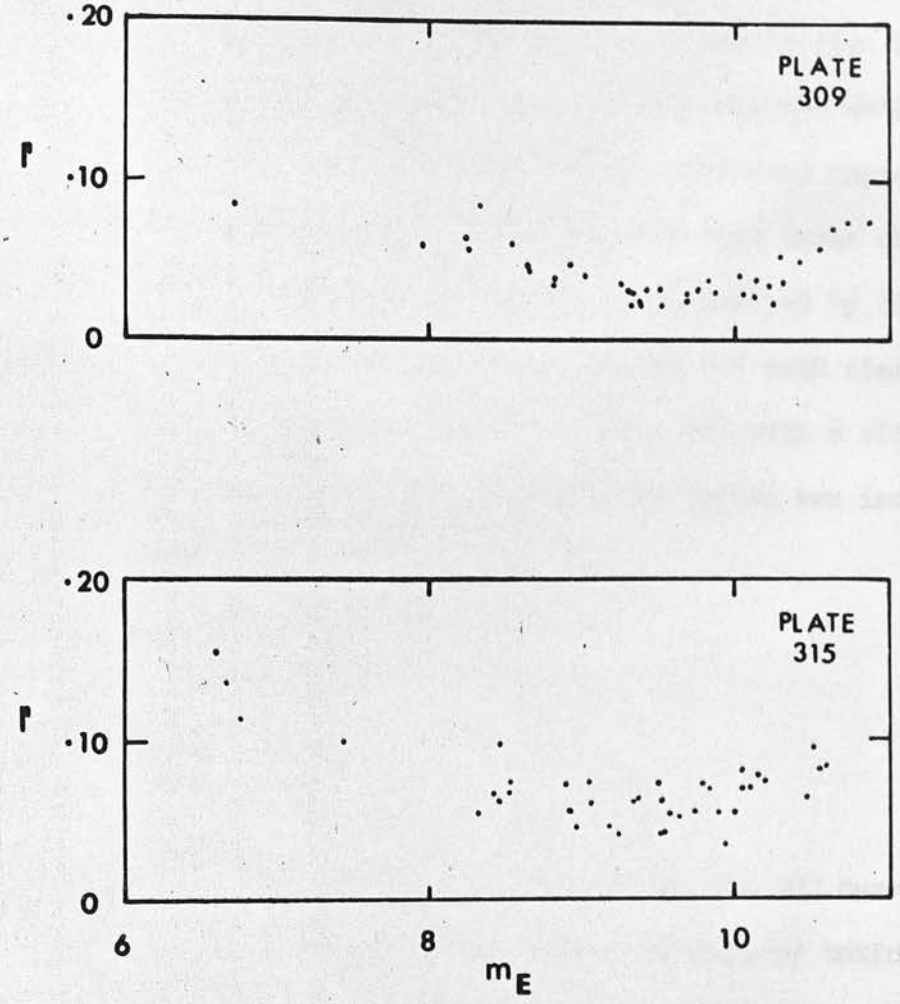

Figure 19. R.m.s. deviation per measure from the MO(40) curves, r, for the individual stars against magnitude for the two multiple image plates.

divided into 5 groups of 8 stars each, and the M□(8) curves and r.m.s. deviations of the stars in each group were calculated. The 5 sets of differences, M□(8) – M□(40), are shown for both plates in Fig. 20. The 'mirror image' effect for the extreme groups arises partly from the method of reduction, but does indicate that, as observing conditions improve, the image sizes of the bright stars decrease relatively more than those of the faint stars. This suggests that better □CC curves may be derived by dividing the magnitude range. The r.m.s. deviations per measure for each star from its M□(8) are now nearly uniform with magnitude (Fig. 21) with a slight tendency to increase for the brighter stars. The group boundaries are indicated by arrows.

4.2 THE □CC CURVES.

Following the results of the previous section, the □CC curves of the polarization plates were derived in two ways – firstly, by taking all the stars together, the M□(all), and secondly, after dividing them into three groups at approximate thirds of the magnitude range, at m(E) = 10.8 and 12.4 respectively (m(E) is the magnitude derived from the polarization plates), giving the M□(Δ m). All the curves for each of the 16 polarization plates are given in Table 8. The r.m.s. deviations per star for the M□ curves, together with the numbers of stars used, are given in Table 9. The r.m.s. deviations of the mean points average ± 0m.0035 for the M□(all), ± 0m.0078 for the

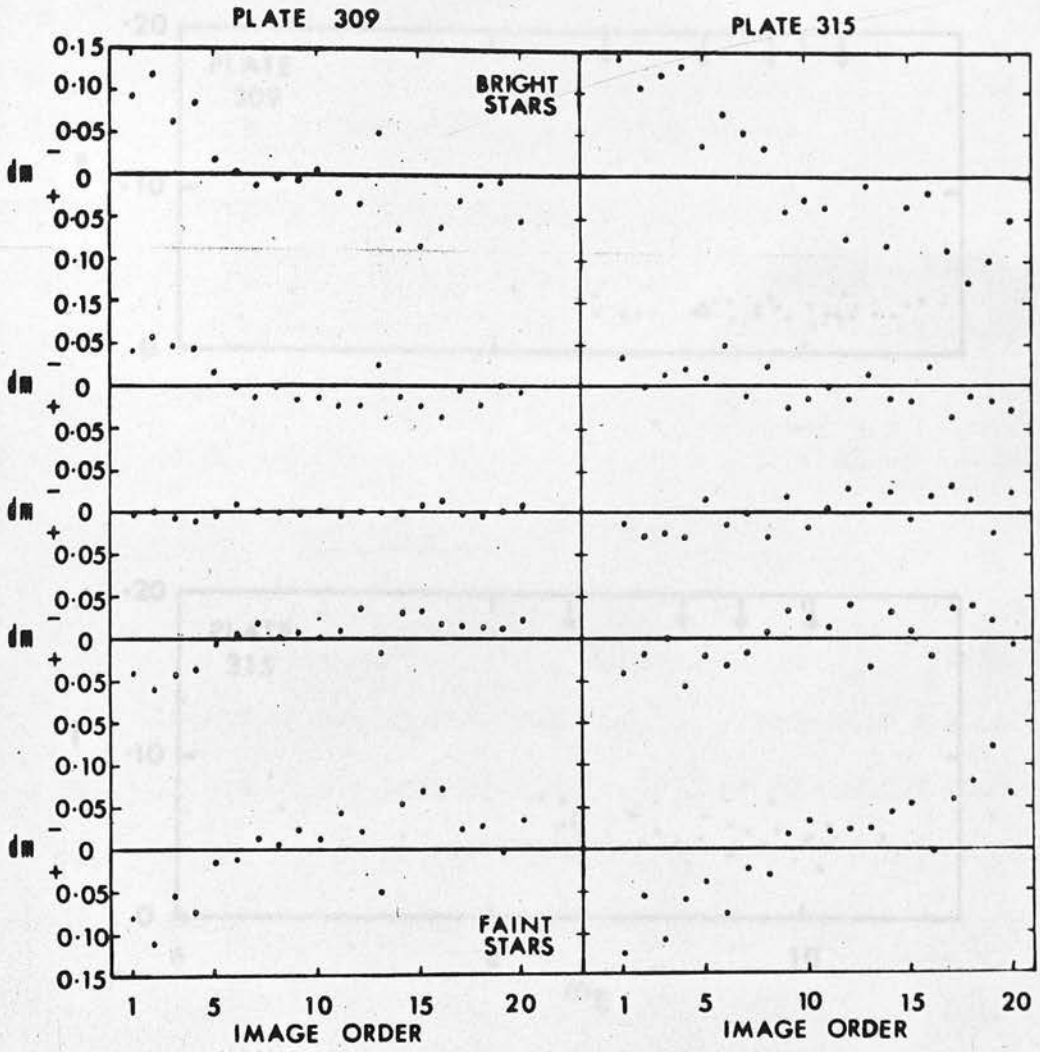

Figure 20. Five sets of differences, M□(8) − M□(40), for the two multiple image plates.

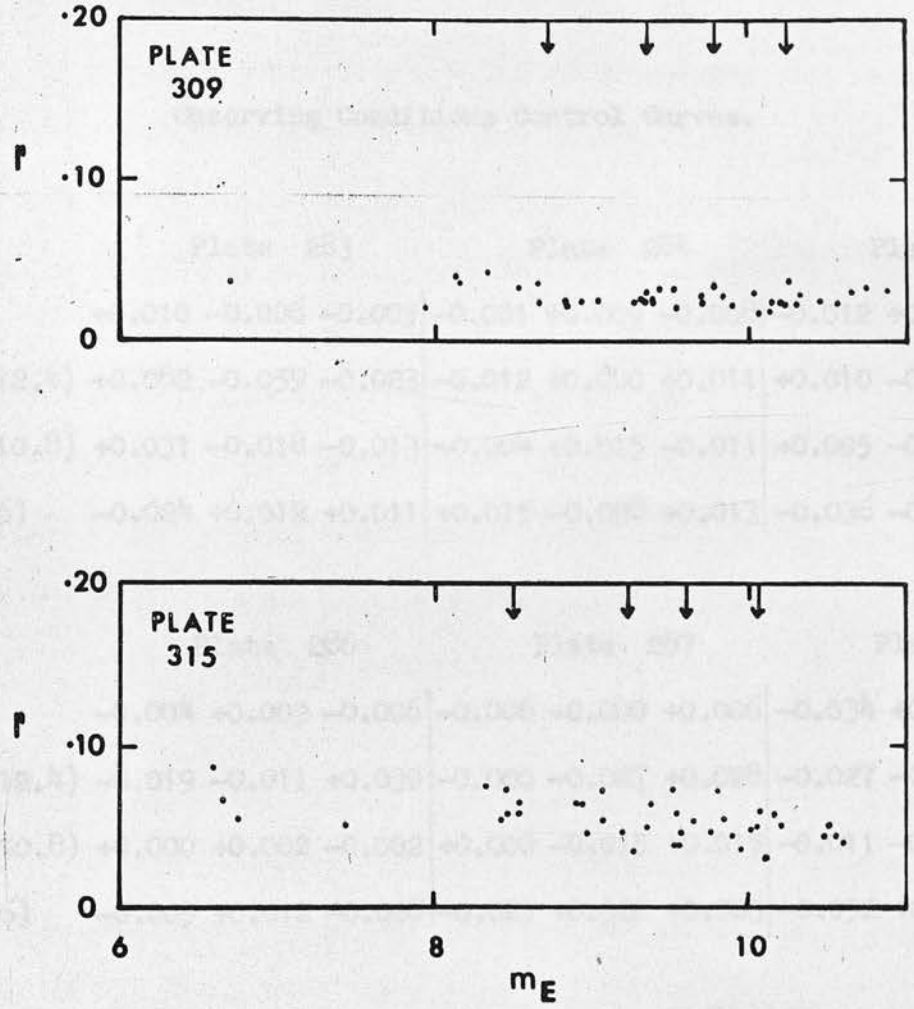

Figure 21. R.m.s. deviation per measure from the MO(8) curves, r, for the individual stars against magnitude for the two multiple image plates.

Table 8.

Observing Conditions Control Curves.

	Plate 283			Plate 284			Plate 285		
M0(all)	+0.010	−0.006	−0.005	−0.001	+0.009	−0.008	−0.012	+0.001	+0.011
M0(13.5 − 12.4)	+0.082	−0.059	−0.023	−0.012	+0.000	+0.011	+0.010	−0.008	−0.002
M0(12.4 − 10.8)	+0.031	−0.018	−0.013	−0.004	+0.015	−0.011	+0.005	−0.002	−0.003
M0(10.8 − 6)	−0.024	+0.012	+0.011	+0.015	−0.028	+0.013	−0.036	−0.002	+0.038

	Plate 286			Plate 287			Plate 288		
M0(all)	−0.004	+0.009	−0.006	−0.006	−0.000	+0.006	−0.034	+0.004	+0.030
M0(13.5 − 12.4)	−0.019	−0.011	+0.030	−0.000	−0.027	+0.028	−0.027	−0.005	+0.032
M0(12.4 − 10.8)	+0.000	+0.002	−0.002	+0.000	−0.015	+0.015	−0.011	−0.007	+0.018
M0(10.8 − 6)	−0.005	+0.012	−0.008	−0.025	+0.022	+0.003	−0.052	+0.031	+0.021

Table 8 (cont.).

	Plate 361			Plate 362		
MO(all)	−0.031	−0.019	+0.050	−0.028	−0.005	+0.033
MO(13.5 − 12.4)	−0.063	+0.036	+0.027	−0.046	+0.034	+0.011
MO(12.4 − 10.8)	−0.032	−0.012	+0.044	−0.021	−0.010	+0.031
MO(10.8 − 6)	−0.012	−0.064	+0.076	−0.014	−0.025	+0.039

	Plate 363			Plate 364		
MO(all)	−0.052	+0.006	+0.047	−0.050	+0.001	+0.048
MO(13.5 − 12.4)	−0.034	−0.035	+0.070	−0.047	−0.002	+0.049
MO(12.4 − 10.8)	−0.059	−0.000	+0.059	−0.052	−0.000	+0.052
MO(10.8 − 6)	−0.042	+0.013	+0.029	−0.030	−0.019	+0.049

	Plate 555			Plate 556			Plate 557		
MO(all)	−0.061	−0.016	+0.077	−0.034	−0.019	+0.053	−0.121	+0.029	+0.092
MO(13.5 − 12.4)	−0.088	+0.004	+0.083	−0.019	−0.004	+0.022	−0.154	+0.056	+0.098
MO(12.4 − 10.8)	−0.072	−0.018	+0.090	−0.023	−0.015	+0.037	−0.129	+0.021	+0.109
MO(10.8 − 6)	+0.072	−0.088	+0.016	−0.018	−0.039	+0.057	+0.043	−0.030	−0.013

	Plate 558			Plate 559			Plate 560		
MO(all)	−0.026	−0.019	+0.045	−0.058	+0.002	+0.055	−0.080	−0.021	+0.101
MO(13.5 − 12.4)	−0.056	−0.044	+0.100	−0.090	−0.008	+0.099	−0.077	−0.042	+0.119
MO(12.4 − 10.8)	−0.020	−0.028	+0.048	−0.061	+0.015	+0.046	−0.088	−0.016	+0.104
MO(10.8 − 6)	−0.014	−0.004	+0.018	+0.024	−0.021	−0.004	−0.036	+0.013	+0.023

Table 9.

R.m.s. Deviations per Star for the M□ Curves.

Plate Number	M□(all) Stars	rms	M□(13.5 – 12.4) Stars	rms	M□(12.4 – 10.8) Stars	rms	M□(10.8 – 6) Stars	rms
283	74	0.030	27	0.073	49	0.033	22	0.022
284	93	0.030	25	0.032	60	0.034	25	0.022
285	100	0.028	28	0.038	57	0.027	16	0.014
286	90	0.029	38	0.051	46	0.024	23	0.027
287	96	0.025	37	0.041	46	0.022	22	0.019
288	105	0.028	45	0.036	38	0.025	22	0.026
361	121	0.032	63	0.036	56	0.027	25	0.015
362	85	0.030	47	0.044	38	0.027	15	0.024
363	89	0.026	52	0.043	36	0.021	21	0.023
364	113	0.028	84	0.045	38	0.018	17	0.016
555	118	0.048	51	0.054	47	0.038	22	0.037
556	127	0.039	53	0.078	45	0.033	30	0.033
557	116	0.048	39	0.044	45	0.035	31	0.042
558	103	0.035	45	0.071	49	0.030	30	0.036
559	116	0.056	48	0.074	48	0.037	27	0.043
560	77	0.031	30	0.050	39	0.024	32	0.043

MO(13.5 to 12.4), ± 0m.0042 for the MO(12.4 to 10.8) and ± 0m.0056 for the MO(10.8 to 6). The differences between the MO(Δ m) curves are usually larger than their r.m.s. deviations, indicating that they are a better approximation than the MO(all), to the actual OCC curve, which varies continuously with magnitude.

Details of the numbers of stars with measures available in the OCC regions, the fraction of these selected for use by the 1.5 r.m.s. deviation cycle, and the distribution of the used stars in the various magnitude ranges are given in Table 10. On average, 63 percent of the available stars were retained in the 1.5 r.m.s. deviation cycle. This supports the use of this method – if the distribution of r.m.s. deviations were Gaussian, only approximately half of the stars would be retained. For only 3 plates is this condition approached.

Only about 1/5 of the stars used are brighter than m(E) = 10.8; the relative proportions of the stars in the fainter groups depend on the plate set. The final column of Table 10 gives the fraction of the stars in the MO(Δ m) rejected by the 1.5 r.m.s. deviation cycle which are in common with stars similarly rejected in the MO(all). On average it is 0.79.

Further support for the 1.5 r.m.s. deviation cycle comes from the fact, already noted, that no star once rejected by that cycle was reinstated during a later cycle of its set.

Table 10.

Numbers of Stars in the OCC Regions.

Plate Number	Stars in OCC Regions	Fraction used in MO(Δm)	Fraction of these in MO: >12.4	12.4–10.8	<10.8	Fraction rejected in MO(Δ m) also rejected in MO(all)
283	142	0.69	0.28	0.50	0.22	0.73
284	153	0.72	0.23	0.54	0.23	0.81
285	166	0.61	0.28	0.56	0.16	0.80
286	172	0.62	0.36	0.43	0.22	0.85
287	177	0.59	0.35	0.44	0.21	0.82
288	178	0.59	0.43	0.36	0.21	0.75
361	217	0.66	0.44	0.39	0.17	0.81
362	151	0.66	0.47	0.38	0.15	0.84
363	164	0.66	0.48	0.33	0.19	0.80
364	213	0.65	0.60	0.27	0.12	0.77
555	229	0.52	0.42	0.39	0.18	0.78
556	230	0.56	0.41	0.35	0.23	0.86
557	219	0.52	0.34	0.39	0.27	0.71
558	194	0.64	0.36	0.40	0.24	0.84
559	174	0.71	0.39	0.39	0.22	0.65
560	149	0.68	0.30	0.39	0.32	0.83
Mean per Plate:	183	0.63	0.38	0.41	0.21	0.79

4.3 VARIATIONS IN THE REGIONAL OCC CURVES.

When the OCC curves for the three regions of any particular plate are compared, significant differences are found and these differences are partially correlated between the plates of a set. To illustrate the effect, the deviations ($O_r - MO$) are listed in Table 11 for the MO(12.4 to 10.8) curves, together with the r.m.s. deviations of the MO. The mean ($O_r - MO$) and its r.m.s. deviation are also given for each plate set.

The maker's tolerance on large-scale variations in the transmission of the polaroid is $\pm$ 3 percent, which was confirmed by actual measurement. This implies that exposure through different areas of polaroid can itself cause magnitude differences of about 0m.03. Let the OCC regions be numbered I, II and III, and the actual pieces of polaroid be numbered 1, 2 and 3, Fig. 22. As the filter is rotated clockwise, each of the regions is exposed through a different piece of polaroid for the 3 exposures, namely

	1st	2nd	3rd	image
region I	1	2	3	
region II	2	3	1	
region III	3	1	2.	

Returning to the data of Table 11, by numbering the magnitude differences of region I 1, 2 and 3 and giving the same number to the corresponding magnitude differences (i.e. to the faintest, or to the brightest, etc.) in the other regions, the following cycles are found for the mean values of the 3 plate sets:

Table 11.

Example Deviations $O_r - MO$.

Plate Number	Rms of MO(Δm)	Region One $O_r - MO$			Region Two $O_r - MO$			Region Three $O_r - MO$		
283	0.005	−0.003	+0.036	−0.033	+0.016	−0.022	+0.005	−0.013	−0.015	+0.028
284	0.004	−0.024	+0.063	−0.038	+0.024	−0.027	+0.003	−0.000	−0.035	+0.036
285	0.004	−0.010	+0.016	−0.007	+0.012	+0.003	−0.016	−0.003	−0.020	+0.022
286	0.004	−0.026	+0.036	−0.010	+0.040	−0.017	−0.023	−0.014	−0.019	+0.033
287	0.003	−0.032	+0.029	+0.003	+0.033	−0.016	−0.017	−0.002	−0.013	+0.014
288	0.004	−0.026	+0.018	+0.007	+0.018	−0.001	−0.018	+0.007	−0.018	+0.011
Mean of Set		−0.020	+0.033	−0.013	+0.024	−0.013	−0.011	−0.004	−0.020	+0.024
Rms of Set		0.010	0.016	0.017	0.010	0.011	0.011	0.007	0.007	0.009
361	0.004	−0.011	−0.009	+0.020	−0.016	+0.013	−0.003	+0.027	−0.004	−0.023
362	0.004	−0.009	+0.024	−0.015	−0.004	+0.005	−0.001	+0.014	−0.030	+0.016
363	0.004	−0.020	+0.027	−0.006	−0.006	+0.009	−0.003	+0.026	−0.036	+0.009
364	0.003	+0.007	−0.009	+0.001	−0.004	+0.006	−0.002	−0.003	+0.003	+0.000
Mean of Set		−0.008	+0.008	0.000	−0.008	+0.008	−0.002	+0.016	−0.017	0.000
Rms of Set		0.008	0.014	0.010	0.005	0.003	0.001	0.012	0.017	0.015
555	0.006	−0.024	+0.013	+0.011	+0.052	−0.018	−0.034	−0.028	+0.005	+0.023
556	0.005	−0.008	+0.001	+0.007	+0.016	+0.000	−0.016	−0.008	−0.001	+0.009
557	0.005	−0.028	−0.008	+0.036	+0.026	+0.010	−0.036	+0.002	−0.002	+0.000
558	0.004	−0.016	+0.002	+0.014	+0.009	+0.003	−0.013	+0.007	−0.005	−0.001
559	0.005	−0.014	+0.008	+0.005	−0.002	+0.008	−0.007	+0.015	−0.017	+0.001
560	0.004	−0.017	+0.003	+0.014	−0.004	+0.008	−0.004	+0.021	−0.010	−0.010
Mean of Set		−0.018	+0.003	+0.014	+0.016	+0.002	−0.018	+0.001	−0.005	+0.004
Rms of Set		0.007	0.006	0.010	0.019	0.009	0.012	0.016	0.007	0.010

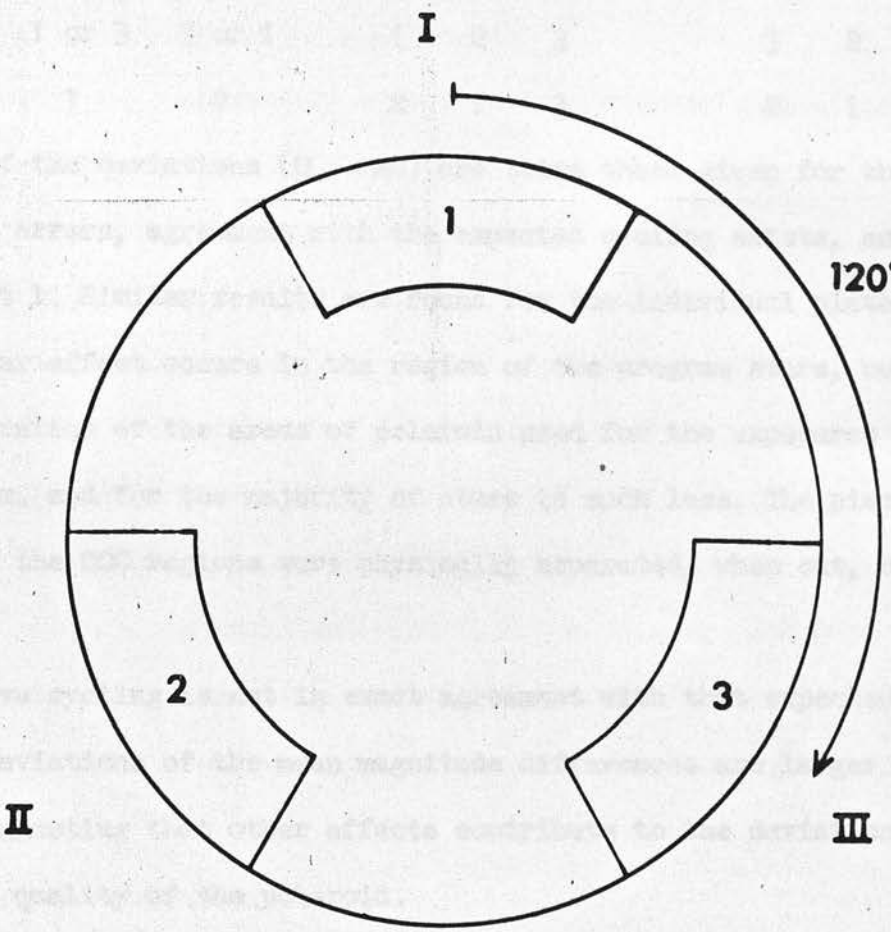

Figure 22. The numbering of the OCC regions, I, II and III, and of the individual pieces of polaroid, 1, 2 and 3.

Set 1			Set 2			Set 3		
1	2	3	1	2	3	1	2	3
2	1 or 3	3 or 1	1	2	3	3	2	1
3	1	2	2	1	3	2	1	3.

The errors of the deviations ($O_+ - MO$) are twice those given for the MO alone. Within these errors, agreement with the expected cycling exists, especially for plate set 1. Similar results are found for the individual plates.

A similar effect occurs in the region of the program stars, but the largest separation of the areas of polaroid used for the exposures of a star is about 2 cm. and for the majority of stars is much less. The pieces of polaroid for the OCC regions were physically separated, when cut, by larger distances.

The above cycling is not in exact agreement with that expected, and also, the r.m.s. deviations of the mean magnitude differences are larger than expected, suggesting that other effects contribute to the deviations.

(1) Optical quality of the polaroid.

In addition to the variation in transmission already noted, visual inspection shows the polaroid to be slightly corrugated, with peaks separated by about 2 cm. This produces lateral displacement of the images and some defocussing, which would be only partially cyclic as the distributions of stars in the regions are very different. The thickness of the polaroid is 380 microns. Variations in thickness of 0.1 percent over part of the 3 mm. diameter area of polaroid through which the beam of light for a particular star passes, can cause elongations of images of a few tenths of a

micron, which correspond to a few hundredths of a magnitude. No precise measures of such variations are yet available.

(2) Distribution of stars with magnitude.

The OCC curve varies continuously with magnitude and the same distribution of magnitude does not occur in all three regions. For the multiple image OCC curves described above, differences as large as 0m.05 are found for groups of stars differing in mean magnitude by only 1/3 of the range of the MO(Δ m).

(3) Variations in sky transparency across the area of a plate.

The centres of the OCC regions are $1^{\circ}.75$ apart and the exposures of the polarization plates were relatively short, 2 or 3.5 minutes. The integrated intensity of starlight transmitted by the atmosphere at such separations and exposures may not be constant. Measures with the Twin 16-inch photoelectric telescope suggest that compensation for astronomical 'seeing' for stars 1° apart may not be complete, but probably does not lead to residual errors exceeding $\pm$ 0m.005.

(4) Polarization of background light.

If the causes of background light are not polarized, its effect, even post-exposing the images, is removed by the OCC method. There is no nebulosity in h and chi Persei and with a sky background of V~19 per sec. arc^2, the effects of partial polarization of the sky background are negligible. Scattered Moonlight is polarized. For plate set 1, the Moon was about 40° below the horizon, while for plate set 2, the Moon was nearly full and 73° away from h and chi Persei. There is no significant difference for the sets of deviations of the two plate sets in Table 11. In the latter case, the position

angle of the expected polarization – at 90° to the great circle joining h and chi Persei and the Moon – is 164°. The measured mean differences of the background fog levels in the three regions for this set are –0.78, +3.81 and –0.73 iris units (those of the other plate sets are fractions of a unit), suggesting a polarized component in position angle 120°. The other polarized contribution comes from artificial sources – the Observatory is situated within the southern edge of Edinburgh. This source can vary considerably.

(5) Variations in emulsion sensitivity.

Lawrence and Reddish (1965) found variations in emulsion sensitivity of ± 0m.023 occuring at separations of 2 cm. The OCC regions are approximately 1×1.5 cm.^{2} in area, but are 4.5 cm. from centre to centre. However, relative brightnesses of close groups of images are preserved.

CHAPTER 5.

THE PHOTOGRAPHIC POLARIZATION MEASURES.

The calibration of the iris readings used the photoelectric magnitudes in the region measured by (1) Johnson and Morgan (1955) and (2) Wildey (1964), given in Table 12.

Column 1 gives the running number of the standards, which was the order of measurement; column 2 the Edinburgh number, as in the Catalogues and Charts; column 3 the number from Oosterhoff (1937); and column 4 the number from Wildey (1964), where the first number is Table 1,2 or 3 in that paper, the second number is the star number in that Table, and the third number or arabic letter, if they exist, give the associated stars in Tables 4,5 or 6 of that paper. The following 6 columns give the UBV measures. The V measures from the two sources have been brought together, as have the B–V and U–B measures respectively. The spectral types are given next, with the following sources: 1 – Johnson and Morgan (1955); 2 – Blanco (1955); 3 – Johnson and Hiltner (1956); and 4 – Hiltner (1956). The final column gives the mean m(E), the magnitude derived from the Ilford R40 panchromatic emulsion.

The photoelectric measures agree to within $\pm$ 0m.01 except for standard stars 6 and 33, and for the red supergiants 41, 45 and 48, all of which are discussed below.

The calibration curves were hand drawn through the centroid of the points and so are dominated by stars with B–V between + 0.2 and + 0.6. The

Table 12.

Photometric Standard Stars.

St.Ed. No.	Oost. No.	Wildey No.	V (1)	V (2)	B − V (1)	B − V (2)	U − B (1)	U − B (2)	Spectral Type	Source	m(E)
1	356	2572	—	10.02	—	+0.34	—	−0.51	—	—	9.97
2	403	2589	1.31	7.44	7.44	+0.72	+0.72	+0.11	+0.11	A2 Iap 1	7.50
3	404	2631	1.31.2	—	12.56	—	+0.42	—	−0.27	— —	12.66
4	—	2639	1.31.3	—	13.45	—	+0.70	—	+0.29	— —	—
5	396	2361	—	8.75	—	+0.38	—	−0.51	—	— —	8.75
6	62	2138	3.13	9.03	9.28	+0.50	+0.44	−0.65	−0.55	Bo IVpe 1	8.79
7	61	2084	3.13.2	—	12.09	—	+0.73	—	+0.40	— —	12.24
8	377	2144	1.25.1	—	12.33	—	+0.54	—	−0.13	— —	12.47
9	376	2178	1.25	6.38	6.38	+0.58	+0.58	+0.02	+0.02	A1 Ia 1	6.43
10	375	2189	1.25.3	—	12.26	—	+0.43	—	−0.30	— —	12.33
11	330	2262	—	10.38	—	+0.44	—	−0.60	—	— —	10.56
12	—	2194	—	13.45	—	+0.42	—	−0.13	—	— —	—
13	329	2165	—	9.86	—	+0.40	—	−0.62	—	— —	9.86
14	339	2227	1.26	8.05	8.05	+0.34	+0.34	−0.55	−0.55	B2 Ib 1	8.05
15	340	2246	3.14	9.90	9.90	+0.32	+0.32	−0.56	−0.56	B2 III 1	9.89
16	341	2251	—	11.56	—	+0.34	—	−0.34	—	B3 V 1	11.53
17	342	2200	—	12.67	—	+0.36	—	−0.25	—	— —	12.69
18	—	2167	—	13.36	—	+0.41	—	−0.13	—	— —	—
19	325	2139	—	11.38	—	+0.27	—	−0.49	—	B2 V 1	11.29
20	324	2133	—	12.21	—	+0.33	—	−0.38	—	— —	12.19
21	323	2088	—	9.45	—	+0.32	—	−0.65	—	— —	9.47
22	—	2241	—	13.58	—	+0.43	—	+0.02	—	— —	—
23	344	2253	—	12.71	—	+0.41	—	−0.10	—	— —	12.58
24	—	2269	—	13.19	—	+0.39	—	−0.19	—	— —	—
25	345	2296	—	8.53	—	+0.30	—	−0.56	—	— —	8.50
26	347	2311	—	9.38	—	+0.30	—	−0.54	—	— —	9.35
27	348	2330	—	11.42	—	+0.24	—	−0.39	—	— —	11.39
28	352	2371	—	9.25	—	+0.32	—	−0.55	—	— —	9.21
29	—	2426	1.29.1	—	13.69	—	+0.49	—	+0.06	— —	—
30	350	2417	1.29	8.31	8.31	+2.29	+2.29	+2.28	+2.28	M4.5 Iab 2	8.12

Table 12 (cont.)

St.Ed. No.	Oost. No.	Wildey No.	V (1)	V (2)	B − V (1)	B − V (2)	U − B (1)	U − B (2)	Spectral Type	Source	m(E)
31 –	2421	1.29.2	–	13.17	–	+0.72	–	+0.32	–	–	–
32 –	2515	3.15.2	–	13.41	–	+0.37	–	−0.16	–	–	–
33 349	2349	1.29.a	12.81	12.81	+0.36	+0.55	−0.28	+0.37	–	–	12.85
34 319	2284	–	9.66	–	+0.40	–	−0.59	–	–	–	9.63
35 320	2185	–	10.92	–	+0.33	–	−0.25	–	B3 V	1	10.93
36 517	2172	2.2	8.50	8.50	+0.16	+0.16	−0.79	−0.79	O6	1	8.46
37 –	2152	2.2.2	–	13.21	–	+1.23	–	+0.40	–	–	–
38 –	1910	3.12.1	–	13.38	–	+0.72	–	+0.18	–	–	–
39 510	1899	3.12	8.53	8.53	+0.32	+0.32	−0.53	−0.53	B2 II	1	8.53
40 508	1781	–	9.21	–	+0.30	–	−0.50	–	–	–	9.20
41 254	1655	1.21	7.81	7.85	+2.28	+2.23	+2.47	+2.43	M2.5 Iab	2	7.97
42 261	1586	3.10	8.96	8.97	+0.32	+0.32	−0.54	−0.54	B1 III	1	9.02
43 –	1628	3.10.1	–	13.56	–	+0.50	–	−0.82	–	–	–
44 262	1575	3.10.2	–	12.12	–	+1.95	–	+1.89	–	–	12.30
45 289	1818	1.23	7.97	7.91	+2.26	+2.27	+2.54	+2.57	M1 Iab	2	8.02
46 –	1211	1.16.b	12.58	12.58	+0.60	+0.60	+0.32	+0.32	–	–	–
47 23	983	1.16.a	–	10.65	–	+1.27	–	+1.26	–	–	10.80
48 22	899	1.16	9.25	9.16	+2.47	+2.47	+2.67	+2.63	M3.5 Ib	2	9.20
49 136	1119	–	12.57	–	+1.40	–	+1.23	–	–	–	12.90
50 145	717	–	9.28	–	+0.30	–	−0.56	–	–	–	9.29
51 –	689	1.15.1	–	13.21	–	+0.48	–	+0.32	–	–	–
52 144	662	1.15	8.18	8.18	+0.30	+0.31	−0.59	−0.59	B1 Ib	1	8.22
53 –	620	1.15.2	–	13.01	–	+0.37	–	−0.16	–	–	–
54 225	800	–	12.25	–	+0.36	–	−0.28	–	–	–	12.21
55 219	978	–	10.59	–	+0.38	–	−0.44	–	B1.5 V	1	10.59
56 227	950	–	11.29	–	+0.36	–	−0.40	–	B2 V	1	11.26
57 228	1015	–	10.57	–	+0.28	–	−0.10	–	–	–	10.51
58 230	1162	1.18	6.66	6.66	+0.51	+0.51	−0.45	−0.45	B2 Ia	1	6.65
59 231	1187	3.9	10.82	10.82	+0.39	+0.39	−0.40	−0.40	B2 IV	1	10.82
60 –	1171	1.18.3	–	13.50	–	+0.60	–	+0.30	–	–	–

Table 12 (cont.)

St.Ed. No.	No.	Oost. No.	Wildey No.	V (1)	V (2)	B − V (1)	B − V (2)	U − B (1)	U − B (2)	Spectral Type	Source		m(E)
61	–	1182	1.18.2	–	13.62	–	+0.52	–	+0.16	–	–		–
62	–	1150	–	13.23	–	+0.98	–	+0.48	–	–	–		–
63	–	1166	3.9.a	13.12	13.12	+0.54	+0.54	−0.10	−0.10	–	–		–
64	206	1181	–	12.65	–	+0.40	–	−0.23	–	–	–		12.62
65	204	1202	3.9.b	12.12	12.12	+0.44	+0.44	−0.22	−0.22	–	–		12.09
66	210	1078	–	9.75	–	+0.34	–	−0.49	–	B1 V	1		9.76
67	–	1000	–	13.23	–	+0.41	–	+0.02	–	–	–		–
68	–	960	–	13.69	–	+0.43	–	0.00	–	–	–		–
69	212	843	–	9.32	–	+0.31	–	−0.53	–	–	–		9.32
70	193	869	–	11.96	–	+0.37	–	−0.20	–	–	–		11.99
71	188	782	–	9.45	–	+0.27	–	−0.55	–	–	–		9.47
72	186	864	–	9.94	–	+0.31	–	−0.49	–	B1 V	1		9.93
73	185	867	–	10.51	–	+0.62	–	+0.12	–	–	–		10.62
74	183	847	–	9.11	–	+0.38	–	−0.52	–	–	–		9.15
75	–	681	3.8.1	–	12.72	–	+0.28	–	−0.35	–	–		–
76	112	339	3.7	8.85	8.85	+0.31	+0.31	−0.61	−0.61	B1 IV	1		8.89
77	113	311	3.7.2	–	12.54	–	+0.42	–	−0.28	–	–		12.51
78	118	230	–	13.68	–	−0.12	–	−0.92	–	–	–		13.28
79	86	49	–	9.08	–	+0.26	–	−0.66	–	B1 II	4		9.06
80	97	16	1.12	6.49	6.49	+0.28	+0.28	−0.65	−0.65	B1 Iab	1		6.47
81	–	66	1.12.1	–	13.20	–	+0.75	–	+0.16	–	–		–
82	96	–	1.11.2	–	12.38	–	+0.27	–	−0.37	–	–		12.27
83	98	3	1.11	7.40	7.39	+0.24	+0.23	−0.66	−0.65	B2 Ib	1		7.38
84	99	7	1.11.1	–	12.08	–	+0.23	–	−0.36	–	–		12.00
85	440	146	–	9.19	–	+0.17	–	−0.67	–	B1 IV	3		9.18

calibrations were stored in the computer in the form of line segments, each specified by its end points and gradient in magnitudes per iris unit. Fainter than V = 11.5 the magnitude interval was 0m.25, brighter than V = 11.5 it was 0m.50.

The magnitude of each star was determined from all the plates on which the first image could be measured. The number of measures, mean magnitude and r.m.s. deviation per measure are given for each star in the Catalogue at the end of this thesis. This r.m.s. deviation is plotted against mean magnitude in Fig. 23. The distribution is smooth to V = 12 and then rises sharply as the plate limit is approached. Six stars having unusually large deviations are discussed below. Omitting these stars, for V < 12.00, the mean r.m.s. deviation per measure is $\pm$ 0m.050.

The magnitude measures for six stars with large r.m.s. deviations are summarised in Table 13. For each plate set, the number of measures, mean magnitude and r.m.s. deviation per measure are given. The mean Julian date of each set is also given. The final column gives the variable star designation from the General Catalogue of Variable Stars (Kukarkin and others, 1958).

The identified variables are semiregular long-period variables, and include standard stars 41 and 48, with differing photoelectric measures. Standard star 45 is star 289, which is FZ Persei, an irregular long-period variable, for which V = 8.02 $\pm$ 0.04.

Stars 89 and 91 appear to be similar, with large differences in mean magnitude and small r.m.s. deviations. Star 453 has large r.m.s. deviations suggesting light variations within the time (about two hours) to obtain one

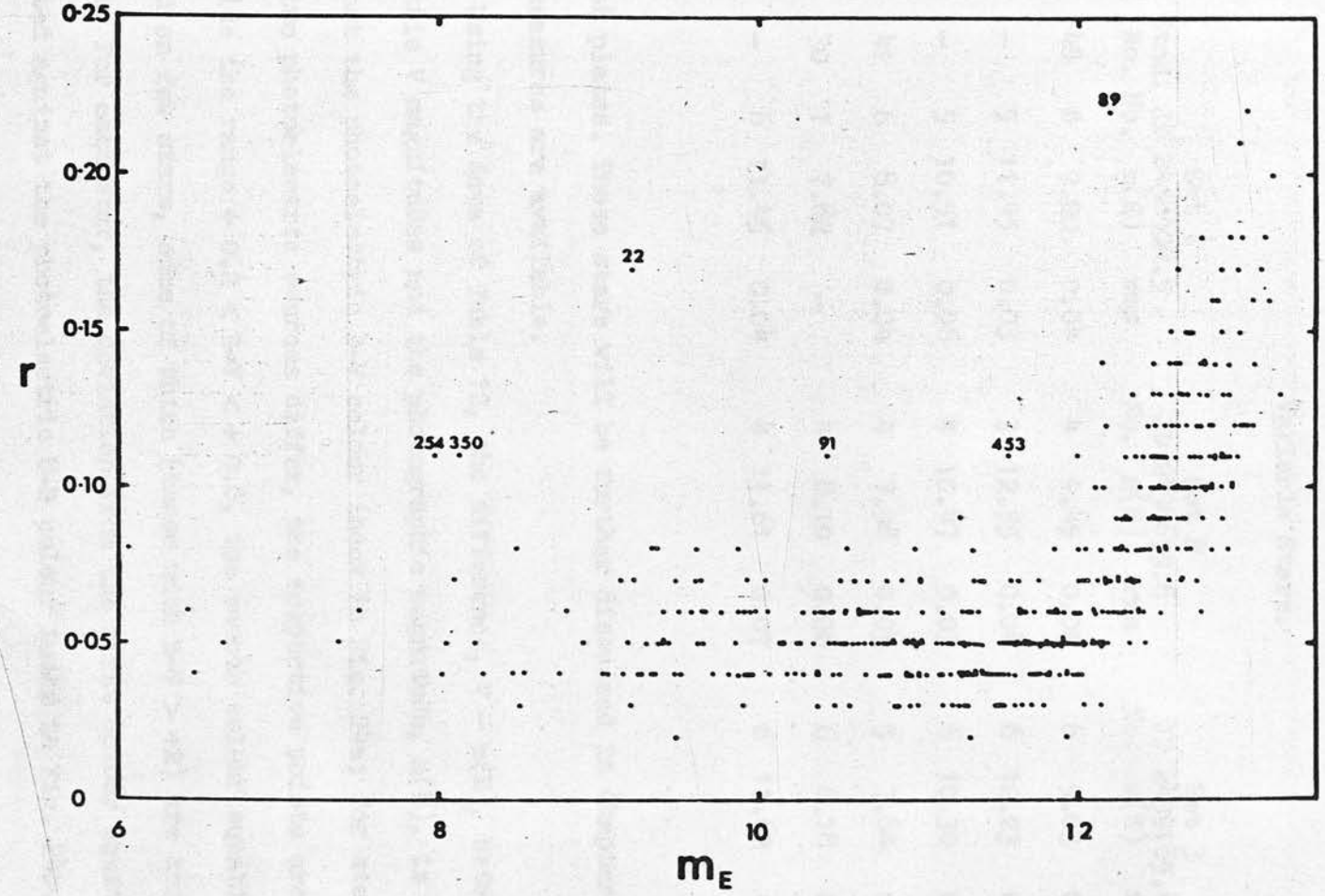

Figure 23. R.m.s. deviation per magnitude measure against magnitude for the 527 stars. Stars with large deviations are numbered.

Table 13.

Variable Stars.

Star No.	Stnd. No.	Set 1 JD 2438404.5 No.	m(E)	rms	Set 2 JD 2438659.6 No.	m(E)	rms	Set 3 JD 2439185.4 No.	m(E)	rms	Variable Designation
22	48	6	9.20	0.04	4	9.45	0.02	6	9.03	0.05	BU Per
89	–	5	11.95	0.03	3	12.55	0.04	6	12.23	0.04	–
91	–	5	10.51	0.06	4	10.47	0.03	6	10.30	0.02	–
254	41	6	8.07	0.04	4	7.98	0.05	5	7.84	0.03	AD Per
350	30	1	7.82	–	4	8.10	0.06	6	8.18	0.03	RS Per
453	–	6	11.45	0.04	4	11.61	0.07	6	11.62	0.08	–

set of plates. These stars will be further discussed in Chapter 6 when their UBV measures are available.

Using the data of Table 12, the difference, $V - m(E)$, between the photoelectric V magnitudes and the photographic magnitude, m(E), is plotted against the photoelectric B–V colour index in Fig. 24a; for stars for which the two photoelectric sources differ, the respective points are joined. Outside the range $+0.2 < B-V < +0.6$, the smooth colour equation found is based on few stars, some of which (those with $B-V > +2$) are known variable stars. For each star, the deviation from the first colour equation, Δ CE, is plotted against the photoelectric U–B colour index in Fig. 24b. Here there is

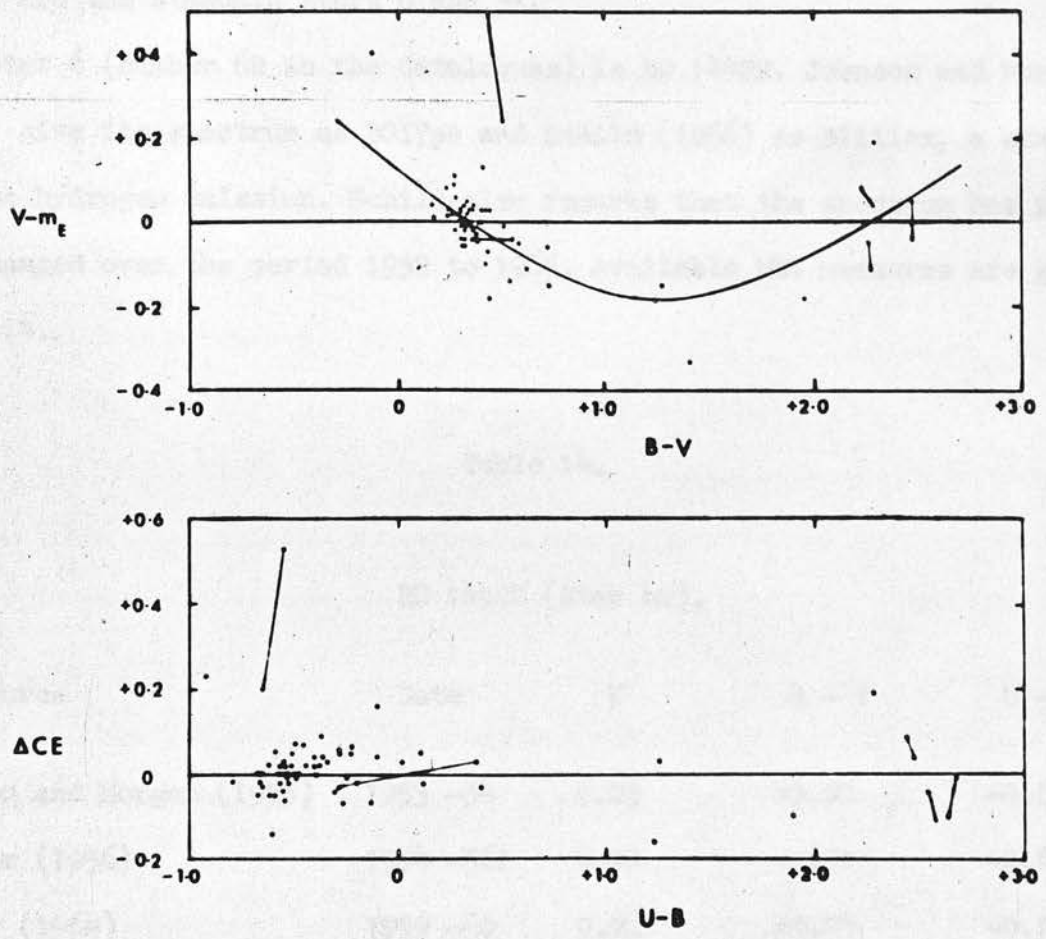

Figure 24. Colour equations between the UBV system and the Ilford R40 emulsion.

no colour equation.

The two other stars noted above for which the photoelectric sources differ are the standard stars 6 and 33.

Star 6 (number 62 in the Catalogues) is HD 14422. Johnson and Morgan (1955) give its spectrum as BOIVpe and Schild (1966) as B1iiiex, a star with extreme hydrogen emission. Schild also remarks that the spectrum has probably not changed over the period 1952 to 1965. Available UBV measures are given in Table 14.

Table 14.

HD 14422 (Star 62).

Source	Date	V	B – V	U – B
Johnson and Morgan (1955)	1953 –54	9.03	+0.50	–0.65
Hiltner (1956)	1954 –56?	8.99	+0.51	–0.64
Wildey (1964)	1959 –60	9.28	+0.44	–0.55
Edinburgh (see text)	1961 Oct.	9.3 (4)	+0.6 (4)	–0.6 (2)
" " "	1964 Jan.	8.80(6)		
" " "	1964 Sep.	8.76(4)		
" " "	1965 Mar.	8.68(5)	+0.56(5)	–0.35(1)
" " "	1966 Feb.	8.68(6)		[8.89(3)]
" " "	1966 Oct.	8.86(5)	+0.55(5)	–0.56(5)
" " "	1968 Jan.	9.03	+0.50	–0.65

The Edinburgh 1961 measures are from rather poor plates; the 1964 and 1966 February V magnitudes are from the polarization plates, corrected by the colour equation of Fig. 24a; the 1965 and 1966 February U measures are from UBV plates corrected by preliminary colour equations to the standard system; and the 1966 October measures are from the UBV measures described in Chapter 6. The 1968 measures are by Sherwood using the Twin 16-inch photoelectric telescope. The U magnitude given in brackets for 1966 February is the same as the actual U magnitude for 1965 March.

The star is variable, but too few observations are yet available. Hill (1967) has found light variations on a short time scale, $\pm$ 0m.04 from 12 observations on 3 nights. The two available spectra were obtained when the magnitude and colours were very similar: spectra taken at other phases would be of great interest.

Available UBV measures for standard star 33 (number 349) are given in Table 15. The sources of the Edinburgh magnitudes are as described for Table 14. The colours of Wildey appear to be in error. Schild (1965) and Reddish (1967) have also noted apparent errors in these colours.

The complete polarization parameters of the 527 stars measured in h and chi Persei are given in the Catalogue at the end of this thesis. In addition to p and θ_o in equatorial coordinates, the Catalogue gives the Stokes parameters, Q and U, in columns 14 and 15 for each star.

Table 15.

Star 349.

Source	Date	V	B − V	U − B
Johnson and Morgan (1955)	1953 –54	12.81	+0.36	–0.28
Wildey (1964)	1959 –60	12.81	+0.55	+0.37
Edinburgh (see text)	1961	12.9	+0.3	–0.4
" " "	1964	12.84		
" " "	1965 –66	12.86	+0.36	–0.28
" " "	1966Feb	12.84		
" " "	1966 Oct.	12.82	+0.36	–0.34

5.1 COMPARISON WITH PHOTOELECTRIC MEASURES:

Polarization parameters have been measured photoelectrically for 64 of the stars measured in the present program (by Hiltner (1951) – reference 1a in the relevant tables; Hiltner (1956) – ref. 1; Hall (1958) – ref. 2; and Serkowski (1965a) – ref. 3).

Table 16 lists the measures for the 15 stars which have photoelectric measures by more than one observer; the Stokes parameters are shown in Fig.25, the corresponding measures for each star being joined. Taking these measures in all 17 possible pairs (since one star was measured by all three), the

Table 16.

Stars with two or more Photoelectric Polarization Measures.

Star Number	HD or BD Number	Source	p	P.A.	Q	U
97	13854	1	0.083	112	-0.060	-0.058
		2	0.078	110	-0.060	-0.050
98	13841	1	0.073	111	-0.054	-0.049
		2	0.062	114	-0.042	-0.046
112	13969	1	0.096	114	-0.064	-0.071
		2	0.110	114	-0.074	-0.082
144	14052	1	0.088	116	-0.054	-0.069
		3	0.089	116	-0.055	-0.070
210	+56 524	2	0.080	111	-0.059	-0.054
		3	0.074	110	-0.057	-0.048
230	14143	1	0.086	117	-0.051	-0.070
		2	0.087	116	-0.054	-0.069
		3	0.083	117	-0.049	-0.067
236	14162	1	0.091	115	-0.058	-0.070
		3	0.088	117	-0.052	-0.071
241	+56 534	2	0.115	114	-0.077	-0.086
		3	0.098	110	-0.075	-0.063
289	14330	1a	0.084	115	-0.054	-0.064
		2	0.095	113	-0.066	-0.068
339	14443	1	0.082	117	-0.048	-0.066
		3	0.082	115	-0.053	-0.063
350	14488	1a	0.076	124	-0.028	-0.070
		3	0.084	124	-0.032	-0.078
376	14433	1	0.086	112	-0.062	-0.060
		2	0.080	117	-0.047	-0.065
396	14476	1a	0.078	113	-0.054	-0.056
		2	0.074	114	-0.050	-0.055
403	14535	1	0.077	111	-0.057	-0.052
		2	0.070	115	-0.045	-0.054
517	14434	1	0.084	116	-0.052	-0.066
		2	0.093	117	-0.055	-0.075

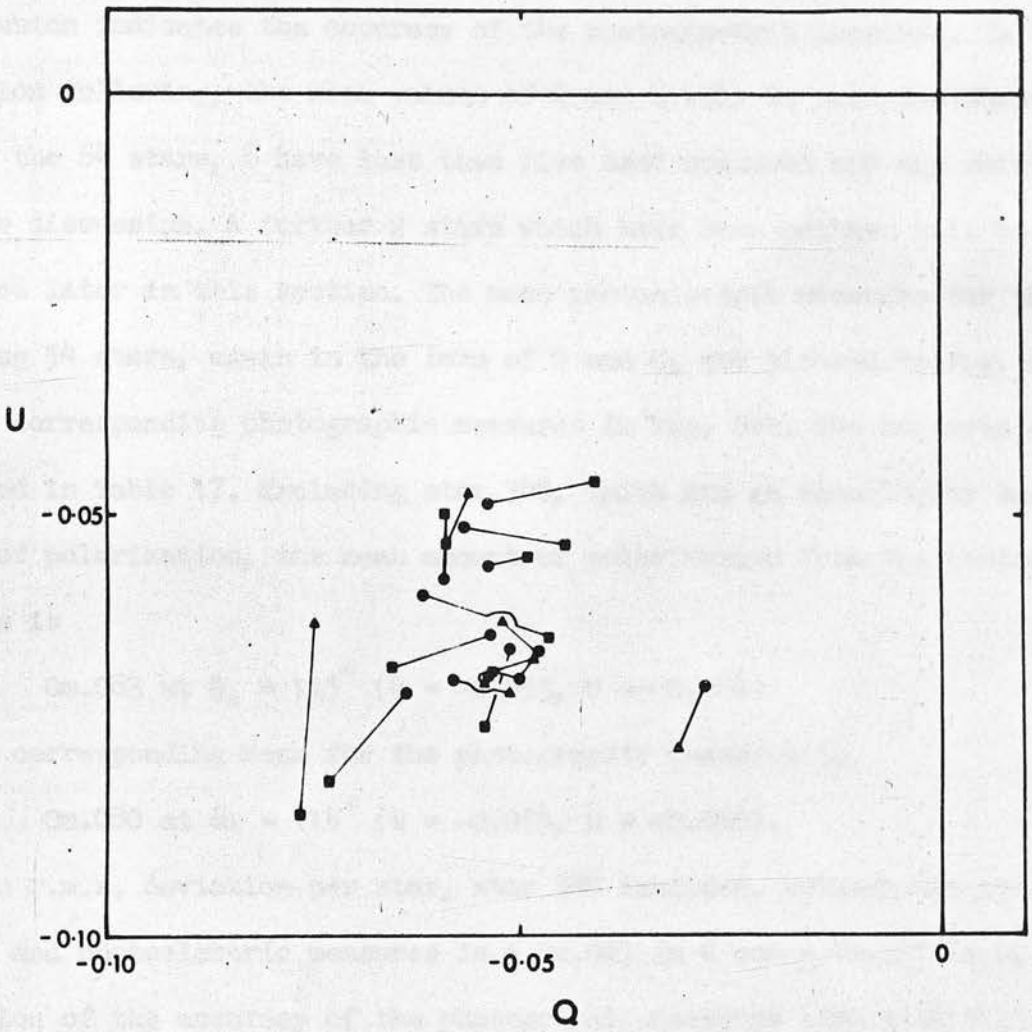

Figure 25. Stokes parameters of stars having more than one photoelectric polarization measure.
• Hiltner (1951) and (1956),
■ Hall (1958) and
▲ Serkowski (1965a).

r.m.s. deviation about the mean values is ± 0m.0037 per measure in both Q and U, which indicates the accuracy of the photoelectric measures. In the discussion following, the mean values of Q and U will be used for these stars.

Of the 64 stars, 8 have less than five used measures and are omitted from the discussion. A further 2 stars which have been omitted will be discussed later in this section. The mean photoelectric measures for the remaining 54 stars, again in the form of Q and U, are plotted in Fig. 26a, and the corresponding photographic measures in Fig. 26b. The measures are collected in Table 17. Excluding star 348, which has an anomalously small amount of polarization, the mean amount of polarization from the photoelectric measures is

$$0^m.083 \text{ at } \theta_o = 115^\circ \quad (Q = -0.053,\ U = -0.064)$$

and the corresponding mean for the photographic measures is

$$0^m.080 \text{ at } \theta_o = 114^\circ \quad (Q = -0.054,\ U = -0.059).$$

The mean r.m.s. deviation per star, star 348 included, between the photographic and photoelectric measures is ± 0m.027 in Q and ± 0m.031 in U, an indication of the accuracy of the photographic measures (see also 5.3). Star 348, whose values are indicated in Fig. 26, has the largest deviation. It should be noted that the Observing Conditions Control curves are less well defined for these bright stars and most of these latter lie in the dense cluster regions where overlapping is probable. The r.m.s. deviations of the magnitude measures were shown in Fig. 23 to be uniform from the brightest stars to those with m(E) = 12. Probably, therefore, the above accuracy in the polarization parameters applies to the same magnitude limit.

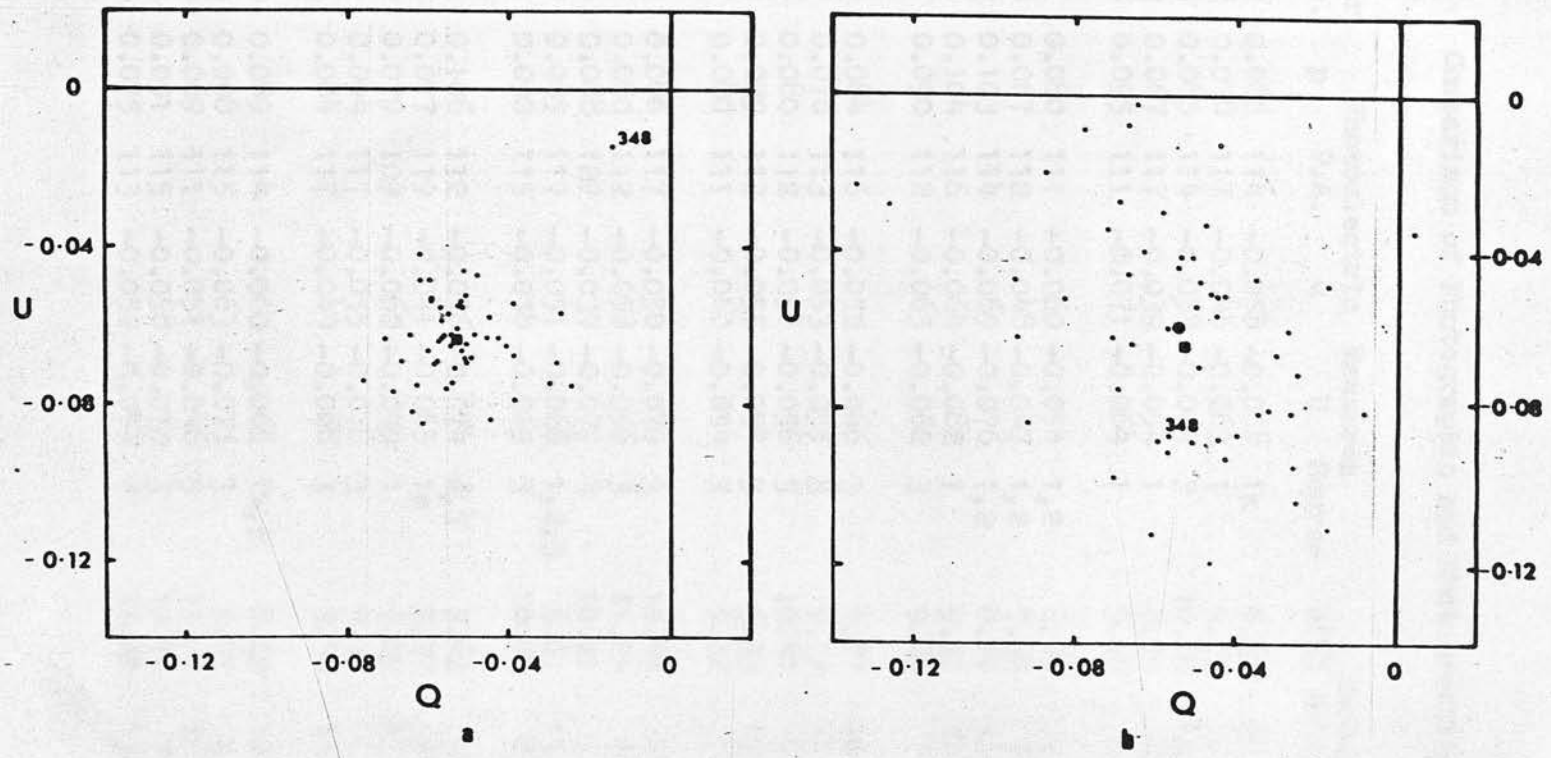

Figure 26. Stokes parameters of stars with photoelectric measures.
(a) the photoelectric measures, with ■ the mean value.
(b) photographic measures of the same stars, with • the mean value.

Table 17.

Comparison of Photographic and Photoelectric Polarization Measures.

Star No.	Photoelectric Measures p	P.A.	Q	U.	Source	Photographic Measures m(E)	No.used	p	P.A.	Q	U
22	0.086	114	−0.058	−0.064	1a	9.20	10	0.086	124	−0.032	−0.080
55	0.078	117	−0.046	−0.063	1	9.81	10	0.065	91	−0.065	−0.002
57	0.085	114	−0.057	−0.063	3	10.84	15	0.080	103	−0.072	−0.034
62	0.067	117	−0.039	−0.054	1	8.79	8	0.078	93	−0.078	−0.009
86	0.095	111	−0.071	−0.064	1	9.06	9	0.068	109	−0.054	−0.041
97	0.080	111	−0.060	−0.054	1,2	6.47	7	0.058	107	−0.048	−0.033
98	0.067	112	−0.048	−0.047	1,2	7.38	7	0.074	114	−0.050	−0.054
112	0.103	114	−0.069	−0.076	1,2	8.89	10	0.081	107	−0.067	−0.046
123	0.104	116	−0.064	−0.082	1	9.37	12	0.069	112	−0.049	−0.048
167	0.090	112	−0.065	−0.062	3	9.40	7	0.090	96	−0.088	−0.020
180	0.084	116	−0.052	−0.066	3	9.87	12	0.086	117	−0.050	−0.069
183	0.076	113	−0.053	−0.055	3	9.15	13	0.070	109	−0.054	−0.044
184	0.080	112	−0.058	−0.056	3	10.47	9	0.124	111	−0.092	−0.084
186	0.079	113	−0.055	−0.057	3	9.93	13	0.082	113	−0.057	−0.059
212	0.080	111	−0.060	−0.054	3	9.32	5	0.136	95	−0.134	−0.023
219	0.086	117	−0.050	−0.070	3	10.59	7	0.068	114	−0.045	−0.051
227	0.080	112	−0.058	−0.056	3	11.26	6	0.112	131	−0.018	−0.111
228	0.088	122	−0.039	−0.079	3	10.51	7	0.046	98	−0.044	−0.013
230	0.085	117	−0.051	−0.068	1,2,3	6.65	15	0.035	138	+0.004	−0.035
231	0.090	115	−0.058	−0.069	3	10.82	8	0.067	115	−0.043	−0.051
241	0.106	112	−0.076	−0.074	2,3	9.62	9	0.113	107	−0.094	−0.062
254	0.077	119	−0.041	−0.065	1a	7.97	15	0.107	119	−0.057	−0.090
261	0.079	109	−0.062	−0.049	1	9.02	13	0.051	125	−0.017	−0.048
281	0.094	117	−0.055	−0.076	3	9.35	6	0.098	106	−0.083	−0.052
288	0.084	117	−0.049	−0.068	3	9.50	13	0.065	104	−0.058	−0.030
289	0.089	114	−0.060	−0.066	1a,2	8.02	12	0.092	112	−0.066	−0.063
290	0.098	115	−0.063	−0.075	3	9.91	6	0.073	123	−0.030	−0.066
296	0.069	111	−0.051	−0.046	3	11.02	15	0.095	123	−0.040	−0.086
316	0.091	115	−0.058	−0.070	3	10.78	7	0.075	125	−0.025	−0.071
317	0.075	113	−0.052	−0.054	3	11.26	13	0.102	123	−0.043	−0.092

Table 17 (cont.)

Star No.	Photoelectric Measures p	P.A.	Q	U	Source	Photographic Measures m(E)	No.used	p	P.A.	Q	U
319	0.076	118	-0.042	-0.063	3	9.63	14	0.106	118	-0.060	-0.088
320	0.076	109	-0.060	-0.047	3	10.93	10	0.128	124	-0.046	-0.119
323	0.095	121	-0.045	-0.084	3	9.47	5	0.098	127	-0.026	-0.094
329	0.063	122	-0.028	-0.057	3	9.86	12	0.102	113	-0.070	-0.075
330	0.078	120	-0.039	-0.068	3	10.56	10	0.072	116	-0.045	-0.056
337	0.079	116	-0.049	-0.062	3	11.51	7	0.102	120	-0.051	-0.089
339	0.082	116	-0.050	-0.065	1,3	8.05	15	0.081	132	-0.008	-0.081
345	0.082	113	-0.057	-0.059	3	8.50	7	0.094	111	-0.071	-0.062
347	0.073	116	-0.045	-0.058	3	9.35	6	0.106	103	-0.095	-0.047
348	0.021	112	-0.015	-0.015	3	11.39	11	0.104	118	-0.057	-0.087
350	0.080	124	-0.030	-0.074	1a,3	8.12	5	0.088	123	-0.035	-0.081
356	0.085	115	-0.055	-0.065	3	9.97	12	0.075	101	-0.070	-0.027
363	0.084	114	-0.056	-0.062	3	10.62	10	0.085	126	-0.026	-0.081
376	0.083	114	-0.054	-0.062	1,2	6.43	13	0.075	106	-0.063	-0.040
389	0.088	112	-0.063	-0.061	3	9.91	11	0.129	96	-0.126	-0.028
396	0.076	114	-0.052	-0.056	1a,2	8.75	9	0.066	123	-0.027	-0.060
403	0.073	113	-0.051	-0.053	1,2	7.50	10	0.069	114	-0.046	-0.051
426	0.075	107	-0.062	-0.042	1	8.48	10	0.066	109	-0.052	-0.041
442	0.075	124	-0.028	-0.070	1	9.60	10	0.068	93	-0.067	-0.008
447	0.079	126	-0.024	-0.075	1	9.64	15	0.059	116	-0.036	-0.047
508	0.092	117	-0.054	-0.074	3	9.20	14	0.120	117	-0.070	-0.098
510	0.096	113	-0.067	-0.069	1	8.53	10	0.106	128	-0.025	-0.104
517	0.088	116	-0.053	-0.071	1,2	8.46	7	0.098	121	-0.045	-0.088
527	0.105	117	-0.062	-0.085	3	10.47	13	0.128	121	-0.061	-0.112

The r.m.s. scatter per star of the photoelectric measures about their mean is ± 0m.011 in Q and ± 0m.010 in U. Comparing this with the accuracy of ± 0m.004 per measure derived above, the scatter of the polarization parameters in h and chi Persei is real.

The computer output of the polarization reduction program for stars 397 and 440 which were previously omitted is reproduced in Fig. 27. The photoelectric measures of these stars – 397 was measured by Hall and 440 by Hiltner – have been added, together with the corresponding magnitude differences. Subtracting the latter magnitude differences from those measured, the deviations are

	+ 0.041	−0.071	+ 0.034	for star 397
and	+ 0.011	−0.056	+ 0.046	for star 440.

In both cases, the second image is too bright, by 0m.11 for star 397 and 0m.08 for star 440, and the enhancement arises from measures on plate set 3. From equation (15) in 2.1, such enhancements could be due to overlapping by stars 2 to 3 magnitudes fainter, i.e. about m(E) = 12.5. From the charts of Oosterhoff (1937) however, there are no possible overlaps to m(pg) = 16. The observing system effects discussed in 2.1, which affect areas of plate 3 mm. in diameter, can also be discounted as the three images of stars on plate set 3 are separated by only 0.8 mm. and nearby stars have not been affected. A filter defect can similarly be discounted. Emulsion defects would require an extraordinary coincidence to be repeated from plate to plate. The occurrence of such errors whose existence was detected only from the existing photoelectric measures, which cannot be seriously questioned, is disturbing.

POLARIZATION REDUCTION OUTPUTS

STAR 397 X= 88.8 Y= 26.0

FOG -0.65 RMS 1.20

MAG 12 9.59 RMS 0.08

POLN 7 PLATES CYCLES 2

USED 6

PLATE	FOG	MAG	DM1	DM2	DM3	RMS	
1	0.11	9.71	0.064	-0.053	-0.011	0.008	
11	-0.89	9.57	0.054	-0.050	-0.004	0.012	
12	-0.38	9.51	0.073	-0.076	0.003	0.009	
14	-0.50	9.52	0.061	-0.046	-0.015	0.013	
15	0.81	9.48	0.077	-0.077	0.000	0.009	
16	-3.89	9.55	0.091	-0.080	-0.011	0.016	
ED PAR			0.071	-0.063	-0.005	0.011	C=-0.0011

POLN 0.154 AT 77 D Q= -0.138 U= 0.069

STARS 1.5 RMSD 1 0.017

2	-1.71	9.64
3	-1.06	9.67
4	0.11	9.62
5	-0.23	9.69
6	-0.86	9.61
7		
8		
9		
10		
13	0.65	9.50

0.032	-0.060	0.029	0.030

PH.EL. POLN 0.080 AT 106 D

WITH ED PAR	0.030	0.008	-0.039

Figure 27. Computer output from the Polarization Reduction Program for Star 397, together with its photoelectric measures.

STAR 440 X=944.3 Y=942.7

FOG -0.93 RMS 1.87

MAG 12 9.18 RMS 0.05

POLN 12 PLATES CYCLES 4

USED 9

PLATE	FOG	MAG	DM1	DM2	DM3	RMS
3	-0.06	9.17	-0.001	0.025	-0.024	0.048
4	1.11	9.21	0.015	0.008	-0.022	0.035
5	-0.23	9.20	0.053	-0.016	-0.037	0.032
6	1.14	9.19	0.078	-0.038	-0.039	0.038
11	-3.89	9.19	-0.000	-0.042	0.042	0.027
12	0.99	9.14	0.049	-0.056	0.007	0.012
13	-2.35	9.12	0.009	-0.071	0.062	0.038
14	-3.50	9.10	0.089	-0.098	0.009	0.046
15	-0.57	9.13	0.013	-0.090	0.078	0.050
ED PAR			0.034	-0.042	0.009	0.038

C=-0.0004

POLN 0.089 AT 69 D Q= -0.067 U= 0.059

STARS 1.5 RMSD 3 0.057

1						
2	1.29	9.25	0.076	0.025	-0.101	0.078
7						
8						
9	-2.02	9.15	0.068	0.043	-0.110	0.086
10						
16	-3.13	9.27	-0.071	-0.037	0.108	0.083

PH.EL. POLN 0.075 AT 116 D

WITH ED PAR 0.023 0.014 -0.037

Figure 27 (cont.). Polarization Reduction for Star 440.

5.2 THE POLARIZATION RESULTS.

For a preliminary presentation of the polarization results, the stars have been divided in two ways: firstly, by magnitude at m(E) = 11.99 – stars brighter have an r.m.s. deviation per magnitude measure of ± 0m.050 and those fainter have errors increasing with decreasing brightness; secondly, by the number of measures used to derive the polarization parameters into 3 groups – those with measures from 10 or more, 9 to 5 and 4 or less plates. The numbers of stars in the various categories are:

number of plates used	16 – 10	9 – 5	⩽ 4
m(E) ⩽ 11.99	191	96	20
m(E) > 11.99	106	98	16.

Details of the number of measures made and the number of measures retained for use after selection by the 1.5 r.m.s. deviation cycle for the bright and for the faint stars separately are given in Table 18. On average, 75 percent of the measures are retained for the bright stars and 73 percent for the faint stars, again supporting the use of this method.

For each plate, the number of stars with polarization measures and the fraction retained for use after application of the 1.5 r.m.s. deviation cycle, are given in Table 19.

The Stokes parameters for the bright stars are plotted in Fig. 28, the stars with 10 or more measures being represented by filled circles, and stars with 9 to 5 measures by open circles. Stars with 4 or less measures are omitted. The faint stars are similarly shown in Fig. 29.

Table 18.

Numbers of Polarization Measures Used.

Number of Measures used	16	15	14	13	12	11	10	9	8	7	6	5	4	3	2	1	0	Total
Stars brighter than m(E) = 12.00																		
Number of Measures made																		
16	3	17	13	21	16	22	10	7	5	11	1							126
15		6	6	13	7	9	8	8	2	7								66
14			3	5	1	5	9	1			3							27
13				3	2	2	3	3	1		1							15
12					1	2		3	1		1							8
11							1	4	4	1	2							12
10							3	6	2	2		1						14
9								2		2	1		1					6
8									2	1		1						4
7										2	2	1	1					6
6											2	2	1					5
5												1	2					3
4													3	1				4
3														2				2
2															3			3
1																4		4
0																	2	2
Stars fainter than m(E) = 12.00																		
16	1	4	10	6	9	6	1	6	4	5								52
15		1	5	7	6	3	10	5	6	1								44
14			1	4	4	7	4	4	2	3	2							31
13					3	3	1	4		2	3							16
12						2	3	3	4	2	1							15
11							3	4	2	1	1	1						12
10							2	4	3	2	1		1					13
9								3	2		3	1	3					12
8										1			2	1				4
7										2	3	5						10
6																		0
5												2		1				3
4													2	1				3
3														3				3
2															1			1
1																1		1
0																		0

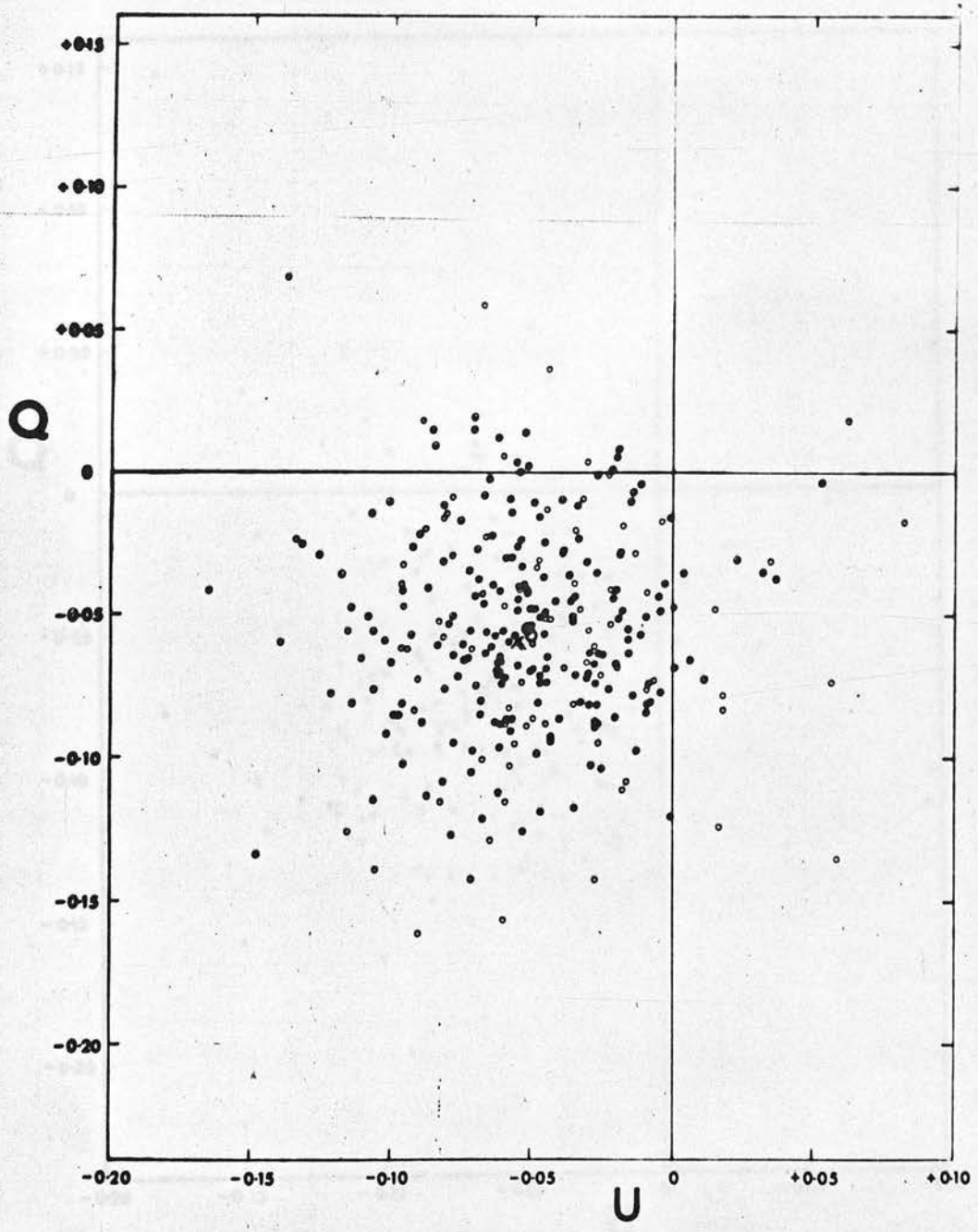

Figure 28. Stokes parameters of stars brighter than m(E) = 12. The mean photographic value is indicated by ×, and the mean values of the two groups by large symbols.

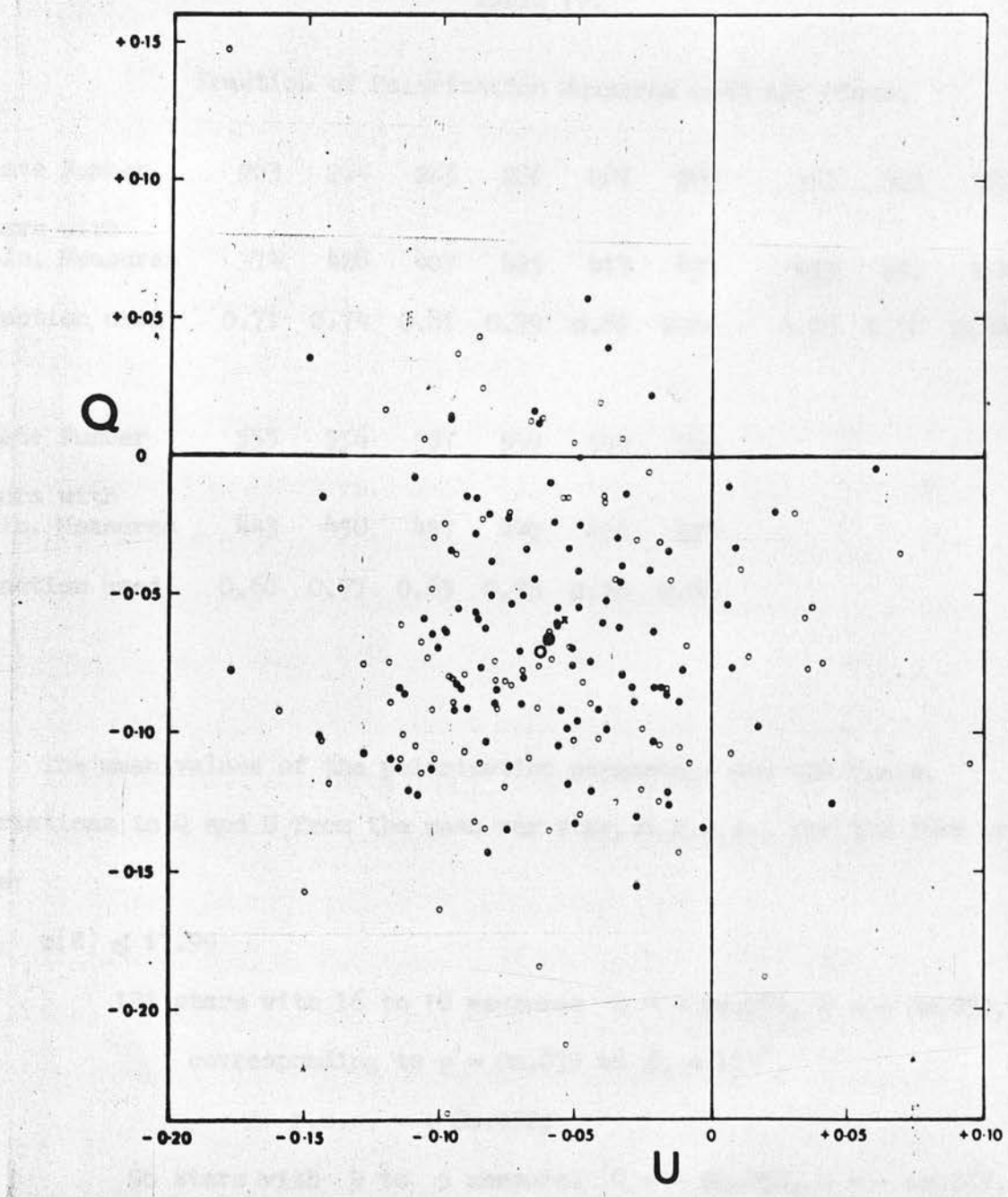

Figure 29. Stokes parameters of stars fainter than m(E) = 12. Symbols as for Fig. 28.

Table 19.

Fraction of Polarization Measures used per Plate.

Plate Number	283	284	285	286	287	288	361	362	363	364
Stars with Poln. Measures	374	428	407	425	417	433	453	458	454	460
Fraction used	0.71	0.74	0.81	0.79	0.82	0.86	0.76	0.78	0.74	0.73

Plate Number	555	556	557	558	559	560
Stars with Poln. Measures	443	458	457	440	436	434
Fraction used	0.68	0.77	0.65	0.73	0.70	0.68

The mean values of the polarization parameters and the r.m.s. variations in Q and U from the mean per star, Δ r.m.s., for the four groups are:

$m(E) \leqslant 11.99$

191 stars with 16 to 10 measures $Q = -0m.051$, $U = -0m.055$, corresponding to $p = 0m.075$ at $\theta_o = 114^\circ$, Δ r.m.s. $= \pm 0m.032$;

96 stars with 9 to 5 measures $Q = -0m.050$, $U = -0m.057$, corresponding to $p = 0m.075$ at $\theta_o = 114^\circ$, Δ r.m.s. $= \pm 0m.044$;

$m(E) \geq 12.00$

106 stars with 16 to 10 measures $Q = -0m.060$, $U = -0m.066$,

corresponding to $p = 0m.089$ at $\theta_o = 114^\circ$,

Δ r.m.s. $= \pm 0m.042$;

98 stars with 9 to 5 measures $Q = -0m.063$, $U = -0m.071$,

corresponding to $p = 0m.095$ at $\theta_o = 114^\circ$,

Δ r.m.s. $= \pm 0m.054$.

It will be recalled that the mean photographic parameters for 54 stars with photoelectric measures obtained in section 5.1 were $p = 0m.080$ at $\theta_o = 114^\circ$ with r.m.s. deviations of $\pm 0m.027$ in Q and $\pm 0m.031$ in U, and also that the photoelectric measures had an intrinsic scatter of $\pm 0m.010$. Comparing these figures with those found above, it is found that:

(1) stars with $m(E) < 12.00$ have a smaller value of p. Examination of Fig. 28 suggests that this is due to a secondary concentration of stars with small values of p. In Chapter 6 it will be shown that many of these are relatively nearby stars with large proper motions;

(2) stars with $m(E) > 12.00$ have a significantly larger value of p. From Fig. 29, there are few stars with small values of p;

(3) the position angle does not vary and is only 1 degree less than the mean photoelectric value;

(4) if the r.m.s. deviations found in the comparison with the photoelectric measures are taken as the errors in the photographic measures, the r.m.s. variation for the bright stars with 10 or more measures indicates an intrinsic scatter in the Stokes parameters of $\pm 0m.016$ for h and chi

Persei, rather larger than from the photoelectric measures. Removing this from the observed r.m.s. deviations found, the errors in the Stokes parameters for the different groups are:

	16 – 10	9 – 5
$m(E) < 12.00$	$\pm$ 0m.029	$\pm$ 0m.041
$m(E) \geq 12.00$	$\pm$ 0m.039	$\pm$ 0m.052.

The photoelectric values of p and θ_o for the 54 stars of section 5.1 are shown in equatorial coordinates in Fig. 30, together with photographic measures of 32 of them which used measures from 16 to 10 plates, the stars having both measures being indicated by large dots. For most stars there is good agreement. The photographic measures of the 191 stars with $m(E) < 12.00$ and 16 to 10 measures used are shown in Fig. 31. There are no areas where there is a systematic deviation from the general trend.

5.3 ERRORS IN THE PHOTOGRAPHIC POLARIZATION MEASURES.

The errors in the Stokes parameters can be estimated theoretically from the error in one magnitude measure derived above and the differentials of equations (8) and (10) in Chapter 2. Dividing both sides by 0.4605, these equations can be written as

$$P \cos 2\theta_o/0.4605 = p \cos 2\theta_o = Q = (10^{-\delta m_1/2.5} - 1)/0.4605$$

and $$P \sin 2\theta_o/0.4605 = p \sin 2\theta_o = U = (10^{-\delta m_2/2.5} - 10^{-\delta m_3/2.5})/(\sqrt{2} \times 0.4605).$$

From these, $$dQ(N) = 2 \times 10^{-\delta m_1/2.5} \times d(\delta m)/\sqrt{N}$$

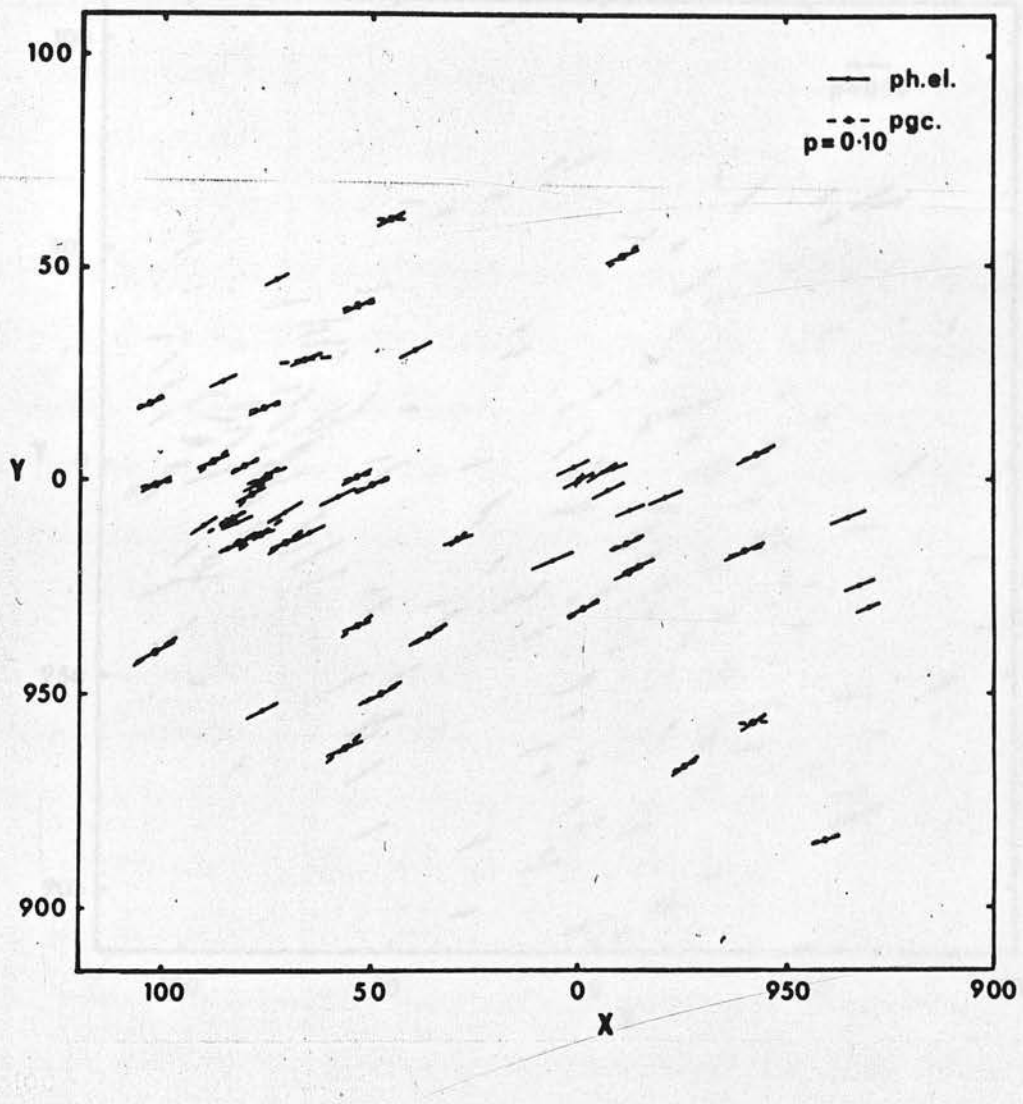

Figure 30. p and θ_o in equatorial coordinates for stars with photoelectric measures and photographic measures from 16 – 10 plates.

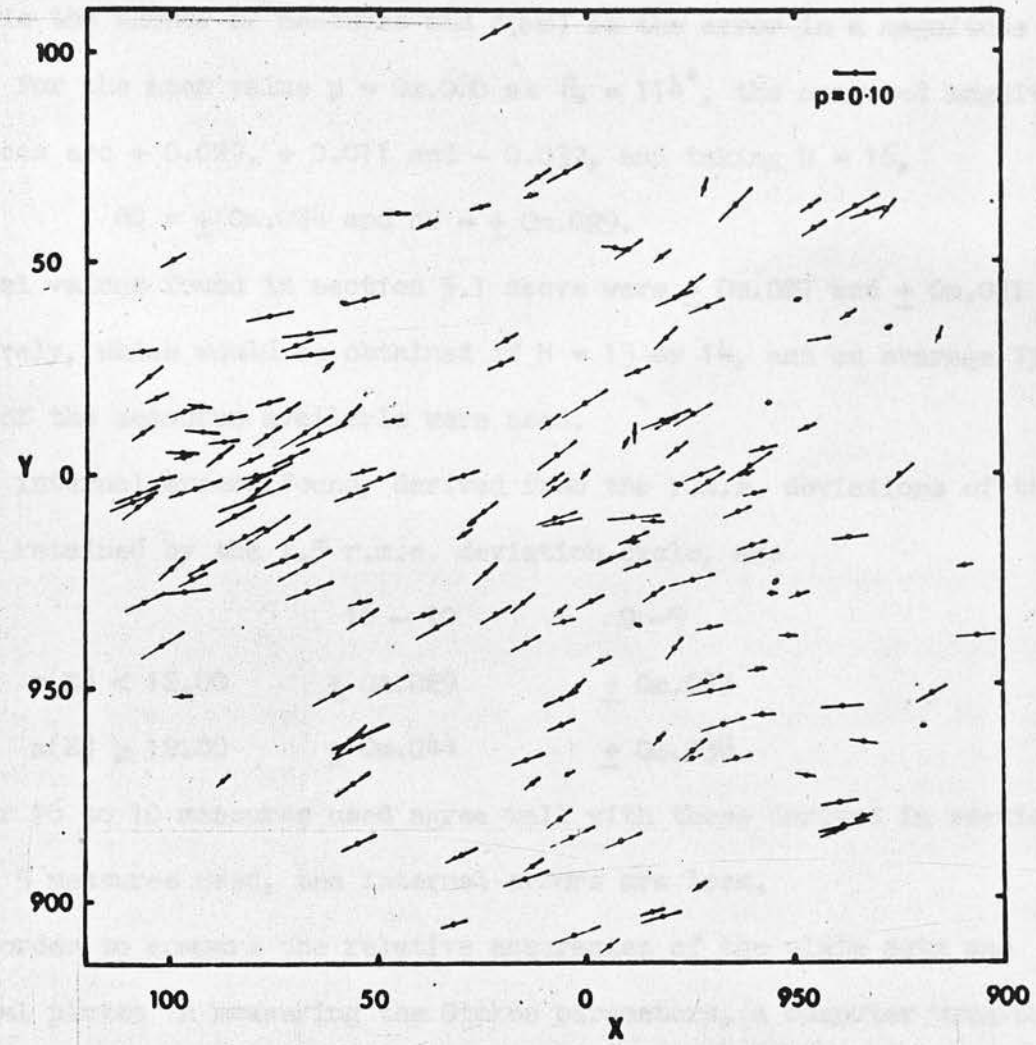

Figure 31. Photographic measures of p and θ_o in equatorial coordinates for 191 stars with m(E) < 12.00 and 16 to 10 used measures.

and $$dU(N) = 2 \times (10^{-\delta m_2/2.5} + 10^{-\delta m_3/2.5}) \times d(\delta m)/\sqrt{3N},$$

where N is the number of measures and $d(\delta m)$ is the error in a magnitude measure. For the mean value p = 0m.080 at $\theta_0 = 114^\circ$, the measured magnitude differences are + 0.029, + 0.011 and − 0.039, and taking N = 16,

$$dQ = \pm\ 0m.024 \text{ and } dU = \pm\ 0m.029.$$

The actual values found in section 5.1 above were ± 0m.027 and ± 0m.031 respectively, which would be obtained if N = 13 or 14, and on avarage 75 percent of the measures available were used.

The internal errors found, derived from the r.m.s. deviations of the measures retained by the 1.5 r.m.s. deviation cycle, are

	16 − 10	9 −5
m(E) < 12.00	± 0m.029	± 0m.023
m(E) ⩾ 12.00	± 0m.044	± 0m.038.

Those for 16 to 10 measures used agree well with those derived in section 5.2. For 9 to 5 measures used, the internal errors are less.

In order to compare the relative accuracies of the plate sets and individual plates in measuring the Stokes parameters, a computer program was written which derived the polarization parameters for any stated combination of plates, compared these with the photoelectric measures available, and derived the r.m.s. deviation per measure. (Results from this program have already been used in section 5.1 for the case when none of the plates were omitted.)

Results for the various plate sets were:

Plate set	no. of plates	r.m.s.Q	r.m.s.U	r.m.s.Q per plate	r.m.s.U per plate
1	6	0.037	0.037	0.091	0.091
2	4	0.051	0.050	0.102	0.100
1 + 2	10	0.027	0.031	0.085	0.098
3	6	0.089	0.072	0.218	0.176
1 + 2 + 3	16	0.027	0.031	0.108	0.124.

Plate set 3, taken far from the meridian, is of very poor quality but plate set 1 is better than plate set 2, although the latter was taken on the meridian. The use of a more homogeneous set of plates taken near the meridian would improve the results.

To compare individual plates, each plate was omitted in turn during the reduction. The best plate is then indicated by the largest r.m.s. deviation, etc. The results are given in Table 20, together with the order of 'goodness'. Plate set 3 is clearly worst, but now plate set 2 is best.

To study further the relative accuracies of the plates, the mean r.m.s. deviation for each plate from the mean magnitude for all stars with $m(E) < 12.00$ was found, see Table 20, and hence another order of 'goodness' was obtained. Plate set 2 is now worst!

Further studies of the properties of photographic plates in recording ranges of brightness and small changes in relative brightness when conditions of background fog level and observing conditions vary would be of interest.

Table 20.

Plate Order from Polarization and from Magnitude Measures.

Plate Number	283	284	285	286	287	288	361	362	363	364
Mean Poln. rms diff., stated plate omitted	.029	.030	.030	.029	.030	.031	.030	.032	.031	.030
'Goodness' order	10	5	9	11	4	2	7	1	2	7
Magnitude rms per plate measure: bright stars only	.047	.048	.040	.064	.050	.053	.053	.057	.060	.055
'Goodness' order	2	3	1	16	5	8	9	12	14	11

Plate Number	555	556	557	558	559	560
Mean Poln. rms diff., stated plate omitted	.029	.030	.029	.028	.028	.029
'Goodness' order	13	5	13	15	16	11
Magnitude rms per plate measure: bright stars only	.051	.048	.062	.052	.054	.058
'Goodness' order	6	4	15	7	10	13

5.4 INSTRUMENTAL POLARIZATION.

No attempt has been made to measure instrumental polarization of the Schmidt telescope directly or to compute it theoretically. Both the agreement found between photoelectric and photographic measures in section 5.1 and also the overall uniformity of the polarization vectors shown in Fig. 31 suggest that any such effect is less than the accuracy achieved, i.e. < 1.5 percent for a single star.

To examine any such effect more directly, a set of 12 polarization plates of a 1° diameter field centred on HD 111469, 12 hrs 46.9 mins, + 27 49.5 (1950), (30 Coma), near the north galactic pole, was obtained in 1965 April. Exposures were 5 minutes each on Ilford R40 emulsion, using Filter 2. The photometric standards of Harris and Upgren (1964) reach V = 11.28 only, but the magnitude scale was extrapolated to m(E) = 12. The reductions were carried out as described above. Since less than 10 stars were available in any one observing conditions control region, the r.m.s. deviations of the mean OCC curves were only 0m.01, and a single OCC curve had to be used over the entire range of 7 magnitudes. The Stokes parameters of 37 stars in the area brighter than m(E) = 12 and with measures from 6 to 12 plates, are given in Table 21, and identified in Chart 10 at the end of this thesis. The mean values are Q = − 0m.015 and U = − 0m.003, with an r.m.s. variation in Q and U of ± 0m.034 per star. These values correspond to p = 0m.015 at a position angle of 95°.

For comparison, in the catalogue of photoelectric measures by Behr (1959), there are 34 stars with $b(1) > 70^{\circ}$. The Stokes parameters of these

Table 21.

Photographic Polarization Measures of Stars at the North Galactic Pole.

No.	N	X	Y	m(E)	rms(m)	n	n	p	P.A.	rms(p)	Q	U	Notes
1	12	111.9	999.8	4.95	0.02	12	8	0.035	102	0.035	-0.032	-0.014	1,2,3
2	12	49.7	40.6	11.22	0.05	11	10	0.063	88	0.032	-0.062	0.005	
3	12	48.5	120.0	11.92	0.06	12	9	0.042	105	0.028	-0.036	-0.021	
4	12	43.7	99.8	11.40	0.04	12	8	0.073	124	0.021	-0.026	-0.068	
5	12	27.8	100.3	11.25	0.04	12	8	0.041	99	0.018	-0.040	-0.012	
6	12	999.9	0.0	5.73	0.05	12	7	0.032	148	0.025	0.014	-0.029	1,2,3
7	12	958.8	48.0	8.76	0.02	12	9	0.067	124	0.026	-0.026	-0.062	1,2,3
8	12	941.4	44.3	11.44	0.04	12	10	0.044	127	0.029	-0.012	-0.042	
9	11	903.7	37.6	11.19	0.04	11	8	0.095	143	0.018	0.026	-0.091	
10	12	918.8	134.4	11.18	0.06	12	11	0.016	153	0.032	0.009	-0.013	
11	12	796.6	117.9	11.80	0.08	12	9	0.040	147	0.031	0.016	-0.037	
12	12	823.8	85.2	11.66	0.06	12	12	0.027	155	0.037	0.017	-0.020	
13	12	792.9	75.6	11.74	0.07	11	10	0.048	101	0.033	-0.044	-0.017	
14	12	899.8	890.8	10.50	0.04	10	6	0.071	58	0.014	-0.032	0.063	2,3
15	12	923.0	869.3	11.33	0.03	12	11	0.013	7	0.021	0.012	0.003	
16	12	930.2	854.3	10.11	0.03	12	10	0.008	163	0.027	0.007	-0.005	1,2,3
17	12	936.2	844.2	11.52	0.04	12	12	0.032	83	0.028	-0.032	0.008	
18	12	943.1	833.2	11.91	0.05	12	9	0.018	63	0.035	-0.011	0.015	
19	6	934.0	771.3	11.22	0.04	6	6	0.046	57	0.023	-0.018	0.043	
20	12	28.2	765.4	6.89	0.03	12	8	0.033	111	0.023	-0.025	-0.022	1,2,3
21	12	989.8	799.4	11.98	0.05	12	10	0.040	63	0.021	-0.024	0.032	
22	12	969.8	799.3	8.79	0.02	12	9	0.089	80	0.030	-0.084	0.030	1,2,3
23	12	966.9	830.9	11.59	0.02	12	12	0.029	179	0.033	0.029	-0.001	
24	12	951.8	848.7	11.43	0.02	12	11	0.038	17	0.027	0.031	0.022	
25	12	959.0	885.7	11.49	0.03	11	8	0.039	58	0.023	-0.017	0.036	
26	12	943.6	905.7	8.23	0.04	12	8	0.054	85	0.023	-0.053	0.009	1,2,3
27	12	922.3	968.9	9.22	0.02	12	7	0.018	58	0.020	-0.008	0.016	1,2,3
28	12	987.8	941.4	11.61	0.05	12	8	0.027	68	0.024	-0.019	0.019	
29	12	985.4	924.7	11.30	0.03	12	8	0.049	23	0.016	0.034	0.035	
30	12	997.7	860.0	9.79	0.03	12	8	0.034	67	0.024	-0.024	0.024	2,3
31	11	24.6	887.5	11.91	0.04	11	8	0.119	3	0.038	0.118	0.014	
32	12	52.8	965.0	11.22	0.04	12	7	0.043	107	0.017	-0.036	-0.023	
33	12	83.0	922.8	10.65	0.02	12	8	0.059	108	0.019	-0.047	-0.034	
34	12	60.5	921.3	11.25	0.05	12	8	0.043	67	0.021	-0.030	0.031	3
35	12	59.6	913.3	10.44	0.03	12	7	0.087	98	0.013	-0.083	-0.024	2

Table 21 (cont.).

No.	N	X	Y	m(E)	rms(m)	n	n	p	P.A.	rms(p)	Q	U	Notes
36	12	104.7	871.4	11.12	0.12	12	10	0.040	64	0.027	−0.024	0.032	
37	12	108.7	886.9	11.67	0.06	12	11	0.027	90	0.032	−0.027	−0.000	

Notes

	1	2	3
Ed.No.	HD Number	BD Number	Harris and Upgren V mag.
1	111812	+28 2156	4.94
6	111469	+28 2153	5.78
7	111348	+28 2152	8.73
14	–	+27 2170	10.47
16	111253	+27 2171	10.11
20	111541	+27 2176	6.89
22	111367	+27 2173	8.81
26	111284	+27 2172	8.15
27	111233	+28 2151	9.18
30	–	+27 2174	9.70
34	–	–	11.28
35	–	+27 2178	–

stars are given in Table 22, with mean values of Q = − 0m.0001 and U = + 0m.0004 and with an r.m.s. variation of ± 0m.0045 in Q and ± 0m.0063 in U.

These results also suggest that any instrumental polarization is negligible within the accuracy achieved.

Table 22.

Stars in Behr's Catalogue with $b^I > +70$.

HD Number	Name	Gal. Lat.	p	P.A.	Q	U
98231	xi UMa	+70.8	0.0012	20	+0.0009	+0.0008
98262	nu UMa	+70.6	0.0004	38	+0.0001	+0.0004
101484	92 Leo	+74.2	0.0002	40	+0.0000	+0.0002
101501	61 UMa	+74.7	0.0020	155	+0.0013	-0.0015
102647	bet Leo	+71.7	0.0006	98	-0.0006	-0.0002
106661	6 Com	+75.8	0.0006	116	-0.0004	-0.0005
106714	7 Com	+82.7	0.0015	104	-0.0013	-0.0007
106760	-	+81.7	0.0015	48	-0.0002	+0.0015
107383	11 Com	+78.9	0.0011	39	+0.0002	+0.0011
107966	13 Com	+85.2	0.0012	10	+0.0011	+0.0004
108225	6 CVn	+77.8	0.0005	138	+0.0001	-0.0005
108381	gam Com	+85.9	0.0005	22	+0.0004	+0.0004
109317	-	+83.7	0.0009	30	+0.0004	+0.0008
109358	bet CVn	+75.9	0.0000	92	0.0000	0.0000
110411	rho Vir	+72.8	0.0004	39	+0.0001	+0.0004
110897	10 CVn	+78.2	0.0009	158	+0.0006	-0.0006
111812	31 Com	+88.5	0.0009	118	-0.0005	-0.0008
112413	alp CVn	+78.9	0.0004	3	+0.0004	+0.0000
113226	eps Vir	+73.0	0.0003	128	-0.0001	-0.0002
113797	14 CVn	+80.6	0.0021	61	-0.0011	+0.0018
113996	41 Com	+85.1	0.0016	79	-0.0015	+0.0006
114376	15 CVn	+77.8	0.0013	27	+0.0008	+0.0010
114447	17 CVn	+77.8	0.0027	41	+0.0004	+0.0027
114710	bet Com	+84.0	0.0009	60	-0.0004	+0.0008
115004	-	+76.0	0.0018	48	-0.0002	+0.0018
115604	20 CVn	+75.3	0.0013	32	+0.0006	+0.0012
117176	70 Vir	+73.0	0.0004	101	-0.0004	-0.0002
118216	-	+75.7	0.0006	121	-0.0003	-0.0005
120136	tau Boo	+72.5	0.0007	72	-0.0006	+0.0004
120477	ups Boo	+71.1	0.0007	158	+0.0005	-0.0005
120539	6 Boo	+74.0	0.0042	44	+0.0002	+0.0042
121370	eta Boo	+71.6	0.0009	133	-0.0009	-0.0001
121710	9 Boo	+74.1	0.0029	79	-0.0027	+0.0011
123999	12 Boo	+70.7	0.0001	147	+0.0000	-0.0001

CHAPTER 6.

THE SPATIAL DISTRIBUTION OF STARS AND INTERSTELLAR MATTER TOWARDS h AND chi PERSEI.

The region of the double cluster in Perseus is one of the most studied regions of the sky. The principal features along the line of sight to the region are shown schematically in Fig. 32.

The distances of the clusters are from Schild (1967), derived from the extensive spectral classifications available for the brighter stars. Other groups of stars deduced by Schild are also shown. The largest group shown is the Perseus I association. From Schild's distances and the diameters of 22 arc minutes derived from star counts by Oosterhoff (1937), the physical diameters of the clusters are about 15 parsecs.

The distribution of interstellar matter has been derived by Grigoreva (1965) in the region $117^{\circ} < l < 124^{\circ}$. h and chi Persei are situated at $l = 135^{\circ}$, but the distribution is believed to be very similar. On traversing the Perseus arm, the interstellar absorption is 1.3 magnitudes.

The distribution in space of the 527 stars to V = 13 in the present program is now investigated using proper motions and new photographic UBV photometry.

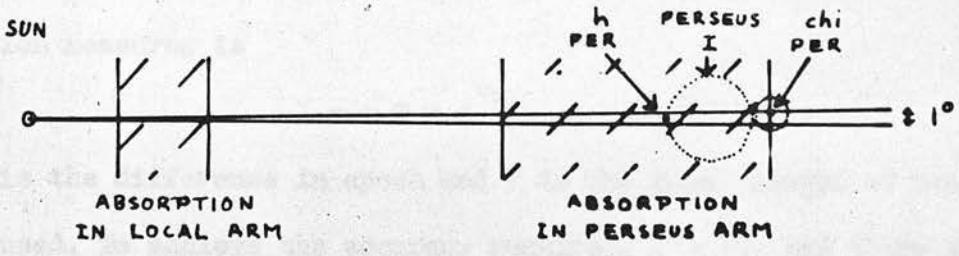

Figure 32. Schematic galactic structure along the line of sight to h and chi Persei.

6.1 PROPER MOTIONS IN THE REGION OF h AND chi PERSEI.

The discrimination of cluster members in h and chi Persei by the use of proper motions is extremely difficult due to the distance of the clusters, more than 2 kiloparsecs, but the identification of nearby stars with large proper motions is possible.

According to Vasilevskis (1962), an indicator of the usefulness of proper motion measures is

$$I = \Delta T \times f^{1/2},$$

where ΔT is the difference in epoch and f is the focal length of the telescope used. To achieve the accuracy required, $I > 150$ and there should be several plate pairs. For the investigation by van Maanen (1944) of h Persei, $I \sim 115$ as the average epoch difference is only 23 years. For the investigation of Lavdovskii (1961), $I \sim 200$ and there are 3 plate pairs. The numbers given to the stars in h and chi Persei by Lavdovskii are given in column 3 of the polarization Catalogue at the end of this thesis. All but 8 of the program stars have proper motions by Lavdovskii. There are 43 stars with annual proper motions > 0.01 arc secs., including the white dwarf, star 230 in Oosterhoff (1937).

The transverse velocity, u, of a star at right angles to the line of sight is related to the annual proper motion of the star, m, and distance, r, in parsecs, by

$$u = 4.74 \times m \times r \text{ km. per sec.}$$

Only 'high' velocity stars have transverse velocities exceeding 30 km. per

sec., the majority of stars having much smaller relative velocities. For a star with a transverse velocity of 30 km. per sec. and annual proper motion of 0.01 arc secs., the distance r = 630 parsecs. The stars in the present program, having larger proper motions and smaller transverse velocities, are probably much nearer.

The proper motions and the photographic polarization measures of these 43 stars are given in Table 23 and their Stokes parameters shown in Fig. 33. For stars brighter than m(E) = 12 and with ten or more used measures, the mean amount of polarization is 0m.035 at 113°.

6.2 PHOTOGRAPHIC UBV PHOTOMETRY OF THE PROGRAM STARS.

The 15 UBV plates are listed in Table 6 in Chapter 3, and there also their measurement and reduction is described. The iris photometer measures were calibrated using the photoelectric standards of Table 12 in Chapter 5. The star images on the coarse grain UBV plates are larger (and reach fainter magnitude limits) than the fine grain polarization plates and some stars could not now be measured as their images were not sufficiently isolated. Some other stars were too red to appear on the B or on the U plates and could not be completely measured. Altogether there are UBV measures for 469 stars.

The r.m.s. deviation per measure from the mean magnitude of each star for the V, B and U plates, plotted against the corresponding mean magnitude, gives diagrams similar to Fig. 23 in Chapter 5. These V, B and U deviations

Table 23.

Polarization Measures of Stars with large Proper Motions.

Star No.	m(E)	Lavdovsky Number	Proper Motion R.A.	Proper Motion Dec.	Number used	p	P.A.	Q	U
6	12.14	271	-0.005	+0.010	7	0.146	155	+0.095	-0.111
10	11.01	284	+0.008	-0.012	9	0.047	136	+0.001	-0.047
13	10.13	265	-0.019	-0.018	14	0.049	122	-0.021	-0.044
14	8.09	390	+0.014	-0.013	11	0.015	104	-0.014	-0.007
17	11.93	658	+0.022	+0.004	10	0.092	126	-0.027	-0.088
23	10.80	984	+0.019	-0.018	12	0.073	82	-0.070	+0.019
24	12.80	898	-0.002	-0.010	5	0.087	113	-0.060	-0.064
31	12.49	546	+0.025	-0.014	11	0.142	125	-0.050	-0.133
40	12.75	763	-0.011	+0.004	8	0.130	104	-0.115	-0.061
42	9.13	1242	+0.029	-0.015	8	0.084	174	+0.082	-0.017
43	11.74	1345	+0.016	-0.017	10	0.087	116	-0.054	-0.068
45	12.63	1335	+0.010	-0.004	6	0.064	84	-0.063	+0.014
52	12.67	1307	+0.012	-0.010	13	0.086	129	-0.019	-0.084
59	10.44	1664	-0.018	-0.006	12	0.020	82	-0.020	+0.006
65	12.94	2052	+0.013	-0.011	6	0.125	110	-0.096	-0.081
70	12.50	1956	-0.006	+0.011	10	0.133	129	-0.027	-0.130
75	10.75	1555	-0.017	+0.011	9	0.077	132	-0.009	-0.076
76	12.36	74	-0.011	+0.004	9	0.095	120	-0.048	-0.082
77	10.89	101	+0.030	-0.021	13	0.048	156	+0.032	-0.035
78	11.15	194	+0.043	-0.004	12	0.018	115	-0.011	-0.014
81	12.70	18	+0.040	-0.024	10	0.013	150	+0.006	-0.011
89	12.20	185	+0.004	+0.010	12	0.060	95	-0.060	-0.010
90	10.65	44	+0.019	+0.019	11	0.040	97	-0.039	-0.009
93	12.63	73	+0.002	-0.020	6	0.123	129	-0.026	-0.120
118	13.28	404	+0.171	-0.020	6	0.078	166	+0.070	-0.036
121	11.84	489	+0.025	+0.012	15	0.043	113	-0.030	-0.031
125	11.29	435	+0.026	-0.015	13	0.012	100	-0.011	-0.004
141	11.00	880	+0.011	+0.012	12	0.053	178	+0.053	-0.003
177	11.15	925	+0.014	+0.007	6	0.047	159	+0.035	-0.031
185	10.62	877	-0.009	-0.006	13	0.035	100	-0.033	-0.012

Table 23 (cont.).

Star No.	m(E)	Lavdovsky Number	Proper Motion R.A.	Dec.	Number used	p	P.A.	Q	U
197	12.64	991	−0.011	−0.006	8	0.085	149	+0.040	−0.075
245	11.52	1146	+0.011	−0.005	13	0.043	132	−0.004	−0.043
246	10.40	1134	+0.014	−0.011	13	0.064	104	−0.057	−0.029
252	12.48	1296	+0.031	−0.015	10	0.034	142	+0.009	−0.033
270	12.14	1473	+0.019	−0.015	9	0.024	97	−0.023	−0.006
294	11.64	1617	+0.034	−0.012	12	0.059	102	−0.054	−0.024
295	10.62	1569	+0.013	−0.001	7	0.071	127	−0.019	−0.068
306	13.23	2143	+0.058	−0.049	9	0.081	144	+0.025	−0.077
362	13.20	2068	+0.010	−0.025	11	0.073	65	−0.046	+0.057
366	12.39	2081	+0.013	+0.001	8	0.114	113	−0.080	−0.082
387	11.89	1711	+0.011	−0.021	13	0.039	133	−0.003	−0.039
401	10.66	2274	+0.019	−0.009	14	0.077	96	−0.075	−0.017
452	12.03	629	−0.004	+0.010	9	0.047	126	−0.015	−0.045

are summarised in Table 24. The extensions of the B and U magnitudes to fainter limits indicates the presence of a number of red stars.

Denoting magnitudes on the Edinburgh system by primed symbols, the difference $V-V'$ is plotted against $B-V$ in Fig. 34. There are few stars outside the range $+0.2 < B-V < +0.6$, and a best straight line was fitted to the observations by taking mean values for the ranges $-0.2 < B-V < +0.8$ and $B-V > +2.0$. Hence,

$$V = V' + 0.075\ (B-V) - 0.049,$$

with an r.m.s. scatter per star about the mean relationship of $\pm$ 0m.064. There was no significant magnitude dependence.

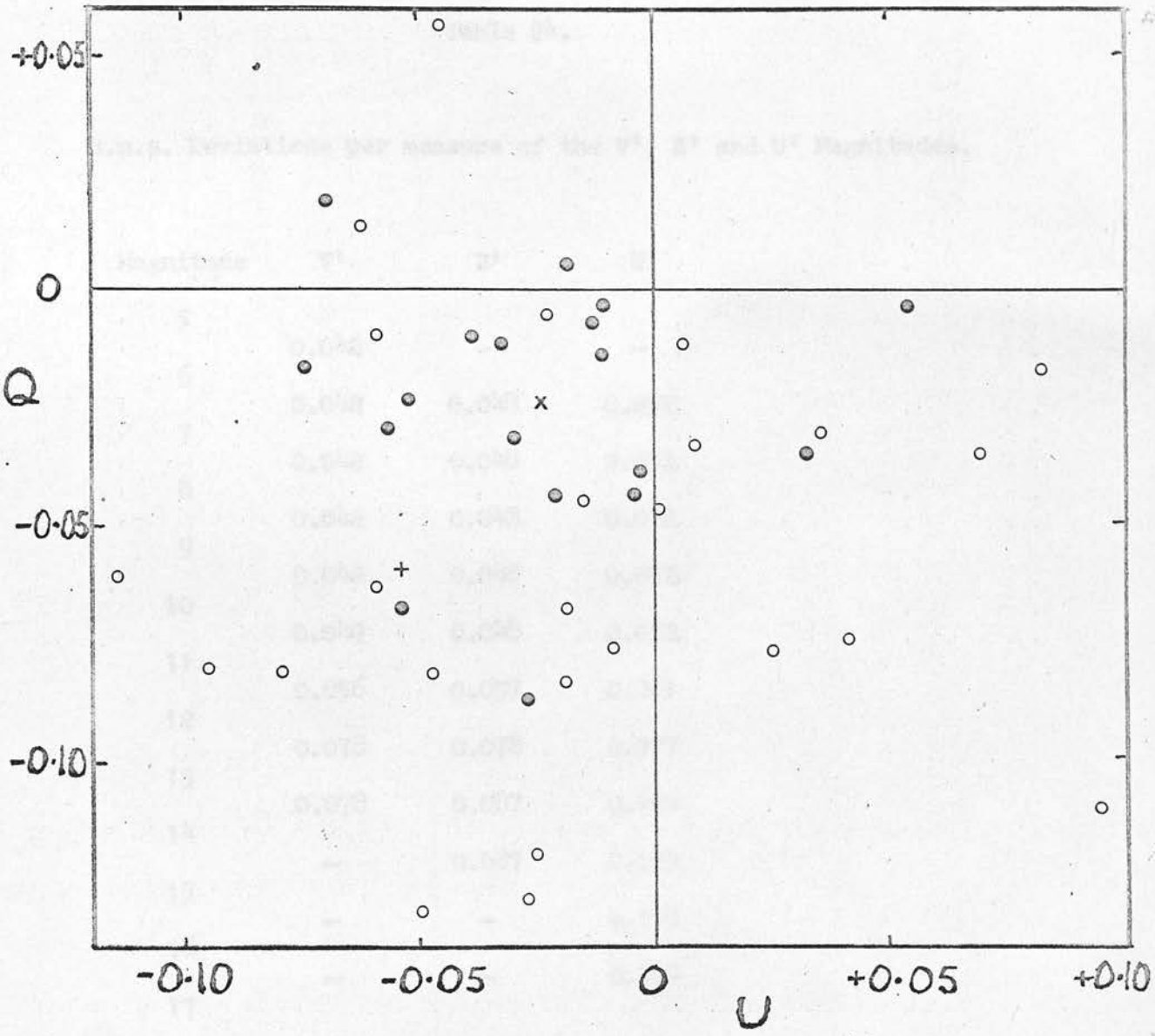

Figure 33. Stokes parameters of stars with annual proper motions larger than 0.01 arc seconds.

Stars brighter than m(E) = 12 and with 5 or more used measures are indicated by filled circles and their mean is ×. The mean photographic value of the cluster stars, Fig. 26b, is +.

Table 24.

R.m.s. Deviations per measure of the V^s, B^s and U^s Magnitudes.

Magnitude	V^s	B^s	U^s
5			
	0.042	–	–
6			
	0.042	0.048	0.052
7			
	0.042	0.048	0.052
8			
	0.042	0.048	0.052
9			
	0.042	0.048	0.052
10			
	0.049	0.048	0.052
11			
	0.056	0.057	0.061
12			
	0.078	0.078	0.077
13			
	0.078	0.087	0.109
14			
	–	0.087	0.109
15			
	–	–	0.109
16			
	–	–	0.109
17			

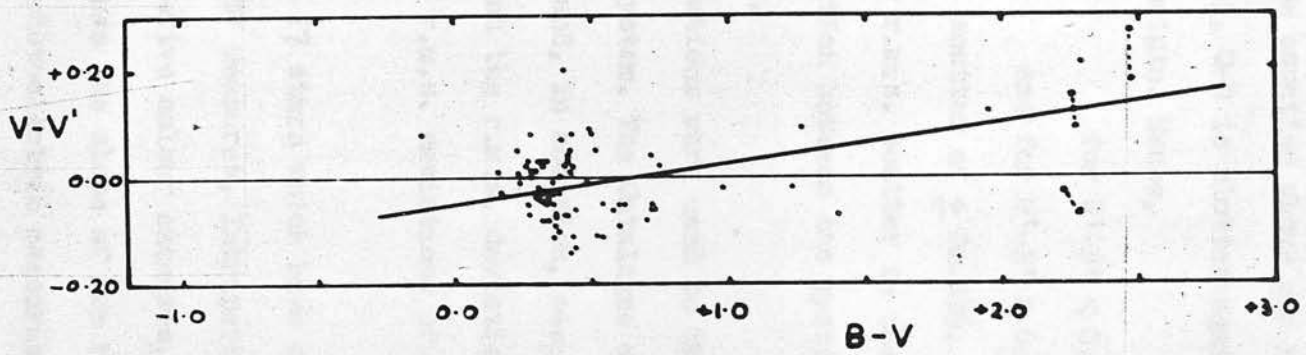

Figure 34. The colour equation between V–V' and B–V. Measures for the long period variables are joined by dashed lines.

-126-

It was found that $B-V = B'-V'$, with an r.m.s. scatter of $\pm$ 0m.032, so that B–V in the equation above can be replaced by $B'-V'$.

In Fig. 35, U–B is plotted against $U'-B'$, and here there is a change of slope at the origin. Hence,

$$\text{for } U'-B' < 0.0, \quad U-B = U'-B'$$

$$\text{and for } U'-B' > 0.0, \quad U-B = 0.881(U'-B'),$$

with an r.m.s. scatter of $\pm$ 0m.026.

The large r.m.s. scatter in the $V-V'$ versus B–V diagram suggests that the transformation between the systems is non-linear, see also Lawrence and Reddish (1965).

These equations were used to transform the Edinburgh measures to the standard UBV system. The Catalogue at the end of this thesis contains these UBV measures, and, in addition, mean coordinates, the number of measures in each colour, and the r.m.s. deviations of the mean V, B–V and U–B values for each star. The r.m.s. deviations of the mean values are summarised in Table 25.

There are 17 stars which have spectral types and both photoelectric and photographic UBV measures. Intrinsic colours derived by Fitzgerald (1967) were used to derive colour excesses, $E(B-V) = B-V - (B-V)_o$ and similarly for E(U–B), and hence the slope of the reddening curve (assumed straight).

From the photoelectric measures, the mean value of $E(U-B)/E(B-V) = 0.72 \pm 0.08$, and from the photographic measures, $E(U-B)/E(B-V) = 0.65 \pm 0.13$. The photoelectric measures thus give a value close to the 'standard' value, 0.73, Allen (1963, p.252), but the mean photographic value differs, again

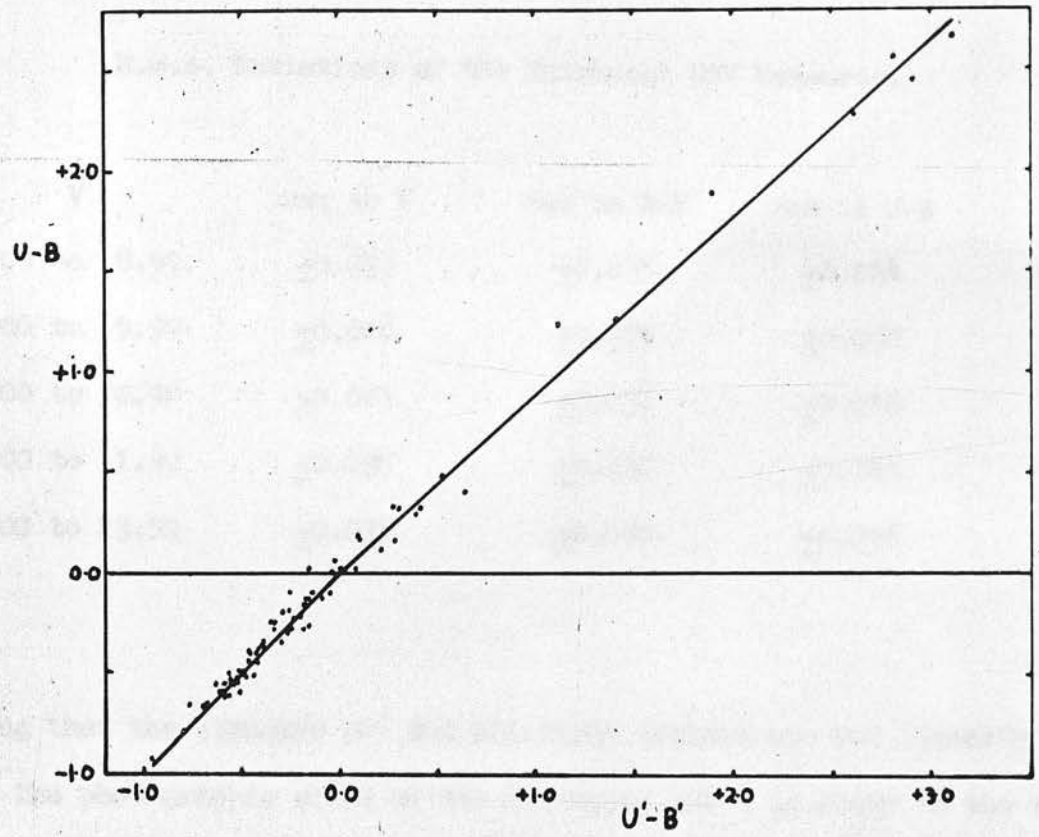

Figure 35. The colour equation between U'—B' AND U—B.

Table 25.

R.m.s. Deviations of the Edinburgh UBV Measures.

V	rms in V	rms in B–V	rms in U–B
5.00 to 8.99	±0.023	±0.035	±0.034
9.00 to 9.99	±0.018	±0.027	±0.032
10.00 to 10.99	±0.023	±0.033	±0.036
11.00 to 11.99	±0.025	±0.040	±0.045
12.00 to 13.50	±0.035	±0.050	±0.056

suggesting that the standard UBV and Edinburgh systems are not linearly related. The photographic slope of the reddening curve is close to the value derived for Perseus in the spectrophotometric study of the reddening law by Nandy (1965).

The two colour diagram, B–V against U–B, is given for the 469 stars in Fig. 36. Separate symbols have been used for special stars as follows:

W white dwarf, star 118;

O star with spectral type O6;

× stars with spectral type B;

A AI stars;

+ stars with annual proper motions > 0.01 arc secs.;

M MI stars.

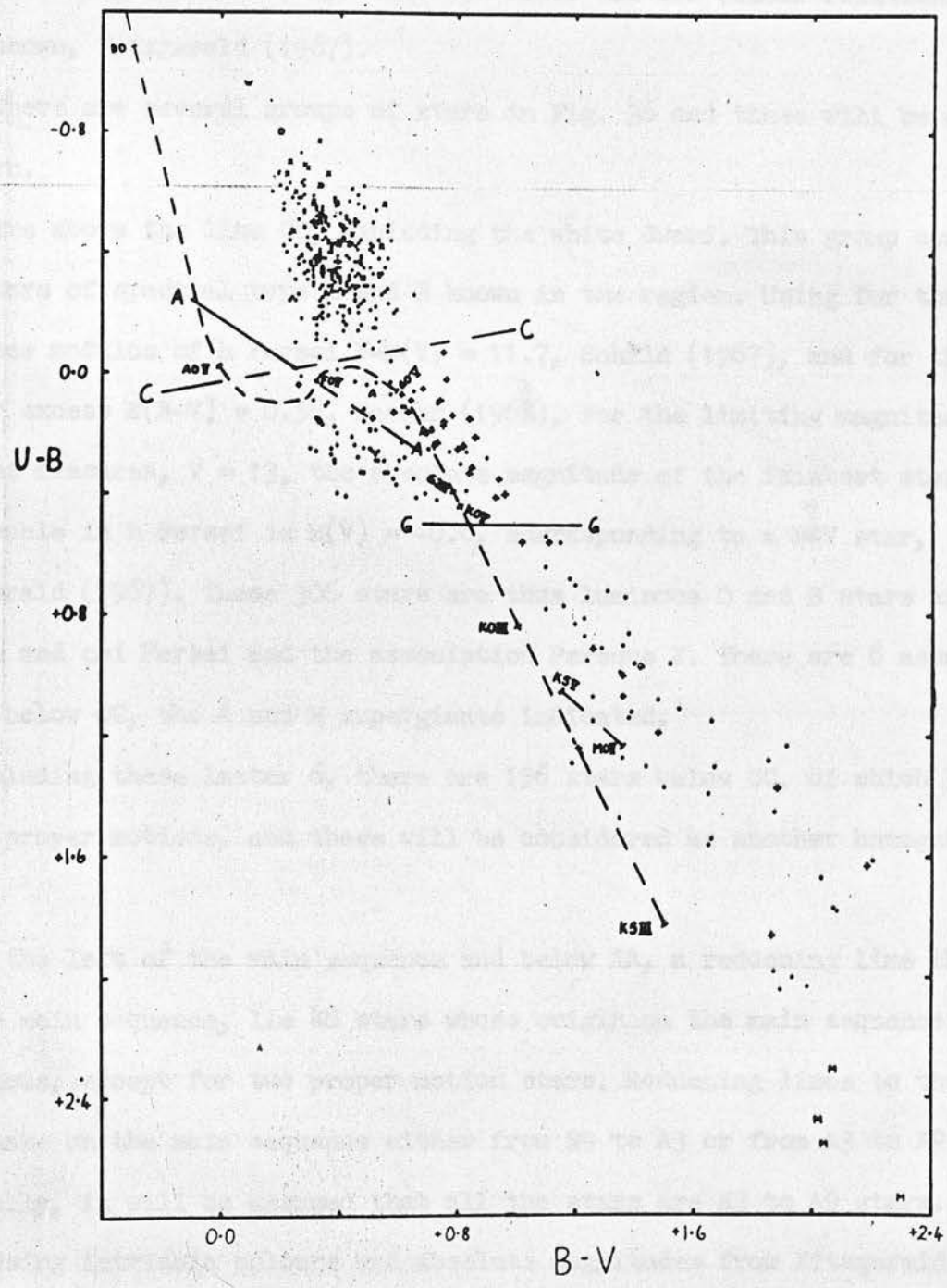

Figure 36. The two colour diagram. See text for symbols.

The luminosity class V and part of the class III two-colour relationships are also shown, Fitzgerald (1967).

There are several groups of stars in Fig. 36 and these will be discussed in turn.

1) stars above the line CC, excluding the white dwarf. This group contains all the stars of spectral type O and B known in the region. Using for the distance modulus of h Persei V-M(V) = 11.7, Schild (1967), and for the colour excess E(B-V) = 0.56, Becker (1963), for the limiting magnitude of the present measures, V = 13, the absolute magnitude of the faintest star observable in h Persei is M(V) = -0.8, corresponding to a B7V star, Fitzgerald (1967). These 306 stars are thus luminous O and B stars associated with h and chi Persei and the association Perseus I. There are 6 associated stars below CC, the A and M supergiants indicated.

2) excluding these latter 6, there are 156 stars below CC, of which 38 have large proper motions, and these will be considered as another homogeneous group.

3) to the left of the main sequence and below AA, a reddening line through F0V on the main sequence, lie 48 stars whose origin on the main sequence is ambiguous, except for two proper motion stars. Reddening lines to these stars originate on the main sequence either from B9 to A3 or from A3 to A9 stars. Initially, it will be assumed that all the stars are A3 to A9 stars.

Using intrinsic colours and absolute magnitudes from Fitzgerald (1967), colour excesses and distance estimates have been derived for these 48 stars, Fig. 37a. The two stars with large proper motions are indicated by crosses.

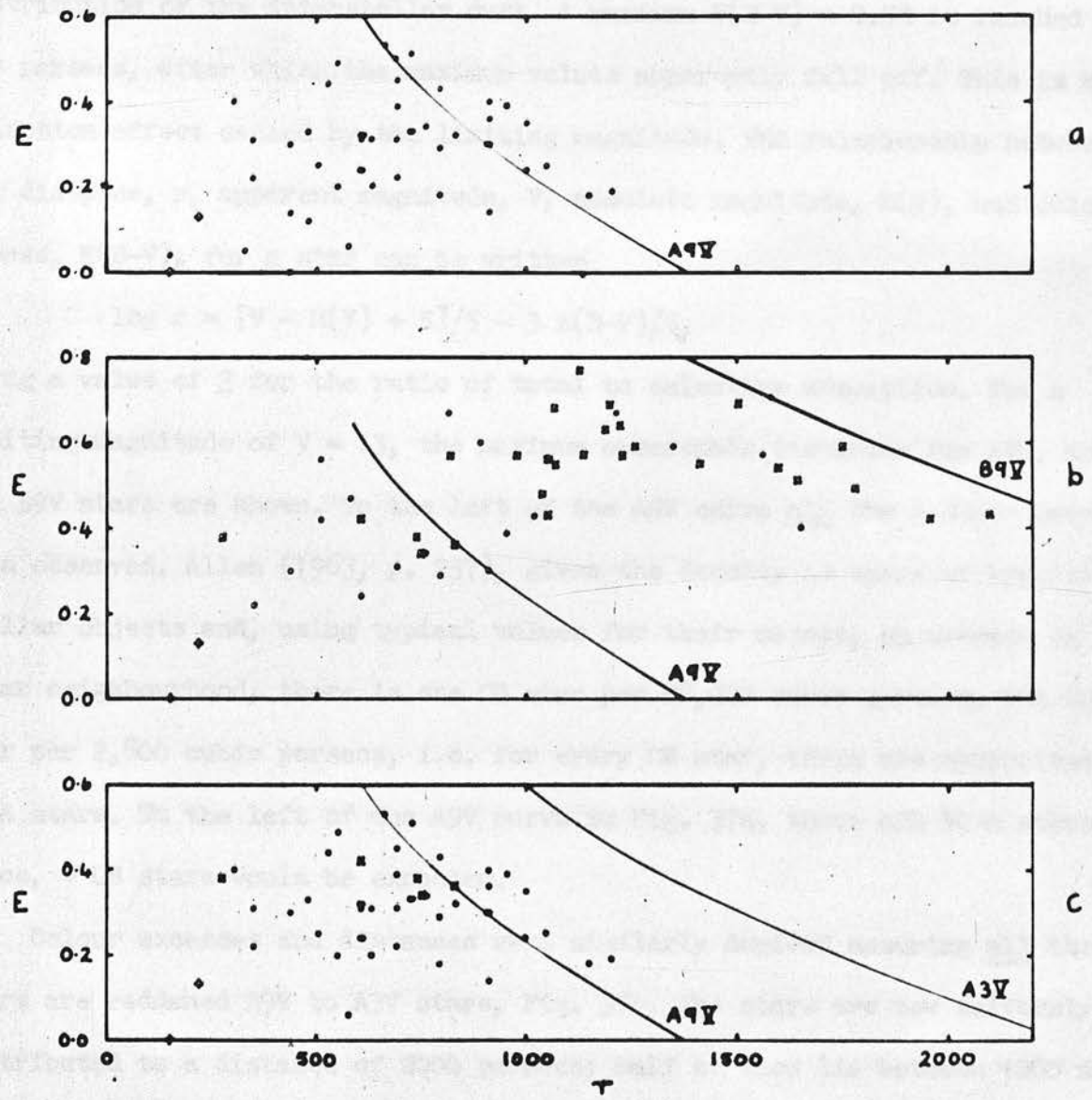

Figure 37. The E(B–V) colour excess, E, against distance for the suspected BA stars, as explained in the text.

The colour excesses have a large scatter, indicating the non-uniformity of distribution of the interstellar dust. A maximum E(B-V) = 0.52 is reached at 700 parsecs, after which the maximum values apparently fall off. This is a selection effect caused by the limiting magnitude. The relationship between the distance, r, apparent magnitude, V, absolute magnitude, M(V), and colour excess, E(B-V), for a star can be written

$$\log r = [V - M(V) + 5]/5 - 3\,E(B-V)/5,$$

using a value of 3 for the ratio of total to selective absorption. For a limiting magnitude of V = 13, the maximum observable distances for A9V, A3V and B9V stars are shown. To the left of the A9V curve all the A stars have been observed. Allen (1963, p. 237), gives the density in space of various stellar objects and, using typical values for their masses, on average in the solar neighbourhood, there is one OB star per 28,000 cubic parsecs, and one A star per 2,800 cubic parsecs, i.e. for every OB star, there are approximately 10 A stars. To the left of the A9V curve in Fig. 37a, there are 40 A stars and hence, 4 OB stars would be expected.

Colour excesses and distances were similarly derived assuming all the stars are reddened B9V to A3V stars, Fig. 37b. The stars are now uniformly distributed to a distance of 2000 parsecs; half of them lie between 1000 and 1600 parsecs – between the spiral arms, which contradicts the accepted distribution of stars in space. To the left of the A9V observable limit, there are 5 stars with spectral types B9V or B9.5V, only one more than the expected number derived from Fig. 37a.

It is now assumed that these 5 stars are BV stars and the remaining 43

stars are A3V to A9V stars, Fig. 37c. The results are now consistent with the accepted structure of the spiral arms, and with the relative numbers of stars. The lack of stars between the A3V and A9V observable limits indicates a real avoidance of the inter-arm region by the earlier A stars. The obscuration rises sharply at about 300 parsecs, in agreement with the result of Grigoreva (1965), but there are still regions of low obscuration in the field – one star at 915 parsecs has a colour excess of 0.14. The mean colour excess for these stars is 0.31.

4) the remaining stars below CC and to the right of AA, i.e. omitting the large proper motion stars, are divided into two groups at GG. Above GG the stars are either unreddened FV to KOV stars or reddened FV stars, and so their position is ambiguous. The stars below GG fall to the right of the class V relationship, and from their brightness, these stars appear to be reddened GIII and KIII stars. Such stars have intrinsic luminosities similar to the BAV stars of group 3 above. The exact nature of these stars is somewhat ambiguous, but they do lie within the local spiral arm.

Omitting the A and M supergiants, therefore, the stars below CC in Fig. 36 belong to the local spiral arm. The distribution of all these stars on the sky is shown in Fig. 38. These stars are distributed over the whole field, with a slight concentration to the north and west.

The remaining stars, shown as dots in Fig. 38, are the OB stars, except for the indicated A and M supergiants. These OB stars are sparse in the north and are concentrated in the cluster regions, although still numerous in the south. The circles, 23 arc mins. in diameter, indicate the cluster regions,

(see Fig. 40)

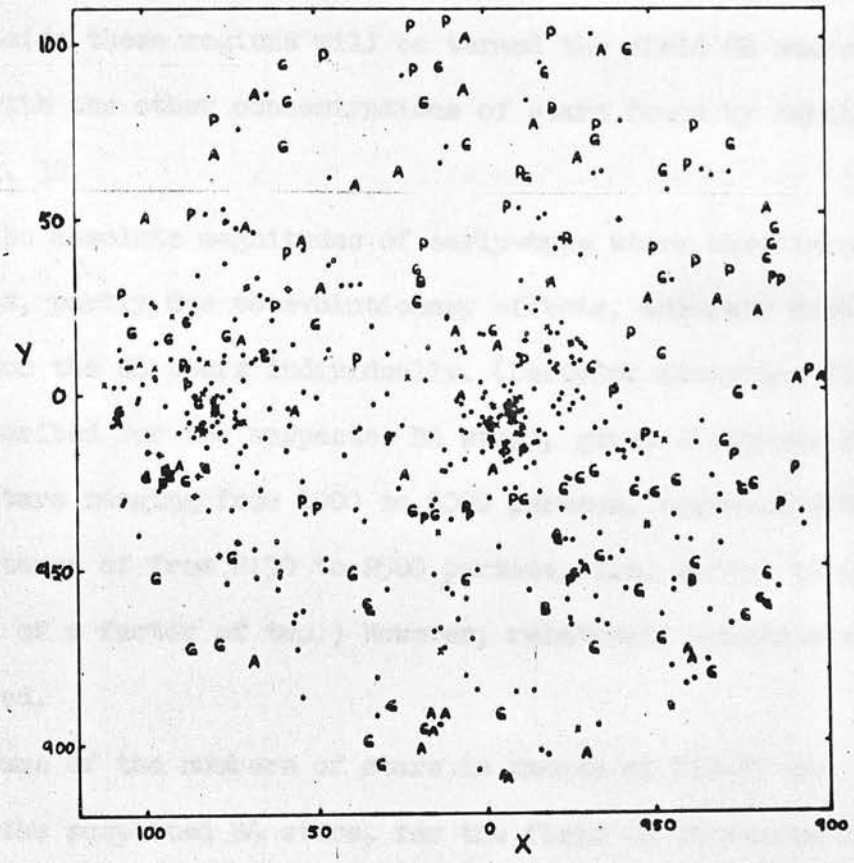

Figure 38. The distribution on the sky in equatorial coordinates of the groups of stars in the local spiral : A – suspected A stars, B – SUSPECTED B stars, P – stars with large proper motions, G – other stars. • – OB stars in the Perseus arm, + stars too crowded to measure, × stars with no UBV magnitudes.

h and chi Persei, with cluster centres as derived by Oosterhoff (1937). The OB stars outside these regions will be termed the field OB stars. They are associated with the other concentrations of stars found by Schild (1967), shown in Fig. 32.

Since the absolute magnitudes of early-type stars have large uncertainties, partly due to evolutionary effects, accurate distances cannot be derived for the OB stars individually. (Deriving distances for the OB stars as described for the suspected BA stars, gives distances for individual stars ranging from 1000 to 5000 parsecs, compared with the expected distance of from 2150 to 2500 parsecs, i.e. errors in the distances of the order of a factor of two.) However, relatively accurate colour excesses can be derived.

Histograms of the numbers of stars in ranges of E(B-V) are shown in Fig. 39 for the suspected BA stars, for the field OB stars and for h Persei and chi Persei. The local spiral arm produces an E(B-V) of approximately 0m.40 - an absorption of 1.2 magnitudes compared with 1.3 magnitudes found by Grigoreva (1965) for the Perseus arm. The OB field stars exhibit a sudden onset at E(B-V) = 0m.47; the steady reduction of their numbers to larger E(B-V) is probably partially due to a selection effect from the limiting magnitude. Both h and chi Persei show symmetric distributions with mean values of 0m.60 and 0m.62 respectively. The range of values of E(B-V) appears to be real, and suggests that interstellar matter is intimately connected with the clusters, although no nebulosity is visible in them.

Plotting schematically the distribution of values of E(B-V) on the sky

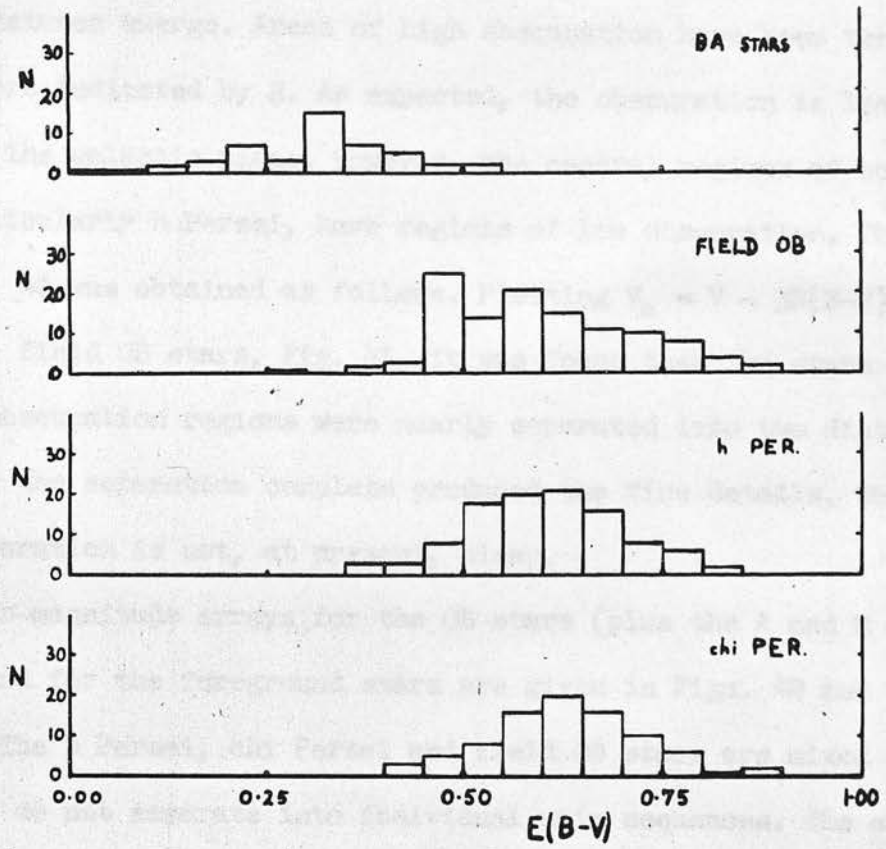

Figure 39. The number, N, of stars in 0m.05 ranges of E(B–V) for various groups of stars.

for all the OB stars, Fig. 40, which also shows galactic coordinates, some interesting features emerge. Areas of high obscuration have been tentatively outlined and are indicated by H. As expected, the obscuration is least furthest from the galactic plane. However, the central regions of both clusters, particularly h Persei, have regions of low obscuration. The fine detail of Fig. 40 was obtained as follows. Plotting $V_o = V - 3E(B-V)$ against $E(B-V)$ for the field OB stars, Fig. 41, it was found that the stars in the high and low obscuration regions were nearly separated into two distinct groups. Making the separation complete produced the fine details. The reason for such a separation is not, at present, clear.

The colour-magnitude arrays for the OB stars (plus the A and M supergiants) and for the foreground stars are given in Figs. 42 and 43 respectively. The h Persei, chi Persei and field OB stars are mixed together, they do not separate into individual main sequences. The suspected BA stars are the brightest and bluest of the foreground stars.

In Chapter 5, 4 possible new variable stars were found. The UBV data for these stars are given in Table 26. If the stars are intrinsic variables and not eclipsing binary systems, Table 26 also gives possible variable types from the UBV photometry.

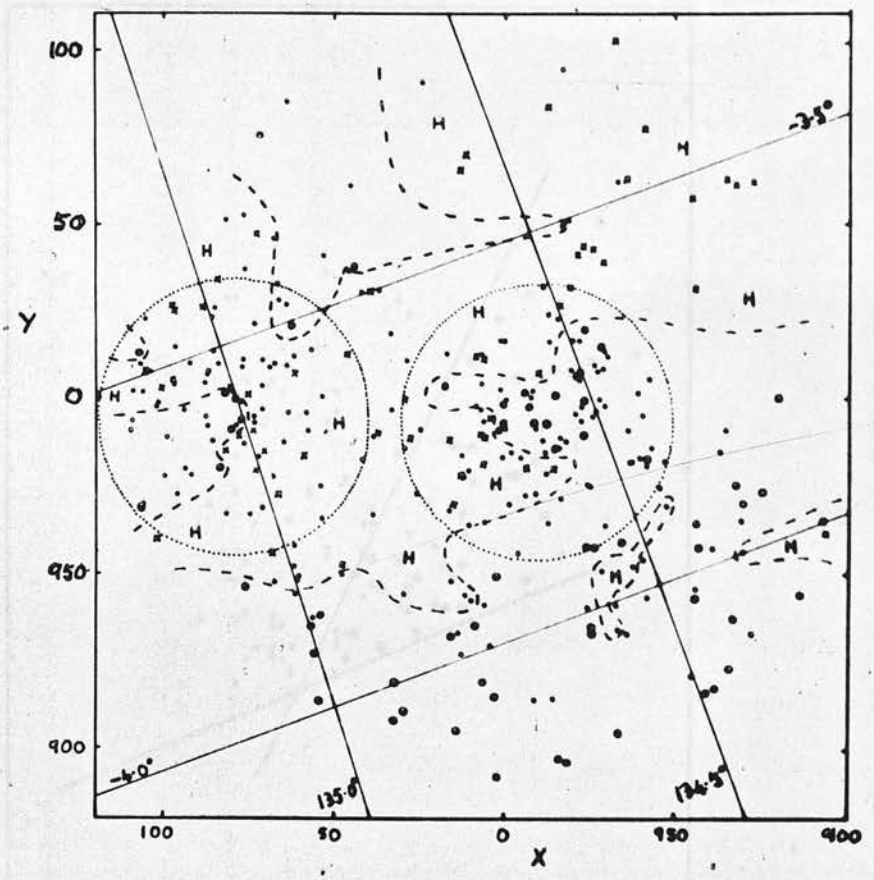

Figure 40. Distribution on the sky of colour excess for the OB stars in the Perseus arm: × – E(B–V) > 0.70; 0 – E(B–V) < 0.50; OTHERS • .

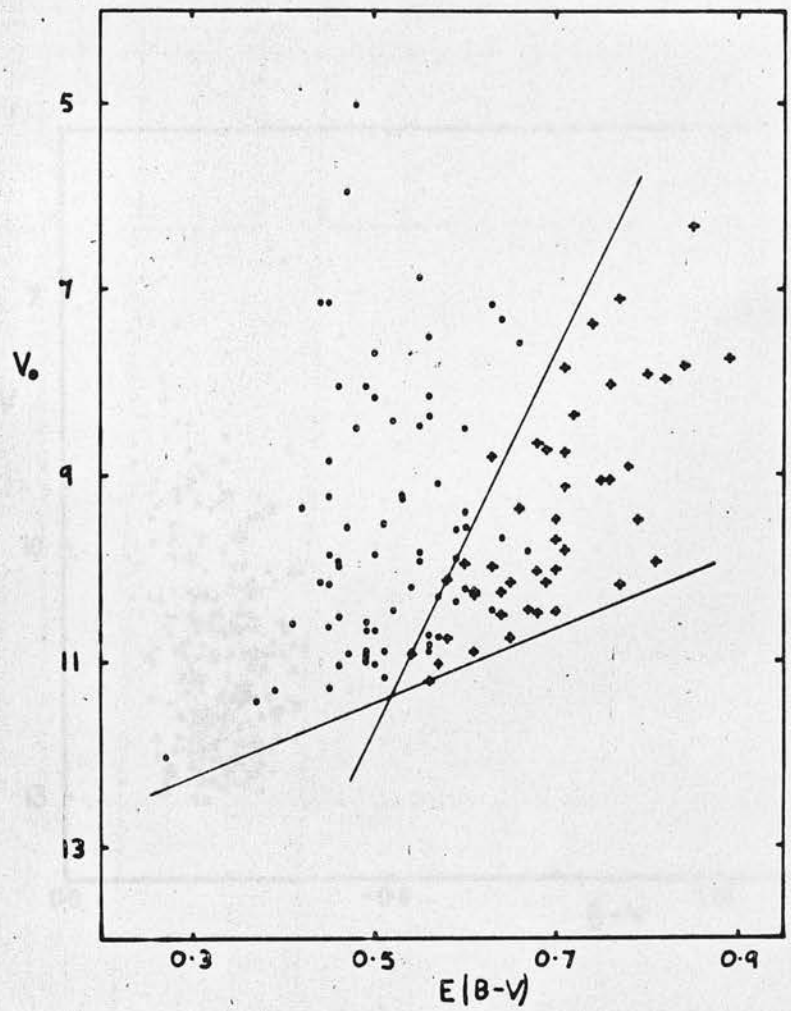

Figure 41. V_o against E(B–V) for the field OB stars in the Perseus spiral arm. + stars in the regions of high obscuration. The division between the two groups is indicated, and also the observational cut–off.

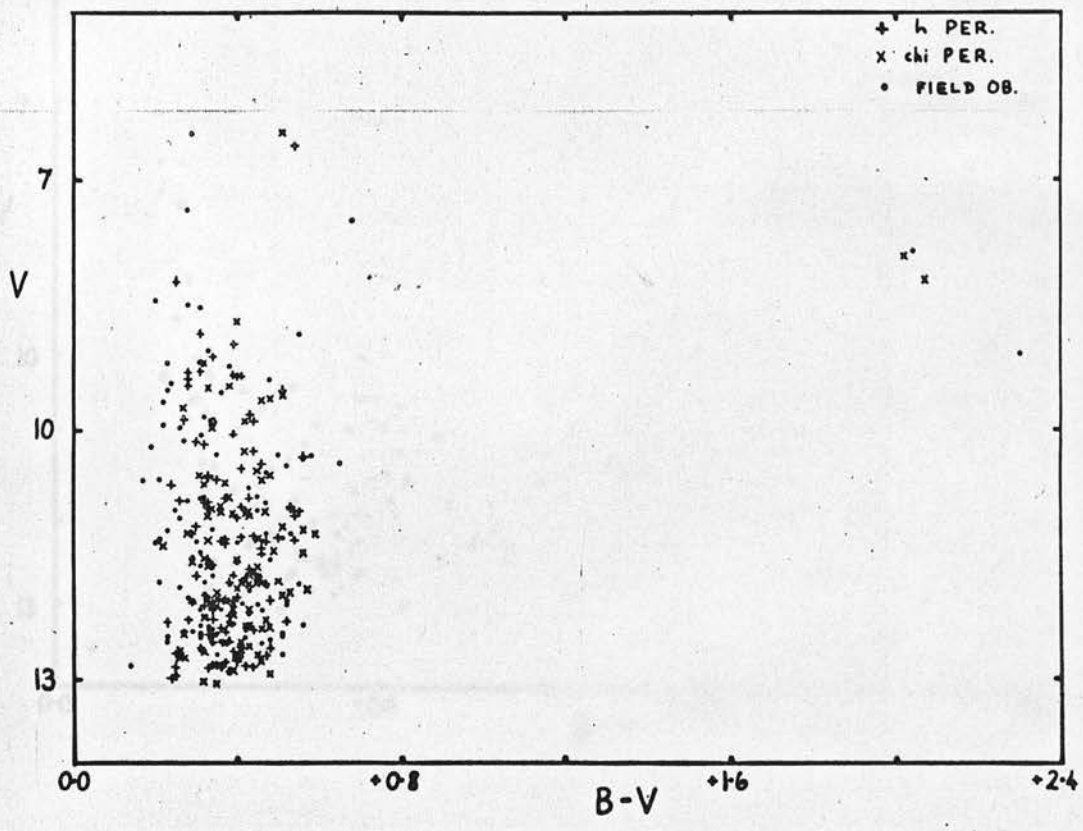

Figure 42. V against B–V for the stars in the Perseus arm.

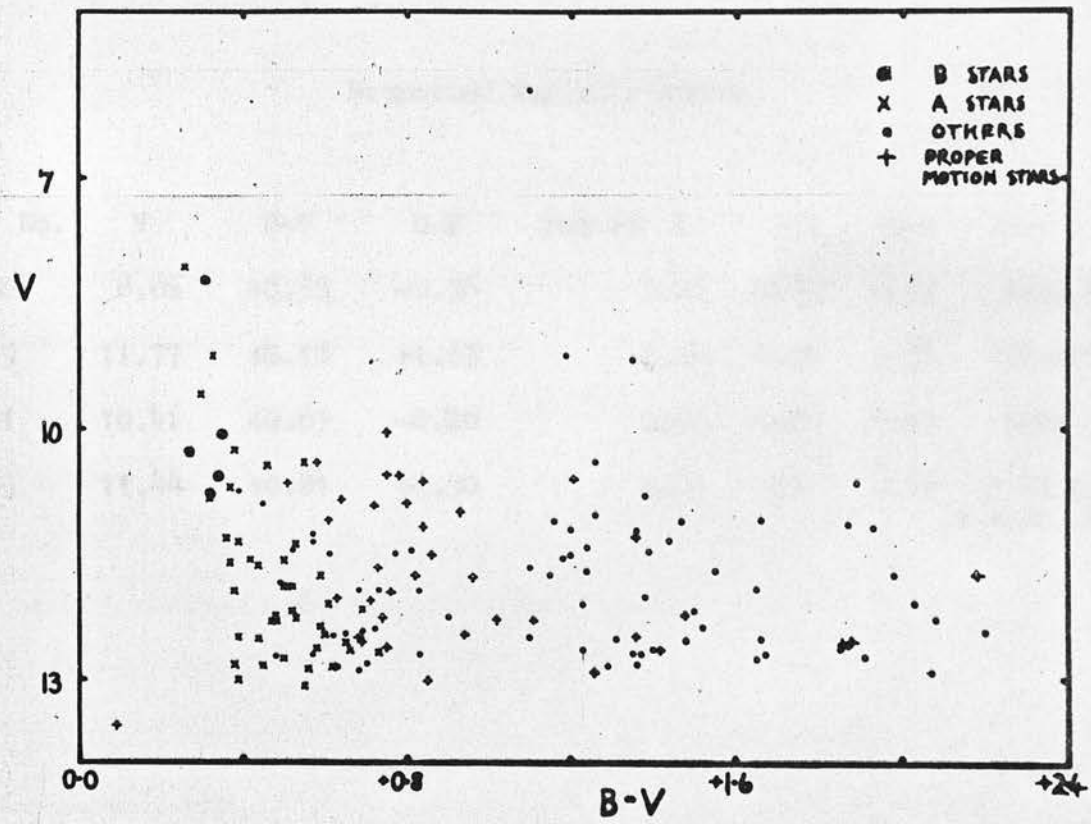

Figure 43. V against B–V array for the stars in the local spiral arm.

Table 26.

Suspected Variable Stars.

Star No.	V	B–V	U–B	rms in V	B–V	U–B	Possible Type
62	8.86	+0.55	–0.56	0.02	0.03	0.03	beta Cephei
89	11.77	+2.18	+1.63	0.04	0.05	0.06	'flash' star
91	10.41	+0.65	–0.26	0.01	0.05	0.05	beta Cephei
453	11.44	+0.81	+0.30	0.03	0.11	0.14	yellow semi–regular or T Tau

CHAPTER 7.

THE POLARIZATION OF STARLIGHT TOWARDS h AND chi PERSEI.

Mean photographic polarization parameters are now presented for the various groups of stars found in Chapter 6. These groups are:

1) proper motion stars;

2) F to M class V to III, stars below CC in Fig. 36;

3) suspected BAV stars;

4) h Persei stars;

5) field OB stars in the Perseus arm;

6) chi Persei stars.

The first three of these groups lie in the local spiral arm, the others in the Perseus arm.

In the polarization Catalogue at the end of this thesis, there are 191 stars with polarization measures used from 10 or more plates, but 12 of these have no UBV measures. Only these 179 stars, with r.m.s. deviations in the Stokes parameters of $\pm$ 0m.029, will be used in the following.

The mean polarization parameters for the various groups are given in Table 27.

The proper motion stars have the smallest amount of polarization, as expected since they are the nearest stars. The next two groups, the F to M class III to V stars and the suspected BAV stars, have equal amounts of polarization, nearly twice that of the proper motion stars. This confirms that

Table 27.

Mean Polarizations for the Groups of Stars towards h and chi Persei.

Star Group	Stars	p	P.A.	rms p	rms P.A.	E(B-V)	p/E(B-V)
1) proper motion	18	0.035	113	±0.010	±16		
2) F to M, V to III	18	0.063	112	±0.012	±10		
3) local BA stars	19	0.064	118	±0.011	± 9	0.31	0.206
4) h Persei	35	0.070	116	±0.006	± 5	0.60	0.117
5) field OB stars	52	0.083	113	±0.006	± 4	0.59	0.141
6) chi Persei	37	0.091	112	±0.007	± 4	0.62	0.147
3) local BA stars							
E(B-V) ≤ 0.32	13	0.063	116	±0.013	±10		
E(B-V) > 0.32	6	0.066	119	±0.017	±11		
4) h Persei							
E(B-V) ≤ 0.60	9	0.078	110	±0.012	± 8		
E(B-V) > 0.60	25	0.071	118	±0.008	± 6		
5) field OB stars							
E(B-V) ≤ 0.59	26	0.084	112	±0.008	± 5		
E(B-V) > 0.59	23	0.081	113	±0.009	± 6		
6) chi Persei							
E(B-V) ≤ 0.62	15	0.090	109	±0.012	± 7		
E(B-V) > 0.62	20	0.094	115	±0.011	± 6		

the F to M group are reddened stars, mostly of class III below GG in Fig. 36, and its stars are similarly distributed in the local spiral arm.

The mean colour excess for the BAV stars is 0.31, giving for the ratio p/E(B-V), a value of 0.206. The maximum value for this ratio from photoelectric polarization measures is 0.195, Schmidt-Kaler (1958). This agreement suggests that the interstellar dust in the local arm is uniformly aligned and has the maximum polarizing efficiency.

For the OB stars in the Perseus arm, the amount of polarization increases in the order h Persei, field OB stars and chi Persei, agreeing with the order in space derived by Schild (1967), Fig. 32. The amount of polarization for h Persei is very little larger than the value for the BAV stars in the local arm, although the colour excess is nearly double. Also the values of p/E(B-V) for the Perseus arm are much less. This suggests that 'depolarization' has occurred, and therefore the alignment of the dust grains is different in the Perseus arm, and hence so is the direction of the presumed magnetic field.

The position angles are all within one r.m.s. deviation of the mean value for all groups, 114°. This suggests that the position angle of the observed polarization, whatever the distance of the star emitting the light, is dominated by the alignment of the nearest effective dust clouds.

In the second part of Table 27, the stars in the last 4 groups have been divided at the value of the mean colour excess into two groups. For the BAV stars, the amount of polarization increases slightly with increase of obscuration, but there are rather few stars. For the OB stars in the Perseus arm, the reverse occurs except for chi Persei. Also, the differences in the

position angles for the two subgroups for h and chi Persei are just significant. This suggests the possibility of local orientations of the dust grains within the clusters, i.e. the possibility of local cluster magnetic fields.

It is therefore concluded: that the polarization observed towards h and chi Persei is largely produced within the local spiral arm; that the orientation of the presumed magnetic field in the Perseus arm is different to that in the local arm; and that there is a possibility of local magnetic fields associated with the clusters themselves.

Krzeminski and Serkowski (1967) have also reached the first conclusion from a study of the cluster Stock 2, 2.5 degrees north of h and chi Persei.

CONCLUSIONS.

A brief discussion of existing catalogues of photoelectric measurements of the polarization of starlight demonstrated the necessity for many more observations. Because of the large amounts of telescope time required for photoelectric polarization measures, these largely concentrate on the brighter stars. There is then a further necessity for an efficient, rapid method for studying the fainter stars. Such a photographic method has been described in this thesis.

The results of the new photographic method agree with photoelectric measures of the same stars, the differences between their Stokes parameters having an r.m.s. deviation of $\pm$ 0m.029. This could be reduced to about $\pm$ 0m.02 for a homogeneous set of high quality plates. The accuracy of the method is limited by the numbers of stars available in the observing conditions control regions, the correction curves varying continuously with magnitude. The astronomical limit on the application of the method is the star density in the region observed. The star density in the cluster regions of h and chi Persei to V = 13 – about 6000 stars per square degree – approaches this limit. Thus, on average, at the galactic equator, the magnitude limit attainable is V = 16 – five magnitudes fainter than the present photoelectric surveys. At present only a one degree diameter field can be observed but this diameter can be doubled. The practical limit on the use of the method is the measurement of the plates. The imminent advent of fully automatic measuring engines under computer control will remove this onerous difficulty. The method will then

become simple and efficient for the determination of the polarization parameters of vast numbers of stars.

The other new photographic method being developed by Treanor (1968), suffers much more severely from the effects of overlapping. The two methods complement each other – Treanor's method is useful for finding regions where there is an interesting configuration of the polarization vectors, and the method discussed here can investigate the polarization more fully with an economy of telescope time.

Using UBV photometry of the stars measured for polarization towards h and chi Persei, groups of stars within the local spiral arm and within the Perseus arm have been distinguished. From the mean photographic polarization values for the various groups, it is concluded that the observed polarization is largely produced within the local spiral arm, confirming Hall's (1958) suggestion and the results of Krzeminski and Serkowski (1967); that the orientation of the presumed magnetic field in the Perseus arm is different to that in the local arm; and that there is a possibility of local magnetic fields associated with the h and chi Persei clusters themselves.

The development of a practicable photographic method for the measurement of the polarization of starlight to very faint magnitude limits is a prologue to extensive investigations of magnetic fields in space, not only in many individual environments in this galaxy, but in nearby galaxies from measures of their brighter stars, and indeed also of

intergalactic magnetic fields from measures of galaxies themselves at such a distance that the images of the galaxies resemble those of stars.

ACKNOWLEDGEMENTS.

The author would like to thank Professor H. A. Brück for his constant interest and encouragement; the Department of Scientific and Industrial Research, now no longer extant, for a studentship during two years; Dr. V. C. Reddish, who designed the filter, for giving the author the opportunity of developing the method and for his encouragement and numerous stimulating discussions; the instrumentation division of the Royal Observatory for their assistance in general and with the iris photometer in particular; and Dr. K. N. Nandy, Mr. L. C. Lawrence and Mr. P. D. Macdonald for assistance with observing.

The description and discussion of the new photographic method for the measurement of the polarization of starlight and the preliminary results achieved, without the aid of the UBV photometry, have already appeared in

Publ. Roy. Obs. Edin., 6, no. 4, 1968. 39 – 122.

REFERENCES.

Allen, C. W., 1963. Astrophysical Quantities, 2nd ed. London, Athlone Press.

Becker, W., 1963. Z. Ap., 57, 117.

Behr, A., 1956. Veröff. Univ. Sternw. Univ. Göttingen, no. 114.

Behr, A., 1959. Veröff. Univ. Sternw. Univ. Göttingen, no. 126.

Blanco, V. M., 1955. Ap. J., 122, 434.

Chandrasekhar, S., 1946. Ap. J., 103, 351.

Chandrasekhar, S., and Fermi, E., 1953. Ap.J., 118, 113.

Coyne, G. V., and Gehrels, T., 1966. A. J., 71, 355.

Coyne, G. V., and Gehrels, T., 1967. A. J., 72, 887.

Fitzgerald, M. P., 1967. Ph. D. Thesis to Case Western Reserve University, Cleveland, Ohio.

Grigoreva, N. B., 1965. Isv. Krimskoi Astr. Obs., 34, 238.

Hall, J. S., 1958. Publ. U. S. Naval Obs., 17, 271.

Harris, D. L., and Upgren, A. R., 1964. Ap. J., 140, 151.

Hill, G., 1967. Ap. J. Suppl., 14, 301.

Hiltner, W. A., 1951. Ap. J., 114, 241.

Hiltner, W. A., 1954. Ap. J., 120, 454.

Hiltner, W. A., 1956. Ap. J. Suppl., 2, 389.

Hiltner, W. A., and Mook, D. E., 1966. Ap. J., 143, 1008.

Hiltner, W. A., and Schild, R. E., 1965. Sky and Telescope, 30, 144.

Hoyle, F., and Ireland, J. G., 1961. M. N. RAS, 122, 35.

Ireland, J. G., 1961. M. N. RAS, 122, 461.

Ireland, J. G., Nandy, K. N., Reddish, V. C., and Wickramasinghe, N. C., 1966. Nature, 212, 990.

Johnson, H. L., 1952. Ap. J., 116, 640.

Johnson, H. L., and Morgan, W. W., 1955. Ap. J., 122, 429.

Johnson, H. L., and Hiltner, W. A., 1956. Ap. J., 123, 267.

Kinman, T. D., Lamla, E., and Wirtanen, C. A., 1966. Ap. J., 146, 964.

Krzeminski, W., and Serkowski, K., 1967. Ap. J., 147, 988.

Kukarkin, B. V., and others, 1958. Obshchii katalog peremennykh zvezd, 2nd ed. Moscow, Akademiya Nauk.

Lavdovskii, V. V., 1961. Trudy Glav. Astr. Obs. Pulkove, Ser. II, 73, 5.

Lawrence, L. C., and Reddish, V. C., 1965. Publ. Roy. Obs. Edin., 3, 280.

Maanen, A. van, 1944. Ap. J., 100, 31.

Mathewson, D. S., 1968. Ap. J. (Letters), 153, L47.

Nandy, K. N., 1965. Publ. Roy. Obs. Edin., 5, 13.

Neckel, T., 1966. Z. Ap., 63, 221.

Oosterhoff, P. Th., 1937. Ann. Sterrew. Leiden, 17, 1.

Reddish, V. C., 1967. M. N. RAS, 135, 251.

Schild, R. E., 1965. Ap. J., 142, 979.

Schild, R. E., 1966. Ap. J., 146, 142.

Schild, R. E., 1967. Ap. J., 148, 449.

Schmidt-Kaler, Th., 1958. Z. Ap., 46, 145.

Seddon, H., and Jones, W., 1966. Publ. Roy. Obs. Edin., 5, 99.

Serkowski, K., 1960. Acta Astr., 10, 227.

Serkowski, K., 1965a. Ap. J., 141, 1340.

Serkowski, K., 1965b. Ap. J., 142, 793.

Serkowski, K., 1966. Ap. J., 144, 857.

Sharpless, S., 1965. Galactic Structure, eds. A. Blaauw and M. Schmidt. Chicago, University of Chicago Press. Chapter 7.

Smith, E. van P., 1956. Ap. J., 124, 43.

Treanor, P. J., 1968. M. N. RAS, 138, 325.

Tripp, W., 1956. Z. Ap., 41, 84.

Vasilevskis, S., 1962. A. J., 67, 699.

Visvanathan, N., 1968. Ap. J. (Letters), 153, L19.

Webb, J. H., and Evans, C. H., 1938. J. Opt. Soc. Amer., 28, 431.

Wildey, R. L., 1964. Ap. J. Suppl., 8, 439.

THE PHOTOGRAPHIC UBV CATALOGUE.

Column 1 Edinburgh number.

2 X coordinate in right ascension: 1 digit = 17.15 arc seconds.

3 Y coordinate in declination: 1 digit = 17.15 arc seconds.

4 number of V measures.

5 number of B measures.

6 number of U measures.

7 V magnitude.

8 B–V colour.

9 U–B colour.

10 r.m.s. deviation of mean V.

11 r.m.s. deviation of mean B–V.

12 r.m.s. deviation of mean U–B.

13 notes: 1 – h Persei stars in Perseus spiral arm.

2 – chi Persei stars in Perseus spiral arm.

3 – field ☐B stars in Perseus spiral arm.

4 – suspected BA stars in local spiral arm.

5 – F to M class V to III stars in local spiral arm.

6 – stars with annual proper motion > 0.01 arc secs.

1	2	3	4	5	6	7	8	9	10	11	12	13
1	916.0	36.9	5	5	5	11.93	0.73	0.10	0.03	0.05	0.05	5
2	914.7	41.0	5	5	5	12.05	0.71	0.18	0.02	0.05	0.07	5
3	914.1	45.9	5	5	4	12.45	2.20	1.61	0.02	0.06	0.17	5
4	916.4	51.2	5	5	5	12.26	0.53	0.26	0.02	0.06	0.06	4
5	926.3	70.3	5	5	5	10.79	1.38	1.14	0.03	0.03	0.04	5
6	936.9	75.7	5	5	5	12.02	0.63	0.13	0.03	0.05	0.07	6
7	927.1	62.1	5	5	5	10.88	0.47	-0.31	0.02	0.04	0.05	3
8	932.4	61.5	5	5	5	11.85	0.55	-0.27	0.02	0.03	0.04	3
9	934.9	63.1	5	5	5	11.33	0.46	-0.56	0.03	0.05	0.05	3
10	938.8	64.7	5	5	5	10.89	0.80	0.25	0.04	0.05	0.05	6
11	945.9	63.2	5	5	5	11.09	1.66	1.54	0.02	0.03	0.04	5
12	944.9	57.7	5	5	5	11.25	0.47	-0.32	0.03	0.04	0.04	3
13	936.7	36.6	5	5	5	10.03	0.75	0.16	0.02	0.03	0.03	6
14	949.3	40.6	3	5	5	8.07	0.26	0.04	0.01	0.02	0.03	4
15	970.7	39.3	5	5	5	9.97	0.45	-0.49	0.01	0.02	0.03	3
16	974.0	42.8	5	5	5	12.36	0.56	-0.38	0.04	0.05	0.04	3
17	974.7	44.1	5	5	5	11.78	0.96	0.40	0.02	0.03	0.03	6
18	976.8	43.9	5	5	5	11.25	0.53	-0.38	0.03	0.03	0.02	3
19	978.7	41.0	5	5	5	10.30	0.50	-0.43	0.03	0.03	0.04	3
20	981.8	50.7	5	5	5	11.87	0.38	-0.30	0.02	0.03	0.04	3
21	983.4	49.7	5	5	5	10.69	0.43	-0.28	0.01	0.03	0.02	3
22	989.4	52.7	5	5	5	9.09	2.30	2.74	0.01	0.04	0.05	3
23	992.9	53.3	5	5	5	10.60	1.21	1.24	0.02	0.02	0.03	6
24	988.7	63.5	5	5	5	12.58	1.86	1.86	0.03	0.05	0.09	6
25	986.8	61.7	5	5	5	12.52	1.66	1.15	0.04	0.07	0.07	5
26	966.9	62.7	5	5	5	12.54	0.36	-0.29	0.04	0.04	0.02	3
27	963.9	63.0	5	5	5	11.57	0.48	-0.29	0.02	0.03	0.03	3
28	971.3	67.1	5	5	5	9.58	0.30	0.25	0.03	0.03	0.03	4
29	966.4	72.5	3	5	5	5.95	1.10	0.78	0.06	0.07	0.03	5
30	958.7	77.7	5	5	5	12.11	0.52	-0.18	0.04	0.05	0.04	3
31	965.9	76.4	5	5	5	12.29	1.02	0.56	0.04	0.05	0.05	6
32	984.8	76.5	5	5	5	12.23	0.48	0.33	0.02	0.05	0.06	4
33	978.9	81.3	5	5	5	10.07	0.35	0.11	0.03	0.03	0.02	4
34	987.1	83.6	5	5	5	10.34	0.56	-0.47	0.03	0.03	0.02	3
35	982.9	94.4	5	5	5	12.45	0.51	-0.15	0.01	0.06	0.06	3

1	2	3	4	5	6	7	8	9	10	11	12	13
36	980.9	91.7	5	5	5	10.65	1.89	2.04	0.03	0.04	0.07	5
37	963.9	97.7	5	5	5	11.63	0.44	0.21	0.02	0.03	0.03	4
38	956.8	97.9	5	5	5	12.38	1.52	0.96	0.03	0.04	0.05	5
39	967.1	102.7	5	5	5	10.31	0.58	-0.20	0.02	0.03	0.04	3
40	979.1	102.7	5	5	4	12.56	1.88	1.37	0.02	0.07	0.09	6
41	5.1	101.1	5	5	5	12.09	0.61	0.23	0.03	0.03	0.03	4
42	11.0	105.9	5	5	5	9.13	0.33	0.16	0.03	0.03	0.06	4
43	21.7	104.4	5	5	5	11.66	0.73	0.23	0.03	0.04	0.05	6
44	24.4	90.3	5	5	5	11.87	0.47	-0.16	0.01	0.02	0.05	3
45	20.9	92.0	5	5	5	12.54	0.69	0.20	0.02	0.07	0.08	6
46	13.2	92.9	5	5	5	9.18	1.35	1.47	0.02	0.03	0.04	5
47	6.1	86.5	5	5	5	12.64	0.66	0.41	0.04	0.06	0.07	4
48	17.7	82.9	5	5	5	12.26	0.90	0.28	0.04	0.04	0.05	5
49	5.2	71.0	5	5	5	11.71	1.55	1.11	0.02	0.05	0.08	5
50	11.4	70.0	5	5	5	9.59	0.50	-0.35	0.02	0.03	0.03	3
51	13.1	65.3	5	5	5	11.30	0.51	-0.33	0.01	0.03	0.03	3
52	18.0	42.3	5	5	5	12.49	1.36	1.07	0.03	0.05	0.11	6
53	25.6	62.7	5	5	5	10.26	0.38	0.30	0.02	0.03	0.03	4
54	38.0	58.7	5	5	5	11.57	0.50	0.19	0.03	0.03	0.05	4
55	45.5	61.1	5	5	5	9.84	0.32	-0.45	0.01	0.02	0.02	3
56	44.7	37.6	5	5	5	12.47	0.31	-0.32	0.02	0.03	0.03	3
57	53.7	40.9	5	5	5	10.82	0.31	-0.38	0.03	0.03	0.04	3
58	54.2	43.1	5	5	5	11.34	0.39	0.40	0.01	0.03	0.04	4
59	58.5	40.3	5	5	5	10.40	0.58	0.13	0.01	0.02	0.03	6
60	68.4	45.7	5	5	5	12.52	0.48	-0.25	0.03	0.04	0.04	3
61	70.1	47.3	5	5	5	12.16	0.69	0.40	0.03	0.05	0.05	4
62	73.0	47.1	5	5	5	8.86	0.55	-0.56	0.02	0.03	0.03	3
63	76.7	52.4	5	5	5	12.73	0.41	-0.22	0.05	0.07	0.05	3
64	81.9	51.1	5	5	5	12.17	0.46	-0.22	0.02	0.04	0.04	3
65	85.9	51.4	5	5	5	12.65	1.42	0.97	0.05	0.06	0.07	6
66	99.7	50.2	5	5	5	10.43	0.46	0.28	0.02	0.03	0.03	4
67	79.2	67.9	5	5	5	12.46	0.60	0.29	0.04	0.06	0.04	4
68	58.8	70.6	5	5	5	12.18	1.50	1.37	0.04	0.08	0.07	5
69	72.1	75.1	5	5	5	12.36	0.33	-0.28	0.03	0.05	0.05	3
70	79.3	78.5	5	5	5	12.23	1.48	1.19	0.04	0.05	0.06	6

1	2	3	4	5	6	7	8	9	10	11	12	13
71	67.1	85.1	5	5	5	11.57	0.42	0.41	0.02	0.03	0.04	4
72	63.7	85.0	5	5	5	10.05	0.31	-0.50	0.01	0.02	0.02	3
73	57.9	83.2	5	5	5	12.54	1.48	1.08	0.04	0.04	0.07	5
74	59.1	93.9	5	5	5	11.94	0.83	0.26	0.04	0.05	0.04	5
75	46.9	96.3	5	5	5	10.62	0.84	0.33	0.03	0.03	0.06	6
76	912.5	30.7	5	5	5	12.27	0.74	0.09	0.02	0.04	0.05	6
77	915.0	31.7	5	5	5	10.84	0.64	0.09	0.03	0.05	0.04	6
78	926.7	34.2	5	5	5	11.00	0.93	0.41	0.01	0.04	0.04	6
79	930.4	25.5	5	5	5	12.37	0.59	0.32	0.01	0.06	0.06	4
80	918.9	21.9	5	5	5	12.68	0.73	0.42	0.04	0.05	0.05	4
81	904.8	5.3	5	5	5	12.47	0.94	0.35	0.04	0.05	0.08	6
82	901.4	2.9	5	5	4	12.86	0.62	0.28	0.04	0.06	0.05	4
83	907.9	2.8	5	5	5	12.17	0.52	0.19	0.02	0.04	0.05	4
84	920.2	0.2	5	5	5	12.17	0.36	-0.19	0.02	0.05	0.05	3
85	924.5	999.4	5	5	5	11.84	0.49	0.04	0.03	0.04	0.02	5
86	935.4	991.1	5	5	4	9.04	0.33	-0.77	0.01	0.02	0.05	3
87	936.6	984.7	4	5	4	10.29	0.35	-0.51	0.03	0.04	0.04	3
88	929.0	985.7	5	5	5	11.02	1.26	1.07	0.01	0.02	0.04	5
89	926.3	981.9	5	5	5	11.77	2.18	1.63	0.04	0.05	0.06	6
90	908.9	978.2	5	5	5	10.56	0.78	0.14	0.03	0.06	0.05	6
91	907.2	964.9	5	5	5	10.41	0.65	-0.26	0.01	0.05	0.05	3
92	906.5	961.6	5	5	5	10.51	0.47	-0.44	0.02	0.03	0.04	3
93	913.0	967.5	4	5	5	12.50	0.68	0.05	0.04	0.06	0.06	6
94	920.6	973.2	4	5	5	12.48	0.62	0.11	0.04	0.06	0.06	5
95	923.7	971.6	5	5	5	10.40	1.26	1.15	0.02	0.04	0.04	5
96	924.6	973.1	4	5	5	12.42	0.27	-0.39	0.02	0.03	0.04	3
97	932.6	975.5	3	5	5	6.46	0.29	-0.68	0.01	0.02	0.02	3
98	930.1	969.9	3	5	5	7.37	0.28	-0.69	0.02	0.02	0.04	3
99	930.6	965.0	5	5	5	12.01	0.33	-0.40	0.02	0.03	0.05	3
100	943.9	964.3	5	5	5	12.15	0.31	-0.32	0.05	0.05	0.06	3
101	951.4	961.4	0									0
102	952.2	961.2	0									0
103	970.5	963.7	5	5	5	11.16	0.30	-0.50	0.02	0.02	0.03	1
104	987.3	964.4	5	5	5	10.82	0.37	-0.43	0.02	0.03	0.06	1
105	954.3	974.5	5	5	5	11.34	0.36	-0.40	0.02	0.03	0.02	3

1	2	3	4	5	6	7	8	9	10	11	12	13
106	955.4	971.7	5	5	4	11.21	1.36	1.27	0.03	0.03	0.05	5
107	952.5	969.2	5	5	5	12.40	0.34	-0.35	0.01	0.04	0.05	3
108	949.3	971.1	5	5	5	11.54	1.18	0.68	0.03	0.05	0.07	5
109	943.3	974.6	5	5	5	12.11	1.23	0.81	0.04	0.06	0.06	5
110	958.2	980.7	5	5	5	12.06	0.33	-0.37	0.04	0.05	0.04	1
111	963.1	981.9	5	5	5	12.53	0.38	-0.34	0.04	0.04	0.04	1
112	960.3	982.9	5	5	5	8.84	0.31	-0.57	0.03	0.03	0.03	1
113	958.6	982.7	5	5	5	12.47	0.33	-0.19	0.03	0.05	0.08	1
114	957.1	985.7	5	5	5	11.75	0.30	-0.37	0.05	0.06	0.03	1
115	953.3	981.8	5	5	5	9.88	0.27	-0.73	0.02	0.03	0.04	1
116	946.4	985.4	0									0
117	948.9	987.3	0									0
118	952.1	987.7	5	5	5	13.56	0.09	-0.96	0.07	0.08	0.05	6
119	963.7	990.7	5	5	5	11.25	0.29	-0.42	0.01	0.03	0.04	1
120	959.4	995.4	4	5	5	11.74	0.39	-0.37	0.04	0.04	0.04	1
121	961.2	999.9	0									6
122	960.8	1.5	5	5	5	11.68	0.43	-0.32	0.02	0.03	0.04	1
123	954.9	5.7	5	5	5	9.34	0.39	-0.56	0.02	0.04	0.04	1
124	946.9	10.7	5	5	5	11.49	0.77	0.26	0.01	0.02	0.03	5
125	955.9	16.7	5	5	5	11.18	0.84	0.15	0.01	0.03	0.03	6
126	950.7	26.1	5	5	5	12.30	0.47	0.33	0.02	0.05	0.05	4
127	943.8	31.3	5	5	5	11.78	0.45	-0.42	0.04	0.05	0.05	3
128	946.6	32.5	5	5	5	11.21	1.20	0.83	0.03	0.05	0.04	5
129	980.0	31.1	5	5	5	12.62	0.58	0.35	0.03	0.05	0.06	4
130	980.7	31.7	5	5	5	10.94	0.53	-0.44	0.01	0.02	0.02	1
131	988.9	32.0	5	4	5	12.01	0.40	-0.31	0.03	0.05	0.05	1
132	983.9	26.7	5	5	5	10.98	0.55	-0.35	0.02	0.03	0.04	1
133	987.4	24.2	5	5	5	9.36	0.40	-0.49	0.02	0.03	0.03	1
134	984.6	23.1	5	5	5	11.72	0.43	-0.21	0.01	0.02	0.03	1
135	987.1	16.4	4	5	5	12.61	0.41	-0.14	0.06	0.07	0.04	1
136	997.7	18.0	5	5	5	12.69	1.35	0.99	0.06	0.07	0.07	5
137	1.5	16.7	5	5	5	10.59	0.35	-0.50	0.02	0.03	0.03	1
138	0.4	16.5	5	5	5	11.83	0.38	-0.43	0.03	0.04	0.04	1
139	996.0	13.1	5	5	5	12.57	0.65	0.35	0.04	0.05	0.04	4
140	990.5	7.1	5	5	5	11.03	0.54	-0.26	0.02	0.02	0.02	1

1	2	3	4	5	6	7	8	9	10	11	12	13
141	988.2	9.5	5	5	5	10.92	0.72	0.24	0.02	0.03	0.02	6
142	978.5	5.1	5	5	5	10.88	0.32	-0.48	0.01	0.02	0.03	1
143	979.0	6.3	5	5	5	12.28	0.28	-0.37	0.02	0.04	0.04	1
144	978.1	7.9	3	5	5	8.22	0.25	-0.60	0.02	0.03	0.03	1
145	980.5	8.5	5	5	5	9.29	0.31	-0.56	0.01	0.02	0.02	1
146	980.7	12.0	0									0
147	980.7	12.7	0									0
148	980.3	16.7	5	5	5	11.99	0.32	-0.37	0.02	0.03	0.03	1
149	980.8	18.1	0									0
150	976.7	19.7	5	5	5	12.82	0.34	-0.18	0.04	0.05	0.05	1
151	977.9	16.7	5	5	5	11.31	0.37	-0.27	0.04	0.04	0.03	1
152	972.0	14.9	5	5	5	12.11	0.32	-0.13	0.01	0.02	0.04	1
153	974.0	14.0	0									0
154	974.0	14.0	0									0
155	970.8	13.6	5	5	5	12.85	0.44	-0.34	0.05	0.05	0.05	1
156	969.9	12.2	5	5	5	11.36	0.37	-0.40	0.01	0.03	0.03	1
157	973.8	9.7	5	5	5	12.42	0.37	-0.32	0.03	0.03	0.02	1
158	972.8	7.9	5	5	5	10.17	0.32	-0.50	0.02	0.03	0.03	1
159	971.1	8.7	5	5	5	12.48	0.34	-0.35	0.04	0.06	0.05	1
160	967.7	7.1	5	5	5	12.50	1.10	0.64	0.03	0.05	0.06	5
161	972.1	999.9	5	5	5	10.04	0.39	-0.37	0.01	0.02	0.03	1
162	970.7	997.9	5	5	5	11.06	0.40	-0.42	0.02	0.02	0.03	1
163	973.3	996.7	5	5	5	11.33	0.36	-0.49	0.02	0.03	0.02	1
164	974.5	994.7	5	5	5	12.23	0.38	-0.37	0.02	0.04	0.05	1
165	976.8	999.3	5	5	5	10.85	0.26	-0.51	0.02	0.03	0.02	1
166	977.7	997.7	5	5	5	10.94	0.33	-0.39	0.02	0.02	0.02	1
167	979.0	995.7	5	5	5	9.39	0.28	-0.64	0.01	0.02	0.02	1
168	977.7	993.6	5	5	5	12.89	0.38	-0.10	0.05	0.05	0.03	1
169	976.8	989.3	5	5	5	12.55	0.34	-0.22	0.02	0.03	0.03	1
170	966.9	977.7	5	5	5	12.85	0.63	0.19	0.02	0.05	0.06	5
171	971.6	975.7	5	5	5	12.70	0.83	0.39	0.05	0.07	0.06	5
172	975.7	975.5	5	5	5	12.83	0.42	-0.29	0.02	0.02	0.03	1
173	974.6	974.7	5	5	5	10.56	0.33	-0.51	0.02	0.03	0.03	1
174	976.2	972.4	5	5	5	9.13	1.19	1.29	0.01	0.03	0.04	5
175	983.7	971.3	5	5	5	10.87	0.33	-0.51	0.02	0.03	0.03	1

1	2	3	4	5	6	7	8	9	10	11	12	13
176	988.6	969.4	5	5	5	11.26	0.57	0.07	0.02	0.03	0.03	5
177	991.8	969.4	5	5	5	11.09	0.61	0.07	0.02	0.03	0.03	6
178	990.9	972.7	5	5	5	12.84	0.36	–0.26	0.03	0.03	0.05	1
179	994.3	972.6	5	5	5	12.38	0.36	–0.23	0.04	0.04	0.05	1
180	998.8	969.7	5	5	5	9.81	0.43	–0.50	0.01	0.02	0.02	1
181	997.9	977.8	5	5	5	12.51	0.44	0.13	0.01	0.02	0.02	4
182	993.9	980.0	5	5	5	10.41	0.46	–0.50	0.03	0.03	0.02	1
183	988.0	978.5	5	5	5	9.12	0.34	–0.48	0.02	0.03	0.03	1
184	985.5	979.5	5	5	5	10.45	0.44	–0.61	0.01	0.02	0.02	1
185	988.8	983.6	0									6
186	988.6	984.7	5	4	5	9.89	0.34	–0.52	0.01	0.03	0.04	1
187	985.3	985.3	5	5	5	12.85	0.25	–0.31	0.05	0.07	0.07	1
188	984.3	985.5	5	5	5	9.47	0.28	–0.59	0.01	0.02	0.03	1
189	982.1	987.7	5	5	5	12.62	0.31	–0.34	0.03	0.03	0.02	1
190	983.9	988.7	5	5	5	12.04	0.39	–0.33	0.04	0.04	0.04	1
191	988.2	990.0	0									0
192	988.5	990.5	0									0
193	988.7	988.0	5	5	5	12.03	0.37	–0.29	0.02	0.03	0.03	1
194	990.2	988.0	0									0
195	990.6	988.2	0									0
196	994.1	985.6	0									0
197	994.4	983.1	5	4	5	12.62	0.75	–0.07	0.05	0.06	0.05	6
198	995.3	983.1	5	4	5	12.08	0.29	–0.42	0.04	0.04	0.03	1
199	0.8	983.0	5	5	5	12.06	0.34	–0.29	0.04	0.04	0.03	1
200	998.4	984.5	5	4	5	12.74	0.40	–0.32	0.02	0.02	0.03	1
201	998.2	986.4	0									0
202	998.0	986.7	0									0
203	998.4	987.2	0									0
204	1.9	990.7	5	5	5	12.16	0.34	–0.20	0.03	0.04	0.05	1
205	4.4	994.2	5	5	5	11.30	0.50	–0.41	0.01	0.02	0.02	1
206	0.7	993.1	5	5	5	12.69	0.25	–0.24	0.05	0.06	0.03	1
207	999.9	991.5	5	5	5	10.13	0.30	–0.41	0.01	0.04	0.04	1
208	999.6	990.6	0									0
209	998.8	990.0	5	4	2	12.71	1.67	1.30	0.04	0.06	0.11	5
210	996.5	990.7	0									0

1	2	3	4	5	6	7	8	9	10	11	12	13
211	990.8	991.2	5	5	5	11.62	0.34	-0.32	0.01	0.02	0.03	1
212	987.7	992.7	5	5	5	9.31	0.28	-0.53	0.00	0.01	0.03	1
213	991.5	993.1	5	4	5	12.31	0.23	-0.46	0.02	0.02	0.04	1
214	992.5	993.5	0									0
215	992.7	993.0	0									0
216	993.6	993.6	0									0
217	993.9	996.0	0									0
218	993.2	996.6	0									0
219	992.8	997.3	5	5	5	10.66	0.24	-0.47	0.02	0.03	0.04	1
220	992.1	996.5	0									0
221	991.3	996.3	0									0
222	990.8	997.4	0									0
223	990.7	998.2	0									0
224	989.5	998.2	0									0
225	985.0	0.7	5	5	5	12.28	0.34	-0.25	0.03	0.04	0.03	1
226	992.5	0.2	5	5	5	12.71	0.40	-0.28	0.04	0.04	0.04	1
227	991.9	2.3	5	5	5	11.28	0.44	-0.46	0.02	0.02	0.02	1
228	994.2	1.9	5	5	5	10.54	0.33	-0.05	0.02	0.02	0.01	1
229	0.6	998.2	5	5	5	12.96	0.25	-0.10	0.03	0.06	0.05	1
230	0.0	0.0	3	5	5	6.60	0.54	-0.42	0.02	0.03	0.03	1
231	1.0	2.9	5	5	5	10.82	0.43	-0.43	0.00	0.02	0.02	1
232	6.9	4.5	5	5	5	11.76	0.45	-0.32	0.03	0.03	0.03	1
233	7.1	998.9	5	5	5	11.94	0.38	0.29	0.02	0.05	0.05	4
234	8.7	998.0	5	5	5	12.78	0.40	-0.22	0.05	0.06	0.05	1
235	7.1	997.0	5	5	5	11.78	0.42	-0.39	0.04	0.05	0.04	1
236	6.5	993.6	5	5	5	9.36	0.41	-0.44	0.01	0.02	0.03	1
237	7.1	989.3	5	5	5	10.93	0.53	-0.32	0.02	0.03	0.04	1
238	6.1	988.7	5	5	5	10.32	0.56	-0.28	0.02	0.03	0.03	1
239	16.5	988.0	5	5	5	11.34	0.47	-0.36	0.02	0.02	0.02	1
240	12.7	984.0	5	5	5	9.90	0.44	-0.43	0.02	0.02	0.03	1
241	6.3	981.0	5	5	5	9.53	0.51	-0.50	0.01	0.01	0.02	1
242	10.6	979.6	5	4	5	12.62	0.48	-0.24	0.04	0.04	0.02	1
243	13.1	977.7	5	5	5	12.04	0.48	-0.32	0.03	0.03	0.05	1
244	12.1	977.6	5	5	5	12.71	0.47	-0.23	0.02	0.04	0.06	1
245	6.1	967.3	5	5	5	11.29	1.36	1.00	0.01	0.03	0.05	6

1	2	3	4	5	6	7	8	9	10	11	12	13
246	5.2	965.7	0									6
247	6.1	964.9	5	4	5	12.66	0.39	-0.20	0.07	0.10	0.07	1
248	10.6	963.9	5	5	5	12.79	0.37	-0.41	0.04	0.05	0.05	1
249	15.3	969.3	5	5	5	11.50	0.46	-0.41	0.02	0.03	0.03	1
250	16.5	968.0	5	5	5	10.93	0.41	-0.47	0.01	0.02	0.03	1
251	15.5	965.6	5	5	5	11.49	0.61	0.11	0.03	0.03	0.04	5
252	18.5	964.7	5	5	5	12.30	1.11	0.56	0.04	0.05	0.07	6
253	21.9	966.9	5	5	5	11.44	0.52	0.03	0.03	0.03	0.02	5
254	36.4	963.8	3	5	5	7.87	2.04	2.56	0.02	0.05	0.05	3
255	38.8	966.9	5	5	5	11.75	0.34	-0.54	0.03	0.03	0.04	3
256	26.5	972.7	5	5	5	12.70	0.51	-0.08	0.04	0.05	0.04	3
257	24.3	976.5	5	5	5	11.90	0.51	0.26	0.01	0.01	0.03	4
258	42.1	982.5	5	5	5	12.16	0.43	-0.32	0.03	0.03	0.03	2
259	38.8	989.3	5	5	5	12.41	0.42	-0.30	0.04	0.05	0.05	3
260	37.6	990.1	5	5	5	12.57	0.46	-0.37	0.05	0.06	0.06	3
261	29.6	985.7	5	5	5	8.98	0.39	-0.56	0.01	0.02	0.02	1
262	28.8	987.9	5	4	4	12.10	2.03	1.67	0.04	0.06	0.08	5
263	27.9	988.5	5	5	5	11.32	0.54	-0.33	0.04	0.04	0.03	1
264	24.8	991.0	5	5	5	11.29	0.41	-0.45	0.00	0.01	0.04	1
265	33.1	996.9	5	5	5	12.10	0.45	-0.24	0.02	0.03	0.02	3
266	29.7	0.0	5	5	4	11.42	0.46	-0.43	0.01	0.02	0.03	1
267	23.0	4.3	0									0
268	18.1	3.3	5	5	5	12.86	0.33	-0.22	0.02	0.04	0.06	1
269	29.3	11.1	5	5	5	12.91	0.38	-0.27	0.03	0.03	0.06	3
270	38.4	10.3	5	5	5	12.04	0.71	0.19	0.01	0.03	0.05	6
271	33.9	18.7	5	5	5	12.49	0.42	-0.16	0.04	0.05	0.05	3
272	17.6	12.7	5	5	5	12.83	0.35	-0.26	0.07	0.08	0.06	1
273	8.8	12.1	5	5	5	11.85	0.47	-0.36	0.01	0.05	0.05	1
274	6.4	11.3	5	5	5	12.30	0.52	-0.22	0.03	0.03	0.03	1
275	6.8	12.9	5	5	5	12.39	0.44	-0.29	0.03	0.03	0.03	1
276	8.8	17.6	5	5	5	12.83	0.45	0.24	0.06	0.07	0.04	4
277	20.4	26.1	5	5	4	11.77	1.98	2.03	0.00	0.05	0.07	5
278	19.4	31.6	4	5	5	8.22	0.31	0.09	0.03	0.03	0.02	4
279	20.5	35.3	4	5	5	12.70	0.57	0.03	0.07	0.09	0.07	5
280	37.0	30.7	5	5	5	12.08	0.39	-0.32	0.03	0.06	0.06	3

1	2	3	4	5	6	7	8	9	10	11	12	13
281	39.8	30.6	5	5	4	9.40	0.48	-0.55	0.02	0.03	0.04	3
282	42.6	30.4	5	5	5	12.73	0.39	-0.35	0.02	0.04	0.06	3
283	46.2	36.3	5	5	5	11.59	0.40	-0.35	0.04	0.04	0.05	3
284	48.6	29.9	5	5	5	11.75	0.59	0.37	0.03	0.04	0.03	4
285	50.0	20.1	5	5	5	12.64	1.23	0.87	0.04	0.06	0.06	5
286	56.8	13.7	5	5	5	11.03	0.43	-0.38	0.02	0.03	0.04	2
287	46.6	12.3	5	5	5	11.26	0.59	-0.21	0.02	0.04	0.06	2
288	53.9	0.5	5	5	5	9.48	0.38	-0.52	0.02	0.03	0.04	2
289	50.0	998.8	3	5	5	7.92	2.02	2.48	0.02	0.04	0.05	2
290	58.5	996.1	5	5	5	9.89	0.42	-0.51	0.01	0.02	0.02	2
291	56.6	995.2	5	4	5	10.70	0.37	0.25	0.01	0.02	0.03	4
292	58.1	991.1	5	5	5	12.34	0.43	-0.42	0.05	0.06	0.05	2
293	54.5	975.1	5	5	5	12.54	0.41	-0.19	0.03	0.04	0.05	2
294	54.8	969.7	5	5	5	11.51	0.86	0.21	0.03	0.06	0.06	6
295	50.5	968.0	5	5	5	10.54	0.75	0.17	0.02	0.04	0.04	6
296	53.9	965.9	5	5	5	11.00	0.42	-0.48	0.04	0.05	0.03	2
297	66.7	972.5	5	5	5	11.20	0.56	-0.49	0.02	0.04	0.04	2
298	71.3	969.1	5	5	5	12.71	0.45	-0.28	0.03	0.04	0.05	2
299	74.9	967.0	4	5	5	12.56	0.37	-0.31	0.01	0.04	0.05	2
300	82.1	967.1	5	5	5	12.25	0.32	-0.36	0.05	0.07	0.06	2
301	96.5	972.5	5	5	5	10.65	0.32	-0.54	0.02	0.02	0.02	2
302	94.9	975.3	5	5	5	10.78	0.32	0.15	0.02	0.03	0.03	4
303	99.7	976.9	5	5	5	12.65	1.40	0.96	0.04	0.06	0.08	5
304	99.9	977.8	5	5	5	11.00	0.36	-0.49	0.02	0.02	0.03	2
305	93.7	980.0	5	5	5	12.54	0.37	-0.34	0.02	0.03	0.04	2
306	94.5	979.0	5	5	5	12.92	1.26	0.91	0.04	0.04	0.06	6
307	93.1	976.9	5	5	5	12.83	1.36	0.90	0.04	0.04	0.08	5
308	92.3	977.9	5	5	5	10.92	0.36	-0.44	0.03	0.04	0.04	2
309	90.2	979.7	5	5	5	12.49	0.39	0.24	0.03	0.05	0.05	4
310	88.5	975.7	5	5	5	11.33	1.44	1.30	0.01	0.04	0.04	5
311	83.7	980.3	5	5	5	12.75	0.27	-0.18	0.02	0.05	0.06	2
312	82.8	979.5	5	5	5	12.89	0.68	0.18	0.04	0.04	0.06	5
313	73.1	979.3	5	5	5	11.17	0.51	-0.40	0.02	0.04	0.03	2
314	67.9	978.5	5	5	5	11.92	0.57	-0.44	0.02	0.05	0.05	2
315	59.0	983.5	5	5	5	11.99	0.51	-0.26	0.03	0.05	0.05	2

1	2	3	4	5	6	7	8	9	10	11	12	13
316	65.5	987.3	5	5	5	10.80	0.38	-0.58	0.02	0.03	0.03	2
317	70.9	985.1	5	5	5	11.31	0.45	-0.50	0.03	0.04	0.03	2
318	72.5	983.4	5	5	5	12.69	0.40	-0.30	0.03	0.04	0.05	2
319	82.1	985.1	5	5	5	9.63	0.48	-0.62	0.02	0.02	0.02	2
320	76.8	986.9	5	5	5	10.95	0.34	-0.34	0.02	0.03	0.03	2
321	78.5	989.1	5	5	5	12.93	0.48	-0.31	0.02	0.05	0.06	2
322	74.1	990.8	5	5	5	11.82	0.50	-0.21	0.04	0.05	0.04	2
323	71.0	992.3	0									0
324	73.8	993.1	5	5	5	12.22	0.39	-0.42	0.00	0.04	0.04	2
325	73.9	995.2	5	5	5	11.33	0.33	-0.50	0.01	0.01	0.02	2
326	71.5	997.1	5	5	5	11.90	0.35	-0.47	0.03	0.06	0.05	2
327	63.9	995.7	5	5	5	12.89	0.39	-0.27	0.03	0.05	0.06	2
328	71.0	4.0	5	5	5	11.73	0.43	-0.20	0.01	0.03	0.05	2
329	75.2	0.9	5	5	5	9.65	0.46	-0.59	0.02	0.03	0.03	2
330	80.8	3.3	5	5	5	10.49	0.45	-0.51	0.04	0.04	0.03	2
331	82.7	1.3	5	5	5	13.02	0.32	-0.18	0.04	0.05	0.06	2
332	83.2	0.2	0									0
333	84.5	997.7	5	5	5	12.81	0.70	0.25	0.04	0.06	0.09	5
334	80.5	998.2	0									0
335	80.0	999.0	0									0
336	79.0	999.6	5	5	5	11.39	0.22	-0.40	0.02	0.02	0.02	2
337	77.7	999.1	5	5	5	11.59	0.29	-0.45	0.02	0.02	0.03	2
338	80.0	997.1	0									0
339	78.9	996.5	0									0
340	80.1	995.5	0									0
341	80.3	994.4	0									0
342	77.9	993.7	5	5	5	12.75	0.26	-0.36	0.05	0.06	0.04	2
343	79.1	992.5	5	5	5	11.03	0.33	-0.62	0.01	0.02	0.03	2
344	80.5	991.1	5	5	5	12.65	0.26	-0.26	0.02	0.03	0.04	2
345	82.4	989.6	0									0
346	83.4	989.2	0									0
347	83.5	990.9	0									0
348	84.8	990.4	0									0
349	85.9	988.1	5	5	5	12.82	0.36	-0.34	0.04	0.05	0.03	2
350	90.4	989.3	4	5	5	8.21	2.07	2.31	0.02	0.04	0.04	2

1	2	3	4	5	6	7	8	9	10	11	12	13
351	99.7	988.9	5	5	5	11.23	0.28	-0.48	0.02	0.03	0.03	2
352	87.1	992.3	5	5	5	9.20	0.32	-0.55	0.01	0.02	0.02	2
353	87.9	994.9	5	5	5	12.26	0.32	-0.38	0.04	0.05	0.04	2
354	94.3	996.9	5	5	5	11.54	0.32	-0.39	0.02	0.03	0.02	2
355	102.5	997.7	5	5	5	11.91	0.40	-0.43	0.01	0.04	0.04	2
356	101.9	999.1	5	5	5	9.97	0.34	-0.44	0.02	0.02	0.02	2
357	100.8	3.1	5	5	5	11.45	0.49	-0.29	0.02	0.03	0.04	2
358	96.8	4.2	4	5	5	10.98	0.43	-0.31	0.03	0.04	0.03	2
359	97.5	5.2	5	5	5	10.98	0.47	-0.39	0.03	0.04	0.04	2
360	101.0	8.9	0									0
361	96.8	7.6	0									0
362	87.9	3.3	5	5	5	13.02	0.85	0.31	0.03	0.05	0.04	6
363	88.6	4.3	5	5	5	10.63	0.37	-0.42	0.02	0.03	0.04	2
364	87.7	7.0	5	5	5	11.00	0.39	-0.44	0.01	0.03	0.03	2
365	87.0	7.8	5	4	5	11.64	0.33	-0.41	0.03	0.04	0.05	2
366	88.7	9.0	0									6
367	92.5	10.1	5	5	5	9.50	0.33	-0.53	0.01	0.02	0.02	2
368	96.7	14.8	5	5	5	12.04	0.37	-0.27	0.04	0.06	0.05	2
369	92.8	16.2	5	5	5	10.91	0.45	0.03	0.01	0.03	0.05	5
370	87.8	20.9	5	5	4	12.73	1.91	1.23	0.03	0.05	0.06	5
371	85.7	13.3	5	5	5	11.77	0.45	-0.24	0.04	0.05	0.05	2
372	84.3	9.9	5	5	5	12.64	0.41	-0.17	0.03	0.04	0.04	2
373	81.9	9.0	0									0
374	76.8	9.1	5	5	5	11.63	0.45	-0.26	0.02	0.03	0.03	2
375	76.8	10.9	5	5	5	12.35	0.42	-0.27	0.02	0.04	0.05	2
376	76.0	16.9	3	5	3	6.43	0.51	0.07	0.01	0.05	0.05	2
377	73.8	21.3	5	5	5	12.37	0.48	-0.09	0.01	0.03	0.05	2
378	71.9	15.3	5	5	5	11.38	0.53	0.29	0.02	0.02	0.03	4
379	71.0	11.1	5	5	5	12.15	0.39	-0.32	0.03	0.05	0.04	2
380	69.0	8.8	5	5	5	12.60	0.43	-0.09	0.02	0.05	0.06	2
381	67.9	9.9	5	5	5	11.56	0.40	-0.37	0.01	0.03	0.04	2
382	64.8	10.6	5	5	5	12.44	0.65	0.06	0.02	0.04	0.05	5
383	64.4	9.2	5	5	5	11.71	0.44	-0.46	0.03	0.03	0.04	2
384	61.9	7.1	5	5	5	12.29	0.47	-0.38	0.02	0.04	0.05	2
385	62.3	12.1	5	5	5	10.54	0.31	-0.49	0.02	0.02	0.03	2

1	2	3	4	5	6	7	8	9	10	11	12	13
386	62.8	21.0	5	5	5	13.05	0.35	-0.11	0.04	0.06	0.04	2
387	62.2	24.9	5	5	5	11.76	0.82	0.24	0.02	0.05	0.06	6
388	64.5	26.6	5	5	5	12.38	0.46	-0.20	0.03	0.04	0.05	2
389	66.6	28.0	5	5	5	9.90	0.34	-0.62	0.02	0.03	0.04	2
390	66.8	32.9	5	5	5	11.83	0.46	-0.29	0.01	0.03	0.04	2
391	70.0	30.2	0									0
392	70.0	30.0	0									0
393	76.6	37.1	5	5	5	10.80	0.45	-0.37	0.01	0.03	0.03	3
394	84.5	33.9	5	5	5	11.48	0.56	-0.23	0.01	0.03	0.03	2
395	85.5	25.6	5	5	5	12.78	0.46	-0.14	0.02	0.02	0.04	2
396	86.0	23.3	4	5	5	8.70	0.40	-0.49	0.02	0.03	0.04	2
397	88.7	26.1	5	5	5	9.59	0.51	-0.29	0.02	0.04	0.05	2
398	91.7	22.3	0									0
399	96.7	24.9	5	5	5	11.96	0.53	-0.33	0.02	0.04	0.04	2
400	97.7	26.0	5	5	5	10.60	0.46	-0.33	0.02	0.03	0.03	2
401	106.7	28.9	5	5	5	10.66	0.51	0.15	0.04	0.04	0.04	6
402	105.0	23.1	5	5	5	11.85	0.43	-0.31	0.04	0.05	0.05	2
403	103.6	18.2	3	5	5	7.49	0.68	0.19	0.02	0.03	0.03	2
404	107.5	13.2	5	5	5	12.67	0.32	-0.16	0.03	0.04	0.06	2
405	106.8	9.7	5	5	5	11.84	0.45	-0.29	0.02	0.05	0.05	2
406	103.9	7.9	5	5	5	12.10	0.34	-0.32	0.04	0.04	0.04	2
407	105.1	7.9	5	5	5	10.53	0.48	-0.35	0.02	0.03	0.03	2
408	111.6	2.8	0									0
409	108.8	2.3	5	5	5	12.33	0.38	-0.34	0.04	0.07	0.10	2
410	106.4	2.3	5	4	5	11.83	0.41	-0.26	0.03	0.04	0.03	2
411	107.7	995.7	5	5	5	10.75	0.39	-0.01	0.04	0.05	0.03	5
412	109.1	993.7	5	5	5	10.26	0.42	-0.52	0.03	0.04	0.03	2
413	107.7	992.3	5	5	5	11.90	0.52	0.27	0.03	0.04	0.05	4
414	109.9	991.3	5	5	5	12.05	0.36	-0.43	0.04	0.05	0.04	2
415	106.5	969.7	5	5	5	9.73	0.27	-0.58	0.02	0.03	0.02	2
416	106.8	968.8	5	5	5	12.46	0.27	-0.39	0.02	0.04	0.04	2
417	917.1	947.9	5	5	5	11.09	1.16	0.77	0.02	0.06	0.07	5
418	914.1	943.9	5	5	5	12.34	0.31	-0.29	0.02	0.05	0.05	3
419	919.3	940.5	5	5	5	11.15	1.87	1.98	0.02	0.03	0.05	5
420	917.3	938.5	5	5	5	12.72	0.48	0.12	0.04	0.05	0.06	5

1	2	3	4	5	6	7	8	9	10	11	12	13
421	923.7	935.6	5	5	5	12.70	1.37	0.74	0.04	0.06	0.09	5
422	927.4	932.7	5	5	5	12.43	0.31	-0.35	0.05	0.05	0.03	3
423	934.6	922.6	5	5	5	12.53	0.36	-0.19	0.02	0.04	0.04	3
424	933.5	919.3	5	5	5	11.34	0.57	-0.04	0.04	0.05	0.03	5
425	938.6	916.7	5	5	5	10.59	0.21	-0.54	0.04	0.04	0.04	3
426	941.0	915.6	4	5	5	8.50	0.28	-0.62	0.01	0.02	0.03	3
427	945.4	909.1	0									0
428	945.7	909.6	0									0
429	945.3	920.6	5	5	5	12.02	0.28	-0.48	0.03	0.06	0.07	3
430	939.2	922.7	4	5	5	11.60	0.37	0.27	0.04	0.05	0.04	4
431	940.4	925.3	5	5	5	12.88	0.56	0.33	0.04	0.05	0.06	4
432	947.9	929.0	5	5	5	11.75	1.15	0.56	0.02	0.05	0.08	5
433	933.6	936.7	5	5	5	9.94	0.22	-0.61	0.02	0.03	0.03	3
434	938.7	945.0	5	5	5	10.58	0.34	0.17	0.02	0.04	0.04	4
435	938.1	950.5	5	5	5	12.39	0.72	0.23	0.02	0.04	0.05	5
436	930.1	956.3	5	5	5	12.13	0.35	-0.45	0.04	0.06	0.04	3
437	938.8	957.3	5	5	5	9.98	0.26	-0.58	0.01	0.03	0.03	3
438	943.2	957.4	5	5	5	11.63	0.31	-0.30	0.02	0.03	0.04	3
439	944.1	945.6	5	5	5	12.71	0.35	-0.27	0.01	0.03	0.04	3
440	944.5	942.6	5	5	5	9.19	0.23	-0.70	0.03	0.03	0.02	3
441	954.5	942.7	5	5	1	12.93	2.07	1.77	0.03	0.07	0.06	5
442	958.3	943.0	5	5	5	9.55	0.36	-0.66	0.02	0.03	0.03	3
443	967.3	940.7	5	5	5	11.82	0.32	-0.37	0.04	0.05	0.04	3
444	966.6	933.9	5	5	5	11.82	0.41	-0.49	0.03	0.06	0.06	3
445	964.1	932.7	5	5	5	11.47	0.31	-0.45	0.02	0.05	0.04	3
446	967.5	926.6	5	5	5	11.47	1.39	1.12	0.02	0.04	0.04	5
447	974.5	932.7	5	5	5	9.67	0.22	-0.66	0.03	0.03	0.02	3
448	974.6	934.7	5	5	5	11.53	0.29	-0.31	0.03	0.03	0.02	3
449	982.5	937.3	5	5	5	10.29	0.27	0.01	0.01	0.03	0.03	4
450	975.5	940.5	5	5	5	10.12	0.27	-0.63	0.02	0.03	0.03	3
451	986.9	943.2	5	5	4	12.60	1.87	1.45	0.02	0.06	0.06	5
452	974.5	945.9	5	5	5	11.95	0.76	0.02	0.01	0.03	0.04	6
453	973.9	947.9	4	5	5	11.44	0.81	0.30	0.03	0.11	0.14	5
454	970.5	948.7	5	5	5	11.88	0.52	0.29	0.03	0.04	0.04	4
455	971.7	950.7	5	5	5	12.02	0.35	-0.52	0.02	0.05	0.05	3

1	2	3	4	5	6	7	8	9	10	11	12	13
456	966.0	952.7	5	5	5	11.42	1.24	0.95	0.02	0.04	0.06	5
457	962.6	951.9	5	5	5	12.33	0.39	-0.39	0.03	0.06	0.06	3
458	959.1	953.7	5	5	5	11.05	0.26	-0.56	0.03	0.06	0.06	3
459	965.8	959.1	5	5	5	12.64	0.31	-0.18	0.03	0.04	0.04	3
460	974.1	957.5	5	5	5	12.42	0.28	-0.33	0.02	0.03	0.03	3
461	975.7	957.7	5	5	5	12.99	0.24	-0.25	0.04	0.05	0.04	1
462	978.3	957.7	5	5	5	11.19	1.93	2.00	0.01	0.05	0.08	5
463	978.6	958.5	5	5	5	11.89	0.50	0.19	0.01	0.03	0.03	4
464	996.5	955.7	5	5	5	10.47	0.41	-0.48	0.01	0.03	0.04	1
465	2.7	949.5	5	5	5	11.35	0.30	-0.36	0.03	0.05	0.04	3
466	6.1	947.1	5	5	5	11.11	1.47	1.15	0.03	0.07	0.09	5
467	6.1	941.1	5	5	5	11.35	0.37	-0.33	0.02	0.03	0.02	3
468	8.6	935.1	5	5	5	12.05	0.29	-0.34	0.02	0.04	0.04	3
469	4.2	929.5	5	5	5	11.19	0.34	-0.55	0.03	0.04	0.04	3
470	6.5	918.7	5	5	5	11.21	0.23	-0.44	0.03	0.03	0.05	3
471	3.3	914.8	5	5	5	11.97	0.32	-0.11	0.01	0.06	0.09	3
472	996.2	908.3	5	5	5	11.93	0.68	0.14	0.03	0.06	0.06	5
473	991.3	913.7	5	5	5	11.65	0.34	-0.47	0.04	0.05	0.04	3
474	986.1	914.3	4	5	4	9.19	0.31	-0.59	0.01	0.03	0.03	3
475	972.6	902.7	0									0
476	966.7	904.2	5	5	5	12.55	0.23	-0.24	0.02	0.03	0.03	3
477	970.7	895.7	5	5	5	12.30	0.48	0.16	0.03	0.04	0.04	4
478	981.8	895.9	4	5	5	11.36	0.20	-0.62	0.04	0.05	0.04	3
479	984.3	897.0	5	5	5	11.31	0.21	-0.56	0.02	0.03	0.03	3
480	994.4	889.0	5	5	5	10.41	0.55	0.33	0.03	0.03	0.05	4
481	995.2	889.7	5	5	5	12.74	0.50	0.25	0.03	0.05	0.06	4
482	2.5	891.6	5	5	5	11.83	0.21	-0.42	0.03	0.04	0.03	3
483	12.9	908.0	5	5	5	11.31	0.36	0.10	0.02	0.04	0.03	4
484	17.2	908.1	5	5	5	13.01	0.39	0.20	0.04	0.06	0.07	4
485	14.7	905.2	5	5	5	10.20	0.19	-0.66	0.01	0.02	0.02	3
486	19.1	904.5	5	5	5	12.52	1.31	0.72	0.03	0.05	0.05	5
487	16.5	903.3	5	5	5	10.83	0.32	0.26	0.03	0.04	0.06	4
488	20.1	898.1	5	5	5	13.08	0.55	0.29	0.06	0.07	0.04	4
489	31.9	894.5	5	5	5	11.51	1.20	0.70	0.04	0.05	0.04	5
490	35.7	901.2	5	5	4	12.29	2.08	1.78	0.04	0.06	0.07	5

1	2	3	4	5	6	7	8	9	10	11	12	13
491	32.9	907.9	4	5	5	12.84	0.14	–0.25	0.04	0.06	0.06	3
492	30.1	910.5	5	5	5	10.61	0.17	–0.60	0.02	0.03	0.03	3
493	29.1	911.0	5	5	5	12.84	1.29	0.91	0.02	0.05	0.08	5
494	32.9	918.7	5	5	5	12.49	0.23	–0.34	0.04	0.05	0.05	3
495	14.1	926.0	0									0
496	12.8	927.0	5	5	5	11.57	0.33	–0.39	0.02	0.05	0.05	3
497	16.1	931.7	5	5	5	12.39	0.33	–0.24	0.04	0.06	0.06	3
498	14.3	932.9	5	5	5	10.85	0.28	–0.54	0.03	0.03	0.03	3
499	10.2	942.6	5	5	5	12.45	0.35	–0.38	0.05	0.05	0.05	3
500	11.8	944.2	5	5	5	12.50	0.31	–0.50	0.02	0.04	0.04	3
501	15.7	947.9	5	5	5	12.38	0.33	–0.38	0.02	0.05	0.05	3
502	14.4	960.2	0									0
503	29.7	944.3	5	5	5	12.57	0.34	–0.38	0.04	0.05	0.04	3
504	34.9	938.6	5	5	4	12.77	1.65	1.39	0.04	0.07	0.06	5
505	35.7	940.3	5	5	5	11.92	1.65	1.56	0.02	0.05	0.05	5
506	40.0	949.0	5	5	5	12.42	0.69	0.20	0.03	0.04	0.04	5
507	47.8	952.7	5	5	5	12.48	0.51	–0.42	0.03	0.03	0.05	3
508	48.1	949.9	4	5	5	9.23	0.38	–0.57	0.03	0.03	0.03	3
509	54.5	938.2	5	5	5	11.90	0.26	–0.38	0.02	0.05	0.05	3
510	56.6	937.3	5	5	5	8.53	0.31	–0.56	0.01	0.03	0.02	3
511	57.3	935.0	5	5	5	9.45	0.24	–0.58	0.02	0.03	0.03	3
512	56.5	927.1	5	5	5	9.52	0.23	–0.63	0.02	0.03	0.02	3
513	54.9	913.5	5	5	5	10.97	0.25	–0.42	0.03	0.03	0.02	3
514	68.9	923.7	5	5	5	12.82	0.38	0.18	0.02	0.04	0.05	4
515	79.0	928.9	5	5	2	12.65	1.85	1.28	0.03	0.04	0.10	5
516	87.0	928.1	5	5	5	11.70	1.24	0.74	0.03	0.03	0.06	5
517	76.5	946.1	4	5	5	8.46	0.20	–0.80	0.01	0.02	0.03	3
518	67.8	947.6	5	5	5	10.69	0.43	–0.43	0.02	0.03	0.03	3
519	61.9	944.4	5	5	5	10.80	0.32	–0.52	0.03	0.04	0.04	3
520	60.9	948.2	5	5	5	11.34	0.40	–0.53	0.03	0.04	0.04	3
521	60.9	949.6	5	5	5	12.22	0.43	–0.50	0.03	0.04	0.05	3
522	62.0	952.3	5	5	5	12.09	0.41	–0.27	0.01	0.06	0.06	3
523	62.0	958.3	5	5	5	12.06	0.52	–0.15	0.02	0.05	0.05	3
524	68.6	955.9	5	5	5	11.93	0.43	–0.57	0.02	0.05	0.05	3
525	74.8	954.2	5	5	5	12.02	1.38	0.86	0.04	0.05	0.11	5

1	2	3	4	5	6	7	8	9	10	11	12	13
526	97.3	948.5	5	5	5	11.66	1.10	0.54	0.04	0.06	0.05	5
527	102.1	960.1	5	5	5	10.43	0.52	-0.54	0.02	0.03	0.02	3

CATALOGUE

Col. 1 Edinburgh number.

2 Oosterhoff (1937) number.

3 Lavdovskii (1961) number.

4 N_m - number of magnitude measures.

5 X coordinate in α direction: 1 digit = 17.15 sec. arc.

6 Y coordinate in δ direction: 1 digit = 17.15 sec. arc.

7 m_E magnitude from Ilford R40 emulsion.

8 rms(m) - r.m.s. deviation per magnitude measure.

9 N_p - number of polarization measures.

10 N_u - number of polarization measures used.

11 p - amount of polarization in magnitudes.

12 P.A. - position angle of the polarization.

13 rms(p) - r.m.s. deviation of the polarization magnitude differences used.

14 Q - Stokes parameter.

15 U - Stokes parameter.

16 Notes: 1 - HD number)
) see lists at end of Catalogue.
2 - BD number)

3 - photoelectric standard stars, Table 8.

4 - variable stars, Tables 9 and 10.

5 - photoelectric polarization measures, Table 14.

6 - stars with large proper motions, Table 15.

No.	Cost.	Lavd.	N_m	X	Y	m_E	rms(m)	N_p	N_u	p	P.A.	rms(p)	Q	U	Notes
1	0	106	16	916.1	37.2	12.05	0.08	16	11	0.032	68	0.022	−0.022	0.022	
2	0	0	16	915.0	41.3	12.10	0.10	16	12	0.030	160	0.040	0.023	−0.020	
3	0	90	15	914.1	46.1	12.69	0.08	14	10	0.077	138	0.039	0.008	−0.077	
4	0	112	16	916.3	51.5	12.28	0.09	16	7	0.121	111	0.023	−0.091	−0.079	
5	0	195	16	926.3	70.5	11.01	0.07	15	9	0.057	124	0.023	−0.021	−0.053	
6	0	271	14	937.1	76.0	12.14	0.14	10	7	0.146	155	0.045	0.095	−0.111	6
7	0	198	14	927.3	62.3	10.86	0.06	14	10	0.066	138	0.030	0.007	−0.066	
8	0	232	15	932.3	61.5	11.86	0.06	14	11	0.096	107	0.023	−0.079	−0.053	
9	0	251	15	935.1	63.3	11.32	0.06	15	10	0.126	118	0.016	−0.071	−0.104	
10	0	284	15	939.0	65.0	11.01	0.07	15	9	0.047	136	0.018	0.001	−0.047	6
11	0	358	15	946.0	63.5	11.34	0.08	15	12	0.069	123	0.024	−0.029	−0.063	
12	154	347	15	945.1	58.0	11.27	0.06	15	11	0.078	122	0.025	−0.034	−0.071	
13	67	265	16	936.7	36.8	10.13	0.05	16	14	0.049	122	0.025	−0.021	−0.044	2,6
14	197	390	16	949.3	40.8	8.09	0.07	16	11	0.015	104	0.023	−0.014	−0.007	1,2,6
15	496	597	16	971.0	39.4	9.98	0.04	16	15	0.101	110	0.022	−0.078	−0.064	2
16	562	649	16	974.2	43.1	12.37	0.07	16	15	0.154	120	0.046	−0.075	−0.134	
17	582	658	16	974.8	44.3	11.93	0.04	10	10	0.092	126	0.033	−0.027	−0.088	6
18	635	707	16	977.1	44.0	11.27	0.05	10	9	0.121	118	0.035	−0.067	−0.100	
19	678	733	16	978.6	41.3	10.33	0.05	16	10	0.104	112	0.016	−0.076	−0.072	2
20	744	786	16	981.7	51.1	11.82	0.04	16	11	0.058	129	0.022	−0.011	−0.057	
21	768	809	16	983.5	49.9	10.71	0.05	16	8	0.174	116	0.011	−0.106	−0.138	
22	899	910	16	989.6	52.8	9.20	0.17	15	10	0.086	124	0.020	−0.032	−0.080	2,3,4,5
23	983	984	16	993.1	53.5	10.80	0.05	16	12	0.073	82	0.026	−0.070	0.019	3,6
24	0	898	16	988.9	63.4	12.80	0.10	9	5	0.087	113	0.023	−0.060	−0.064	6
25	0	863	14	986.9	61.9	12.77	0.12	13	12	0.086	128	0.054	−0.021	−0.084	
26	0	556	16	967.1	62.8	12.47	0.11	15	10	0.086	108	0.035	−0.069	−0.051	
27	0	513	16	964.1	63.3	11.62	0.07	15	15	0.120	135	0.038	0.000	−0.120	
28	0	615	16	971.3	67.4	9.57	0.06	14	13	0.052	158	0.029	0.037	−0.037	2
29	0	547	16	966.3	72.6	6.06	0.08	13	6	0.018	130	0.011	−0.003	−0.017	2
30	0	475	16	958.9	77.7	12.17	0.07	12	8	0.141	119	0.042	−0.076	−0.119	
31	0	546	16	966.1	76.5	12.49	0.09	13	11	0.142	125	0.041	−0.050	−0.133	6
32	0	838	16	984.8	76.6	12.24	0.09	12	10	0.072	118	0.028	−0.040	−0.060	
33	0	754	15	979.2	81.5	10.03	0.07	11	6	0.147	147	0.010	0.059	−0.135	2
34	0	882	15	987.3	83.7	10.37	0.04	11	9	0.144	130	0.022	−0.027	−0.142	2
35	0	812	15	983.1	94.6	12.40	0.11	10	10	0.091	95	0.052	−0.090	−0.015	
36	0	787	15	981.2	91.8	10.83	0.05	10	9	0.099	120	0.034	−0.049	−0.086	
37	0	526	15	964.0	97.9	11.63	0.06	8	8	0.078	120	0.036	−0.038	−0.068	
38	0	460	9	956.5	98.6	12.62	0.09	9	4	0.144	127	0.028	−0.038	−0.139	
39	0	560	15	967.3	102.9	10.38	0.06	10	5	0.100	117	0.009	−0.058	−0.082	
40	0	763	11	979.2	103.1	12.75	0.07	9	8	0.130	104	0.038	−0.115	−0.061	6
41	0	1169	15	5.4	101.3	12.10	0.06	10	9	0.141	115	0.031	−0.091	−0.107	
42	0	1242	15	11.1	106.0	9.13	0.07	10	8	0.084	174	0.023	0.082	−0.017	2,6
43	0	1345	15	21.7	104.6	11.74	0.07	10	10	0.087	116	0.037	−0.055	−0.068	6
44	0	1361	15	24.4	90.3	11.87	0.06	10	9	0.144	122	0.029	−0.064	−0.128	
45	0	1335	14	20.8	92.2	12.63	0.08	10	6	0.064	84	0.027	−0.063	0.014	6
46	0	1270	15	13.5	93.0	9.33	0.04	10	9	0.079	142	0.017	0.018	−0.077	2
47	0	1178	14	6.2	86.6	12.66	0.10	9	6	0.112	117	0.031	−0.064	−0.091	
48	0	0	16	17.6	83.0	12.33	0.07	10	9	0.159	112	0.042	−0.114	−0.110	
49	0	1159	16	5.2	71.2	11.90	0.05	13	10	0.105	118	0.027	−0.059	−0.087	
50	0	1231	16	11.5	70.1	9.64	0.06	14	11	0.078	124	0.030	−0.030	−0.072	2
51	0	1258	16	13.2	65.6	11.31	0.04	15	11	0.040	107	0.017	−0.033	−0.023	
52	1470	1307	15	18.2	42.7	12.67	0.10	15	13	0.086	129	0.050	−0.019	−0.084	6
53	0	1371	16	25.6	62.9	10.27	0.04	16	14	0.051	104	0.028	−0.045	−0.024	2
54	1685	1477	16	38.2	58.9	11.60	0.05	16	10	0.061	114	0.019	−0.041	−0.045	
55	0	1535	16	45.6	61.3	9.81	0.04	16	10	0.065	91	0.019	−0.065	−0.002	2,5
56	1759	1562	16	44.7	37.8	12.38	0.06	16	15	0.092	118	0.059	−0.052	−0.076	
57	1873	1619	15	53.7	40.9	10.84	0.05	15	15	0.080	103	0.045	−0.072	−0.034	2,5
58	1884	1622	16	54.2	43.1	11.39	0.04	16	9	0.058	118	0.014	−0.032	−0.048	
59	1932	1664	16	58.3	40.4	10.44	0.05	15	12	0.020	82	0.026	−0.019	0.006	2,6
60	2067	1790	16	68.3	45.8	12.51	0.13	15	14	0.054	138	0.049	0.006	−0.054	
61	2084	1814	15	70.2	47.4	12.24	0.06	9	9	0.138	125	0.039	−0.048	−0.129	3
62	2138	1856	16	73.2	47.1	8.79	0.06	11	8	0.078	93	0.034	−0.078	−0.009	1,2,3,4,5
63	2195	1902	16	76.7	52.4	12.78	0.14	16	11	0.134	134	0.046	−0.003	−0.134	
64	2298	1990	15	82.1	51.2	12.17	0.07	14	13	0.088	130	0.046	−0.017	−0.086	
65	2364	2052	16	86.1	51.5	12.94	0.18	12	6	0.125	110	0.035	−0.096	−0.081	6
66	2554	2208	16	99.8	50.2	10.46	0.06	16	14	0.078	118	0.037	−0.044	−0.065	
67	0	1948	16	79.3	68.1	12.55	0.09	14	10	0.158	130	0.033	−0.028	−0.155	
68	0	1679	15	59.1	70.7	12.42	0.08	14	12	0.125	111	0.037	−0.094	−0.083	
69	0	1844	15	72.2	75.2	12.28	0.06	12	9	0.150	113	0.043	−0.102	−0.109	
70	0	1956	15	79.5	78.5	12.50	0.10	11	10	0.133	129	0.048	−0.027	−0.130	6

No.	Oost.	Lavd.	N_m	X	Y	m_E	rms(m)	N_p	N_u	p	P.A.	rms(p)	Q	U	Notes
71	0	1787	15	67.3	85.2	11.60	0.03	5	4	0.161	121	0.013	−0.075	−0.142	
72	0	1746	9	63.9	85.1	10.05	0.06	5	5	0.110	120	0.035	−0.056	−0.095	2
73	0	1667	13	57.8	83.3	12.79	0.14	11	6	0.106	132	0.028	−0.012	−0.105	
74	0	1686	15	59.2	94.0	12.01	0.07	10	10	0.086	120	0.039	−0.044	−0.074	
75	0	1555	15	46.9	96.3	10.75	0.04	10	9	0.077	132	0.037	−0.009	−0.076	6
76	0	74	16	912.4	31.1	12.36	0.11	16	9	0.095	120	0.025	−0.048	−0.082	6
77	0	101	14	915.1	32.0	10.89	0.07	14	13	0.048	156	0.037	0.032	−0.035	6
78	0	194	16	926.9	34.4	11.15	0.05	16	12	0.018	115	0.027	−0.011	−0.014	6
79	5	216	16	930.3	25.6	12.44	0.12	16	12	0.094	126	0.031	−0.028	−0.089	
80	0	130	15	919.1	22.1	12.89	0.17	15	12	0.078	131	0.056	−0.011	−0.077	
81	0	18	15	905.0	5.5	12.70	0.15	15	10	0.013	150	0.042	0.006	−0.011	6
82	0	0	14	901.3	3.2	12.94	0.14	11	10	0.055	67	0.053	−0.039	0.039	
83	0	39	16	908.0	3.1	12.16	0.10	15	13	0.038	123	0.045	−0.016	−0.034	
84	0	134	15	920.3	0.4	12.10	0.06	15	10	0.065	117	0.025	−0.039	−0.053	
85	0	173	16	924.6	999.6	11.84	0.06	16	13	0.098	131	0.027	−0.012	−0.097	
86	49	244	16	935.4	991.3	9.06	0.04	16	9	0.068	109	0.016	−0.054	−0.041	2,3,5
87	63	255	16	936.7	985.0	10.25	0.05	16	15	0.092	97	0.033	−0.090	−0.021	2
88	1	201	16	929.2	986.1	11.18	0.05	15	9	0.057	70	0.022	−0.044	0.037	
89	0	185	14	926.3	982.1	12.20	0.22	14	12	0.060	95	0.034	−0.060	−0.010	4,6
90	0	44	15	909.1	978.3	10.65	0.06	15	11	0.040	97	0.023	−0.039	−0.009	6
91	0	29	15	907.3	965.3	10.42	0.11	15	8	0.082	95	0.018	−0.080	−0.015	4
92	0	24	15	906.5	961.7	10.54	0.08	15	13	0.101	93	0.031	−0.101	−0.010	
93	0	73	15	913.2	967.6	12.63	0.10	13	6	0.123	129	0.019	−0.026	−0.120	6
94	0	135	10	920.7	973.5	12.54	0.12	9	8	0.068	85	0.036	−0.067	0.013	
95	0	158	15	923.8	971.9	10.59	0.07	15	7	0.090	114	0.017	−0.061	−0.067	2
96	0	168	15	924.9	973.3	12.27	0.08	9	6	0.056	98	0.012	−0.054	−0.015	3
97	16	225	15	932.7	975.5	6.47	0.04	15	7	0.058	107	0.018	−0.048	−0.033	1,2,3,5
98	3	210	15	930.3	970.1	7.38	0.05	15	7	0.074	114	0.014	−0.050	−0.054	1,2,3,5
99	7	211	14	930.6	965.3	12.00	0.08	14	12	0.065	110	0.033	−0.050	−0.042	3
100	140	326	16	943.8	964.4	12.14	0.08	16	13	0.047	121	0.042	−0.023	−0.042	
101	229	396	16	951.6	961.6	11.15	0.06	16	12	0.051	89	0.024	−0.051	0.003	
102	237	403	16	952.1	961.4	12.23	0.08	16	15	0.128	113	0.049	−0.090	−0.091	
103	487	575	16	970.4	963.8	11.11	0.05	15	14	0.068	100	0.033	−0.064	−0.022	
104	834	842	16	987.4	964.6	10.81	0.04	16	11	0.020	78	0.028	−0.019	0.008	
105	250	418	16	954.4	974.7	11.29	0.05	16	11	0.016	135	0.022	−0.000	−0.016	
106	268	424	16	955.4	971.9	11.45	0.04	16	11	0.027	91	0.023	−0.027	−0.001	
107	242	406	16	952.4	969.4	12.33	0.06	16	13	0.102	100	0.040	−0.096	−0.035	
108	196	378	16	949.3	971.3	11.74	0.04	16	10	0.058	109	0.017	−0.046	−0.036	
109	136	320	16	943.3	974.8	12.32	0.05	16	14	0.108	119	0.033	−0.055	−0.092	
110	306	452	16	958.2	980.9	11.97	0.06	16	10	0.093	106	0.022	−0.078	−0.050	
111	376	502	14	963.2	982.1	12.51	0.08	13	9	0.111	114	0.015	−0.073	−0.083	
112	339	472	16	960.3	983.2	8.89	0.05	14	10	0.081	107	0.017	−0.067	−0.046	1,2,3,5
113	311	456	16	958.4	982.8	12.51	0.11	12	9	0.256	124	0.052	−0.097	−0.237	3
114	289	441	16	957.2	985.7	11.68	0.05	16	7	0.100	108	0.020	−0.081	−0.058	
115	245	413	15	953.3	982.1	9.84	0.05	14	9	0.101	99	0.017	−0.096	−0.032	2
116	164	351	16	946.4	985.7	11.61	0.05	16	8	0.104	101	0.019	−0.096	−0.039	
117	190	376	16	948.8	987.6	12.06	0.07	15	8	0.148	123	0.016	−0.060	−0.136	
118	230	404	8	952.1	987.8	13.28	0.13	7	6	0.078	166	0.042	0.070	−0.036	3,6
119	380	507	16	963.6	991.1	11.17	0.05	16	15	0.068	112	0.029	−0.048	−0.048	
120	326	467	15	959.5	995.6	11.71	0.03	15	11	0.061	103	0.025	−0.055	−0.026	
121	356	489	16	961.3	0.2	11.84	0.05	16	15	0.043	113	0.029	−0.030	−0.031	6
122	350	483	16	960.9	1.7	11.66	0.05	16	15	0.136	124	0.032	−0.053	−0.125	
123	260	430	16	957.5	5.9	9.37	0.05	15	12	0.069	112	0.015	−0.049	−0.048	2,5
124	174	361	16	947.0	10.9	11.60	0.05	16	11	0.051	112	0.018	−0.036	−0.036	
125	278	435	16	955.9	16.8	11.29	0.05	16	13	0.012	100	0.028	−0.011	−0.004	6
126	214	401	16	950.9	26.3	12.26	0.08	15	8	0.045	77	0.023	−0.041	0.019	
127	138	333	16	943.8	31.6	11.76	0.05	16	12	0.059	97	0.023	−0.057	−0.014	
128	168	363	16	946.6	32.7	11.37	0.06	13	9	0.031	123	0.017	−0.013	−0.028	
129	705	751	15	979.9	31.3	12.67	0.09	15	12	0.100	140	0.036	0.017	−0.099	
130	729	770	16	980.8	31.8	10.97	0.05	15	11	0.077	134	0.030	−0.004	−0.077	
131	888	897	15	989.0	32.2	12.01	0.05	15	7	0.069	131	0.019	−0.009	−0.069	
132	777	803	16	983.8	26.8	11.00	0.05	16	8	0.184	120	0.016	−0.090	−0.161	
133	839	861	16	987.3	24.4	9.40	0.05	16	13	0.073	111	0.020	−0.055	−0.048	2
134	789	821	16	984.6	23.3	11.65	0.03	15	7	0.085	117	0.015	−0.050	−0.069	
135	838	858	13	987.2	16.7	12.59	0.12	13	9	0.108	137	0.030	0.007	−0.107	
136	1119	1054	16	997.7	18.1	12.90	0.11	16	8	0.107	98	0.028	−0.102	−0.029	3
137	1196	1113	16	1.4	16.9	10.55	0.06	14	6	0.066	110	0.020	−0.051	−0.043	2
138	1174	1097	16	0.3	16.6	11.77	0.03	15	10	0.138	121	0.017	−0.067	−0.121	
139	1062	1023	16	996.0	13.4	12.64	0.07	15	8	0.110	124	0.026	−0.042	−0.102	
140	919	916	16	990.3	7.4	11.02	0.06	14	11	0.038	154	0.026	0.023	−0.030	

No.	Oost.	Lavd.	N_m	X	Y	m_E	rms(m)	N_p	N_u	p	P.A.	rms(p)	Q	U	Notes
141	851	880	16	988.3	9.6	11.00	0.04	15	12	0.053	178	0.028	0.053	−0.003	6
142	670	722	16	978.3	5.5	10.87	0.03	15	13	0.065	128	0.030	−0.015	−0.064	
143	695	730	16	979.3	6.6	12.17	0.07	15	11	0.071	121	0.029	−0.034	−0.062	
144	662	712	12	978.2	7.9	8.22	0.05	4	3	0.075	110	0.006	−0.057	−0.048	1,2,3,5
145	717	757	12	980.3	8.6	9.29	0.05	2	2	0.052	71	0.014	−0.041	0.032	2,3
146	725	767	16	980.9	12.1	11.42	0.04	15	12	0.061	118	0.028	−0.035	−0.051	
147	731	768	16	981.0	12.7	10.67	0.07	14	13	0.137	111	0.051	−0.102	−0.091	
148	714	758	16	980.3	16.9	11.92	0.02	12	6	0.106	118	0.016	−0.059	−0.088	
149	730	769	16	981.0	18.4	12.61	0.10	16	14	0.111	95	0.072	−0.110	−0.018	
150	626	691	16	976.8	19.8	12.77	0.11	16	11	0.164	114	0.043	−0.108	−0.122	
151	658	716	15	977.9	16.9	11.26	0.04	11	8	0.117	120	0.022	−0.057	−0.102	
152	515	606	16	972.0	15.1	12.00	0.05	16	9	0.051	87	0.018	−0.050	0.005	
153	551	646	16	974.1	14.1	10.47	0.06	13	11	0.114	119	0.025	−0.062	−0.096	2
154	549	645	13	973.8	13.5	12.68	0.10	7	5	0.217	113	0.034	−0.150	−0.157	
155	494	591	15	970.8	13.7	12.84	0.10	9	4	0.060	102	0.027	−0.055	−0.025	
156	475	582	14	969.9	12.4	11.33	0.04	14	6	0.073	133	0.013	−0.006	−0.073	
157	547	635	14	973.8	9.9	12.37	0.08	14	8	0.140	116	0.027	−0.085	−0.111	
158	530	626	11	973.0	8.1	10.15	0.05	5	4	0.069	96	0.014	−0.068	−0.014	2
159	505	596	11	971.4	8.9	12.33	0.13	7	5	0.184	105	0.052	−0.160	−0.092	
160	440	553	14	967.7	7.3	12.61	0.14	11	8	0.157	113	0.043	−0.107	−0.114	
161	517	605	16	972.1	0.2	9.93	0.06	16	11	0.096	110	0.021	−0.074	−0.060	2
162	491	585	16	970.7	998.1	11.03	0.05	16	15	0.109	122	0.034	−0.048	−0.098	
163	538	625	11	973.4	996.6	11.31	0.03	10	8	0.083	100	0.023	−0.078	−0.029	
164	563	641	10	974.4	994.9	12.15	0.06	10	9	0.114	122	0.030	−0.051	−0.103	
165	622	682	16	976.8	999.6	10.78	0.06	13	9	0.063	121	0.025	−0.029	−0.055	
166	649	705	15	977.6	997.9	10.93	0.05	15	11	0.021	89	0.026	−0.021	0.000	
167	692	731	13	979.3	995.9	9.40	0.06	9	7	0.090	96	0.018	−0.088	−0.020	2,5
168	647	696	14	977.7	993.9	12.92	0.11	12	8	0.195	125	0.051	−0.064	−0.184	
169	623	680	15	976.8	989.6	12.48	0.10	14	11	0.127	131	0.049	−0.016	−0.126	
170	431	540	13	967.2	977.7	12.90	0.11	12	8	0.111	133	0.055	−0.008	−0.111	
171	509	589	11	971.5	975.7	12.80	0.10	10	9	0.111	113	0.045	−0.076	−0.081	
172	596	656	15	975.6	975.6	12.83	0.12	11	9	0.158	119	0.062	−0.084	−0.134	
173	572	640	16	974.6	975.0	10.53	0.05	16	15	0.118	105	0.034	−0.102	−0.059	2
174	604	663	16	976.3	972.6	9.25	0.04	16	9	0.056	107	0.013	−0.047	−0.031	2
175	769	792	16	983.6	971.5	10.86	0.03	16	15	0.068	125	0.033	−0.024	−0.064	
176	860	868	15	988.6	969.6	11.27	0.04	9	7	0.034	119	0.026	−0.018	−0.029	
177	943	925	16	991.8	969.6	11.15	0.04	9	6	0.047	159	0.021	0.035	−0.031	6
178	932	912	15	991.1	972.9	12.84	0.12	9	6	0.121	115	0.061	−0.079	−0.091	
179	1012	980	16	994.3	972.6	12.36	0.07	11	9	0.042	100	0.048	−0.040	−0.014	
180	1141	1063	16	998.9	969.9	9.87	0.04	16	12	0.086	117	0.022	−0.050	−0.069	2,5
181	1114	1039	15	997.7	977.9	12.51	0.08	14	6	0.122	86	0.022	−0.121	0.016	
182	1001	974	13	993.8	980.1	10.45	0.05	13	12	0.082	111	0.030	−0.060	−0.055	
183	847	857	16	988.0	978.6	9.15	0.04	15	13	0.070	109	0.020	−0.054	−0.044	2,3,5
184	803	817	13	985.5	979.6	10.47	0.04	10	9	0.124	111	0.018	−0.092	−0.084	2,5
185	867	877	14	988.7	983.9	10.62	0.06	14	13	0.035	100	0.027	−0.033	−0.012	2,3,6
186	864	874	16	988.6	984.9	9.93	0.04	13	13	0.082	113	0.021	−0.057	−0.059	2,3,5
187	801	816	12	985.3	985.6	12.86	0.14	7	6	0.077	98	0.086	−0.074	−0.020	
188	782	800	9	984.3	985.8	9.47	0.07	6	4	0.157	107	0.008	−0.131	−0.087	2,3
189	746	778	16	982.1	987.9	12.52	0.11	13	12	0.105	107	0.035	−0.086	−0.060	
190	778	795	16	983.9	988.9	11.99	0.05	16	15	0.055	88	0.037	−0.055	0.004	
191	859	875	15	988.5	989.9	10.67	0.06	11	10	0.134	95	0.039	−0.132	−0.025	
192	876	878	10	988.9	990.7	12.65	0.13	3	3	0.174	124	0.038	−0.066	−0.161	
193	869	876	16	988.7	988.2	11.99	0.06	11	8	0.079	106	0.019	−0.067	−0.042	3
194	911	902	15	990.3	988.1	11.32	0.04	11	8	0.025	114	0.025	−0.017	−0.018	
195	923	913	14	990.6	988.4	13.07	0.22	8	7	0.066	152	0.065	0.037	−0.055	
196	1014	988	11	994.2	985.7	12.97	0.10	8	4	0.129	109	0.031	−0.101	−0.081	
197	1023	991	13	994.3	983.4	12.64	0.13	10	8	0.085	149	0.062	0.041	−0.075	6
198	1047	1002	13	995.4	983.2	12.03	0.05	7	6	0.043	101	0.027	−0.040	−0.017	
199	1184	1093	13	0.9	983.2	12.11	0.05	7	5	0.041	114	0.015	−0.028	−0.030	
200	1126	1050	16	998.3	984.6	12.74	0.12	14	7	0.057	116	0.038	−0.036	−0.044	
201	1122	1049	16	998.1	986.5	12.24	0.08	15	9	0.068	150	0.023	0.034	−0.058	
202	1129	1051	15	998.3	986.9	12.95	0.11	14	9	0.102	97	0.034	−0.099	−0.025	
203	1128	1057	16	998.3	987.4	12.15	0.05	14	14	0.162	111	0.039	−0.119	−0.110	
204	1202	1111	13	2.0	990.8	12.09	0.06	2	2	0.095	178	0.031	0.095	−0.007	3
205	1232	1132	13	4.4	994.5	11.27	0.04	7	4	0.088	146	0.016	0.034	−0.081	
206	1181	1092	10	0.8	993.2	12.62	0.17	1	1	0.339	6	0.000	0.332	0.071	3
207	1161	0	9	0.0	991.6	10.22	0.04	0	0						2
208	1155	1069	16	999.4	990.9	12.52	0.06	4	4	0.210	107	0.033	−0.174	−0.118	
209	1138	1065	16	998.9	990.1	12.95	0.08	10	4	0.068	147	0.023	0.028	−0.062	
210	1078	1025	13	996.4	990.9	9.76	0.06	2	2	0.102	132	0.016	−0.011	−0.101	2,3,5

No.	Oost.	Lavd.	N_m	X	Y	m_E	rms(m)	N_p	N_u	p	P.A.	rms(p)	Q	U	Notes
211	926	915	7	990.9	991.6	11.55	0.04	1	1	0.103	116	0.000	−0.062	−0.082	
212	843	855	11	987.8	992.9	9.32	0.08	6	5	0.136	95	0.014	−0.134	−0.023	2,3,5
213	939	927	7	991.4	993.1	12.15	0.05	3	3	0.316	61	0.195	−0.172	0.265	
214	963	943	7	992.6	993.4	10.95	0.03	1	1	0.283	116	0.000	−0.176	−0.222	
215	977	958	8	992.6	993.3	10.97	0.08	0	0						
216	991	972	15	993.5	993.9	11.32	0.05	3	3	0.082	117	0.040	−0.048	−0.067	
217	1004	983	16	993.9	996.1	10.82	0.06	1	1	0.231	109	0.000	−0.181	−0.143	
218	986	976	13	993.4	996.8	12.48	0.12	12	9	0.126	131	0.050	−0.019	−0.125	
219	978	964	16	993.0	997.6	10.59	0.05	10	7	0.068	114	0.014	−0.045	−0.051	2,3,5
220	956	939	15	992.2	996.7	12.54	0.10	12	8	0.126	110	0.034	−0.097	−0.080	
221	936	928	14	991.4	996.4	10.37	0.04	4	4	0.114	109	0.022	−0.091	−0.069	2
222	929	0	16	990.8	997.7	10.27	0.06	8	8	0.070	99	0.028	−0.066	−0.022	2
223	930	921	15	990.9	998.3	12.29	0.06	11	8	0.102	128	0.019	−0.026	−0.099	
224	896	896	16	989.4	998.5	12.47	0.09	15	9	0.087	98	0.030	−0.084	−0.023	
225	800	818	15	985.3	0.9	12.21	0.07	15	10	0.135	118	0.033	−0.075	−0.112	3
226	965	951	15	992.5	0.4	12.60	0.10	15	10	0.194	102	0.035	−0.177	−0.078	
227	950	940	15	991.9	2.5	11.26	0.04	7	6	0.112	131	0.019	−0.017	−0.111	3,5
228	1015	992	16	994.3	1.9	10.51	0.05	11	7	0.046	98	0.018	−0.044	−0.013	2,3,5
229	1179	1096	15	0.5	998.5	12.86	0.11	14	13	0.085	97	0.085	−0.082	−0.021	
230	1162	1081	16	0.0	0.1	6.65	0.05	16	15	0.035	138	0.030	0.004	−0.035	1,2,3,5
231	1187	1101	13	1.4	3.0	10.82	0.04	12	8	0.067	115	0.030	−0.043	−0.051	3,5
232	1278	1166	16	7.1	4.6	11.73	0.05	16	11	0.122	127	0.020	−0.035	−0.117	
233	1284	1174	16	7.3	998.9	11.86	0.06	16	13	0.057	127	0.031	−0.016	−0.055	
234	1296	1183	14	8.6	998.2	12.78	0.10	14	11	0.079	99	0.062	−0.075	−0.024	
235	1283	1175	15	7.3	997.0	11.76	0.04	14	12	0.079	127	0.026	−0.022	−0.076	
236	1268	1161	10	6.4	993.6	9.43	0.05	4	4	0.031	120	0.024	−0.015	−0.027	1,2,5
237	1282	1171	15	7.3	989.5	10.95	0.04	15	10	0.103	108	0.019	−0.084	−0.060	
238	1257	1149	15	6.0	988.8	10.36	0.04	14	10	0.104	102	0.026	−0.096	−0.041	2
239	1438	0	16	16.3	987.9	11.36	0.04	15	8	0.091	117	0.012	−0.053	−0.074	
240	1364	1229	16	12.5	983.9	9.95	0.04	16	9	0.067	108	0.012	−0.054	−0.040	2
241	1261	1151	16	6.3	981.1	9.62	0.05	16	9	0.113	107	0.015	−0.094	−0.062	2,5
242	1333	1205	15	10.5	979.6	12.63	0.10	15	11	0.119	121	0.034	−0.057	−0.105	
243	1378	1239	16	13.2	977.9	12.02	0.04	13	12	0.096	106	0.029	−0.081	−0.051	
244	1358	1219	16	12.2	977.7	12.71	0.11	15	14	0.055	104	0.050	−0.048	−0.026	
245	1258	1146	16	6.2	967.6	11.52	0.04	16	13	0.043	132	0.029	−0.004	−0.043	6
246	1242	1134	16	5.3	965.6	10.40	0.06	16	13	0.064	104	0.022	−0.057	−0.029	2,6
247	1254	1147	16	6.0	964.9	12.63	0.14	14	12	0.089	131	0.050	−0.012	−0.089	
248	1331	1202	16	10.6	963.9	12.84	0.16	16	10	0.116	113	0.033	−0.080	−0.085	
249	1412	1268	16	15.3	969.6	11.48	0.03	16	11	0.079	130	0.019	−0.014	−0.078	
250	1439	1280	16	16.4	968.2	10.92	0.04	16	7	0.093	154	0.017	0.057	−0.073	
251	1414	1267	14	15.4	965.6	11.58	0.05	13	9	0.066	8	0.020	0.063	0.018	
252	1467	1296	14	18.4	964.9	12.48	0.09	14	10	0.034	142	0.035	0.009	−0.033	6
253	1499	1327	16	21.8	966.9	11.52	0.03	16	12	0.093	120	0.026	−0.047	−0.081	
254	1655	1444	15	36.3	963.8	7.97	0.11	15	15	0.107	119	0.026	−0.057	−0.090	1,2,3,4,5
255	1681	1470	16	38.8	966.9	11.66	0.05	14	10	0.066	108	0.022	−0.053	−0.039	
256	1548	1364	16	26.3	972.9	12.76	0.13	15	14	0.133	145	0.066	0.044	−0.126	
257	1525	1351	16	24.3	976.6	11.91	0.06	16	13	0.081	132	0.035	−0.007	−0.080	
258	1721	1502	16	42.3	982.6	12.13	0.05	14	11	0.161	112	0.037	−0.115	−0.112	
259	1686	1471	16	38.8	989.2	12.42	0.05	16	15	0.133	112	0.041	−0.095	−0.092	
260	1671	1463	15	37.4	990.2	12.54	0.09	15	12	0.074	114	0.038	−0.049	−0.055	
261	1586	1392	16	29.4	985.8	9.02	0.04	16	13	0.051	125	0.025	−0.017	−0.048	1,2,3,5
262	1575	1389	16	28.8	987.9	12.30	0.09	16	7	0.126	106	0.021	−0.107	−0.068	3
263	1566	1378	16	27.8	988.6	11.34	0.04	16	12	0.034	119	0.023	−0.018	−0.029	
264	1539	1354	16	25.0	991.0	11.26	0.04	16	11	0.092	127	0.018	−0.026	−0.088	
265	1625	1430	16	33.3	996.9	12.15	0.03	16	14	0.087	117	0.037	−0.051	−0.070	
266	1590	1393	16	29.4	999.9	11.43	0.04	16	11	0.082	106	0.022	−0.070	−0.043	
267	1516	1343	16	23.3	4.5	10.97	0.05	16	7	0.050	144	0.017	0.015	−0.048	
268	1465	1302	15	18.1	3.6	12.83	0.11	15	8	0.037	119	0.026	−0.019	−0.031	
269	1587	1394	15	29.3	11.1	12.84	0.10	14	11	0.063	106	0.042	−0.053	−0.034	
270	1680	1473	16	38.3	10.2	12.14	0.05	16	9	0.024	97	0.018	−0.023	−0.006	6
271	1633	1436	16	33.8	18.9	12.49	0.10	16	14	0.089	125	0.038	−0.029	−0.084	
272	1460	1299	13	17.3	12.9	12.78	0.06	13	9	0.138	111	0.042	−0.104	−0.092	
273	1298	1191	16	8.7	12.2	11.82	0.04	15	13	0.071	127	0.032	−0.020	−0.068	
274	1266	1164	16	6.3	11.6	12.30	0.09	16	11	0.129	125	0.037	−0.044	−0.121	
275	1276	1168	16	6.8	12.9	12.38	0.06	16	13	0.122	106	0.043	−0.103	−0.065	
276	1304	1195	16	8.8	17.6	12.81	0.10	15	9	0.086	130	0.042	−0.016	−0.084	
277	1490	1325	16	20.3	26.3	11.90	0.05	16	14	0.067	114	0.036	−0.045	−0.049	
278	1482	1316	16	19.3	31.6	8.27	0.04	16	13	0.063	118	0.023	−0.035	−0.052	1,2
279	1491	1328	16	20.3	35.6	12.81	0.13	16	12	0.106	129	0.059	−0.021	−0.104	
280	1670	1464	14	37.1	31.0	12.04	0.03	5	5	0.151	112	0.027	−0.109	−0.105	

No.	Cost.	Lavd.	N_m	X	Y	m_E	rms(m)	N_p	N_u	p	P.A.	rms(p)	Q	U	Notes
281	1702	1490	16	39.7	30.7	9.35	0.08	6	6	0.098	106	0.039	−0.083	−0.052	2,5
282	1733	1512	14	42.5	30.6	12.73	0.11	4	4	0.177	132	0.064	−0.018	−0.176	
283	1770	1540	16	46.2	36.6	11.60	0.04	16	6	0.046	121	0.015	−0.022	−0.041	
284	1793	1559	13	48.6	29.9	11.82	0.06	8	7	0.085	141	0.029	0.018	−0.083	
285	1819	1572	16	50.2	20.1	12.85	0.08	16	14	0.063	101	0.062	−0.058	−0.024	
286	1908	1647	16	57.0	13.9	11.05	0.04	15	11	0.068	136	0.021	0.001	−0.068	
287	1772	1539	16	46.4	12.4	11.33	0.06	16	10	0.058	95	0.017	−0.058	−0.010	
288	1870	1609	16	53.8	0.6	9.50	0.04	16	13	0.065	104	0.015	−0.058	−0.030	2,5
289	1818	1571	16	50.1	998.8	8.02	0.04	16	12	0.092	112	0.017	−0.066	−0.063	1,2,3,4,5
290	1924	1653	14	58.4	996.0	9.91	0.04	14	6	0.073	123	0.011	−0.030	−0.066	2,5
291	1903	1640	16	56.5	995.2	10.67	0.04	16	14	0.097	111	0.029	−0.072	−0.065	
292	1917	1652	15	58.0	991.1	12.30	0.07	15	12	0.123	107	0.030	−0.101	−0.070	
293	1878	1610	16	54.4	975.1	12.58	0.07	16	9	0.128	119	0.022	−0.067	−0.109	
294	1880	1617	16	54.8	969.8	11.64	0.03	16	12	0.059	102	0.022	−0.054	−0.023	6
295	1816	1569	16	50.3	967.9	10.62	0.05	16	7	0.071	127	0.012	−0.019	−0.068	6
296	1862	1604	16	53.8	965.9	11.02	0.05	16	15	0.095	123	0.032	−0.040	−0.087	5
297	2033	1754	16	66.6	972.7	11.36	0.04	16	15	0.126	110	0.030	−0.097	−0.081	
298	2089	1809	16	71.3	969.0	12.76	0.12	15	12	0.142	108	0.049	−0.115	−0.083	
299	2148	1866	16	75.1	967.0	12.55	0.08	16	12	0.114	116	0.047	−0.070	−0.090	
300	2271	1966	16	82.0	967.0	12.25	0.07	16	12	0.104	107	0.040	−0.087	−0.057	
301	2485	2165	15	96.4	972.7	10.62	0.06	12	12	0.123	98	0.047	−0.118	−0.036	
302	2468	2151	16	95.2	975.2	10.73	0.06	15	10	0.085	118	0.024	−0.047	−0.071	
303	2536	2195	13	99.8	977.0	13.03	0.12	8	3	0.096	107	0.040	−0.079	−0.055	
304	2539	2199	14	99.8	977.8	11.02	0.05	14	11	0.085	132	0.028	−0.009	−0.084	
305	2455	2134	16	93.7	980.0	12.52	0.09	13	10	0.104	108	0.042	−0.083	−0.063	
306	2460	2143	15	94.5	979.0	13.23	0.20	14	9	0.081	144	0.049	0.025	−0.077	6
307	2450	2129	10	93.2	976.9	13.15	0.17	4	3	0.165	164	0.094	0.140	−0.087	
308	2433	2114	16	92.3	978.0	10.92	0.05	16	12	0.082	118	0.021	−0.045	−0.068	
309	2411	2086	15	90.3	979.7	12.56	0.11	11	7	0.192	119	0.026	−0.101	−0.164	
310	2382	2071	15	88.4	975.9	11.63	0.05	15	9	0.048	108	0.017	−0.038	−0.028	
311	2310	2003	15	83.7	980.2	12.68	0.15	14	11	0.083	113	0.058	−0.057	−0.060	
312	2295	1985	12	82.9	979.6	13.01	0.21	11	5	0.096	77	0.027	−0.086	0.043	
313	2119	1837	13	73.4	979.5	11.21	0.05	12	11	.089	112	0.028	−0.064	−0.061	
314	2053	1766	16	67.7	978.6	11.97	0.04	16	14	0.148	119	0.027	−0.078	−0.126	
315	1928	1660	15	59.1	983.7	12.00	0.04	15	8	0.106	130	0.018	−0.019	−0.104	
316	2024	1744	16	65.3	987.5	10.78	0.05	16	7	0.075	125	0.016	−0.025	−0.071	5
317	2085	1810	16	70.9	985.1	11.26	0.09	16	13	0.102	123	0.021	−0.043	−0.092	5
318	2110	1830	16	72.4	983.5	12.70	0.08	15	15	0.168	110	0.056	−0.129	−0.108	
319	2284	1978	16	82.2	985.1	9.63	0.07	16	14	0.106	118	0.032	−0.060	−0.088	2,3,5
320	2185	1890	16	76.9	987.0	10.93	0.04	14	10	0.128	124	0.023	−0.046	−0.119	3,5
321	2211	1911	10	78.4	989.1	12.97	0.10	5	5	0.232	70	0.072	−0.180	0.148	
322	2140	1851	13	74.1	990.8	11.88	0.04	9	9	0.129	105	0.035	−0.111	−0.065	
323	2088	1811	15	71.2	992.3	9.47	0.02	7	5	0.098	127	0.023	−0.026	−0.094	2,3,5
324	2133	1846	16	73.7	993.1	12.19	0.06	16	7	0.104	114	0.021	−0.070	−0.077	3
325	2139	1850	10	73.9	995.1	11.29	0.03	1	1	0.107	133	0.000	−0.009	−0.107	3
326	2094	1821	14	71.4	997.0	11.80	0.05	11	9	0.143	116	0.030	−0.087	−0.113	
327	2006	1728	15	63.8	995.9	12.87	0.16	9	9	0.152	111	0.063	−0.114	−0.101	
328	2091	1822	16	71.3	3.9	11.68	0.05	16	15	0.105	115	0.038	−0.068	−0.080	
329	2165	1874	16	75.3	1.0	9.86	0.08	16	12	0.102	113	0.024	−0.070	−0.075	2,3,5
330	2262	1951	16	80.7	3.3	10.56	0.03	16	10	0.072	116	0.016	−0.045	−0.056	3,5
331	2297	1989	14	82.6	1.4	12.99	0.12	14	13	0.097	86	0.073	−0.096	0.013	
332	2308	1994	15	83.3	0.3	12.91	0.13	14	6	0.049	90	0.032	−0.048	−0.000	
333	2329	2013	14	84.4	997.9	12.91	0.09	10	7	0.087	117	0.039	−0.052	−0.070	
334	2255	1947	16	80.4	998.4	10.66	0.06	16	13	0.091	114	0.035	−0.062	−0.067	
335	2242	1936	16	79.8	998.9	10.81	0.06	11	6	0.039	105	0.011	−0.034	−0.020	
336	2229	1926	16	79.2	999.8	11.28	0.05	15	14	0.096	103	0.035	−0.087	−0.041	
337	2196	1899	16	77.6	999.0	11.51	0.05	10	7	0.102	120	0.021	−0.051	−0.089	5
338	2245	1938	14	80.1	997.0	12.44	0.08	11	9	0.099	115	0.035	−0.064	−0.076	
339	2227	1928	15	79.2	996.5	8.05	0.05	15	15	0.081	132	0.028	−0.008	−0.081	1,2,3,5
340	2246	1939	11	80.3	995.7	9.89	0.03	4	4	0.093	127	0.027	−0.027	−0.089	2,3
341	2251	1937	16	80.3	994.4	11.53	0.05	14	10	0.199	111	0.025	−0.148	−0.133	3
342	2200	1904	16	77.7	993.8	12.69	0.10	16	9	0.148	108	0.027	−0.118	−0.089	3
343	2232	1924	6	79.2	992.5	10.99	0.03	2	2	0.081	105	0.005	−0.070	−0.041	
344	2253	1945	14	80.5	991.1	12.58	0.09	9	9	0.114	102	0.057	−0.103	−0.048	3
345	2296	1979	15	82.4	989.8	8.50	0.03	7	7	0.094	111	0.027	−0.071	−0.062	2,3,5
346	2309	2002	15	83.5	989.0	12.77	0.14	7	5	0.220	128	0.045	−0.054	−0.213	
347	2311	2005	13	83.5	990.9	9.35	0.04	6	6	0.106	103	0.039	−0.095	−0.047	2,3,5
348	2330	2019	16	84.7	990.2	11.39	0.04	12	11	0.104	118	0.026	−0.057	−0.087	3,5
349	2349	2034	16	85.9	988.0	12.85	0.12	16	8	0.145	100	0.036	−0.137	−0.048	3
350	2417	2090	11	90.3	989.3	8.12	0.11	8	5	0.088	123	0.013	−0.035	−0.081	1,2,3,4,5

No.	Oost.	Lavd.	N_m	X	Y	m_E	rms(m)	N_p	N_u	p	P.A.	rms(p)	Q	U	Notes
351	2540	2200	14	99.6	988.9	11.19	0.04	13	8	0.109	131	0.014	−0.016	−0.108	
352	2371	2056	13	87.3	992.2	9.21	0.07	3	3	0.066	163	0.013	0.055	−0.038	2,3
353	2379	2067	12	87.9	994.9	12.22	0.06	8	4	0.229	99	0.017	−0.218	−0.070	
354	2462	2147	16	94.3	996.9	11.49	0.03	14	11	0.140	108	0.028	−0.114	−0.081	
355	2579	2234	15	102.4	997.7	11.90	0.05	15	9	0.116	109	0.018	−0.091	−0.073	
356	2572	2226	16	101.9	999.0	9.97	0.06	13	12	0.075	101	0.030	−0.070	−0.027	2,3,5
357	2555	2213	16	100.7	3.0	11.51	0.03	16	7	0.076	109	0.017	−0.059	−0.047	
358	2505	2175	16	97.0	4.1	10.98	0.05	16	15	0.050	96	0.037	−0.048	−0.011	
359	2513	2185	15	97.3	5.1	10.98	0.05	15	13	0.085	87	0.037	−0.084	0.010	
360	2566	2217	15	101.3	8.9	10.46	0.06	15	7	0.043	129	0.023	−0.009	−0.042	
361	2507	2176	11	97.0	7.7	12.50	0.09	7	5	0.100	122	0.020	−0.044	−0.089	
362	2381	2068	13	87.8	3.1	13.20	0.16	12	11	0.073	65	0.062	−0.046	0.057	6
363	2392	2077	16	88.4	4.3	10.62	0.06	15	10	0.085	126	0.029	−0.026	−0.081	2,5
364	2377	2069	15	87.5	6.9	11.00	0.04	12	9	0.030	86	0.034	−0.030	0.004	2
365	2372	2061	16	87.3	7.7	11.61	0.05	15	13	0.082	94	0.036	−0.081	−0.011	
366	2395	2081	16	88.9	9.0	12.39	0.10	16	8	0.114	113	0.023	−0.080	−0.082	6
367	2444	2123	14	92.4	9.9	9.49	0.06	13	10	0.087	85	0.025	−0.086	0.015	2
368	2504	2178	16	96.7	14.8	11.98	0.05	15	14	0.091	109	0.052	−0.071	−0.056	
369	2452	2136	16	92.9	16.1	10.91	0.04	16	13	0.063	84	0.038	−0.062	0.013	
370	2383	2072	15	87.7	20.9	13.01	0.15	15	9	0.158	118	0.039	−0.088	−0.132	
371	2351	2041	16	85.7	13.4	11.80	0.05	16	11	0.087	100	0.020	−0.081	−0.031	
372	2328	2014	14	84.3	10.0	12.68	0.12	12	10	0.153	83	0.048	−0.149	0.035	
373	2285	1982	16	81.9	8.9	12.68	0.09	14	8	0.109	111	0.029	−0.080	−0.074	
374	2191	1901	14	77.1	9.1	11.69	0.04	14	10	0.087	125	0.022	−0.029	−0.082	
375	2189	1894	13	76.9	10.8	12.33	0.07	7	7	0.149	105	0.056	−0.128	−0.075	3
376	2178	1885	15	76.2	16.9	6.43	0.06	15	13	0.075	106	0.028	−0.063	−0.040	1,2,3,5
377	2144	1855	15	73.7	21.4	12.47	0.10	15	13	0.079	112	0.029	−0.057	−0.055	3
378	2105	1832	16	71.9	15.2	11.41	0.04	16	14	0.077	124	0.027	−0.030	−0.071	
379	2090	1816	8	71.4	11.1	12.10	0.05	5	3	0.166	99	0.012	−0.157	−0.054	
380	2070	1794	16	69.2	8.9	12.65	0.07	15	14	0.125	111	0.057	−0.093	−0.085	
381	2057	1777	16	67.9	9.9	11.56	0.04	16	12	0.159	122	0.023	−0.071	−0.142	
382	2022	1740	14	64.9	10.7	12.51	0.10	10	8	0.088	82	0.050	−0.084	0.024	
383	2014	1736	16	64.3	9.2	11.72	0.04	16	13	0.140	113	0.029	−0.096	−0.102	
384	1977	1703	16	61.9	7.1	12.25	0.07	16	14	0.109	105	0.037	−0.094	−0.056	
385	1983	1709	15	62.3	12.1	10.50	0.04	12	9	0.092	114	0.031	−0.061	−0.069	
386	2000	1725	14	63.0	20.9	13.05	0.12	14	7	0.130	127	0.032	−0.035	−0.125	
387	1985	1711	16	62.3	24.9	11.89	0.05	16	13	0.039	133	0.028	−0.003	−0.039	6
388	2019	1741	16	64.3	26.9	12.34	0.07	16	11	0.153	114	0.030	−0.103	−0.113	
389	2049	1765	16	66.4	28.0	9.91	0.06	16	11	0.129	96	0.021	−0.126	−0.028	2,5
390	2051	1768	16	67.1	32.9	11.84	0.05	16	11	0.135	116	0.025	−0.082	−0.108	
391	2079	1805	16	70.0	30.6	9.66	0.06	16	10	0.089	113	0.013	−0.061	−0.064	2
392	2086	1813	16	70.3	30.0	11.64	0.06	16	15	0.085	111	0.036	−0.062	−0.058	
393	2190	1895	16	76.4	37.1	10.81	0.07	16	14	0.124	101	0.037	−0.114	−0.047	
394	2336	2026	16	84.3	33.9	11.56	0.05	16	8	0.125	139	0.016	0.017	−0.124	
395	2353	2037	16	85.4	25.7	12.81	0.13	10	8	0.100	100	0.034	−0.094	−0.036	
396	2361	2049	16	86.2	23.2	8.75	0.04	16	9	0.066	123	0.024	−0.027	−0.060	1,2,3,5
397	2402	2083	12	88.8	26.0	9.59	0.08	7	6	0.154	77	0.011	−0.138	0.069	2
398	2435	2116	16	91.7	22.2	12.48	0.13	13	7	0.074	140	0.040	0.013	−0.073	
399	2509	2179	16	96.9	24.9	12.04	0.05	16	14	0.101	123	0.037	−0.042	−0.093	
400	2520	2189	11	97.8	26.0	10.63	0.06	7	7	0.170	97	0.041	−0.165	−0.042	2
401	2625	2274	16	106.8	28.9	10.66	0.05	15	14	0.077	96	0.047	−0.075	−0.017	6
402	2603	2257	16	105.2	23.0	11.87	0.05	16	11	0.093	126	0.022	−0.027	−0.089	
403	2589	2240	16	103.4	18.1	7.50	0.06	16	10	0.069	114	0.018	−0.047	−0.051	1,2,3,5
404	2631	2284	16	107.4	13.1	12.66	0.07	16	12	0.122	105	0.051	−0.106	−0.059	3
405	2622	2271	15	106.9	9.7	11.88	0.05	15	13	0.072	124	0.036	−0.027	−0.067	
406	2591	2242	16	104.0	7.9	12.09	0.06	13	6	0.184	110	0.016	−0.141	−0.118	
407	2601	2256	15	105.3	7.9	10.54	0.06	11	9	0.152	102	0.041	−0.140	−0.060	
408	2677	2317	15	111.7	2.9	12.57	0.14	14	11	0.046	110	0.058	−0.035	−0.030	
409	2646	2291	16	109.1	2.3	12.17	0.12	11	10	0.120	114	0.032	−0.080	−0.090	
410	2612	2269	16	106.3	2.2	11.81	0.04	9	9	0.144	106	0.038	−0.122	−0.077	
411	2628	2276	15	107.6	995.6	10.78	0.04	15	11	0.130	111	0.026	−0.098	−0.085	
412	2649	2294	15	109.3	993.7	10.24	0.05	15	13	0.125	112	0.024	−0.089	−0.087	
413	2633	2282	16	107.8	992.2	11.93	0.05	16	15	0.106	127	0.036	−0.028	−0.102	
414	2656	2301	15	109.9	991.2	12.03	0.05	15	10	0.130	123	0.024	−0.052	−0.119	
415	2605	2262	16	106.4	969.8	9.71	0.04	16	12	0.109	116	0.018	−0.068	−0.085	2
416	2611	2267	16	106.8	968.8	12.45	0.09	16	12	0.057	117	0.047	−0.033	−0.046	
417	0	104	15	917.1	948.2	11.26	0.05	14	14	0.087	119	0.037	−0.047	−0.073	
418	0	77	14	913.9	944.1	12.29	0.11	14	9	0.140	106	0.024	−0.119	−0.074	
419	0	120	14	919.3	940.5	11.34	0.07	13	13	0.017	107	0.049	−0.014	−0.010	
420	0	103	15	917.3	938.7	12.79	0.14	15	10	0.108	121	0.043	−0.050	−0.096	

No.	Oost.	Lavd.	N_m	X	Y	m_E	rms(m)	N_p	N_u	p	P.A.	rms(p)	Q	U	Notes
421	0	150	14	923.6	935.7	13.09	0.16	12	7	0.189	138	0.038	0.019	−0.188	
422	0	187	15	927.4	933.1	12.41	0.11	14	10	0.166	120	0.042	−0.083	−0.144	
423	0	229	15	934.5	922.7	12.47	0.14	13	7	0.117	106	0.019	−0.099	−0.063	
424	0	223	15	933.5	919.4	11.41	0.07	15	14	0.047	108	0.038	−0.038	−0.027	
425	0	264	15	938.6	917.1	10.51	0.07	15	15	0.120	104	0.041	−0.107	−0.055	
426	0	282	15	941.0	915.7	8.48	0.08	13	10	0.066	109	0.035	−0.052	−0.041	1,2,5
427	0	330	15	945.5	909.2	12.68	0.13	12	10	0.067	83	0.042	−0.065	0.016	
428	0	331	15	945.7	909.7	12.77	0.18	15	10	0.060	178	0.042	0.060	−0.005	
429	0	329	15	945.3	920.6	11.99	0.11	15	9	0.129	121	0.020	−0.059	−0.115	
430	0	268	15	939.3	922.8	11.57	0.05	13	13	0.096	98	0.036	−0.093	−0.026	
431	0	277	15	940.3	925.4	12.95	0.13	15	13	0.091	99	0.058	−0.087	−0.029	
432	180	356	15	947.9	929.2	11.97	0.05	15	11	0.054	82	0.026	−0.052	0.014	
433	30	226	15	933.5	936.9	9.87	0.06	15	13	0.072	84	0.030	−0.071	0.015	2
434	87	269	15	938.9	945.2	10.55	0.06	14	13	0.108	94	0.035	−0.107	−0.014	
435	81	262	15	938.0	950.6	12.58	0.15	15	8	0.037	163	0.024	0.031	−0.021	
436	4	208	15	930.3	956.4	12.09	0.05	15	10	0.133	116	0.025	−0.083	−0.104	
437	90	270	10	939.0	957.3	9.92	0.07	6	5	0.091	84	0.030	−0.089	0.019	2
438	133	315	15	943.3	957.5	11.58	0.07	9	4	0.088	95	0.018	−0.087	−0.016	
439	143	319	14	943.9	945.7	12.71	0.15	13	6	0.094	116	0.016	−0.059	−0.074	
440	146	325	12	944.3	942.7	9.18	0.05	12	9	0.089	69	0.038	−0.067	0.059	1,2,3
441	251	414	7	954.4	943.0	13.10	0.14	3	3	0.017	161	0.061	0.013	−0.011	
442	309	443	16	958.3	943.2	9.60	0.07	10	10	0.068	93	0.045	−0.067	−0.008	2,5
443	432	534	15	967.3	940.9	11.78	0.05	14	10	0.120	107	0.019	−0.100	−0.067	
444	420	523	16	966.7	934.1	11.72	0.06	15	7	0.125	103	0.013	−0.112	−0.056	
445	383	500	16	963.9	932.9	11.40	0.05	14	14	0.078	104	0.030	−0.069	−0.038	
446	0	533	16	967.6	926.7	11.69	0.05	16	8	0.078	115	0.021	−0.050	−0.060	
447	566	621	16	974.6	932.9	9.64	0.05	15	15	0.059	116	0.041	−0.036	−0.047	2,5
448	565	620	16	974.6	934.9	11.48	0.04	16	13	0.088	128	0.033	−0.020	−0.086	
449	748	774	16	982.4	937.4	10.23	0.05	16	12	0.049	133	0.026	−0.004	−0.048	2
450	590	648	15	975.5	940.5	10.06	0.04	15	9	0.060	87	0.020	−0.060	0.006	2
451	831	835	14	987.0	943.3	12.86	0.11	11	9	0.034	84	0.065	−0.033	0.007	
452	560	629	16	974.4	946.1	12.03	0.07	16	9	0.047	126	0.019	−0.015	−0.045	6
453	542	616	16	973.9	948.1	11.56	0.11	16	7	0.022	91	0.021	−0.022	−0.001	4
454	484	570	16	970.3	948.8	11.93	0.04	16	11	0.120	103	0.024	−0.109	−0.051	
455	508	587	16	971.7	950.9	11.96	0.05	16	16	0.098	111	0.040	−0.073	−0.065	
456	406	520	16	965.9	953.0	11.63	0.06	15	9	0.082	96	0.021	−0.081	−0.016	
457	372	495	16	962.6	952.1	12.31	0.07	15	9	0.128	107	0.027	−0.105	−0.073	
458	323	455	16	959.3	953.8	10.93	0.05	15	13	0.050	99	0.036	−0.047	−0.015	
459	405	521	15	965.9	959.2	12.62	0.12	14	11	0.051	115	0.043	−0.033	−0.040	
460	544	623	14	973.9	957.6	12.35	0.07	12	7	0.055	98	0.030	−0.053	−0.015	
461	593	651	16	975.8	957.8	13.00	0.17	7	7	0.097	86	0.057	−0.096	0.013	
462	663	703	16	978.3	957.9	11.39	0.07	11	9	0.051	114	0.018	−0.034	−0.038	
463	673	709	16	978.7	958.6	11.85	0.08	16	16	0.073	140	0.033	0.012	−0.072	
464	1067	1013	16	996.4	955.9	10.47	0.03	15	10	0.056	116	0.022	−0.035	−0.044	2
465	1212	1117	16	2.7	949.5	11.30	0.04	16	15	0.074	132	0.024	−0.008	−0.073	
466	1255	1141	16	6.2	947.3	11.37	0.05	16	14	0.094	115	0.034	−0.062	−0.071	
467	1252	1140	15	6.1	941.2	11.32	0.02	15	13	0.080	113	0.032	−0.056	−0.057	
468	1293	1177	16	8.7	935.2	12.01	0.06	16	14	0.084	114	0.030	−0.057	−0.062	
469	1226	1126	16	4.2	929.6	11.15	0.03	16	14	0.044	117	0.030	−0.026	−0.035	
470	0	1139	15	6.5	918.7	11.13	0.04	15	12	0.079	125	0.027	−0.027	−0.074	
471	0	1115	16	3.3	914.9	11.92	0.05	16	11	0.122	115	0.032	−0.078	−0.094	
472	0	998	15	996.2	908.3	12.03	0.05	15	14	0.142	109	0.042	−0.113	−0.086	
473	0	899	16	991.4	913.8	11.66	0.06	14	14	0.111	112	0.043	−0.081	−0.076	
474	0	810	15	986.0	914.3	9.26	0.04	15	7	0.141	117	0.020	−0.082	−0.115	
475	0	588	16	972.9	902.9	10.35	0.06	16	13	0.046	122	0.028	−0.020	−0.041	
476	0	519	16	966.7	904.3	12.53	0.11	16	14	0.164	114	0.051	−0.112	−0.121	
477	0	562	16	970.6	895.9	12.35	0.11	16	12	0.067	126	0.036	−0.021	−0.063	
478	0	743	16	981.8	895.9	11.25	0.03	16	14	0.109	106	0.034	−0.093	−0.057	
479	0	783	16	984.2	897.1	11.22	0.03	15	13	0.063	106	0.033	−0.053	−0.033	
480	0	954	16	994.4	889.1	10.47	0.03	15	10	0.060	128	0.017	−0.015	−0.058	
481	0	979	16	995.3	889.8	12.89	0.15	16	13	0.145	93	0.062	−0.144	−0.015	
482	0	1091	16	2.5	891.7	11.70	0.05	16	13	0.130	110	0.031	−0.099	−0.085	
483	0	1214	14	12.9	908.2	11.31	0.04	13	11	0.068	124	0.034	−0.026	−0.063	
484	0	1276	14	17.2	908.3	13.10	0.12	9	4	0.165	90	0.023	−0.165	0.001	
485	0	1244	16	14.6	905.2	10.17	0.04	16	11	0.131	108	0.019	−0.107	−0.076	2
486	0	1295	16	19.1	904.3	12.79	0.09	15	11	0.115	111	0.027	−0.085	−0.077	
487	0	1262	16	16.4	903.3	10.84	0.05	16	7	0.033	98	0.024	−0.031	−0.009	2
488	0	1308	14	20.0	898.3	13.17	0.18	12	11	0.034	102	0.048	−0.032	−0.013	
489	0	1403	16	31.9	894.5	11.76	0.05	16	16	0.074	107	0.037	−0.062	−0.041	
490	0	1433	16	35.5	901.3	12.58	0.13	15	13	0.091	108	0.054	−0.074	−0.054	

No.	Oost.	Lavd.	N_m	X	Y	m_E	rms(m)	N_p	N_u	p	P.A.	rms(p)	Q	U	Notes
491	0	1417	16	33.1	907.9	12.73	0.10	16	8	0.176	108	0.028	−0.144	−0.102	
492	0	1384	16	30.0	910.4	10.55	0.05	16	12	0.093	115	0.024	−0.060	−0.072	2
493	0	1376	15	29.2	911.0	13.07	0.12	15	10	0.086	124	0.034	−0.033	−0.079	
494	0	1418	16	32.9	918.8	12.41	0.06	15	13	0.079	107	0.032	−0.065	−0.044	
495	0	1235	15	14.1	925.9	12.61	0.11	14	13	0.113	121	0.040	−0.053	−0.099	
496	0	1215	15	12.8	927.1	11.51	0.04	15	12	0.054	125	0.035	−0.019	−0.051	
497	1421	1263	16	15.9	931.8	12.32	0.09	16	11	0.089	103	0.031	−0.081	−0.038	
498	1387	1245	16	14.2	932.9	10.79	0.04	16	11	0.086	110	0.023	−0.066	−0.056	
499	1319	1201	16	10.2	942.6	12.39	0.08	16	13	0.088	95	0.041	−0.087	−0.016	
500	1344	0	16	11.8	944.3	12.48	0.11	16	7	0.143	133	0.021	−0.012	−0.143	
501	1417	1265	15	15.7	948.0	12.30	0.08	15	12	0.176	107	0.036	−0.145	−0.101	
502	1391	1247	16	14.4	960.3	10.37	0.03	16	13	0.086	119	0.018	−0.045	−0.074	2
503	1582	1388	16	29.6	944.3	12.54	0.11	16	7	0.131	112	0.024	−0.096	−0.089	
504	1639	1434	15	34.9	938.5	13.01	0.11	14	9	0.043	142	0.041	0.011	−0.041	
505	1645	1439	16	35.6	940.3	12.13	0.07	16	12	0.107	124	0.027	−0.038	−0.099	
506	1695	1478	16	39.8	949.0	12.51	0.10	13	11	0.100	113	0.045	−0.071	−0.071	
507	1777	1538	16	47.8	952.8	12.55	0.08	16	13	0.117	106	0.057	−0.098	−0.063	
508	1781	1544	15	48.0	949.9	9.20	0.03	15	14	0.120	117	0.028	−0.071	−0.098	1,2,3,5
509	1864	1602	16	54.5	938.2	11.82	0.05	14	10	0.156	114	0.027	−0.106	−0.114	
510	1899	1631	16	56.6	937.3	8.53	0.04	16	10	0.106	128	0.019	−0.025	−0.104	1,2,3,5
511	1901	1637	16	57.3	934.9	9.40	0.05	16	14	0.093	114	0.025	−0.061	−0.070	2
512	0	1623	16	56.3	927.1	9.47	0.04	16	11	0.103	123	0.020	−0.043	−0.094	2
513	0	1601	16	54.9	913.5	10.92	0.04	16	11	0.095	115	0.025	−0.060	−0.074	
514	0	1722	15	68.9	923.7	12.90	0.10	14	7	0.102	79	0.025	−0.095	0.037	
515	2204	0	14	79.0	928.8	13.02	0.18	13	9	0.106	94	0.051	−0.105	−0.014	
516	2354	2040	16	87.1	928.1	11.98	0.06	16	12	0.051	130	0.034	−0.009	−0.050	
517	2172	1877	16	76.5	946.0	8.46	0.04	16	7	0.098	121	0.009	−0.045	−0.088	1,2,3,5
518	2048	1764	16	67.8	947.6	10.70	0.06	16	7	0.114	106	0.016	−0.096	−0.062	
519	1960	1681	16	61.8	944.3	10.74	0.05	16	9	0.171	114	0.017	−0.116	−0.125	
520	1951	1674	16	61.1	948.1	11.34	0.05	16	13	0.107	117	0.032	−0.062	−0.087	
521	1950	1673	16	61.0	949.5	12.18	0.05	16	16	0.122	131	0.037	−0.016	−0.121	
522	1966	1692	16	61.9	952.1	12.14	0.05	16	14	0.106	115	0.034	−0.070	−0.080	
523	1965	1693	16	61.8	958.1	12.09	0.05	15	13	0.076	103	0.033	−0.068	−0.034	
524	2056	1766	16	68.6	955.8	11.92	0.05	16	7	0.167	125	0.015	−0.060	−0.156	
525	2145	1860	15	75.0	954.1	12.27	0.08	13	11	0.066	82	0.043	−0.064	0.018	
526	2495	2168	16	97.3	948.3	11.90	0.05	16	11	0.054	90	0.027	−0.054	0.001	
527	2563	2224	16	102.1	959.9	10.47	0.05	16	13	0.128	121	0.029	−0.061	−0.112	5

HD STARS MEASURED IN h AND χ PERSEI

HD. NO.	ED. NO.	HD NO.	ED. NO.	HD NO.	ED. NO.
13841	98	14162	236	14422	62
13854	97	14210	278	14433	376
13890	426			14434	517
13900	440	14250	261	14443	339
13910	14	14270	254	14476	396
		14321	508		
13969	112	14330	289	14488	350
14052	144	14357	510	14535	403
14143	230				

BD STAR'S MEASURED IN h AND χ PERSEI

BD. NO.	ED. NO.	BD. NO.	ED. NO.	BD. NO.	ED. NO.
+57 541	42	506	34	549	55
		508	133	550	508
+56 468	95			551	289
470	98	+56 510	212	552	57
471	97	511	183		
472	433	512	22	+56 553	288
473	86	513	186	554	512
		514	185	555	510
+56 474	13			556	511
476	87	+56 516	222	557	290
477	437	517	221		
478	426	518	219	+56 558	59
479	440	521	228	560	72
		523	464	561	389
+56 480	14			562	391
481	115	+56 524	210	563	323
482	123	528	180		
484	442	529	207	+56 565	62
485	112	530	230	566	329
		531	137	567	517
+56 486	29			568	376
487	28	+56 532	246	570	339
488	15	533	238		
489	161	534	241	+56 572	340
491	158	535	236	573	319
		536	50	574	345
+56 492	153			576	347
493	447	+56 538	240	577	396
494	450	539	46		
495	173	540	502	+56 578	352
496	19	541	485	580	364
		542	487	581	363
+56 497	174			482	397
499	33	+56 543	278	583	350
500	144	544	53		
501	167	545	261	+56 584	367
502	145	546	492	587	400
		547	254	590	356
+56 503	449			591	403
504	188	+56 548	281	592	415
505	184				

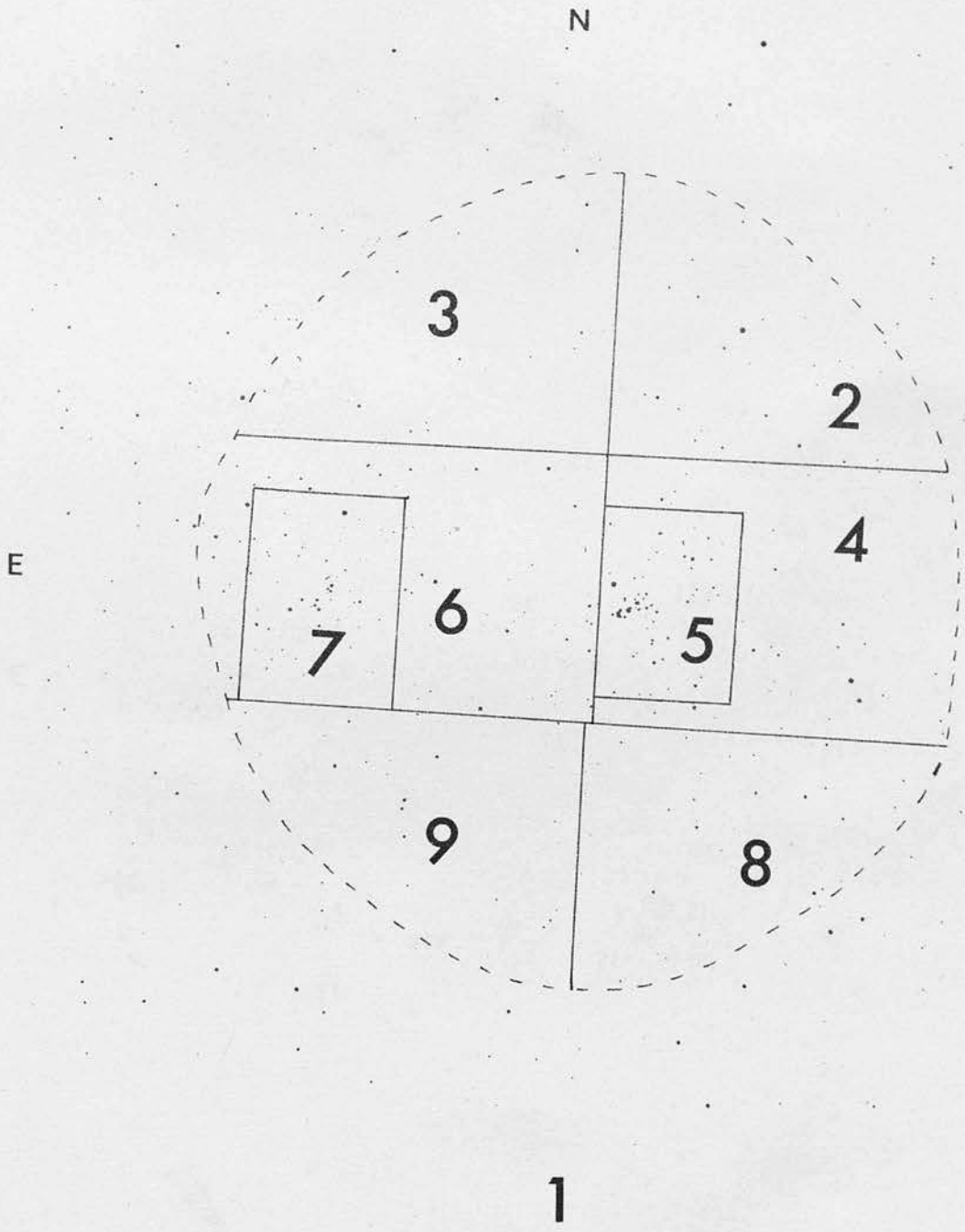

Master chart, showing the areas of h and χ Persei covered by charts 1-9.
Chart 10 shows the area of the North Galactic Pole.

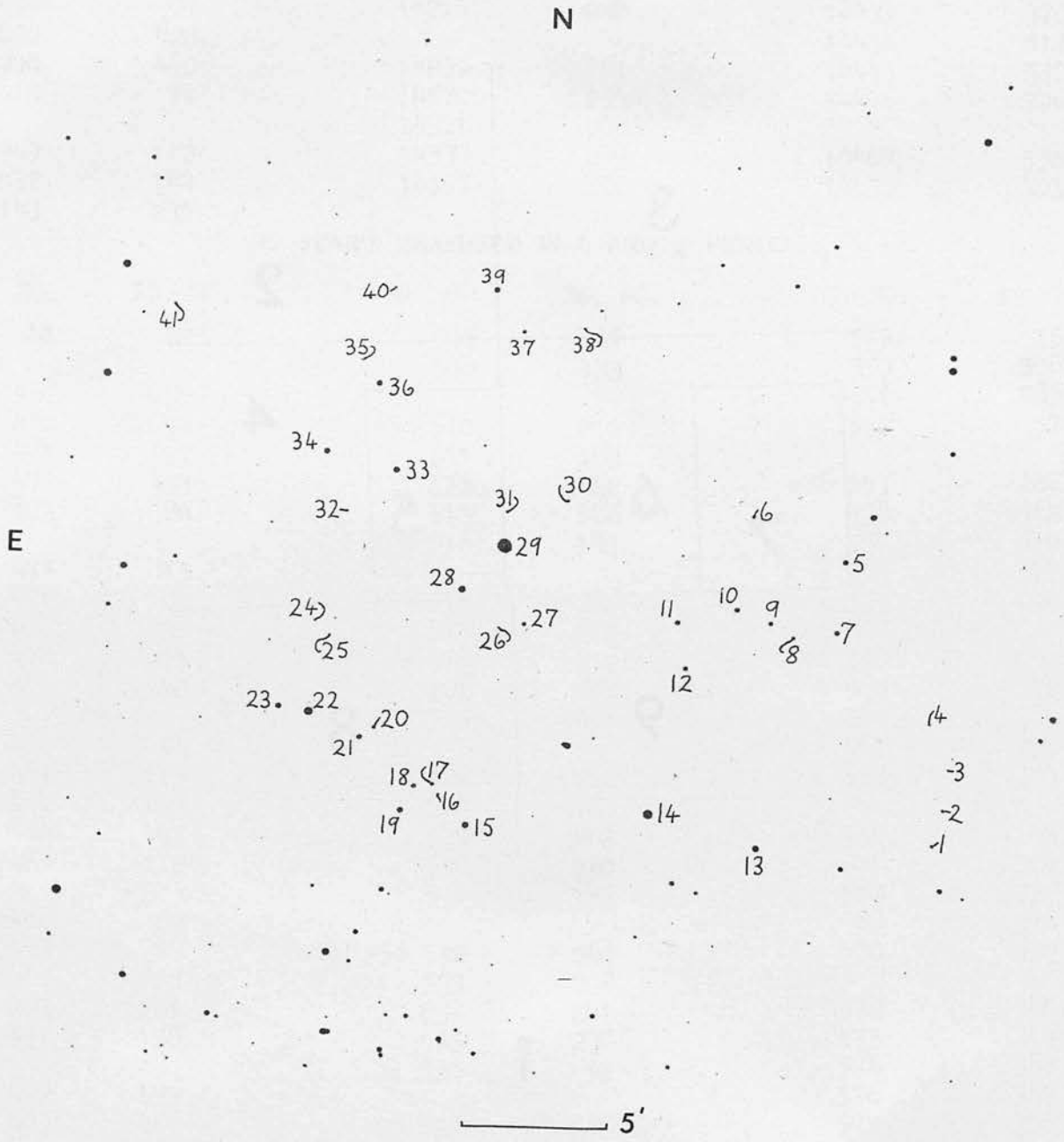
N
E
41
40
39
35
37
38
36
34
33
32
31
30
16
29
5
28
24
27
11
10
9
7
25
26
8
12
23
22
20
14
21
18
17
16
3
19
15
14
2
1
13
5'

2

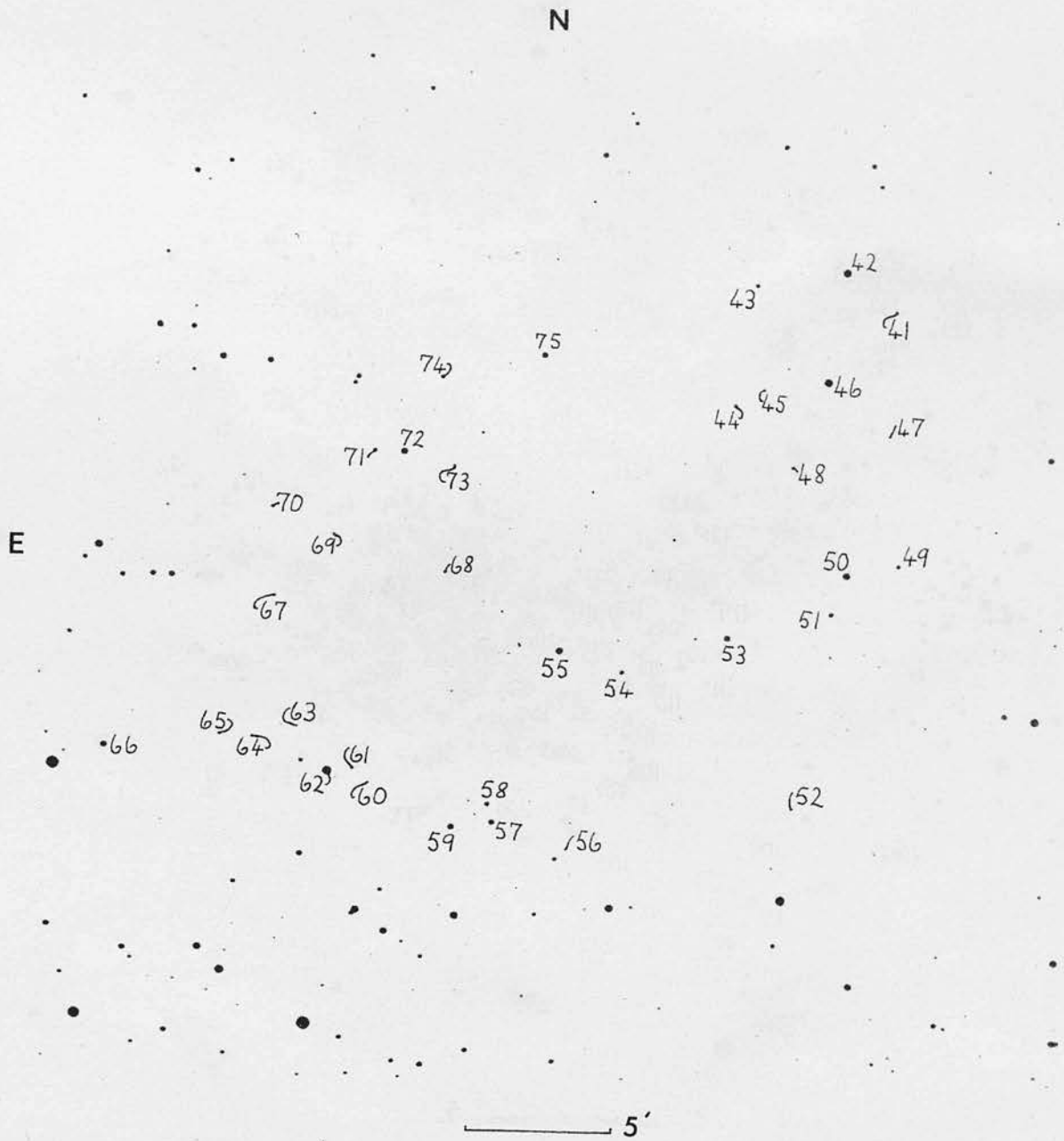
N
E
42
43
41
75
74
46
45
44
47
72
71
73
48
70
69
68
50
49
67
51
53
55
54
65
63
66
64
61
62
60
58
52
59
57
56
5′

3


N
E
78
128
131
130
129
127
77
76
132
133
134
126
79
80
125
124
81
123
82
122
83
85
84
121
120
86
119
118
117
88
114
116
87
112
113
89
90
111
110
115
97
109
96
94
105
108
106
98
95
107
93
91
100
99
104
103
101
102
92
5'

4

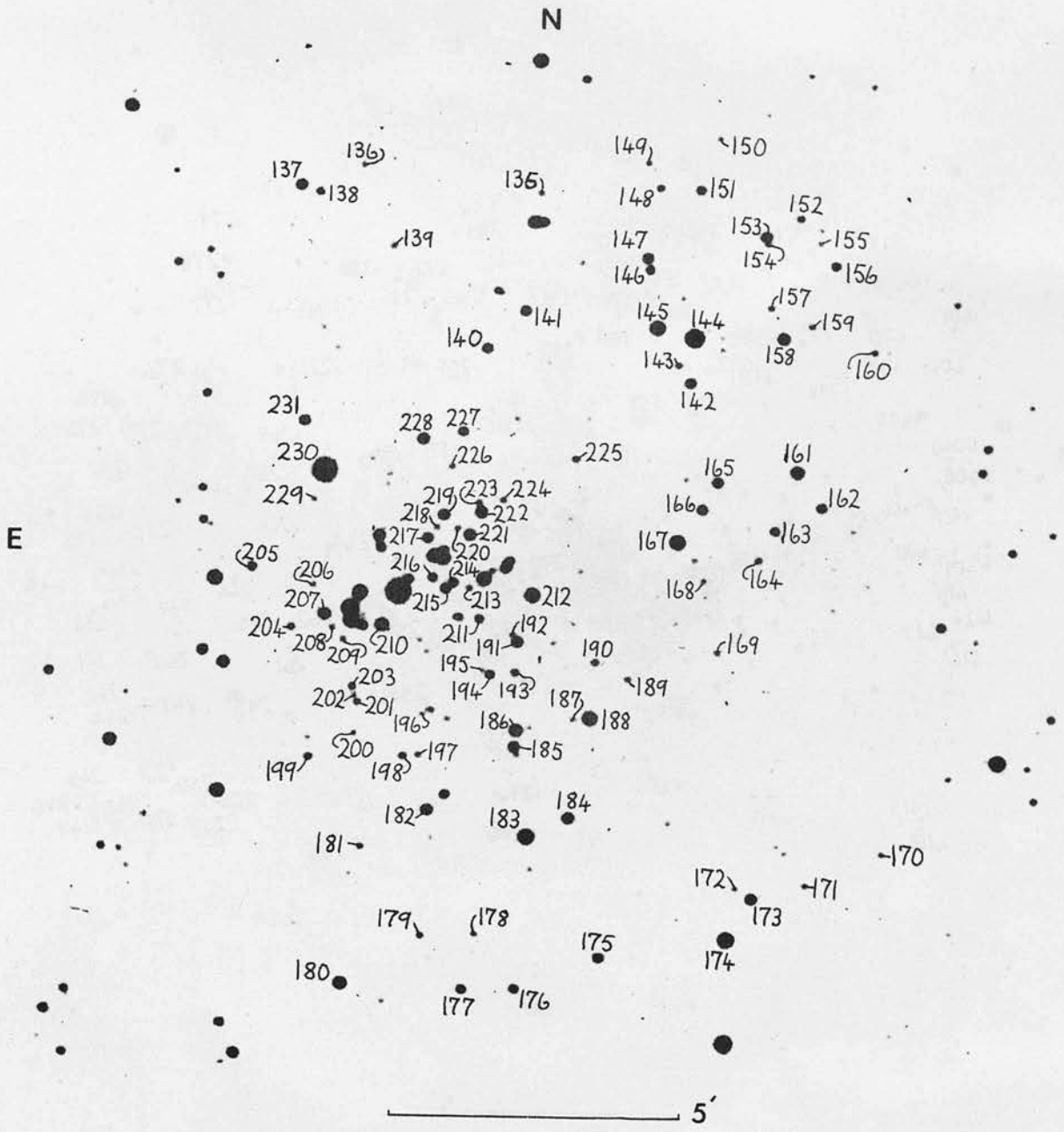
N
E
136
137
138
139
149
150
148
151
152
153
155
154
147
146
156
157
141
145
144
159
140
143
158
160
142
231
228
227
230
226
225
165
161
229
219
223
224
166
162
218
222
217
221
167
163
205
220
206
216
214
164
207
215
213
212
168
204
211
192
208
209
210
191
190
169
195
203
194
193
187
189
202
201
196
186
188
200
197
185
199
198
184
182
183
181
170
172
171
179
178
173
175
174
180
177
176
5′

5

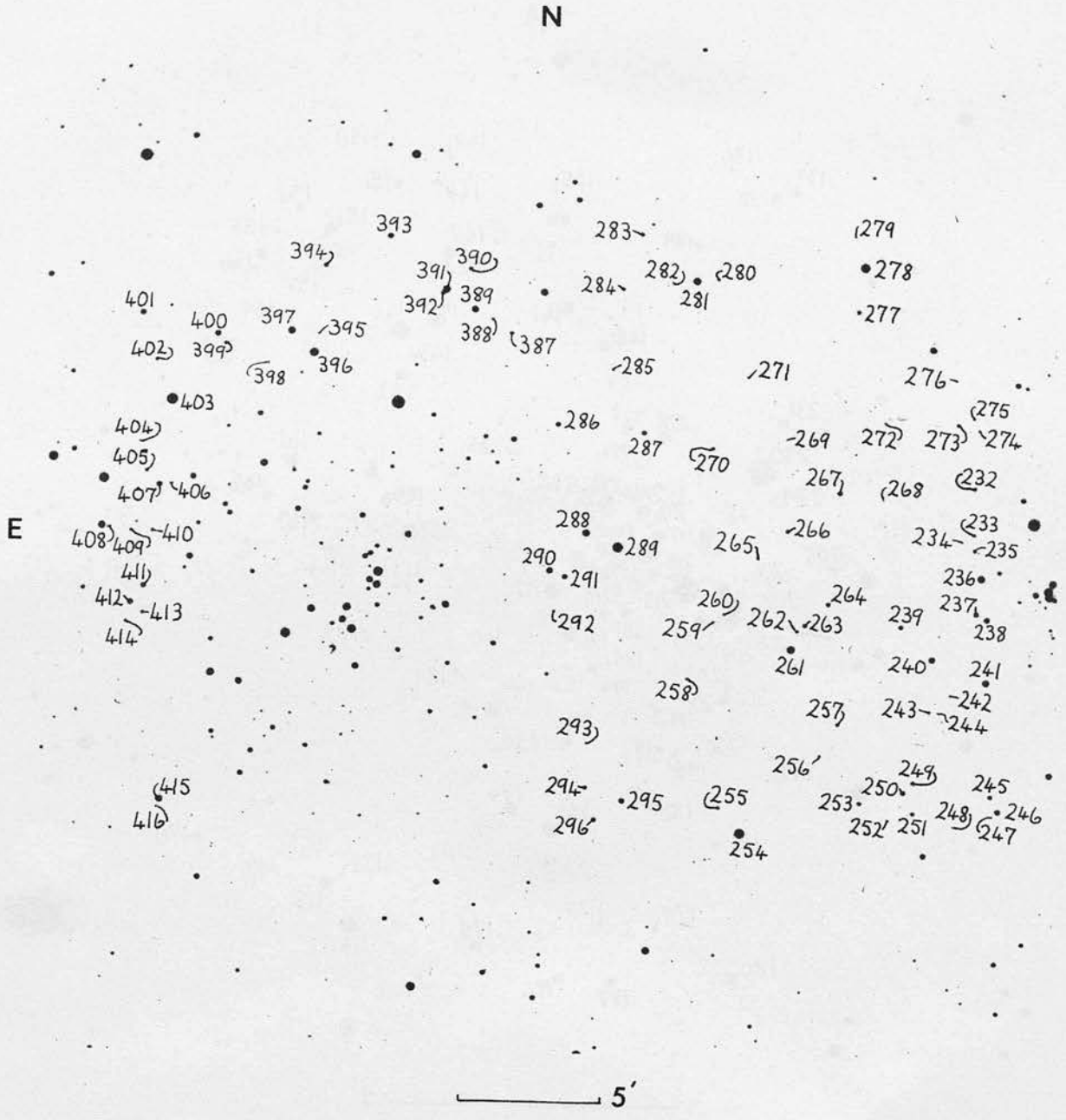

6

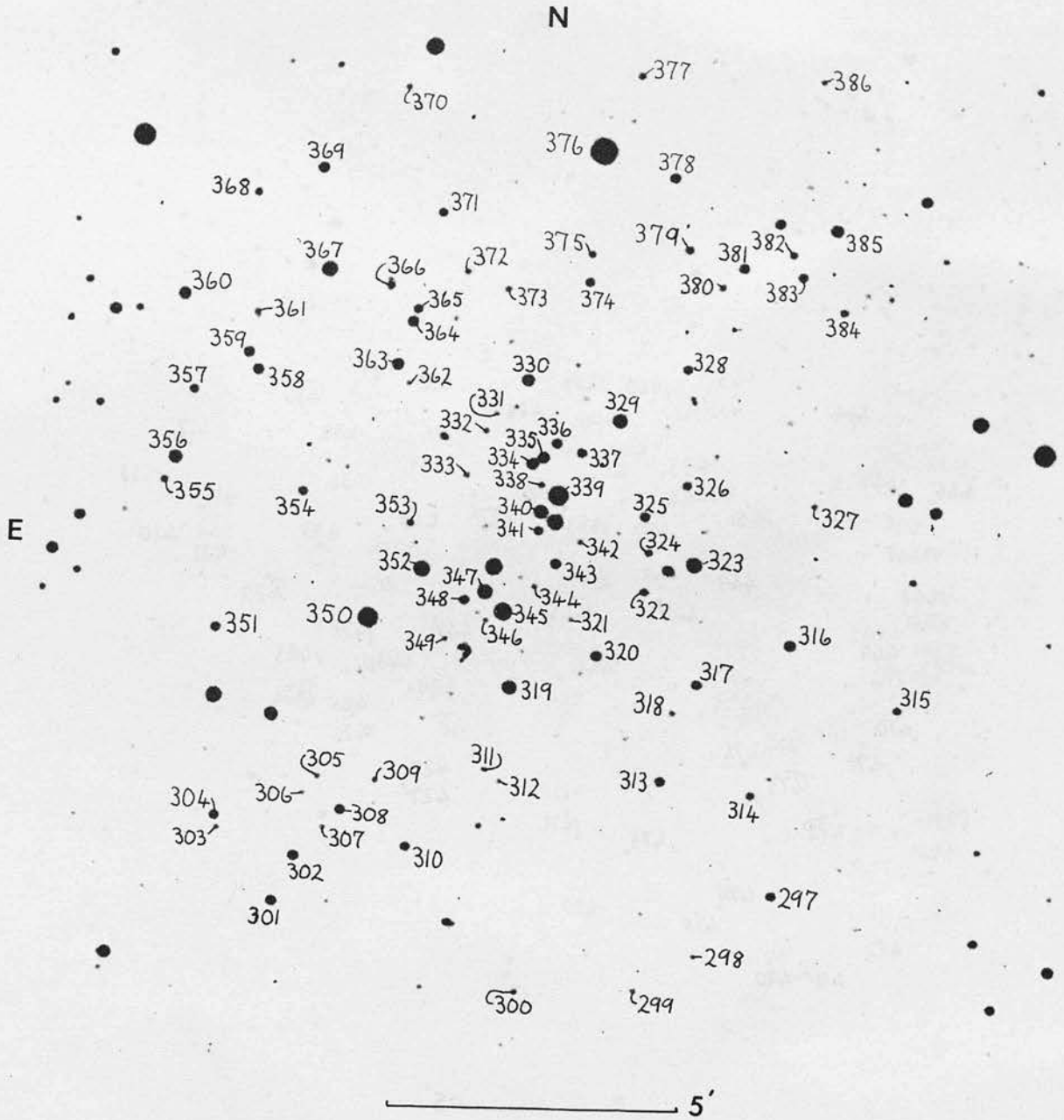
N
E
377
386
370
369
376
378
368
371
367
375
379
381
382
385
366
372
360
380
383
365
373
374
361
384
364
359
363
330
328
362
357
358
331
329
332
336
356
335
337
334
333
338
339
326
355
354
353
340
325
327
341
342
324
352
347
343
323
348
344
322
350
345
321
351
349
346
316
320
317
319
318
315
305
309
311
313
304
306
312
314
308
303
307
310
302
297
301
298
300
299
5′

7

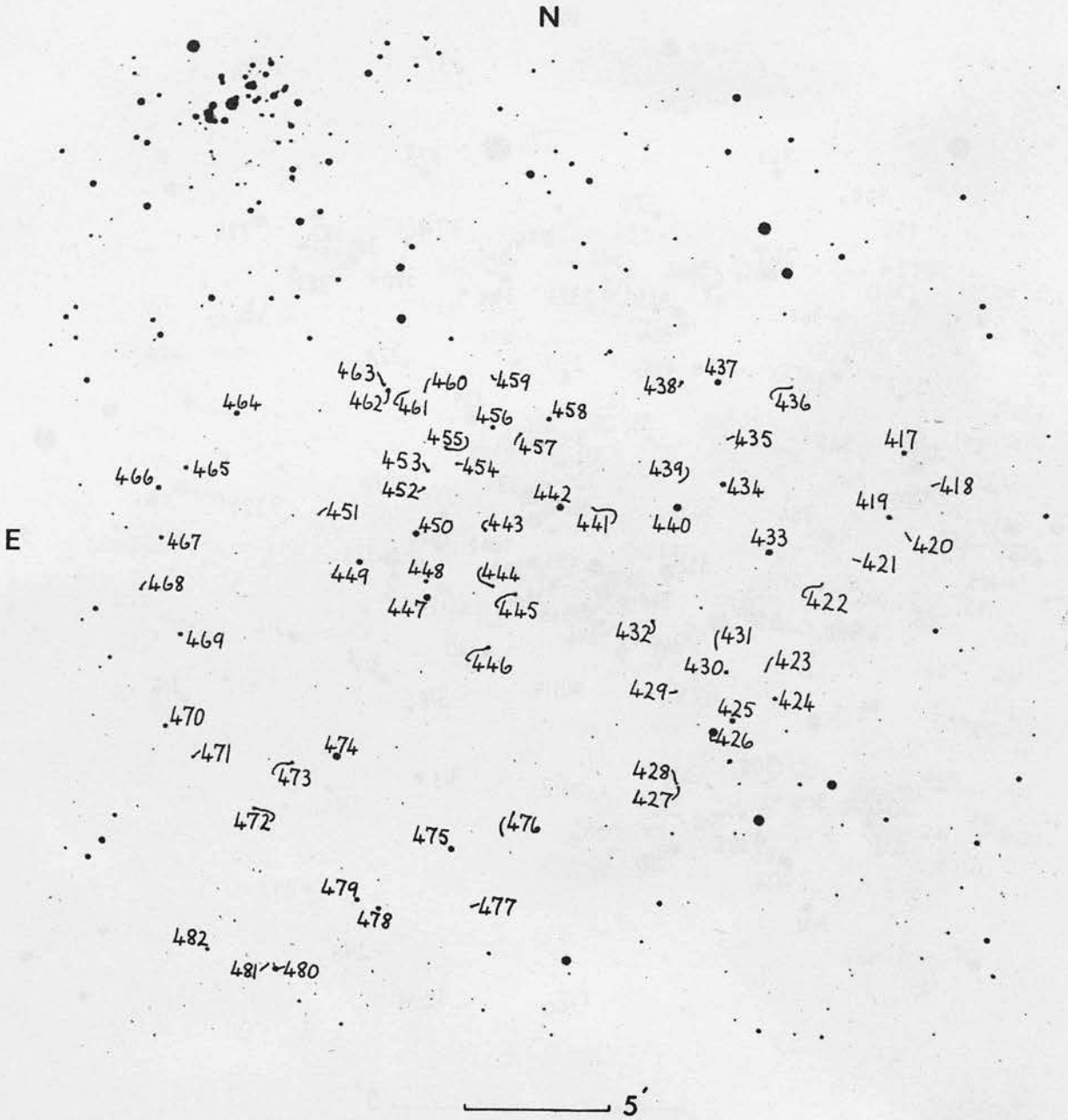
N
E
463
460
459
438
437
464
462
461
456
458
436
455
457
435
417
453
454
439
466
465
452
434
418
442
419
451
450
443
441
440
433
420
467
449
448
444
421
468
447
445
422
469
432
431
446
430
423
429
470
425
424
426
471
474
473
428
427
472
475
476
479
478
477
482
481
480
5′

8


N
E
527
525
524
523
522
521
520
518
507
508
506
502
501
500
503
499
526
517
519
505
504
510
509
511
498
497
496
495
515
516
512
514
494
513
492
493
491
484
483
485
486
487
490
488
489
5′

9

DE 72294 D/233409 K7 TCL